

Optimisation of Study Design in the Pharmacokinetics of Anticancer Drugs

Samantha Jane Carmichael

BSc (Hons), MSc, MRPharmS



Table of Contents

Table of Contents	i
List of Tables	vi
List of Figures	viii
List of Equations	xx
Declaration	xxv
Acknowledgements	xxvi
Abstract	xxvii

Chapter 1: Optimisation of Study Design in the Pharmacokinetics of Anticancer Drugs.	1.1
1.1 Introduction.....	1.2
1.2 Pharmacokinetics and Pharmacokinetic Modelling.....	1.4
1.3 Population PK Study Design	1.14
1.4 Dose Adaptation for Anticancer Chemotherapy Using Pharmacokinetics.	1.25
1.5 Aims of Thesis.....	1.30

Chapter 2: Methods	2.1
2.1 Introduction.....	2.2
2.2 Data Simulation	2.4
2.2.1 Parameter Distributions	2.4
2.2.2 Pharmacokinetic Models.....	2.6
2.2.2.1 One-Compartment Model.....	2.6
2.2.2.2 Two-Compartment Model	2.6
2.2.3 Random Error on Concentration.....	2.8
2.3 Parameter Estimation.....	2.9
2.3.1 NONMEM	2.9
2.3.2 Summary Statistics	2.14

Chapter 3: Use of Sensitivity Analysis to Define 'Optimal' Sampling Strategies	3.1
3.1 Introduction.....	3.2
3.2 Mathematical Proofs.....	3.4
3.2.1 One-Compartment IV Bolus.....	3.4
3.2.2 Two-Compartment IV Bolus.....	3.9
3.3 Comparison of Derived 'Optimal' Sampling Times with Those Obtained in Simulated Populations.....	3.10
3.3.1 Introduction.....	3.10
3.3.2 Methods.....	3.10
3.3.3 Results.....	3.14
3.3.3.1 One-Compartment IV Bolus PK Model.....	3.14
3.3.3.2 Two-Compartment IV Bolus.....	3.26
3.3.4 Discussion.....	3.41
3.3.4.1 One-Compartment Model.....	3.41
3.3.4.2 Two-Compartment Model.....	3.42
3.4 Conclusion.....	3.45
Chapter 4: Limited Sampling in a One-Compartment IV Bolus Pharmacokinetic Model (Two Sampling Times)	4.1
4.1 Introduction.....	4.2
4.2 Comparison of Two Sampling Designs based on Sensitivity Analysis.....	4.4
4.2.1 Methods.....	4.4
4.2.1.1 Data Simulation.....	4.4
4.2.1.2 Sampling Designs.....	4.4
4.2.1.3 Data Analysis.....	4.5
4.2.2 Results.....	4.8
4.2.3 Discussion.....	4.14
4.3 Comparison of NONMEM FO and FOCE Methods.....	4.16
4.3.1 Methods.....	4.16
4.3.1.1 Data Simulation.....	4.16
4.3.1.2 Data Analysis.....	4.16
4.3.2 Results.....	4.18

4.3.3	Discussion.....	4.27
4.4	Comparison of Results from 10 Sets of 500 subjects with those from 100 sets of 500 Subjects.....	4.30
4.4.1	Methods	4.30
4.4.1.1	Data Simulation	4.30
4.4.1.2	Data Analysis.....	4.30
4.4.2	Results.....	4.31
4.4.3	Discussion.....	4.35
4.5	Conclusion	4.36

Chapter 5:	Limited Sampling in a One-Compartment IV Bolus Pharmacokinetic Model	5.1
5.1	Introduction.....	5.2
5.2	Methods	5.5
5.2.1	Data Simulation	5.5
5.2.2	Two-Sample Designs.....	5.5
5.2.3	Three-Sample Designs.....	5.6
5.2.4	Data Analysis.....	5.7
5.3	Results.....	5.11
5.3.1	Two-Sample Designs.....	5.11
5.3.2	Three-Sample Designs.....	5.22
5.4	Discussion.....	5.34
5.5	Conclusion	5.41

Chapter 6: Limited Sampling in a Two-Compartment IV Bolus Pharmacokinetic Model.....	6.1
6.1 Introduction.....	6.2
6.2 Methods	6.4
6.2.1 Data Simulation	6.4
6.2.2 Sampling Schedules.....	6.6
6.3 Results.....	6.10
6.4 Discussion.....	6.20
Chapter 7: Application of Limited Sampling Design to Two Anticancer Drugs	7.1
7.1 One-Compartment PK Model - Carboplatin (Simulated Data)	7.2
7.1.1 Introduction.....	7.2
7.1.2 Methods	7.3
7.1.2.1 Data Simulation	7.3
7.1.2.2 Sampling Schedules.....	7.3
7.1.2.3 Data Analysis.....	7.6
7.1.3 Results.....	7.9
7.1.4 Discussion.....	7.20
7.2 Two-Compartment PK Model - Antagonist G 6 hour IV Infusion (Clinical Data).....	7.25
7.2.1 Introduction.....	7.25
7.3 Phase I Study	7.27
7.3.1 Methods	7.27
<i>Antagonist G Administration & PK Sampling Schedule.....</i>	<i>7.27</i>
<i>Individual PK Analyses</i>	<i>7.28</i>
<i>Population PK Analysis</i>	<i>7.28</i>
7.3.2 Results.....	7.29
7.4 Optimal Design for Antagonist G.....	7.43
7.4.1 Methods	7.43
7.4.1.1 Data Simulation	7.43
7.4.2 Results.....	7.44
7.5 Antagonist G Simulations.....	7.47

7.5.1	Methods	7.47
7.5.1.1	Data Simulation	7.47
7.5.1.2	Sampling Schedules.....	7.47
7.5.1.3	Data Analysis.....	7.48
7.5.2	Results.....	7.49
7.5.3	Discussion.....	7.62
7.6	Conclusion	7.66
Chapter 8:	Conclusions and Further Investigations	8.1
Appendix 1:	Mathematical Proofs	A1.1
	Introduction.....	A1.2
	One-Compartment IV Bolus	A1.2
	Two-Compartment IV Bolus	A1.9
Appendix 2:	Simulation Programs	A2.1
	Input File for One-Compartment IV Bolus Simulations	A2.2
	Simulation Program for a One-Compartment IV Bolus PK Model.....	A2.3
	Simulation Program for a One-Compartment IV Bolus PK Model with Fixed Sampling Times (Selects Optimal Sampling Times for each Individual)	A2.6
	Simulation Programs for a One-Compartment IV Bolus PK Model with Three Sampling Times	A2.9
	Input File for Two-Compartment IV Bolus Simulations.....	A2.15
	Simulation Program for a Two-Compartment IV Bolus PK Model.....	A2.16
	Input File for Two-Compartment IV Infusion Simulations.....	A2.19
	Simulation Program for a Two-Compartment IV Infusion PK Model.....	A2.20
Appendix 3:	Presentations	A3.1
	References	R.1

List of Tables

Chapter 1

Table 1.1 Limited sampling strategies for anticancer drugs, designed using the regression approach.	1.17
---	------

Chapter 3

Table 3.1 Effect of high concentrations on population standard deviation, using the one-compartment PK model ($\omega_{Cl} = 3$ l/h, $t = 5.0$ hr).....	3.25
---	------

Table 3.2 Effect of high concentrations on population standard deviation, using the one-compartment PK model ($\omega_{Cl} = 5$ l/h, $t = 5.0$ hr).....	3.25
---	------

Table 3.3 Times of peak concentration variance due to each parameter (from Figures 3.18-3.21).	3.29
--	------

Chapter 4

Table 4.1 Mean pharmacokinetic parameter values used to simulate data for comparison of Designs 1 and 2 (table 4.2).....	4.6
---	-----

Table 4.2 Sampling designs for a one-compartment IV bolus PK model using two fixed sampling times.....	4.7
---	-----

Table 4.3 Summary of bias and imprecision results using Designs 1 and 2 with NONMEM for estimation of PK parameters.....	4.13
---	------

Table 4.4 Mean pharmacokinetic parameter values used to simulate data for comparison of NONMEM FO and FOCE methods	4.17
---	------

Chapter 5

Table 5.1 Mean pharmacokinetic parameter values used to simulate data.....	5.8
---	-----

Table 5.2 Sampling designs for evaluation of sampling windows with two sampling times.....	5.8
---	-----

Table 5.3 Sampling schedules for three sampling times on a one-compartment IV bolus PK model ($t_{1/2} = 0.69$ hr).....	5.10
---	------

Table 5.4 Comparing mean %Bias and %Imprecision for two-sample design 8 with a $50\%*t_{1/2}$ sampling window and the three-sample runs with $50\%*t_{1/2}$ sampling windows (designs 10b, 11b and 12b). Results shown for a standard deviation of clearance = 3 l/h.....	5.33
--	------

Chapter 6

Table 6.1 Pharmacokinetic parameter values for designs 13 to 19 (Table 6.2)... 6.5

Table 6.2 Sampling schedules for simulation of the two-compartment IV bolus PK model..... 6.8

Chapter 7

Table 7.1 Mean pharmacokinetic parameter values for carboplatin simulations. 7.4

Table 7.2 Sampling schedules for carboplatin using a one-compartment IV bolus PK model..... 7.7

Table 7.3 Summary and results of individual NONMEM analyses. 7.30

Table 7.4 Summary of the Antagonist G population model development with NONMEM using data from patients 13-24..... 7.38

Table 7.5 Summary of parameter estimates during development of Antagonist G population model using data from patients 13-24..... 7.39

Table 7.6 Pharmacokinetic parameter values for optimal sampling design for Antagonist G..... 7.43

Table 7.7 'Optimal' sampling times for Antagonist G. 7.46

List of Figures

Chapter 1

Figure 1.1 One-compartment pharmacokinetic model with IV bolus dose (D), volume of distribution (V) and first-order elimination (k_e). C represents the concentration of drug attained in the body following administration of the dose. 1.6

Figure 1.2 Two-compartment pharmacokinetic model with IV bolus dose (D), inter-compartmental transfer (k_{12} & k_{21}), volume of distribution of the central (V_1) and peripheral (V_2) compartments and first-order elimination (k_{10}). C_1 and C_2 represent the concentration of drug attained in the central and peripheral compartments, respectively, following administration of the dose. 1.9

Figure 1.3 Representation of the linear trapezoidal rule. $AUC_{t_i}^{t_{i+1}}$ is the area between t_i and t_{i+1} . C_i and C_{i+1} are the corresponding concentration measurements and Δt is the time interval (Gabrielsson et al. 1997). 1.19

Chapter 2

Figure 2.1 Examples of bias and imprecision within populations of results. Distributions of results are shown that are (a) unbiased and precise, (b) biased, but precise, (c) unbiased, but imprecise and (d) biased and imprecise. 2.16

Chapter 3

Figure 3.1 Change in concentration variance ($(\text{mg/l})^2$) over time when $Cl = 10$ l/h, $V = 10$ l, $\omega_{Cl} = 3$ l/h, $\omega_V = 0$ l and dose = 100mg. 3.7

Figure 3.2 Change in concentration variance ($(\text{mg/l})^2$) over time when $Cl = 10$ l/h, $V = 10$ l, $\omega_{Cl} = 0$ l/h, $\omega_V = 3$ l and dose = 100mg. 3.7

Figure 3.3 Organisation of simulated populations for calculation of observed concentration variance for comparison with that predicted from the equations derived in section 3.2. 3.13

Figure 3.4 Plot of concentration variance over time for ten simulations of 5000 subjects and the derived concentration variance when $\omega_{Cl} = 3$ l/h (no random error). 3.16

Figure 3.5 Plot of concentration variance over time for ten simulations of 5000 subjects and the derived concentration variance when $\omega_{Cl} = 3$ l/h (random error). 3.16

Figure 3.6 Concentration variance across time for $\omega_{Cl} = 1$ l/h (no random error).	3.17
Figure 3.7 Concentration variance across time for $\omega_{Cl} = 2$ l/h (no random error).	3.17
Figure 3.8 Concentration variance across time for $\omega_{Cl} = 3$ l/h (no random error).	3.18
Figure 3.9 Concentration variance across time for $\omega_{Cl} = 4$ l/h (no random error).	3.18
Figure 3.10 Concentration variance across time for $\omega_{Cl} = 5$ l/h (no random error).	3.19
Figure 3.11 Concentration variance across time for $\omega_{Cl} = 1$ l/h (random error).	3.19
Figure 3.12 Concentration variance across time for $\omega_{Cl} = 2$ l/h (random error).	3.20
Figure 3.13 Concentration variance across time for $\omega_{Cl} = 3$ l/h (random error).	3.20
Figure 3.14 Concentration variance across time for $\omega_{Cl} = 4$ l/h (random error).	3.21
Figure 3.15 Concentration variance across time for $\omega_{Cl} = 5$ l/h (random error).	3.21
Figure 3.16 Histograms of concentration at 1.0 hr and 5.0 hr when $\omega_{Cl} = 3$, with the one-compartment model (n=5000).	3.23
Figure 3.17 Histograms of concentration at 1.0 hr and 5.0 hr when $\omega_{Cl} = 5$, with the one-compartment model (n=5000).	3.24
Figure 3.18 Plot of concentration variance over time showing the effect of increasing variance in clearance (Cl) from 10 to 50%, with the two-compartment PK model.	3.27
Figure 3.19 Plot of concentration variance over time showing the effect of increasing variance in volume of the central compartment (V_1) from 10 to 50%, with the two-compartment PK model.	3.27
Figure 3.20 Plot of concentration variance over time showing the effect of increasing variance in volume of the peripheral compartment (V_2) from 10 to 50%, with the two-compartment PK model.	3.28
Figure 3.21 Plot of concentration variance over time showing the effect of increasing variance in inter-compartmental clearance (Q) from 10 to 50%, with the two-compartment PK model.	3.28

Figure 3.22 Plot of concentration variance over time for ten simulations of 5000 subjects and the derived concentration variance when $\omega_{Cl} = 3$ l/h (no random error).....	3.32
Figure 3.23 Plot of concentration variance over time for ten simulations of 5000 subjects and the derived concentration variance when $\omega_{Cl} = 3$ l/h (random error).	3.32
Figure 3.24 Concentration variance across time for $\omega_{Cl} = 1$ l/h (no random error).	3.33
Figure 3.25 Concentration variance across time for $\omega_{Cl} = 2$ l/h (no random error).	3.33
Figure 3.26 Concentration variance across time for $\omega_{Cl} = 3$ l/h (no random error).	3.34
Figure 3.27 Concentration variance across time for $\omega_{Cl} = 4$ l/h (no random error).	3.34
Figure 3.28 Concentration variance across time for $\omega_{Cl} = 5$ l/h (no random error).	3.35
Figure 3.29 Concentration variance across time for $\omega_{Cl} = 1$ l/h (random error).3.35	
Figure 3.30 Concentration variance across time for $\omega_{Cl} = 2$ l/h (random error).3.36	
Figure 3.31 Concentration variance across time for $\omega_{Cl} = 3$ l/h (random error).3.36	
Figure 3.32 Concentration variance across time for $\omega_{Cl} = 4$ l/h (random error).3.37	
Figure 3.33 Concentration variance across time for $\omega_{Cl} = 5$ l/h (random error).3.37	
Figure 3.34 Histograms of Concentration at 0.5 hr and 5.0 hr when $\omega_{Cl} = 3$, with the Two-Compartment Model.	3.39
Figure 3.35 Histograms of Concentration at 0.5 hr and 5.0 hr when $\omega_{Cl} = 5$, with the Two-Compartment Model.	3.40

Chapter 4

Figure 4.1 Sampling times for Designs 1 and 2 shown on the concentration variance curve. The curves show the contribution of each parameter (Var (Cl) and Var (V)) to the total concentration variance curve (Var Total).....	4.7
Figure 4.2 Bias ($\pm 95\%$ CI) and imprecision of the NONMEM population estimates of clearance (\overline{Cl}), using Designs 1 and 2.	4.10

Figure 4.3 Comparison of mean individual simulated values of clearance with the mean NONMEM posthoc values.....	4.10
Figure 4.4 Bias ($\pm 95\%$ CI) and imprecision of the NONMEM population estimates of volume of distribution (\bar{V}), using Designs 1 and 2	4.11
Figure 4.5 Comparison of mean individual simulated values of volume of distribution with the mean NONMEM posthoc values	4.11
Figure 4.6 Bias ($\pm 95\%$ CI) and imprecision of the NONMEM population estimates of standard deviation in clearance (ω_{Cl}), using Designs 1 and 2.....	4.12
Figure 4.7 Bias ($\pm 95\%$ CI) and imprecision of the NONMEM population estimates of standard deviation in volume of distribution (ω_V), using Designs 1 and 2.	4.12
Figure 4.8 Bias ($\pm 95\%$ CI) and imprecision of the NONMEM population estimates of proportional intra-subject random error in concentration (σ_I), using Designs 1 and 2.	4.13
Figure 4.9 Bias (mean and 95% CI) and imprecision results for the estimates of population mean clearance.	4.21
Figure 4.10 Bias (mean and 95% CI) and imprecision results for the estimates of population mean volume of distribution.....	4.22
Figure 4.11 Bias (mean and 95% CI) and imprecision results for the estimates of the standard deviation of the population clearance distribution (ω_{Cl}).....	4.23
Figure 4.12 Bias (mean and 95% CI) and imprecision results for the estimates of the standard deviation of the distribution of the population volume of distribution (ω_V).....	4.24
Figure 4.13 Bias (mean and 95% CI) and imprecision results for the estimates of the proportional error component (σ_I).....	4.25
Figure 4.14 Bias (mean and 95% CI) and imprecision results for the estimates of the additive error component (σ_2).	4.26
Figure 4.15 Comparison of average bias and imprecision in the estimation of clearance (Cl), using either 100 or 10 sets of 500 subjects.	4.32
Figure 4.16 Comparison of average bias and imprecision in the estimation of volume of distribution (V), using either 100 or 10 sets of 500 subjects.....	4.32

Figure 4.17 Comparison of average bias and imprecision in the estimation of standard deviation of clearance (ω_{Cl}), using either 100 or 10 sets of 500 subjects.	4.33
Figure 4.18 Comparison of average bias and imprecision in the estimation of standard deviation of volume of distribution (ω_V), using either 100 or 10 sets of 500 subjects.	4.33
Figure 4.19 Comparison of average bias and imprecision in the estimation of the proportional random error component (σ_1), using either 100 or 10 sets of 500 subjects.	4.34
Figure 4.20 Comparison of average bias and imprecision in the estimation of the additive random error component (σ_2), using either 100 or 10 sets of 500 subjects.	4.34

Chapter 5

Figure 5.1 Sampling times for designs 3 to 8 shown on the concentration variance curve. The boxes represent the distribution of the sampling window around the 1.0hr sample.	5.9
Figure 5.2 Concentration variance components and the sampling times for designs 10 to 12 shown on the concentration variance curve. The boxes represent the distribution of the sampling window around the second and third samples. The black boxes represent the $10\%*t_{1/2}$ sampling window and the blue and green boxes represent the $50\%*t_{1/2}$ sampling windows on the second and third time, respectively.....	5.10
Figure 5.3 Bias (mean \pm 95% CI) results for the estimates of population mean clearance. The results for designs 3-9 are shown as the simulated ω_{Cl} increased from 1 to 3, from left to right.	5.16
Figure 5.4 Imprecision results for the estimates of population mean clearance. The results for designs 3-9 are shown as the simulated ω_{Cl} increased from 1 to 3, from left to right.	5.16
Figure 5.5 Bias (mean \pm 95% CI) results for the estimates of population mean volume of distribution. The results for designs 3-9 are shown as the simulated ω_{Cl} increased from 1 to 3, from left to right.	5.17
Figure 5.6 Imprecision results for the estimates of population mean volume of distribution. The results for designs 3-9 are shown as the simulated ω_{Cl} increased from 1 to 3, from left to right.	5.17

Figure 5.7 Bias (mean \pm 95% CI) results for the estimates of standard deviation of the population clearance distribution (ω_{Cl}). The results for designs 3-9 are shown as the simulated ω_{Cl} increased from 1 to 3, from left to right. 5.18

Figure 5.8 Imprecision results for the estimates of the standard deviation of the population clearance distribution (ω_{Cl}). The results for designs 3-9 are shown as the simulated ω_{Cl} increased from 1 to 3, from left to right..... 5.18

Figure 5.9 Bias (mean \pm 95% CI) results for the estimates of standard deviation of the population volume distribution (ω_V). The results for designs 3-9 are shown as the simulated ω_{Cl} increased from 1 to 3, from left to right..... 5.19

Figure 5.10 Imprecision results for the estimates of the standard deviation of the population volume distribution (ω_V). The results for designs 3-9 are shown as the simulated ω_{Cl} increased from 1 to 3, from left to right..... 5.19

Figure 5.11 Bias (mean \pm 95% CI) results for the estimates of the proportional error component (σ_1). The results for designs 3-9 are shown as the simulated ω_{Cl} increased from 1 to 3, from left to right. 5.20

Figure 5.12 Imprecision results for the estimates of the proportional error component (σ_1). The results for designs 3-9 are shown as the simulated ω_{Cl} increased from 1 to 3, from left to right. 5.20

Figure 5.13 Bias (mean \pm 95% CI) results for the estimates of the additive error component (σ_2). The results for designs 3-9 are shown as the simulated ω_{Cl} increased from 1 to 3, from left to right. 5.21

Figure 5.14 Imprecision results for the estimates of the additive error component (σ_2). The results for designs 3-9 are shown as the simulated ω_{Cl} increased from 1 to 3, from left to right. 5.21

Figure 5.15 %Bias and %Imprecision of the estimation of clearance (\overline{Cl}) with windows of 10% of the half life around the second two sampling times..... 5.26

Figure 5.16 %Bias and %Imprecision of the estimation of clearance (\overline{Cl}) with windows of 50% of the half life around the second two sampling times..... 5.26

Figure 5.17 %Bias and %Imprecision of the estimation of volume (\overline{V}) with windows of 10% of the half life around the second two sampling times..... 5.27

Figure 5.18 %Bias and %Imprecision of the estimation of volume (\overline{V}) with windows of 50% of the half life around the second two sampling times..... 5.27

Figure 5.19 %Bias and %Imprecision of the estimation of standard deviation of clearance (ω_{Cl}) with windows of 10% of the half life around the second two sampling times.....	5.28
Figure 5.20 %Bias and %Imprecision of the estimation of standard deviation of clearance (ω_{Cl}) with windows of 50% of the half life around the second two sampling times.....	5.28
Figure 5.21 %Bias and %Imprecision of the estimation of standard deviation of volume (ω_V) with windows of 10% of the half life around the second two sampling times.	5.29
Figure 5.22 %Bias and %Imprecision of the estimation of standard deviation of volume (ω_V) with windows of 50% of the half life around the second two sampling times.	5.29
Figure 5.23 %Bias and %Imprecision of the estimation of random proportional error on concentration (σ_1) with windows of 10% of the half life around the second two sampling times.....	5.30
Figure 5.24 %Bias and %Imprecision of the estimation of random proportional error on concentration (σ_1) with windows of 50% of the half life around the second two sampling times.....	5.30
Figure 5.25 %Bias and %Imprecision of the estimation of additive random error on concentration (σ_2) with windows of 10% of the half life around the second two sampling times.....	5.31
Figure 5.26 %Bias and %Imprecision of the estimation of additive random error on concentration (σ_2) with windows of 50% of the half life around the second two sampling times.....	5.31

Chapter 6

Figure 6.1 Sampling times based on sensitivity analysis for the two-compartment IV bolus PK model.	6.7
Figure 6.2 Plot of log concentration against time, using the population average parameter values from table 6.1, showing the sampling times according to peaks in concentration variance from each parameter (X) and the empirical sampling times (O).....	6.9
Figure 6.3 Bias (%B) and imprecision (%I) in the estimation of clearance (Cl) using designs 13 to 19. The set of three results for each design represents increasing variability in clearance, i.e., from left to right represents ω_{Cl} increasing from 1 l/h to 3 l/h.....	6.12

- Figure 6.4** Bias (%B) and imprecision (%I) in the estimation of the volume of distribution of the central compartment (V_1) using designs 13 to 19. The set of three results for each design represents increasing variability in clearance, i.e., from left to right represents ω_{Cl} increasing from 1 l/h to 3 l/h. 6.12
- Figure 6.5** Bias (%B) and imprecision (%I) in the estimation of the volume of distribution of the peripheral compartment (V_2) using designs 13 to 19. The set of three results for each design represents increasing variability in clearance, i.e., from left to right represents ω_{Cl} increasing from 1 l/h to 3 l/h. 6.13
- Figure 6.6** Bias (%B) and imprecision (%I) in the estimation of the inter-compartmental clearance (Q) using designs 13 to 19. The set of three results for each design represents increasing variability in clearance, i.e., from left to right represents ω_{Cl} increasing from 1 l/h to 3 l/h. 6.13
- Figure 6.7** Bias (%B) and imprecision (%I) in the estimation of the standard deviation of clearance (ω_{Cl}) using designs 13 to 19. The set of three results for each design represents increasing variability in clearance, i.e., from left to right represents ω_{Cl} increasing from 1 l/h to 3 l/h. 6.16
- Figure 6.8** Spread of the bias estimates for the standard deviation of clearance (ω_{Cl}) using designs 13 to 19. (–) is the mean of the ten bias values. The set of three results for each design represents increasing variability in clearance, i.e., from left to right represents ω_{Cl} increasing from 1 l/h to 3 l/h. 6.16
- Figure 6.9** Bias (%B) and imprecision (%I) in the estimation of the standard deviation of the volume of the central compartment (ω_{V_1}) using designs 13 to 19. The set of three results for each design represents increasing variability in clearance, i.e., from left to right represents ω_{Cl} increasing from 1 l/h to 3 l/h. ... 6.17
- Figure 6.10** Bias (%B) and imprecision (%I) in the estimation of the standard deviation of the volume of the peripheral compartment (ω_{V_2}) using designs 13 to 19. The set of three results for each design represents increasing variability in clearance, i.e., from left to right represents ω_{Cl} increasing from 1 l/h to 3 l/h. ... 6.17
- Figure 6.11** Bias (%B) and imprecision (%I) in the estimation of the standard deviation of the inter-compartmental clearance (ω_Q) using designs 13 to 19. The set of three results for each design represents increasing variability in clearance, i.e., from left to right represents ω_{Cl} increasing from 1 l/h to 3 l/h. 6.18
- Figure 6.12** Bias (%B) and imprecision (%I) in the estimation of proportional random error on concentration (σ_I) using designs 13 to 19. The set of three results for each design represents increasing variability in clearance, i.e., from left to right represents ω_{Cl} increasing from 1 l/h to 3 l/h. 6.18

Figure 6.13 Bias (%B) and imprecision (%I) in the estimation of additive random error on concentration (σ_2) using designs 13 to 19. The set of three results for each design represents increasing variability in clearance, i.e., from left to right represents ω_{Cl} increasing from 1 l/h to 3 l/h. 6.19

Chapter 7

Figure 7.1 Sensitivity analysis of concentration variance using carboplatin parameter values. The variance in concentration from a simulated population of 5000 subjects was compared to that predicted. Two sampling times were based on the peaks in concentration variance due to the components clearance and volume of distribution. A third sampling time was selected from the intersect of the variance curves due to these components. 7.4

Figure 7.2 Plot of concentration vs time for the mean values of clearance and volume, with the sampling times. 7.8

Figure 7.3 Carboplatin sampling designs shown on the concentration variance curve. 7.8

Figure 7.4 Mean percentage bias (%B) \pm 95% confidence interval and imprecision (%I) for the estimation of carboplatin clearance, using designs 20-28. 7.14

Figure 7.5 Comparison of mean simulated values with NONMEM population estimates of carboplatin clearance. 7.14

Figure 7.6 Mean percentage bias (%B) \pm 95% confidence interval and imprecision (%I) for the estimation of carboplatin volume of distribution, using designs 20-28. 7.15

Figure 7.7 Comparison of mean simulated values with NONMEM population estimates of carboplatin volume of distribution. 7.15

Figure 7.8 Mean percentage bias (%B) \pm 95% confidence interval and imprecision (%I) for the estimation of the standard deviation of carboplatin clearance, using designs 20-28. 7.16

Figure 7.9 Comparison of mean simulated values with NONMEM population estimates of standard deviation of carboplatin clearance. 7.16

Figure 7.10 Mean percentage bias (%B) \pm 95% confidence interval and imprecision (%I) for the estimation of the standard deviation of carboplatin volume of distribution, using designs 20-28. 7.17

Figure 7.11 Comparison of mean simulated values with NONMEM population estimates of standard deviation of carboplatin volume of distribution. 7.17

Figure 7.12 Mean percentage bias (%B) \pm 95% confidence interval and imprecision (%I) for the estimation of the proportional random error of carboplatin concentration, using designs 20-28.	7.18
Figure 7.13 Comparison of mean simulated values with NONMEM population estimates of proportional error of carboplatin concentration.	7.18
Figure 7.14 Mean percentage bias (%B) \pm 95% confidence interval and imprecision (%I) for the estimation of the additive random error of carboplatin concentration, using designs 20-28.	7.19
Figure 7.15 Comparison of mean simulated values with NONMEM population estimates of additive error of carboplatin concentration.	7.19
Figure 7.16 Individual Antagonist G profiles of measured and predicted concentrations versus time.	7.31
Figure 7.17 Box and whisker plots of individual parameter estimates for Antagonist G. (V_2 is shown without subject 2, value = 119l).....	7.34
Figure 7.18 Plots of individual parameter estimates for Antagonist G against dose. (V_2 is shown without subject 2, value = 119l).....	7.37
Figure 7.19 Individual Antagonist G profiles of measured, population predicted and individual predicted concentrations versus time.....	7.40
Figure 7.20 Population and individual predicted concentrations versus measured concentrations for patients 13 to 24.....	7.42
Figure 7.21 Sampling times based on sensitivity analysis for the two-compartment IV infusion of Antagonist G.....	7.45
Figure 7.22 ‘Optimal’ sampling times from NONMEM population analysis Run 3 and dose of 622mg. Comparison with sampling times used in phase I study. ...	7.46
Figure 7.23 Mean percentage bias(%B) \pm 95% confidence interval and imprecision (%I) for the estimation of the clearance (\overline{Cl}) of Antagonist G, using designs 29-31.....	7.51
Figure 7.24 Comparison of mean simulated values with NONMEM population estimates of Antagonist G clearance.	7.51
Figure 7.25 Mean percentage bias (%B) \pm 95% confidence interval and imprecision (%I) for the estimation of the volume of distribution of the central compartment (\overline{V}_1) of Antagonist G, using designs 29-31.....	7.52

Figure 7.26 Comparison of mean simulated values with NONMEM population estimates of Antagonist G volume of the central compartment (\bar{V}_1).....	7.52
Figure 7.27 Mean percentage bias (%B) \pm 95% confidence interval and imprecision (%I) for the estimation of the volume of distribution of the peripheral compartment (\bar{V}_2) of Antagonist G, using designs 29-31.	7.53
Figure 7.28 Comparison of mean simulated values with NONMEM population estimates of Antagonist G volume of the peripheral compartment (\bar{V}_2).....	7.53
Figure 7.29 Mean percentage bias (%B) \pm 95% confidence interval and imprecision (%I) for the estimation of the inter-compartmental clearance (\bar{Q}) of Antagonist G, using designs 29-31.....	7.54
Figure 7.30 Comparison of mean simulated values with NONMEM population estimates of Antagonist G inter-compartmental clearance (\bar{Q}).....	7.54
Figure 7.31 Mean percentage bias (%B) \pm 95% confidence interval and imprecision (%I) for the estimation of the standard deviation of clearance of Antagonist G (ω_{Cl}), using designs 29-31.	7.57
Figure 7.32 Comparison of mean simulated values with NONMEM population estimates of standard deviation of Antagonist G clearance (ω_{Cl}).....	7.57
Figure 7.33 Mean percentage bias (%B) \pm 95% confidence interval and imprecision (%I) for the estimation of the standard deviation of the volume of distribution of the central compartment of Antagonist G (ω_{V_1}), using designs 29-31.	7.58
Figure 7.34 Comparison of mean simulated values with NONMEM population estimates of standard deviation of Antagonist G volume of the central compartment (ω_{V_1}).....	7.58
Figure 7.35 Mean percentage bias (%B) \pm 95% confidence interval and imprecision (%I) for the estimation of the standard deviation of the volume of distribution of the peripheral compartment of Antagonist G (ω_{V_2}), using designs 29-31.....	7.59
Figure 7.36 Comparison of mean simulated values with NONMEM population estimates of standard deviation of Antagonist G volume of the peripheral compartment (ω_{V_2}).....	7.59

Figure 7.37 Mean percentage bias (%B) \pm 95% confidence interval and imprecision (%I) for the estimation of the standard deviation of the inter-compartmental clearance of Antagonist G (ω_Q), using designs 29-31.....	7.60
Figure 7.38 Comparison of mean simulated values with NONMEM population estimates of standard deviation of Antagonist G inter-compartmental clearance (ω_Q)	7.60
Figure 7.39 Mean percentage bias (%B) \pm 95% confidence interval and imprecision (%I) for the estimation of the proportional intra-subject error in Antagonist G concentration (σ_I), using designs 29-31.....	7.61
Figure 7.40 Comparison of mean simulated values with NONMEM population estimates of standard deviation of the proportional intra-subject error in Antagonist G concentration (σ_I)	7.61
Figure 7.41 Comparison of a set of 500 simulated parameter estimates with NONMEM posthoc parameter estimates, using 14 fixed sampling times (Design 29). The line of identity is shown in pink.....	7.64
Figure 7.42 Comparison of the simulated concentrations for 500 subjects with the NONMEM population predicted concentrations (PRED) and the NONMEM posthoc predicted concentrations for each individual (IPRED), using 14 fixed sampling times (Design 29). The line of identity is shown in red and the linear regression lines (and corresponding equations) for the PRED and IPRED concentrations are shown in blue and purple, respectively.	7.65

List of Equations

Chapter 1

$$k_e = \frac{Cl}{V} \dots\dots\dots \text{Equation 1.1} \dots\dots\dots 1.5$$

$$t_{1/2} = \frac{0.693}{k_e} \dots\dots\dots \text{Equation 1.2} \dots\dots\dots 1.7$$

$$C_t = \frac{D}{V} e^{-k_e \cdot t} \dots\dots\dots \text{Equation 1.3} \dots\dots\dots 1.7$$

$$k_{12} = \frac{Q}{V_1} \dots\dots\dots \text{Equation 1.4} \dots\dots\dots 1.8$$

$$k_{21} = \frac{Q}{V_2} \dots\dots\dots \text{Equation 1.5} \dots\dots\dots 1.8$$

$$C_t = Ae^{-\alpha t} + Be^{-\beta t} \dots\dots\dots \text{Equation 1.6} \dots\dots\dots 1.8$$

$$AUC = k \cdot C_{t(best)} + b \dots\dots\dots \text{Equation 1.7} \dots\dots\dots 1.15$$

Chapter 2

$$\Theta_i = \bar{\Theta} + \eta_i^\Theta \dots\dots\dots \text{Equation 2.1} \dots\dots\dots 2.4$$

$$C_{ij}^* = \frac{D}{V_i} \cdot e^{-\frac{Cl_i}{V_i} \cdot t_{ij}} \dots\dots\dots \text{Equation 2.2} \dots\dots\dots 2.6$$

$$C_{ij}^* = A_i e^{-\alpha_i t_{ij}} + B_i e^{-\beta_i t_{ij}} \dots\dots\dots \text{Equation 2.3} \dots\dots\dots 2.6$$

$$C_{ij}^* = A_i(e^{\alpha_i T_{ij}} - 1)e^{-\alpha_i t_{ij}} + B_i(e^{\beta_i T_{ij}} - 1)e^{-\beta_i t_{ij}} \dots\dots \text{Equation 2.4} \dots\dots 2.7$$

$$C_{ij} = C_{ij}^* + \varepsilon_{ij} \dots\dots \text{Equation 2.5} \dots\dots 2.8$$

$$C_{ij} = C_{ij}^* \dots\dots \text{Equation 2.6} \dots\dots 2.8$$

$$C_{ij} = C_{ij}^* + \varepsilon_{1ij}(C_{ij}^*) \dots\dots \text{Equation 2.7} \dots\dots 2.8$$

$$C_{ij} = C_{ij}^* + \varepsilon_{2ij} \dots\dots \text{Equation 2.8} \dots\dots 2.8$$

$$C_{ij} = C_{ij}^* + \varepsilon_{1ij}(C_{ij}^*) + \varepsilon_{2ij} \dots\dots \text{Equation 2.9} \dots\dots 2.8$$

$$y_{ij} = f(X_{ij}, \Theta, \eta_i, \varepsilon_{ij}) \dots\dots \text{Equation 2.10} \dots\dots 2.10$$

$$L_i(\psi, \Omega) = \int l_i(\eta, \psi) . h(\eta; \Omega) . d\eta \dots\dots \text{Equation 2.11} \dots\dots 2.10$$

$$L(\psi, \Omega) = \prod_i L_i(\psi, \Omega) \dots\dots \text{Equation 2.12} \dots\dots 2.10$$

$$\text{Bias} = \frac{NM - T}{T} \times 100\% \dots\dots \text{Equation 2.13} \dots\dots 2.14$$

$$\overline{\text{Bias}} = \frac{\sum \text{Bias}}{n} \dots\dots \text{Equation 2.14} \dots\dots 2.14$$

$$\overline{\text{Bias}} \pm t_{\alpha/2} . \text{SEM} \dots\dots \text{Equation 2.15} \dots\dots 2.14$$

$$\text{Imprecison} = \frac{\sqrt{\frac{\Sigma(NM - \overline{NM})^2}{n - 1}}}{\overline{T}} \times 100\% \dots\dots \text{Equation 2.16} \dots\dots 2.15$$

$$\overline{NM} = \frac{\sum NM}{n} \dots \text{Equation 2.17} \dots 2.15$$

$$\bar{T} = \frac{\sum T}{n} \dots \text{Equation 2.18} \dots 2.15$$

Chapter 3

$$C_i = f(\theta_i, D, t) \dots \text{Equation 3.1} \dots 3.3$$

$$\omega_C^2 = \sum_i \left(\frac{\partial C}{\partial \theta_i} \right)^2 \omega_{\theta_i}^2 \dots \text{Equation 3.2} \dots 3.3$$

$$C_i = \frac{D}{V} \cdot e^{-\frac{Cl \cdot t}{V}} \dots \text{Equation 3.3} \dots 3.4$$

$$\omega_C^2 = \left(\frac{\partial C}{\partial Cl} \right)^2 \cdot \omega_{Cl}^2 + \left(\frac{\partial C}{\partial V} \right)^2 \cdot \omega_V^2 \dots \text{Equation 3.4} \dots 3.4$$

$$\frac{\partial C}{\partial Cl} = -\frac{t}{V} \cdot C \dots \text{Equation 3.5} \dots 3.4$$

$$\frac{\partial C}{\partial V} = \frac{1}{V^2} (Cl \cdot t - V) \cdot C \dots \text{Equation 3.6} \dots 3.4$$

$$\omega_C^2 = \frac{t^2 C^2}{V^2} \cdot \omega_{Cl}^2 + \frac{(Cl \cdot t - V)^2}{V^4} \cdot C^2 \cdot \omega_V^2 \dots \text{Equation 3.7} \dots 3.4$$

$$\omega_C^2 = \frac{t^2 C^2}{V^2} \cdot \omega_{Cl}^2 \dots \text{Equation 3.8} \dots 3.5$$

$$t_1 = \frac{V}{Cl} = \frac{1}{k_e} = 1.44 \cdot t_{1/2} \dots \text{Equation 3.9} \dots 3.5$$

$$\omega_C^2 = \frac{(Cl \cdot t - V)^2}{V^4} \cdot C^2 \cdot \omega_V^2 \dots \text{Equation 3.10} \dots 3.5$$

$$t = \frac{1}{k_e} \dots \text{Equation 3.11} \dots 3.5$$

$$t = \frac{2V}{Cl} = \frac{2}{k_e} \dots \text{Equation 3.12} \dots 3.5$$

$$C_t = C_t^* + \varepsilon \dots \text{Equation 3.13} \dots 3.8$$

$$(\omega_{C_t}^2) = (\omega_{C_t^*}^2) + (\omega_{\varepsilon}^2) \dots \text{Equation 3.14} \dots 3.8$$

$$C_t = Ae^{-\alpha t} + Be^{-\beta t} \dots \text{Equation 3.15} \dots 3.9$$

$$\omega_C^2 = \left(\frac{\partial C}{\partial Cl}\right)^2 \cdot \omega_{Cl}^2 + \left(\frac{\partial C}{\partial V_1}\right)^2 \cdot \omega_{V_1}^2 + \left(\frac{\partial C}{\partial V_2}\right)^2 \cdot \omega_{V_2}^2 + \left(\frac{\partial C}{\partial Q}\right)^2 \cdot \omega_Q^2$$

..... Equation 3.16 3.9

$$\text{Variance} = (SD)^2; SD = \sqrt{\frac{\sum (x - \bar{x})^2}{n - 1}} \dots \text{Equation 3.17} \dots 3.11$$

Chapter 6

$$C_{ij}^* = A_i e^{-\alpha_i \cdot t_{ij}} + B_i e^{-\beta_i \cdot t_{ij}} \dots \text{Equation 6.1} \dots 6.4$$

$$C_{ij} = C_{ij}^* (1 + \varepsilon_{1ij}) + \varepsilon_{2ij} \dots \text{Equation 6.2} \dots 6.4$$

Chapter 7

$C_{ij} = C_{ij}^* \times e^{\varepsilon_{ij}}$ **Equation 7.1** 7.28

$C_{ij} = C_{ij}^* \times e^{\varepsilon_{1ij}} + \varepsilon_{2ij}$ **Equation 7.2** 7.28

Declaration

In accordance with the regulations of the University of Edinburgh, I declare that this thesis has been composed by myself entirely and that the work presented is my own, except where acknowledgement has been indicated in the text.

Samantha Jane Carmichael

March 2001

Acknowledgements

This research was supported by funding from the Imperial Cancer Research Fund (ICRF) and was carried out in the ICRF Medical Oncology Unit, within the Western General Hospital in Edinburgh. Additional support was received from the Department of Medicine & Therapeutics, Western Infirmary, University of Glasgow.

Firstly, I wish to thank Dr Andrew W. Kelman for carrying out the task of writing the computer programs required for the simulations in this thesis (Appendix 2). Without those none of this would have been possible.

I would like to express my gratitude to all the staff within both the ICRF Medical Oncology Unit and the Department of Medicine & Therapeutics, University of Glasgow for their support and kindness over the time I have spent in both places.

Most importantly, I would like to thank my supervisors Dr Andrew W. Kelman and Dr Lilian S. Murray from the Department of Medicine & Therapeutics; and Dr Duncan I. Jodrell from the ICRF Medical Oncology Unit for their constant support, encouragement and advice.

Abstract

Natural variability between individuals results in a fixed dose of drug having different effects in different people. In the case of anticancer agents either an underdose or overdose of drug can be life threatening. Hence, understanding the mechanisms or causes of this variability is essential to optimise therapy, especially for cancer patients.

Since drug induced effects (pharmacodynamics (PD)) can often be linked to the post administration drug concentration (pharmacokinetics, PK), one method of investigating the variability in effect, using a 'population pharmacokinetic study', is to describe causes of variability in drug concentration in terms of demographic or pathological factors. The resultant statistical model may then be used for dose adjustment, and this may have particular importance in specific 'at risk' patient groups, e.g., the elderly, neonates or those with renal or hepatic dysfunction.

The population approach allows the analysis of sparse data sets, in which each individual contributes only a small number of samples, but a large number of subjects is required. The accuracy of the population parameter estimates of the PK model is dependent on various factors of the design of the study. In particular, interest has concentrated on comparing model parameter estimates obtained from designs with different sampling times to study whether there is a set of times which might be regarded as "optimal".

"Optimal sampling strategies" are based upon the concept of 'information-rich' times within a concentration-time profile.

In this thesis, the selection of optimal sampling times was based on sensitivity analysis and applied to the one and two-compartment PK models. Simulation studies were used to show that parameter estimates obtained using an optimal design method with a reduced number of samples were as good as, if not better than, those obtained

from PK studies in which the sampling times were selected empirically. In addition, the effect of adding sampling windows around the “optimal” times offered improved estimation of the inter-subject variability parameters, when compared to designs with fixed sampling times. This result has particular relevance in a clinical setting where a sample may not be collected at the stipulated time, but is still useful in the analysis if the “actual” sampling time is recorded accurately.

Further simulations were based on published sampling designs for the anticancer drug carboplatin, and these were used for comparison with the results when an “optimal design” was used.

Finally, a population analysis was carried out on data from a phase I clinical trial of the broad-spectrum neuropeptide antagonist, Antagonist G. The parameter values were used to design an “optimal” sampling strategy. As the sample times of the optimal strategy were different to those used in the clinical study, further simulations were used to compare the designs.

Using sensitivity analysis to design sampling strategies for population PK studies allowed the selection of a minimum number of sampling times, but still resulted in accurate estimation of the parameters of the one and two-compartment PK models. These sampling times provide a basis for PK study design, around which further samples could be added to improve the identification of the model and also the estimation of parameters and their inter and intra-subject variability.

Chapter 1

1 Optimisation of Study Design in the Pharmacokinetics of Anticancer Drugs.

1.1 Introduction

The treatment of patients with cytotoxic chemotherapy for cancer is becoming increasingly common. Cancer statistics show that two people in five will be diagnosed with some form of the disease at some time in their lives and that cancer is responsible for a quarter of all deaths in the UK. As a result, many organisations are currently investigating new ways of preventing and treating the many types of cancer (CRC 1999; CRC 2000).

In addition to surgery and radiotherapy, a common mode of treatment is with anticancer drugs. The term chemotherapy encompasses several types of drugs with different mechanisms of action. However the common aim of the use of these drugs is to maximise tumour response to the drugs with minimal toxic side effects to the patient. When any drug is administered to a patient, natural variability between individuals means that the same dose can have different effects in different people. The implications specific to anticancer agents are that both an underdose and an overdose of drug can be life threatening (Evans et al. 1989). Hence, understanding the mechanisms or causes of this variability is essential for optimising therapy for cancer patients.

The study of the absorption, distribution and metabolism of a drug after administration is termed pharmacokinetics (PK) and the effect that a drug has on the body is termed the pharmacodynamics (PD). Collection and analysis of pharmacodynamic information allows the interactions between the drug and the target to be quantified in such a way as to describe the full range of action (Gabrielsson et al. 1997). Responses to drugs can be measured in two ways: continuously like blood pressure or heart-rate; or dichotomously, where there is either a response or not, e.g., an epileptic seizure, cancer or death. The response to the drug can be linked to the drug concentration and relationships between

dose/concentration and therapeutic/toxic effects can be established (Gambus 1996; Troconiz 1996). In oncology this has been applied to carboplatin therapy where the *AUC*, as a measure of exposure to the drug is related to the degree of leucocytopenia observed (Kobayashi et al. 1993; Desoize et al. 1994b; Masson et al. 1997; van Warmerdam 1997). However, pharmacodynamic relationships may not be found for all drugs and all cancers (van Warmerdam et al. 1995). One reason for this is that in many cases more than one drug is administered simultaneously (phase III or later) and therefore it is difficult to assign toxicity/response to a particular agent (Evans et al. 1989). Correlations made between drug concentration and effect are especially useful in pre-clinical situations where information from animal studies is extrapolated to humans. Often concentrations achieved are similar, but the doses administered vary hugely (Evans et al. 1989; Danhof 1996).

The investigation into the variability in PK parameters across patients is termed 'population pharmacokinetics (PK)' (Whiting et al. 1986; Aarons 1991) and the aim is to describe the variability in PK parameters in terms of biological factors. A desired outcome is to use these biological factors to modify dosages, particularly in specific 'at risk' patient groups, e.g., the elderly, neonates or those with renal or hepatic dysfunction (Whiting et al. 1986). The regulatory agency in the U.S., the Food and Drug Administration, has encouraged the routine incorporation of population PK studies into the early phases of drug development (Peck et al. 1992; Sun et al. 1999).

The aim of the studies described in this thesis is to investigate the efficiency of different study designs in the estimation of population PK parameters. This is of particular importance in oncology where patients may have a short life expectancy and should not be subjected to lengthy conventional PK studies.

1.2 Pharmacokinetics and Pharmacokinetic Modelling.

Pharmacokinetics

Pharmacokinetics (PK) is the study of drug absorption, distribution, metabolism and elimination. Post-administration, the drug concentration-time profile can be used to develop mathematical models relating the dose administered to the concentrations observed in biological fluids, e.g., blood or urine. Information gained from understanding these relationships can be used in three different ways: description, prediction or explanation (Gabrielsson et al. 1997). The description of the data allows definition of the model parameters. This in turn leads to the predictive use of the model in new situations, e.g., expected concentrations when a new patient receives the drug, given certain biological parameters. Pharmacokinetic modelling can also be used to explain unexpected observations, e.g., when sub-populations that handle the drug differently exist within a population of patients, for instance, patients with hepatic or renal dysfunction (Whiting et al. 1986; Sun et al. 1999).

Pharmacokinetic Models

The most commonly used PK models involve compartmental methods of analysis in which the body can be considered as a series of compartments or spaces into which drugs are administered or distribute. Regression models and curve-fitting techniques are then used to estimate the model parameters and to define the concentration-time profile and the drug transfer between compartments (Gabrielsson et al. 1997). While the compartments are often not identifiable in terms of specific organs of the body, they nevertheless provide a useful tool to suggest information about physiological processes after drug administration (Rescigno 1999). Both Rescigno (1999) and Williams (1990) provide detailed derivation of the parameters used in compartmental analyses.

The common assumption of such models is that first-order processes govern drug transfer, i.e., the rate of change of the amount of drug within the compartment is proportional to the amount present. Clearance (Cl) and volume of distribution (V)

are the pharmacokinetic model parameters used to describe the time-course of drug concentration.

Clearance is a measure of drug elimination and is measured as the volume of fluid cleared per unit time. Total measured clearance is the sum of all modes of elimination of the drug, e.g. hepatic metabolism, renal filtration. In this thesis clearance is measured in litres per hour (l/h).

Volume of distribution relates the amount of drug in the body to the measured concentration. It is a theoretical volume of fluid that the drug would have to equilibrate in to achieve the observed concentration. This is affected by binding to plasma proteins as only the drug in the plasma is measured and not that which distributes into tissues. If a drug is highly protein bound, then most of it will remain in the plasma (giving a high concentration) and it will have a low volume of distribution. Conversely, if a drug is highly tissue bound, then little will remain in plasma, giving low concentrations and a high volume of distribution. In this thesis volume of distribution is measured in litres (l).

The simplest PK model is the one-compartment model, in which the drug is considered to distribute throughout a single compartment after the administration of an IV bolus dose (D) (figure 1.1). In this case, clearance and volume of distribution lead to the definition of another important PK parameter, the elimination rate constant, k_e , which is measured in units of 'per time', e.g., per hour (h^{-1}) which is used in this thesis, and

$$k_e = \frac{Cl}{V} \quad \text{Equation 1.1}$$

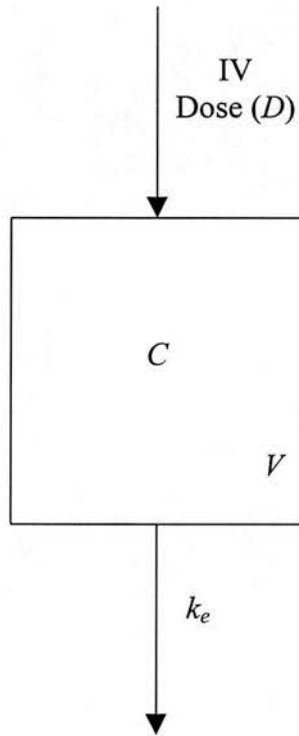


Figure 1.1 One-compartment pharmacokinetic model with IV bolus dose (D), volume of distribution (V) and first-order elimination (k_e). C represents the concentration of drug attained in the body following administration of the dose.

Another useful concept is that of half-life ($t_{1/2}$), i.e., the time taken for the concentration to decrease by 50% of its previous value and

$$t_{1/2} = \frac{0.693}{k_e} \quad \text{Equation 1.2}$$

This is measured in units of time, i.e., hours (h) in this thesis. The parameters Cl and V govern the time-course of drug concentration post-administration and these may be altered in disease states. Indeed, even normal healthy subjects will show variability in these parameters and it is the identification of this variability that is the subject of the study designs investigated in this thesis.

In a one-compartment PK model, the drug concentration in plasma (or compartment) is described by

$$C_t = \frac{D}{V} e^{-k_e t} \quad \text{Equation 1.3}$$

The one-compartment model makes the assumption that the administered drug equilibrates instantaneously between plasma and tissue, but often this is not the case and the distribution into tissue is slower. Additional compartments may be added to the model in order to describe the distribution of drug into peripheral tissues and organs, resulting in the addition of exponential terms to equation 1.3. A two-compartment model consists of a 'central' compartment, into which the drug is administered and a peripheral compartment into which it distributes (figure 1.2). The central compartment may be considered to include blood and all tissues in rapid equilibrium with the blood, and the peripheral compartment the rest of the body. Following drug administration into a two-compartment system, first-order processes may again be used to describe drug transfer between compartments.

Each compartment is associated with a volume of distribution, V_1 and V_2 for the central and peripheral compartments, respectively. Two clearance terms are required for a two-compartment model - the elimination clearance and the inter-compartmental clearance, Q , which describes the transport of drug between the compartments. Elimination from the body is assumed to occur from the central

compartment and the rate constant for this clearance term is represented in figure 1.2 by k_{10} . The inter-compartmental rate constants k_{12} and k_{21} represent the transport from the central to the peripheral compartment and vice versa and are related to Q as follows.

$$k_{12} = \frac{Q}{V_1} \quad \text{Equation 1.4}$$

$$k_{21} = \frac{Q}{V_2} \quad \text{Equation 1.5}$$

Following IV administration, the concentration profile is described by a bi-exponential equation, i.e.,

$$C_t = Ae^{-\alpha t} + Be^{-\beta t} \quad \text{Equation 1.6}$$

where A , α , B and β are the model parameters. The macroscopic rate constants α and β depend on the microscopic rate constants, k_{12} , k_{21} and k_{10} . These relationships and those involving Cl , V_1 , V_2 and Q are defined in Appendix 1.

In this thesis, this model will be parameterised using Cl , V_1 , V_2 and Q .

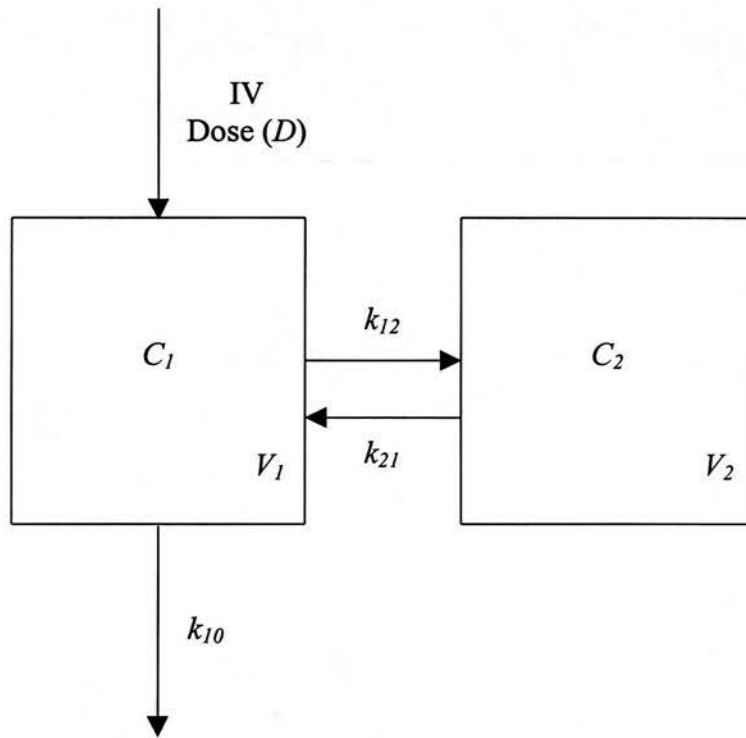


Figure 1.2 Two-compartment pharmacokinetic model with IV bolus dose (D), inter-compartmental transfer (k_{12} & k_{21}), volume of distribution of the central (V_1) and peripheral (V_2) compartments and first-order elimination (k_{10}). C_1 and C_2 represent the concentration of drug attained in the central and peripheral compartments, respectively, following administration of the dose.

Physiologically-Based Pharmacokinetic Models

More complicated multi-compartment PK models involve considering specific organs or tissues connected by the arterial and venous blood flow network, e.g., liver, brain, muscle and fat. These are known as physiologically-based PK (PBPK) models and use physiological values of blood flow rates and tissue weights coupled with blood and tissue/gas partition coefficients to describe the pharmacokinetics of compounds - often in a toxicological setting (Clewell et al. 1994; Spear et al. 1994; Nestorov et al. 1997). This allows the description of the PK of a compound within different species, by altering the values of the physico-chemical constants.

Classical Pharmacokinetic Studies

During Phase I of drug development the aim is generally to investigate the tolerability of new drugs administered within a controlled environment. These studies are generally carried out using healthy volunteers and involve the collection of 10-15 blood samples from a small number of subjects after administration of the drug. This allows the PK parameters for each individual to be estimated with reasonable accuracy, using regression methods and is sometimes termed the 'individual approach' (Bellissant et al. 1998). As each individual is inherently different, the pharmacokinetic parameter values will vary within the group. Therefore, in order to describe the population, estimates of the variability within the population are required in addition to estimates of mean PK parameter values.

The 'standard 2-stage' method is often used to analyse data from classical PK studies, where firstly each individual's PK parameters are estimated by regression methods. The second stage involves calculating the mean values of the parameters within the population and also estimates of their variability (Sheiner 1984). This method may result in different subjects being described by different PK models (one or two-compartment) due to limits of quantification in the chemical analysis of the data (Vozech et al. 1996). Another limitation of this type of study is the assumption that the parameter estimates for each individual are the true values for that subject,

and this leads to overestimation of the variability within the population. In addition, effects of covariates cannot be included in the model.

The field of oncology is quite different from other areas of developmental therapeutics in that anticancer drugs cannot be administered to healthy volunteers and Phase I studies rely upon patients who have exhausted all conventional treatment for their disease. In some ways this could be considered an advantage in that the data is collected from the 'target population' who would receive the drug from the start, rather than waiting until a Phase II clinical trial for the first administration to patients.

Population Pharmacokinetic Studies

The population approach to pharmacokinetic studies considers the whole population as the unit of analysis and not each individual subject (Whiting et al. 1986; Aarons 1991; Sun et al. 1999). This method utilises information from previous PK studies and the analysis of sparse data sets, in which each individual contributes only a small number of samples. In this situation it would be difficult to identify the PK model accurately using the individual approach, but in the population setting each individual is treated as a random sample from a larger population. Hence, large numbers of subjects are required and the accuracy of the population estimates obtained has a greater dependency on the number of subjects than the number of samples per subject (Vozech et al. 1996; Samara et al. 1997). Another difference between population and classical PK studies is that all data is analysed simultaneously, using the same PK model (Vozech et al. 1996; Bellissant et al. 1998). 'Rich' data sets from classical PK studies can also be analysed using population methods, to ensure that all individuals are described by the same PK model.

The program most commonly used for population PK data analysis is NONMEM which employs the statistical method of non-linear mixed effect regression modelling (Boeckman et al. 1992; Kobayashi et al. 1993; Samara et al. 1997; Beal et al. 1998). The mixed effect model allows estimation of both fixed effects (e.g., the model

parameters like Cl and V) and random effects (e.g., the variability between subjects) simultaneously. The equations of the statistical models are intractable and must be solved using iterative methods based on the maximum likelihood principle for the parameter estimates. A Bayesian estimation algorithm may also be combined with the maximum likelihood estimation methods within NONMEM in order to calculate individual pharmacokinetic parameters for each subject. The NONMEM algorithms used in this thesis are described in section 2.3.1.

The population approach to PK estimation can be used at all stages in drug development, although in Phase I studies the classical approach is generally used. These represent the first administration of new drugs to humans (Vozech et al. 1996; Samara et al. 1997). Certain situations exist in which population studies may be implemented at the Phase I stage e.g., the study of anti-cancer drugs, although even in this case a certain number of patients will require full PK profiles to be collected. In particular, special Phase I studies may be carried out in the elderly and ‘at risk’ groups with impaired physiological function, where supporting data exist from previous classical PK studies (Samara et al. 1997).

Phases II and III of drug development tend to recruit large numbers of patients in order to confirm therapeutic efficacy of the new drug or to compare it to a similar marketed competitor, not to explore pharmacokinetic details (Aarons et al. 1996). However, if PK samples can be incorporated in an existing protocol, there may be a significant amount of information to be gained in this clinical setting. Other factors (covariates, e.g., demographics, physiological factors) which affect the pharmacokinetic behaviour of the drug can be investigated and these may aid in explaining the variability in the PK parameters (Levy 1998). This may identify patient subgroups who may require specific dose adjustment (Samara et al 1997) and also whether therapeutic drug monitoring (TDM) may be required for the drug. Clinically, not all drugs or all anti-cancer drugs require pharmacokinetic monitoring, but those which have been identified from initial PK experiments as having steep concentration-effect curves or a large degree of PK variability will benefit (Vozech et

al. 1996). This will apply particularly when risk factors requiring dose modification are difficult to identify.

1.3 Population PK Study Design

A major issue in the design of population PK studies is the selection of the sampling times. The number of samples per subject is often sparse and times may exist which result in more accurate estimates of the PK parameters than others (D'Argenio et al. 1983). In addition, accurate dosing and sampling histories must be obtained as inaccurate recording leads to unreliable parameter estimates (Sheiner 1984; Sun et al. 1996). Jia et al (1996) showed in a limited population study using simulated data in which the times were subject to error, that if the population model assumed no error, then there was little effect on the estimates of the fixed effects. However, the estimation of the random effects was erratic, i.e. biased and imprecise. If the time error was included in the analysis the estimates of the error in sample timing were poor.

Equally important for the performance of population PK studies is the handling of the samples once they are acquired. Hence, the necessity to incorporate the PK protocols conveniently into the existing clinical trial protocols, in terms of the clinical and nursing staff taking the samples and taking into account that the principal objective of the study is not the PK analysis (Aarons et al. 1996; Hon et al. 1998).

Several methods exist with which to select the sampling times for population PK studies.

Limited Sampling Strategies

The term 'limited sampling strategies' has been used to refer to methods in which PK parameters are estimated from a reduced number of samples compared to classical PK studies. The reduced number of samples per subject may allow large-scale population PK studies to be undertaken, where cost of the analysis of samples has been an issue. Other study 'costs' that may be reduced are out-of-hours staffing to collect samples and overnight stays in hospitals.

The most common method used to develop a limited sampling strategy is that of forward stepwise multiple regression. This enables the estimation of a single PK parameter from only 2-3 samples. In order to validate the limited sampling strategy designed with the regression approach, the total number of concentration-time profiles are split into two data sets - the training and validation sets. The training set is used to develop the model, which is then tested using the validation data set.

The collection of full concentration-time profiles in a number of patients is initially required, in order to determine parameter estimates for comparison with those estimated with the limited sampling strategy (van Warmerdam et al. 1994b). A regression analysis is then carried out using all of the concentrations obtained from the initial study, and the time point giving the highest correlation with the pharmacokinetic parameter of interest, e.g., *AUC*, is identified. Thus a linear relationship of the form:

$$AUC = k \cdot C_{t(best)} + b \quad \text{Equation 1.7}$$

is obtained, where *k* and *b* are constants representing the slope of the linear regression and intercept, respectively. $C_{t(best)}$ is the concentration measured at the time with the highest correlation for estimating *AUC*.

For a three-sample strategy, the next two best time points will be entered in a stepwise manner to improve the performance of the model. However, it has been shown that the single time-point which best predicts the pharmacokinetic parameter does not necessarily produce the best limited sampling model when included in a three-point model (Jodrell et al. 1996). For this reason, all subsets regression seems more appropriate, where the limited sampling model will include the group of three times that best predict the parameter. Sallas (1995) used this method to examine limited sampling strategies of 1-3 samples for data collected in a 4-way crossover trial of two formulations of cyclosporin G. In order to resemble an outpatient setting, the effect of limiting the samples to fall within 4 hours postdose was examined (the half-life of the drug was 5 hr). When time constraints were introduced the tendency was for imprecision and bias to increase, although not to unacceptable levels. The

sampling schedules with three samples offered improved parameter estimation over the schedules with one or two samples.

Limited sampling models designed using regression analysis can only be used for dose regimens which are an exact copy of the original (van Warmerdam et al. 1994b). Errors in the timing of the samples will give different concentrations to those the limited sampling strategy was developed from and hence, errors in the estimated parameter. However, the relevance of sampling time errors, will also depend upon which part of the concentration-time curve the sample occurs, i.e., a dependency on distribution or elimination half-life. If an early sample, which should be taken during a short half-life distribution phase, is taken wrongly, then this may cause greater estimation error in the parameter than a sample taken at a slightly different time during the longer half-life elimination phase (van Warmerdam et al. 1994b). Patients with variable pharmacokinetics require the limited sampling strategy to be validated in their population.

Most limited sampling strategies developed using anticancer drugs use the method of forward stepwise regression (table 1.1). This is most common as it is a quick and easy method which does not require that the PK model is defined with initial estimates of parameter variance (van Warmerdam 1997).

Table 1.1 Limited sampling strategies for anticancer drugs, designed using the regression approach.

Anticancer Drug	Reference
5-Fluorouracil	(Moore et al. 1993)
Amonafide	(Ratain et al. 1987; Ratain et al. 1988)
Busulphan	(Hassan et al. 1996).
Carboplatin	(van Warmerdam et al. 1994a; Ghazal-Aswad et al. 1996; van Warmerdam et al. 1996b)
Cladribine	(Liliemark et al. 1996)
Cyclophosphamide	(Egorin et al. 1989)
Docetaxel	(Lustig et al. 1997)
Doxorubicin	(Ratain et al. 1991)
Etoposide	(Gentili et al. 1993; Holz et al. 1995; Sessa et al. 1995; Lum et al. 1997)
Irinotecan and it's active metabolite SN38	(Chabot 1995; Mick et al. 1996; Mathijssen et al. 1999)
Paclitaxel	(Huizing et al. 1995)
Topotecan	(Minami et al. 1996; van Warmerdam et al. 1996a)
Vinblastine	(Ratain et al. 1987)

A second method of selecting sampling times for a limited sampling strategy is to use the trapezoidal method for calculation of *AUC* (Sallas 1995; Duffull et al. 1999). The trapezoidal rule is a method of calculating the *AUC* by summing the areas of the trapezoids between each of the sampling times (figure 1.3) (Gabrielsson et al. 1997).

Limited sampling strategies were chosen by empirically selecting a predefined number of sampling times which give a calculated *AUC* close to that provided from the full data set, when the trapezoidal rule is used. Sallas (1995) combined the linear with the log-linear method and showed that this gave results with comparable accuracy to those obtained when a regression-type limited sampling strategy was used on the cyclosporin G data described previously. Again, the time constraint of sampling within 4 hours was used in this study and did not result in differences in imprecision and bias of the PK estimates.

Duffull et al (1999) used a method where the *AUC* was split into a predefined number of equally sized trapezoids and the sampling times selected accordingly. Various numbers of replicate samples were investigated and a combination of four samples with three replicates was shown have similar accuracy to the conventional sampling schedule of twelve samples. This method would also provide flexibility in a clinical setting in that patients would have a larger volume of blood taken, but at fewer times than during a classical sampling schedule. The blood sample would be split into the required number of replicates and reduce errors induced by assay variability.

However, the use of the trapezoidal rule to define sampling times resulted in designs that had fixed sampling times for all patients, similar to the regression-type designs and again, only one PK parameter was being estimated. Similarly, these designs cannot be extrapolated to drugs with pharmacokinetic models or administration schedules different to that which was used to develop the model.

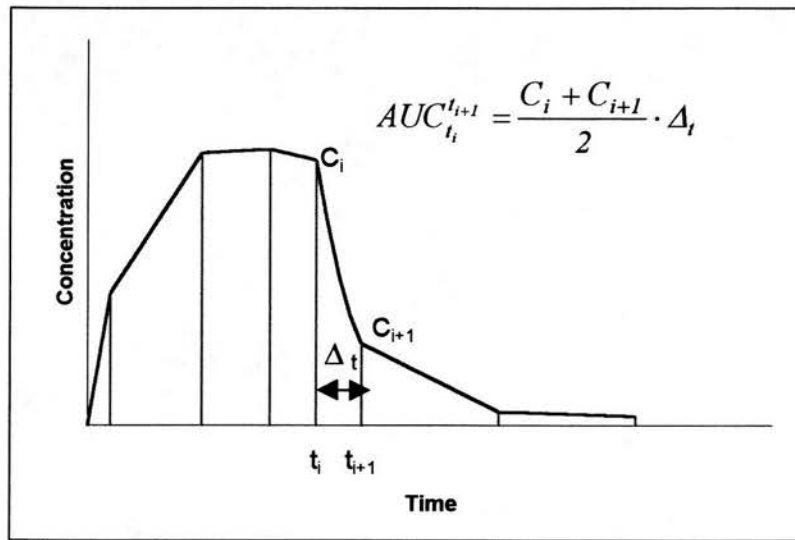


Figure 1.3 Representation of the linear trapezoidal rule. $AUC_{t_i}^{t_{i+1}}$ is the area between t_i and t_{i+1} . C_i and C_{i+1} are the corresponding concentration measurements and Δ_t is the time interval (Gabrielsson et al. 1997).

Due to the restriction of sampling all subjects at the same fixed times when limited sampling strategies are designed using the previous approach, other authors have investigated limited sampling strategies where the sampling times varied for different individuals. In these simulation studies the data were analysed using the population approaches within the NONMEM program, allowing estimates of all PK parameters to be obtained simultaneously. The sampling times were selected either 'empirically' across the minimum and maximum times that the study would be carried out (Al-Banna et al. 1990), or within time windows, that mimicked outpatient clinic times (Jonsson et al. 1996). In addition, both of these studies investigated the number of samples required to give the most precise parameter estimates.

Al Banna et al (1990) used simulated data and initially considered that if a minimum of two samples were to be taken that one sample should be as early as possible and the other should be as late as possible, i.e., at the times of maximal and minimal response respectively. First, the early sample was fixed and the late sample varied at two-hour intervals. Secondly, the effect of adding a third sample to the existing two was examined where the early and late times were fixed and the third point was inserted between them. The results showed that fixed effects were accurately estimated with 2-3 points, but random effects were poorly estimated with two points and adding the third improved precision and bias. Varying the sampling times in the two-sample model showed benefits for different parameter estimates at different times. However, the addition of the third sample improved all parameter estimates, regardless of the timing.

The effect of fixing the number of samples within a study, to mimic a cost constraint, was also evaluated by varying the number of samples per patient. Studies using different number of patients were compared using:

$$50 \text{ patients} \times 2 \text{ points} = 100 \text{ samples}$$

$$33 \text{ patients} \times 3 \text{ points} = 99 \text{ samples}$$

Reducing the number of samples per patient, but increasing the number of patients was shown to reduce bias and imprecision of parameters.

In addition to specifying the time window in which samples could randomly be taken, Jonsson et al (1996) also compared the numbers of samples required to identify a pharmacokinetic model, by the use of both simulated and clinical data. The simulated data examined the effect of drug half-life ($t_{1/2}$) on the precision of the parameter estimates, by the use of both a short (6 hr) and a long (12 hr) $t_{1/2}$. The times of the samples were restricted to the times of outpatient clinics which meant that sampling could only take place between 10am-12pm and 2-4pm. Some patients had only one sample taken either in the morning or afternoon. Others had two samples taken on two separate occasions in the combinations of morning-morning, afternoon-afternoon, morning-afternoon or afternoon-morning. This showed that two samples were better than one for identifying the PK model and estimating the parameters. In addition, of the patients who had two samples taken, having one early and one late improved the estimates of the variability of the parameters compared to having two early or two late. Improved precision was noted for the estimation of the volume of distribution parameter when the $t_{1/2}$ was shorter as more information was gained about the fall in concentration within the restricted sampling window.

These examples showed that increasing the amount of data per subject improved parameter estimates, i.e., two samples were better than one sample (Jonsson et al. 1996) and three samples were better than two samples (Al-Banna et al. 1990). When the number of samples was 2-3, and a restriction was placed on the total number of samples which could be taken, then increasing the number of subjects (and reducing the number of samples per subject) was more efficient than increasing the number of samples per subject. However, if the number of samples was 1-2, then it was more beneficial to increase the number of samples to two in some subjects and reduce the number of patients.

It was also shown that using population methods to analyse sparse data instead of mathematical equations allowed flexibility in sampling within a clinical setting, so fulfilling the aspect of incorporating population PK studies conveniently within other clinical visits.

Optimal Sampling Strategies

The collection of sparse data in population PK studies has raised questions as to the reliability of model parameter estimates obtained from various sampling schedules. 'Optimal' sampling strategies are based upon the concept of 'information-rich' times within a concentration-time profile which may offer improved parameter estimates over other sampling times. In order to construct an optimal sampling schedule the pharmacokinetic model must be known, along with the 'true' values of the parameters and information about the residual error models (van Warmerdam et al. 1994b; Jacquez 1998).

The most frequently used design criterion for selecting optimal sampling times is D-optimality (Box et al. 1959). D-optimality uses the population mean values of the parameters to minimise the determinant of the inverse of Fisher Information Matrix, which effectively selects sampling times when concentration variance is maximal with respect to the PK parameters. The D-optimality design criterion does not incorporate information about the PK parameter variance. Although design criteria that incorporate prior parameter uncertainty into their sampling designs would be expected to provide more robust parameter estimates, it has been shown that designs based on D-optimality perform equally well in terms of bias and precision. The designs incorporating information about parameter uncertainty tend to be similar to the D-optimal designs, but that may be a factor of the population sizes and amount of variability in the parameters in studies so far (Hashimoto et al. 1991; Mentré et al. 1995a; Tod et al. 1998). Tod et al (Tod et al. 1998) demonstrated that the EID criterion gave similar sampling times to those defined with D-optimality when the variability on the parameters was low, but when it was higher the sampling times shifted to a later time. The EID criterion minimises the **E**xpectation of the **I**nverse of the **D**eterminant of the Fisher information matrix over an accepted range of parameters.

Another question raised within the limited-sampling scenario is whether sampling times should be fixed for all individuals. Random sampling around the optimal sampling times defined by D-optimality was shown to improve the precision and

accuracy of the parameter estimates in two simulation studies. However, sampling around non-optimal times gave inferior parameter estimates (Hashimoto et al. 1991; Mentré et al. 1995a).

For a one-compartment PK model, a two sample design derived from D-optimality would give the first sampling time to be the earliest possible and the second as the first time plus $1.44 * t_{1/2}$, for an additive intra-subject random-error model. For a proportional intra-subject random-error model the second time would be the latest time possible (Endrenyi 1981). Within a Bayesian context, the variance on the parameters has also been shown to affect the optimal times within a population, with high variances giving times that were different to those obtained at lower variance and lower variances giving the expected D-optimal times (Merlé et al. 1995).

Optimal sampling strategies are often coupled to either Bayesian or sequential/adaptive techniques to improve their robustness to errors in parameter estimates and actual timing of samples. A Bayesian design involves the sequential updating of the population parameters with each new patient's data until the estimates are stable (Thomson et al. 1992; van Warmerdam et al. 1994b). Sequential/adaptive study designs use the previous patients' data to update the population parameter estimates and derive the optimal times to sample the next patient (D'Argenio 1981; Drusano et al. 1988). These times have been shown to settle into stable sampling schedules with both simulated (D'Argenio 1981) and clinical (Drusano et al. 1988) data. However, initially each patient may have different sampling times.

The examples in the studies by D'Argenio and Drusano show that using optimal sampling times to estimate pharmacokinetic parameters produced parameter estimates that were as accurate, if not better than those produced using full, conventional sampling protocols.

An important property of optimal sampling is that replicate times are often suggested, e.g., four optimal sampling times might result in two samples taken at two

different times (D'Argenio et al. 1997). This arises due to the assumption that the only experimental error is due to assay error, which of course is unrealistic in biological systems where inter-patient variability is also a factor (D'Argenio 1981).

The major restriction in the implementation of optimal sampling versus the limited sampling strategies described previously is that the pharmacokinetic model requires to be defined before selection of sampling times can occur (Drusano et al. 1988; van Warmerdam et al. 1994b; Sallas 1995). Errors in the definition of the model will lead to sub-optimal times being selected and inferior parameter estimates. However, sampling strategies designed around 'optimal' times are more robust than those based on empirical or regression methods. In addition, extrapolation to other dosing schedules is possible as it is the PK model which is important in the selection of the times.

Optimal sampling theory has been applied to a lesser extent than the regression methods, in the development of limited sampling strategies in oncology. The drugs analysed in this way include carboplatin (Peng et al. 1995), cisplatin (Desoize et al. 1994a), docetaxel (Baille et al. 1997) irinotecan (Nakashima et al. 1995) and EO9 (McLeod et al. 1996). The sampling times from these experiments are also coupled to Bayesian techniques to provide robust sampling strategies. This in turn permits sampling at sub-optimal times to give accurate parameter estimates, i.e., allowing for errors in the timing of samples that may occur in a clinical setting.

1.4 Dose Adaptation for Anticancer Chemotherapy Using Pharmacokinetics

Currently, doses of anticancer drugs are individualised for each patient on the basis of body surface area (BSA). This method was adopted after it was shown that the use of BSA was a simple method of scaling doses between neonates and adults and also between different animal species (Rosenthal 1988; Desoize et al. 1994b). In general, this method assumes that the efficiency of the organs of elimination (e.g., liver, kidney) is correlated better with BSA than body weight, i.e., larger people require larger doses to produce the same effect. However, total body clearance has only been partially correlated to BSA (van Warmerdam 1997) and hence other methods of dose-individualisation for oncology patients are required. There are various possibilities for adapting doses of anticancer drug for individual patients in order to optimise treatment (Desoize et al. 1994b).

- Adaptation depending on physiological functions.

Hepatic and renal function can easily be tested from standard blood tests. As one or the other of these routes primarily eliminates most drugs, this will aid in preventing the induction of toxicity by accumulation of drug. In addition, the doses of pro-drugs and liver enzyme inducing drugs can be modified according to the patient's ability to metabolise, e.g., cyclophosphamide and epirubicin. The dose of carboplatin is routinely modified based on renal function and is described later.

- Adaptation depending on intratumoural drug concentration.

The testing of intratumoural drug concentrations is difficult for both ethical and practical reasons, as tumours are rarely readily accessible. In addition, the blood flow into tumours is usually poor compared to areas like the bone marrow where most toxicity occurs. Therefore even if it were simple to check, drug levels in the tumour it would not necessarily be appropriate for measuring toxicity. However, recent advances have allowed non-invasive monitoring of tumour uptake of certain drugs, using the technique of magnetic resonance spectroscopy (MRS) and the closely related technique of magnetic resonance imaging (MRI) (Griffiths et al.

2000). Chemicals present within the body can be detected, identified and quantified by the inclusion of certain isotopes or radiolabelled isotopes in the drug molecule. Both 5-fluorouracil and ifosfamide have been monitored at clinical concentrations in both animals and humans using this method.

- Adaptation depending on toxicity.

Since the philosophy in chemotherapy is to administer the highest dose tolerable to the patient, consideration also has to be given to methods of maximising the dose given to an individual. The experience of mild toxicity is used as a marker of the dose (Evans et al. 1989). If a patient experiences no toxicity, then the dose may also not be adequate for a clinical effect on the tumour and may be increased (Newell 1994).

The reduction in blood cell counts is the pharmacodynamic effect of anticancer therapy most often correlated to a PK parameter. This can take the form of monitoring the absolute granulocyte or platelet nadir or monitoring the percentage reduction from baseline. Reduced clearance of carboplatin has been associated with a higher degree of thrombocytopenia and mathematical equations have been derived to calculate an individualised dose to give a desired platelet nadir (Egorin et al. 1985).

- Adaptation depending on plasma drug concentration.

Evaluating the plasma levels of a drug is the simplest method as plasma is a readily accessible fluid. When accompanied by hepatic and renal function tests, information on elimination is gained for incorporation into a pharmacokinetic model for specific patient sub-groups.

Four requisites must be fulfilled in order to make pharmacokinetic monitoring appropriate in clinical practice (Masson et al. 1997):

- narrow therapeutic index
- a large degree of inter-patient variability

- difficult monitoring of therapeutic/toxic effects, otherwise dose could easily be adjusted on the basis of pharmacological effect, e.g., blood pressure
- existence of a relationship between the pharmacokinetics and the pharmacodynamics.

Thus, it is clear from these definitions that identification of PK parameters and definition of pre-determined target concentrations for anticancer drugs could improve the use of both new and existing chemotherapeutic agents (van Warmerdam 1997). However, routine PK monitoring in oncology is limited to only one drug – methotrexate due to the lack of evidence of improved outcomes (Moore et al. 1987).

Methotrexate is active against a variety of tumour types and is routinely used in combination chemotherapy regimens. Relationships have been established between increased methotrexate clearance and relapse of leukaemic children. In addition it has also been shown that remission rates were higher in children who had a steady-state plasma concentration greater than $16\mu\text{M}$ (Newell 1989). These observations have led to the use of very high doses in the treatment of childhood acute lymphoblastic leukaemia (increases from $25\text{mg}/\text{m}^2$ to $33\text{g}/\text{m}^2$) which have improved the treatment outcome of this disease (Masson et al. 1997). The gastrointestinal mucosa are particularly sensitive to methotrexate and mucositis is one of the main side effects of methotrexate therapy, in addition to myelosuppression. Regimens that produce mucositis do not always cause myelosuppression and a link to prolonged low levels of drug has also been recognised (Dollery 1999).

The availability of an antidote to methotrexate toxicity (folinic acid/leucovorin) has aided the introduction of high-dose regimens and the plasma drug levels of methotrexate are monitored to predict toxicity. The dose of folinic acid rescue therapy is then adjusted accordingly, rather than the dose of methotrexate (Newell 1989). When methotrexate is being administered, consideration should also be given to drug interactions that can increase plasma levels of methotrexate, e.g., NSAIDs and other drugs that inhibit the renal excretion (Loadman et al. 1994).

Although pharmacokinetic monitoring is not routine in oncology, several alternative methods of achieving optimal doses of anticancer drugs have been investigated (Newell 1994; van Warmerdam et al. 1995; Masson et al. 1997; Canal et al. 1998).

***A priori* dose adjustment.**

Pre-treatment patient characteristics are useful for making dose adjustments for drugs for which relationships have been established between the pharmacokinetics or pharmacodynamics and a physiological function (Canal et al. 1998). Commonly this refers to liver and renal function, but disease states and demographic variables can also be involved. Dose reductions based on hepatic data are generally empirical as serum levels of hepatic enzymes and bilirubin are not good indicators of the actual metabolic capacity (Koren et al. 1992; Donelli et al. 1998).

Dose modifications of anti-cancer drugs based on renal function are well-documented (Kintzel et al. 1995). The most common example of an anticancer drug which is dose-adjusted on the basis of renal function is carboplatin where large inter-patient variability in toxicity arises due to variations in individuals' renal function. Both toxicity and response to carboplatin have been correlated with the pharmacokinetics, and dose modifications have been made to attain a desired level of thrombocytopenia or drug exposure as measured by *AUC* (Egorin et al. 1985; Jodrell et al. 1992).

Calvert et al (1989) demonstrated that carboplatin *AUC* could be determined by the pre-treatment renal function, and optimisation of the target *AUC* has reduced the incidence of life-threatening thrombocytopenia. Carboplatin is now routinely administered using a dosing formula to attain a desired *AUC* based on renal function (*GFR*) rather than on a mg/m^2 basis (Calvert 1989). The formula for calculating the dose was originally based on a formal creatinine clearance being measured using $^{51}\text{Cr-EDTA}$, but in clinical practice the Cockcroft and Gault formula is often used to calculate it from serum creatinine levels (Cockcroft et al. 1976). This routinely leads to potential under estimation of the *GFR* and hence the carboplatin dose. A second

formula is becoming more regularly used in which the actual carboplatin clearance (Cl_{Carbo}) is calculated (Chatelut et al. 1995) based on the serum creatinine measurement, removing the need for formal dynamic measurement of renal function.

- Calvert Formula (Calvert et al. 1989).

$$Dose(mg) = AUC * (GFR + 25)$$

where GFR is measured by ^{51}Cr -EDTA.

- Chatelut Formula (Chatelut et al. 1995).

$$Cl_{Carbo}(ml/min) = 0.134 * wt(kg) + \frac{218 * wt(kg) * (1 - 0.00457 * age(years)) * (1 - (0.314 * C))}{Cr(\mu M)}$$

where $C=1$ for females and 0 for males. The dose is then calculated from:

$$Dose(mg) = AUC * Cl_{Carbo}.$$

***A posteriori* dose adjustment.**

Dose adjustment based on individual PK assessment after repeated or continuous dosing is a method of achieving a desired AUC for subsequent cycles of treatment or steady state concentration (C_{SS}) during continuous infusion (Canal et al. 1998).

The technique of adaptive control with feedback utilises patient characteristics and information from population pharmacokinetic studies to determine an initial 'test' dose. Blood samples are taken during treatment and the patient-specific PK characteristics are determined. Comparison of these to the population estimates used to determine the initial dose allows dose modifications to be calculated to attain predefined targets. This method was examined for the drug suramin, which was associated with neurotoxicity at plasma concentrations greater than 300-350 $\mu g/ml$ (Scher et al. 1992; Jodrell et al. 1994; Eisenberger et al. 1995).

1.5 Aims of Thesis.

There is extensive literature on the pharmacokinetics and pharmacodynamics of both new and existing anticancer drugs. It is also clear that the use of such drugs may be improved by pharmacokinetic monitoring, given their narrow therapeutic indices and the serious consequences of both toxicity and therapeutic failure. However, before adaptive dosing techniques become routine in oncology, significant advantages will have to be demonstrated in terms of cost-benefit and therapeutic outcomes. This will require the collection of prospective data using pharmacokinetic-pharmacodynamic monitoring approaches.

The aim of the work described in this thesis was to investigate several aspects of PK study design which might be important in the field of oncology. Specifically, the techniques used to generate and analyse data and also to judge model performance are described in chapter 2. Ultimately, this work was carried with a view to the development of a tool which may be useful clinically, i.e., the selection of a limited number of PK samples per patient may allow adaptive dosing techniques to be undertaken more frequently.

In chapter 3, the concept of optimal sampling times is developed for both a one and two-compartment system.

Chapter 4 reports on a comparison of an 'optimal' design with an alternative design in the one-compartment case. In addition, two of the NONMEM algorithms were compared as to which would provide the least biased and imprecise parameter estimates for sparse data analysis.

The effect of using sampling windows based around 'optimal' sampling times is investigated in chapter 5 and the results when additional samples are added to the minimum number specified for a one-compartment PK model are also presented. These effects are examined for the two-compartment case in chapter 6, where an 'optimal' sampling strategy is compared to an empirical design.

In chapter 7, published data on carboplatin and data obtained from a phase I clinical trial of the novel anticancer drug, Antagonist G (a broad spectrum neuropeptide antagonist), are used as examples for the design strategies developed in the previous chapters.

Finally chapter 8 summarises the work undertaken and places it in perspective for application in oncology.

Chapter 2

2 Methods

2.1 Introduction

Pharmacokinetic data analysis allows the definition of models and estimation of parameters which relate administered drug dose to the concentrations achieved. These models can then be used to make predictions for new subjects (Gabrielsson et al. 1997).

Examination of concentration-time data from a small group of healthy volunteers would not give PK parameter estimates representative of the large group of patients likely to receive the drug and hence the population approach to pharmacokinetics was developed (Whiting et al. 1986; Aarons 1991). This sampling approach involves large numbers of individuals, each of whom donate a small number of samples. Usually these individuals are patients rather than healthy volunteers.

As estimates of the variability of the PK parameters within the population are also required in order to describe the population the use of large numbers of subjects in the population approach allows more accurate characterisation of the population than the small number of subjects used in classical PK studies. Definition of (and assumptions about) the distribution of the PK parameters within the population of subjects is important in both the analysis of the data and also in the use of any results for making predictions about new subjects. Several computer programs used to analyse PK data make the assumption that the PK parameter has a Normal or Lognormal distribution within the population (Samara et al. 1997; Bellissant et al. 1998). In this thesis all parameter distributions were assumed to be Normal.

In order to obtain the best possible estimates of the parameters from the sparse data obtained using the population PK approach, the dosing history and sampling times have to be accurately recorded. In addition, the sparse nature of the data means that some thought should be given to the design of the study before it takes place. For example, how many samples to take per subject and more specifically when to take them. Times may exist where information about parameters is maximal, leading to a

so-called 'optimal' design. Optimal sampling techniques of selecting sampling times have been described in Chapter 1.

This thesis examines the effects of different study designs in which the sampling times were selected according to maxima in the expected concentration variance in the population (see chapter 3). Several study designs were investigated involving different sampling schedules and the ability to estimate the mean population PK parameter distributions was examined (Chapters 4,5, 6, and 7).

The methods used to simulate the populations, estimate the PK parameters and summarise the results are described in this chapter.

2.2 Data Simulation

Concentration-time data were simulated by

- (a) Generating individual PK parameters (Cl , V , etc) using a random number generator.
- (b) Calculating the expected concentration at each time point based on the above parameters for the individual.
- (c) Calculating an observed concentration by the addition of random error to the expected concentration at each observation time.
- (d) Repeating steps (a) to (c) for each subject sampled from the population.

The number of individuals, PK models and the sampling schedules are described later in this thesis (chapters 4, 5, 6 and 7).

2.2.1 Parameter Distributions

In this thesis, each PK parameter was sampled from a Normally distributed population, with a mean value of $\bar{\theta}$ and standard deviation of ω_{θ} .

Thus, an individual PK parameter could be written as:

$$\theta_i = \bar{\theta} + \eta_i^{\theta} \quad \text{Equation 2.1}$$

where η_i^{θ} was the random individual deviation of θ_i from the population mean value $\bar{\theta}$ for the i th individual. These individual deviations, η_i^{θ} , were Normally distributed with mean of zero and standard deviation equal to ω_{θ} .

If a negative PK parameter resulted from the simulation then the simulation was repeated until a positive value was obtained. This procedure did not significantly skew the distributions even where the variability in the parameter was high. This can be attributed to the fact that the only parameter examined with a variability of greater than 10% CV was clearance and the mean value was generally 10 l/h. Hence, in a

Normal distribution the 95% prediction interval was 0.2 to 19.8 l/h for 50% variability and less than 2.5% of the data would be expected to be negative.

2.2.2 Pharmacokinetic Models

2.2.2.1 One-Compartment Model

For the one-compartment IV bolus PK model the individual pharmacokinetic parameters clearance (Cl_i) and volume of distribution (V_i) were sampled from Normally distributed populations with population mean values of \overline{Cl} and \overline{V} , respectively. The standard deviations of clearance and volume of distribution were ω_{Cl} and ω_V , respectively and it was assumed that there was no covariance between Cl and V .

Concentration-time profiles for a one-compartment model were calculated from:

$$C_{ij}^* = \frac{D}{V_i} \cdot e^{-\frac{Cl_i}{V_i} \cdot t_{ij}} \quad \text{Equation 2.2}$$

where C_{ij}^* was the expected drug concentration for the i th individual measured at the j th time, t_{ij} , following a single IV bolus dose, D .

2.2.2.2 Two-Compartment Model

The two-compartment model was parameterised in terms of clearance (Cl), volume of distribution of the central compartment (V_1), volume of distribution of the peripheral compartment (V_2) and the inter-compartmental clearance (Q). The relationships between these parameters and those used to simulate the concentration-time profiles are given in Appendix 1. The data for a two-compartment IV bolus PK model were calculated from:

$$C_{ij}^* = A_i e^{-\alpha_i t_{ij}} + B_i e^{-\beta_i t_{ij}} \quad \text{Equation 2.3}$$

where C_{ij}^* was the expected drug concentration for the i th individual measured at the j th time following a single IV bolus dose. A_i and B_i were constants, α_i , and β_i were the macro rate constants of the i th individual, and t_{ij} was the corresponding sample time.

The equation for simulating the concentration-time profiles for a two-compartment IV infusion model was:

$$C_{ij}^* = A_i \left(e^{\alpha_i T_{ij}} - 1 \right) e^{-\alpha_i t_{ij}} + B_i \left(e^{\beta_i T_{ij}} - 1 \right) e^{-\beta_i t_{ij}} \quad \text{Equation 2.4}$$

T_{ij} was equal to t_{ij} until the end of infusion, after which it was equal to the infusion time.

For individual subjects Cl_i , V_{1i} , V_{2i} and Q_i were sampled from Normally distributed populations with means \overline{Cl} , \overline{V}_1 , \overline{V}_2 , \overline{Q} and standard deviations ω_{Cl} , ω_{V_1} , ω_{V_2} , ω_Q , respectively. Again, it was assumed that there was no covariance between Cl , V_1 , V_2 and Q .

2.2.3 Random Error on Concentration

In reality all measured concentrations incorporate a small random error and to mimic this, each simulated concentration was subject to the addition of a random error.

Thus, if C_{ij}^* is the expected concentration simulated according to Equations 2.2 – 2.4, then the observed concentration C_{ij} is obtained from:

$$C_{ij} = C_{ij}^* + \varepsilon_{ij} \quad \text{Equation 2.5}$$

where ε_{ij} represents the random concentration error. This section summarises the error models used in this thesis.

In the simplest case no error is added to the simulated concentrations, i.e.,

$$C_{ij} = C_{ij}^* \quad \text{Equation 2.6}$$

In the next case the expected concentration, C_{ij}^* , is subject to the addition of a random proportional error component (ε_{1ij}), i.e.,

$$C_{ij} = C_{ij}^* + \varepsilon_{1ij}(C_{ij}^*) \quad \text{Equation 2.7}$$

A third error model adds a random additive component (ε_{2ij}) to the expected concentration:

$$C_{ij} = C_{ij}^* + \varepsilon_{2ij} \quad \text{Equation 2.8}$$

In the final case the observed concentration is obtained by the addition of both a proportional and an additive error component, i.e.,

$$C_{ij} = C_{ij}^* + \varepsilon_{1ij}(C_{ij}^*) + \varepsilon_{2ij} \quad \text{Equation 2.9}$$

ε_{1ij} and ε_{2ij} were sampled from $\varepsilon_1 \sim N(0, \sigma_1^2)$ and $\varepsilon_2 \sim N(0, \sigma_2^2)$.

2.3 Parameter Estimation

2.3.1 NONMEM

The use of the NONMEM (**Non-Linear Mixed Effects Modelling**) computer program allows the definition of the distributions of the PK parameters across the population of patients (estimation of means and variances), along with similar distributions for intra-subject variability terms. Models including covariate fixed effects such as demographical or clinical data, which affect specific PK parameters, may also be developed (Boeckman et al. 1992).

Several estimation algorithms are implemented in NONMEM, each making different assumptions or mathematical simplifications.

The data from each individual within a population must be considered initially: each individual, i , has several concentration measurements, y_{ij} , obtained at times t_j , so that y_i is the vector of all concentrations measured from individual i . The data for each individual is considered to be a function of two statistical sub-models. The first is known as the inter-individual model, which governs the distribution of the PK parameters within the population as a whole. The PK parameters (clearance, volume of distribution etc.) for individual i differ from the population mean values, θ , by η_i (the inter-individual error) and the η 's within the population are assumed to be Normally distributed with a mean of zero and variance-covariance described by a matrix, Ω . The second sub-model is the intra-individual model, which has also been referred to as the random errors on concentration. This accounts for deviations in observed concentrations from that calculated from the individual's PK parameters. These random errors (ε_i) are also assumed to be Normally distributed with means of zero and variance-covariance described by a matrix, Σ . In general ψ is defined as a vector, which combines information from both of these sub-models along with other information that affects the values of y_i , i.e., the population average values of the PK parameters (θ) and the dosing history. The general equation for an individual's observations is:

$$y_{ij} = f(X_{ij}, \Theta, \eta_i, \varepsilon_{ij}) \quad \text{Equation 2.10}$$

where X_{ij} represents the independent variables that affect y_{ij} , e.g., dose and time.

For each individual NONMEM calculates the Likelihood ($L_i(\psi, \Omega)$) of the measurements y_i occurring within the population using equation 2.11:

$$L_i(\psi, \Omega) = \int l_i(\eta, \psi) \cdot h(\eta; \Omega) \cdot d\eta \quad \text{Equation 2.11}$$

where the probability that any individual's η_i are sampled from a Normal distribution with a mean of 0 and a variance-covariance matrix of Ω is given by $h(\eta; \Omega)$ and the likelihood that an individual deviates from the mean parameters, ψ , by η_i is given by $l_i(\eta, \psi)$.

The Likelihood of making all of the observations for all of the individuals within the population is then given by:

$$L(\psi, \Omega) = \prod_i L_i(\psi, \Omega) \quad \text{Equation 2.12}$$

Ideally, NONMEM would estimate the fixed and random effects parameters simultaneously such that $L(\psi, \Omega)$ in equation 2.12 is maximised. In fact, $-2\log L$ is minimised with respect to ψ and Ω to give a value that is known as the Objective Function and this value is useful for model comparison. However, the integration to evaluate $L_i(\psi, \Omega)$ in equation 2.11 is intractable and numerical approximations must be used. Each estimation method in NONMEM makes a different approximation to $L_i(\psi, \Omega)$.

Two of the estimation methods included in the NONMEM (version V) package are used in this thesis: the First-Order (FO), and the First-Order Conditional Estimation (FOCE) methods.

The FO method was the original NONMEM population estimation method. The integration of Equation 2.11 for calculation of the Objective function leads to terms that require calculation of the variance-covariance matrix of the individual's observations and also the expected values of y_i . An exact solution can only be

obtained when the functions governing the random errors in equation 2.10 (η_i and ε_{ij}) are linear. However, linear approximation of these functions can be attained by the use of a first-order Taylor Series expansion. This is an approximation for complicated functions in mathematics and consists of a series of terms involving differentiation of the original function.

The linearisation uses a first-order Taylor series expansion of the random errors about their expected values, i.e., zero for both η_i and ε_i . A simple description of the FO method is that η_i for each individual is set to zero, and the model parameters (ψ) and the variance-covariance matrix (Ω) are estimated. During estimation with the FO method, the objective function $L(\psi, \Omega)$ from equation 2.12 is maximised once for the population. Thus, the FO method produces estimates of the population fixed and random effects, but not of the individual's random effects (Beal et al. 1998). These can be obtained after the estimation of the fixed effects using a Bayesian estimation method to produce the 'posthoc' individual parameter estimates.

The FOCE method is an extension of the FO method where the η_i for each individual, the model parameters (ψ) and the variance-covariance matrix (Ω) are estimated simultaneously. This is based on a method originally proposed by Lindstrom and Bates (1990). The η are therefore **conditional** upon the values of ψ and Ω . This involves maximising the objective function $L(\psi, \Omega)$ from equation 2.11 each time different values of ψ , Ω and η are tried for each individual. This leads to the FOCE method being computationally more intensive than the FO method.

The choice of intra-individual error model also influences the way that the random errors are estimated with the FOCE method. If the intra-individual error model has a proportional component, then the variability of the observations, y_{ij} , (σ^2) is dependent on the mean values, which in turn are dependent on the η_i . This dependence does not occur where only an additive random error component is used. NONMEM includes two versions of the FOCE method - one that ignores this interaction between the random inter- and intra-individual errors (the default method) and one that accounts

for it. In this thesis the FOCE with interaction method is used when intra-individual error models include proportional components.

The conditional method (FOCE) is recommended when the functions governing the random errors are non-linear, e.g., this can occur with a multiple dosing history; or the FO method has given unsatisfactory results, e.g., bias in plots of observed versus population predicted values of data. However, it is also recommended that satisfactory results obtained using the FO method are checked with a conditional method to determine if any improvement in the fit of the model can be made.

Detailed explanation of the estimation algorithms used in NONMEM can be found within the NONMEM Users Guide Part VII, (Beal et al. 1998).

The NONMEM results obtained with the simulated data in this thesis were judged for satisfactory estimation by a combination of the following criteria:

(a) Examination of Goodness of fit plots:

- simulated concentration values vs the population concentration values predicted from NONMEM.
- simulated concentration values vs the individual concentration values predicted from NONMEM.
- individual simulated parameter values vs individual parameter values obtained from NONMEM.
- simulated values of η vs the individual estimates obtained from NONMEM.

(b) Examination of residual plots which are the plots of the differences between the individual subject's NONMEM estimates and the mean values within the population:

- residuals vs the NONMEM predicted values of the concentrations
- residuals vs the NONMEM individual predicted values of the concentrations.

(c) Examination of weighted residual plots which are the plots of the differences between the NONMEM estimates and the mean values within the population, weighted by the variability of the data within the population:

- weighted residuals vs the NONMEM predicted values of the concentrations
- weighted residuals vs the NONMEM individual predicted values of the concentrations.

This allowed more weight to be placed on data about which there was more confidence (less variability).

Results were considered satisfactory when there was no evidence of patterns within the residual plots and the residual values were small. In addition, the goodness of fit plots were required to be close to the line of unity.

2.3.2 Summary Statistics

In general, for each PK study design in this thesis, concentration-time data for ten sets of 500 subjects were simulated and analysed with NONMEM, leading to ten NONMEM population estimates of the PK parameters for each design. The results for each design were summarised by determination of the bias and imprecision of the ten population parameter estimates.

Bias is a measure of the difference between the estimated population parameter mean and the simulated value and was calculated using Equation 2.13 (Sheiner et al. 1981).

$$Bias = \frac{NM - T}{T} \times 100\% \quad \text{Equation 2.13}$$

where NM is the population parameter estimated by NONMEM and T is the true value of the parameter from the simulated data.

The bias results are presented as a mean (\overline{Bias}) and 95% confidence interval obtained from the number of NONMEM runs (n), i.e.,

$$\overline{Bias} = \frac{\sum Bias}{n} \quad \text{Equation 2.14}$$

and the 95% confidence interval was calculated from:

$$\overline{Bias} \pm t_{\alpha/2} \cdot SEM \quad \text{Equation 2.15}$$

where $t_{\alpha/2}$ is the Student's t-statistic corresponding to the two-tailed 95% confidence level for $n-1$ degrees of freedom and SEM is the standard error of the mean bias. The use of confidence intervals to compare different study designs was possible as n was constant at 10.

The imprecision is a measure of the spread of the parameter estimates around the average value of the parameter. This was calculated for each set of NONMEM runs (n) using the standard deviation of the NONMEM population estimates, expressed as a percentage of the mean of the simulated values and is described in Equation 2.16 (Barford 1967).

$$\text{Imprecision} = \frac{\sqrt{\frac{\sum (NM - \overline{NM})^2}{n-1}}}{\overline{T}} \times 100\% \quad \text{Equation 2.16}$$

where

$$\overline{NM} = \frac{\sum NM}{n} \quad \text{Equation 2.17}$$

and

$$\overline{T} = \frac{\sum T}{n} \quad \text{Equation 2.18}$$

For example, for 10 sets of 500 individuals, $n = 10$ and there would be 10 sets of NONMEM population parameter estimates (NM) from which the average could be calculated (\overline{NM}). There would also be 10 true values from which the mean true value could be calculated, \overline{T} , for the corresponding data sets.

To illustrate these concepts, examples of bias and imprecision within populations of results are shown in Figure 2.1. The four distributions show results that are

- (a) unbiased and precise
- (b) biased, but precise
- (c) unbiased, but imprecise
- (d) biased and imprecise

The ideal results would have zero bias and imprecision, as described in (a) above, although less than 15% is acceptable, by convention.

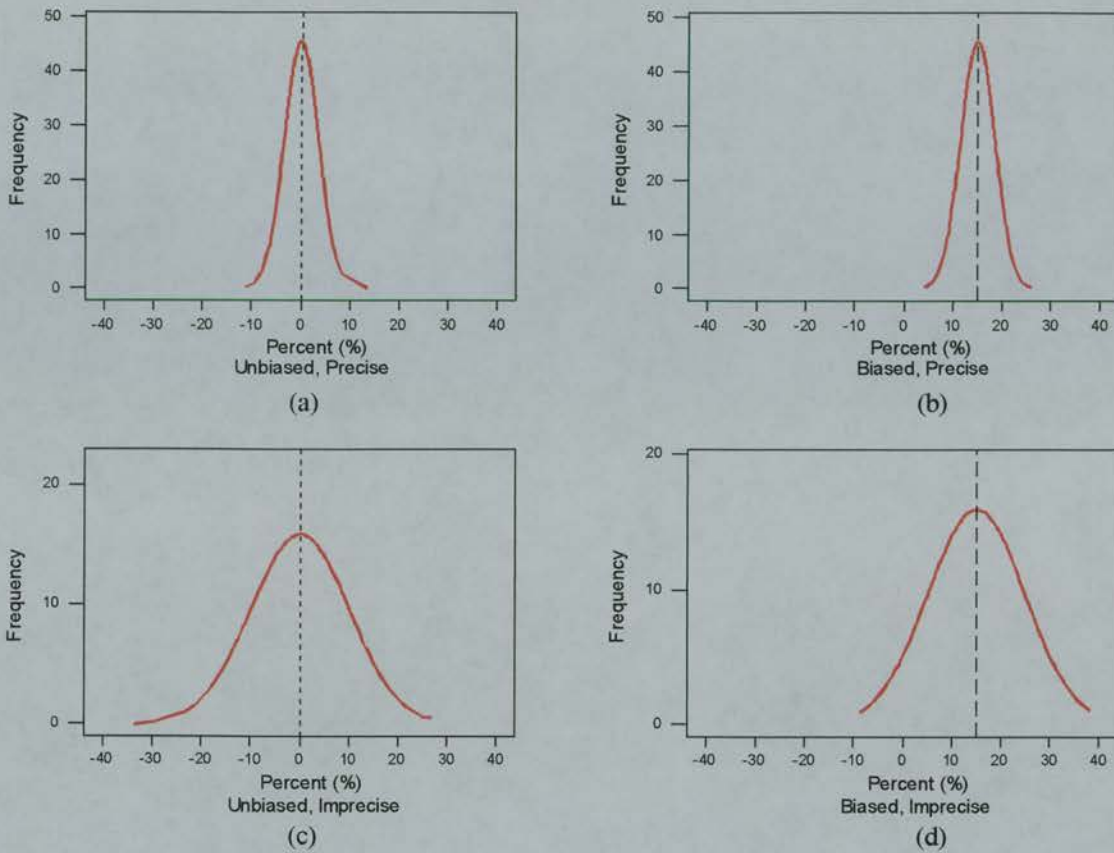


Figure 2.1 Examples of bias and imprecision within populations of results. Distributions of results are shown that are (a) unbiased and precise, (b) biased, but precise, (c) unbiased, but imprecise and (d) biased and imprecise.

Chapter 3

3 Use of Sensitivity Analysis to Define 'Optimal' Sampling Strategies

3.1 Introduction

Sensitivity analysis is often carried out in the area of risk assessment and can incorporate physiologically based pharmacokinetic (PBPK) models used to determine the effects of toxic chemicals and drugs on different organs and tissues of the body (Clewell et al. 1994; Spear et al. 1994; Nestorov et al. 1997). The effects of the variability in the model input parameters (e.g., dose, blood flow rates into specific organs, organ/tissue weights) on the model output parameter (e.g., concentration in a specific organ/tissue) can be examined over time (Hetrick et al. 1991). Sensitivity analysis involves defining the times at which the model output is most sensitive to changes in each model parameter. This is achieved by examining the partial derivatives of the output with respect to each of the input parameters (Gabrielsson et al. 1997). The total variability in the output parameter can be related to factors from each of the input parameters.

This technique has also been applied within the context of therapeutic drug monitoring of gentamicin and theophylline. These drugs have narrow therapeutic indices and are routinely monitored pharmacokinetically to reduce toxicity by the individualisation of dosing. Sensitivity analysis was used to determine at which times blood samples should be taken to minimise errors in the calculation of the elimination rate constant k_e and hence the dose required to achieve a specified concentration (Berg et al. 1983).

The aim of this chapter is to use sensitivity analysis as the basis for defining sampling times for limited sampling pharmacokinetic studies in the population setting. In this case the output parameter is the concentration (C_t) following an IV bolus dose of drug, and the input parameters of the model are clearance (Cl) and volume of distribution (V) for a one-compartment PK model. In the case of a two-compartment PK model the input parameters are total clearance (Cl), volume of distribution of the central compartment (V_1), volume of distribution of the peripheral

compartment (V_2) and the inter-compartmental clearance (Q). These are related to the macro constants A , α , B & β , and the micro constants k_{12} , k_{21} & k_{10} as described in Appendix 1.

The drug concentration at any time (t) is a function of the pharmacokinetic parameters, θ_i , and the dose administered (D), i.e.,

$$C_t = f(\theta_i, D, t) \quad \text{Equation 3.1}$$

The variance in C_t , ω_C^2 , can then be expressed as:

$$\omega_C^2 = \sum_i \left(\frac{\partial C}{\partial \theta_i} \right)^2 \omega_{\theta_i}^2 \quad \text{Equation 3.2}$$

where $\omega_{\theta_i}^2$ represents a measure of the variability in the parameters, θ_i , assuming no covariance between the parameters. Thus, the overall variance in the observed concentration can be related to the variance component associated with each parameter.

In theory, taking concentration measurements at the time(s) at which the variance in concentration is greatest within a population will give the maximum information about the PK parameters (Gabrielsson et al. 1997). Hence, deriving the times of maximum concentration variance should reveal specific sampling times, which may be, in some sense, 'optimal'. This demands, however, that approximate parameter values be known.

3.2 Mathematical Proofs

3.2.1 One-Compartment IV Bolus

If we assume that a dose distributes instantaneously into one compartment following an IV bolus administration, the concentration will be given by (Gabrielsson et al. 1997):

$$C_t = \frac{D}{V} \cdot e^{-\frac{Cl \cdot t}{V}} \quad \text{Equation 3.3}$$

where C_t = Concentration, D = Dose, V = Volume of Distribution, Cl = Clearance and t = time after injection.

Assuming no covariance between Cl and V , then equation 3.2 gives:

$$\omega_C^2 = \left(\frac{\partial C}{\partial Cl} \right)^2 \cdot \omega_{Cl}^2 + \left(\frac{\partial C}{\partial V} \right)^2 \cdot \omega_V^2 \quad \text{Equation 3.4}$$

In this case Cl and V are the mean population parameter values and ω_{Cl}^2 and ω_V^2 are the respective variances in the population. ω_C^2 is the expected variance in concentration due to the variability in the parameters across the population.

Taking the first derivatives of concentration with respect to each of the parameters allows calculation of 'sensitivity' to change in the parameters. Thus (Appendix 1):

$$\frac{\partial C}{\partial Cl} = -\frac{t}{V} \cdot C \quad \text{Equation 3.5}$$

and

$$\frac{\partial C}{\partial V} = \frac{1}{V^2} (Cl \cdot t - V) \cdot C \quad \text{Equation 3.6}$$

so that

$$\omega_C^2 = \frac{t^2 C^2}{V^2} \cdot \omega_{Cl}^2 + \frac{(Cl \cdot t - V)^2}{V^4} \cdot C^2 \cdot \omega_V^2 \quad \text{Equation 3.7}$$

Therefore, the time-points which should be most informative for the estimation of each parameter can be determined. For example, setting ω_V^2 to zero allows the component of variation in C due to variation in Cl to be studied, i.e.,

$$\omega_C^2 = \frac{t^2 C^2}{V^2} \cdot \omega_{Cl}^2 \quad \text{Equation 3.8}$$

ω_C^2 is maximal when $\frac{\partial}{\partial t} \omega_C^2 = 0$ and Appendix 1 shows that this occurs when:

$$t_1 = \frac{V}{Cl} = \frac{1}{k_e} = 1.44 \cdot t_{1/2} \quad \text{Equation 3.9}$$

where k_e is the elimination rate constant and $t_{1/2}$ is the half-life of the drug.

An example of the curve represented by Equation 3.8 is shown in Figure 3.1.

Similarly, setting ω_{Cl}^2 to zero allows the concentration variance component due to the variation in V to be examined:

$$\omega_C^2 = \frac{(Cl \cdot t - V)^2}{V^4} \cdot C^2 \cdot \omega_V^2 \quad \text{Equation 3.10}$$

Turning points again arise when $\frac{\partial}{\partial t} \omega_C^2 = 0$ i.e., when

$$t = \frac{1}{k_e} \quad \text{Equation 3.11}$$

$$\text{and } t = \frac{2V}{Cl} = \frac{2}{k_e} \quad \text{Equation 3.12}$$

In this case $t = \frac{1}{k_e}$ corresponds to a minimum, i.e., giving least information about V ,

whereas $t = \frac{2}{k_e}$ is a maximum associated with a peak in the concentration variance.

Also, $t = 0$ corresponds to a peak in ω_C^2 , although it is not a turning point and at this time, $\omega_C^2 = C^2 \cdot \frac{\omega_V^2}{V^2}$.

Equation 3.10 is illustrated in Figure 3.2 and it can be seen that the variability at $t = 0$ is much greater than that at $t = \frac{2}{k_e}$.

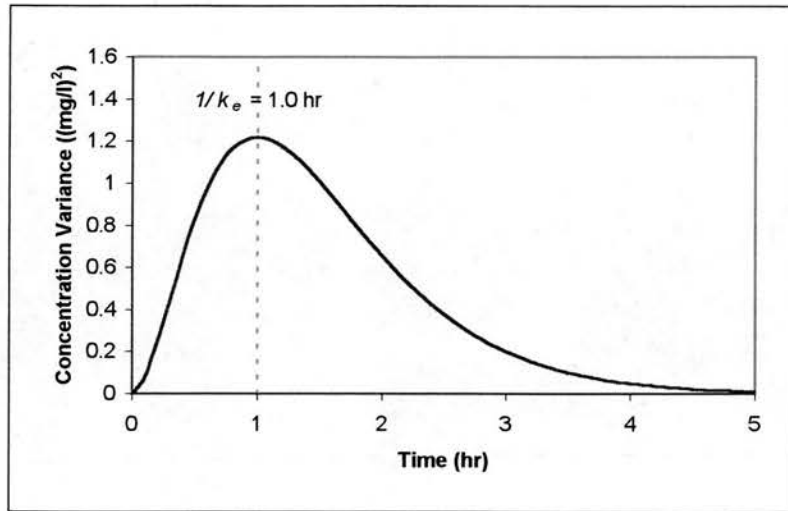


Figure 3.1 Change in concentration variance $((\text{mg/l})^2)$ over time when $Cl = 10 \text{ l/h}$, $V = 10\text{l}$, $\omega_{Cl} = 3 \text{ l/h}$, $\omega_V = 0 \text{ l}$ and dose = 100mg.

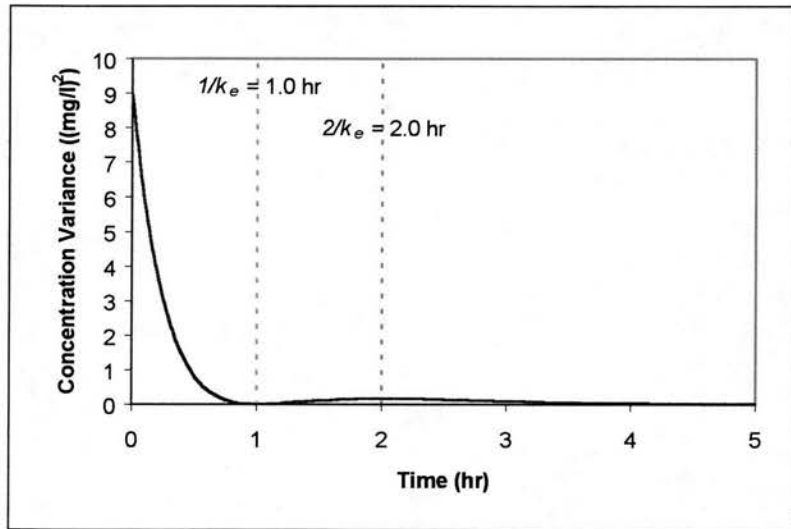


Figure 3.2 Change in concentration variance $((\text{mg/l})^2)$ over time when $Cl = 10 \text{ l/h}$, $V = 10\text{l}$, $\omega_{Cl} = 0 \text{ l/h}$, $\omega_V = 3 \text{ l}$ and dose = 100mg.

If, in addition, the observed concentration, C_t , is associated with random error, this will add to the overall concentration variability:

$$C_t = C_t^* + \varepsilon \quad \text{Equation 3.13}$$

where C_t^* is the expected concentration. Therefore the variance in concentration is dependent on both the expected concentration variance and that of the error component(s), (ω_ε^2) as shown below for equation 3.14.

$$(\omega_{C_t}^2) = (\omega_{C_t^*}^2) + (\omega_\varepsilon^2) \quad \text{Equation 3.14}$$

The mathematical proofs of the effects of random error on the concentration variance are shown in Appendix 1.

3.2.2 Two-Compartment IV Bolus

Similarly, if we assume that the dose distributes into a two-compartment system following an IV bolus, the concentration will be given by (Gabrielsson et al. 1997):

$$C_t = Ae^{-\alpha t} + Be^{-\beta t} \quad \text{Equation 3.15}$$

where C_t = Concentration; A, B = model constants; α, β = the model macro rate constants and t = time after injection.

The two-compartment PK model is parameterised in this thesis using: the total clearance (Cl), the volume of distribution of the central compartment (V_1), the volume of distribution of the peripheral compartment (V_2) and the inter-compartmental clearance (Q). These are related to the constants (A, B), the macro rate constants (α, β) and the micro rate constants (k_{10}, k_{12} & k_{21}) as described in Appendix 1.

Again, assuming no covariance between any of the parameters, the variance in concentration can be expressed as:

$$\omega_C^2 = \left(\frac{\partial C}{\partial Cl}\right)^2 \cdot \omega_{Cl}^2 + \left(\frac{\partial C}{\partial V_1}\right)^2 \cdot \omega_{V_1}^2 + \left(\frac{\partial C}{\partial V_2}\right)^2 \cdot \omega_{V_2}^2 + \left(\frac{\partial C}{\partial Q}\right)^2 \cdot \omega_Q^2$$

Equation 3.16

where ω_{Cl}^2 , $\omega_{V_1}^2$, $\omega_{V_2}^2$ and ω_Q^2 are population variances associated with the population mean values for Cl , V_1 , V_2 and Q , respectively, and ω_C^2 is the variance of C in the population. As before, the total variance in concentration can be attributed to the sum of the components due to each parameter (Equation 3.16) and these are defined in Appendix 1.

The expressions for the variance components were intractable, and so the times giving rise to maxima in the concentration variance were determined graphically in Figures 3.18 to 3.21.

3.3 Comparison of Derived 'Optimal' Sampling Times with Those Obtained in Simulated Populations

3.3.1 Introduction

Before utilising the sampling times obtained from the sensitivity analysis described in section 3.2, it was necessary to evaluate how well those equations predicted concentration variability. This was achieved by comparing the concentration variance predicted from the equations to that which was observed in simulated populations of 5000 subjects. The concentration variability obtained by each method was examined for both the magnitude of variability and times of peak variability.

It was shown that at CV of less than 30% on the parameter Cl , both 'concentration variance-time' curves could be superimposed from each method. However when variability in the parameters was higher the times of peak concentration variance shifted slightly to later times in the simulated populations, for the one-compartment model. Divergence of the curves was also noted with the higher CV in Cl . The shift in peak time was not noted with the two-compartment model, although the divergence was, but to a lesser extent than that seen with the one-compartment model.

It was concluded that the equations derived in section 3.2 predicted concentration variability reliably at lower levels of variability in the parameters, but that examination of simulated populations was required in situations of higher variability in the population PK parameters.

3.3.2 Methods

Concentration-time data were simulated for populations of 5000 subjects, following an IV bolus dose of 100mg as described in section 2.2. Ten groups of populations were simulated for each of the one- and two-compartment PK models. Five groups represented the situation with no random intra-subject error on concentration and five represented the situation with the inclusion of random intra-subject error on

concentration. Within each group there were ten sets of 5000 subjects and each of the five groups represented a different value for the SD of clearance. See the organisation chart in figure 3.3.

One-Compartment PK Model

In the case of the one-compartment PK model, the population mean values were set to 10 l/h and 10 l for clearance and volume, respectively, giving an average value for half-life ($t_{1/2}$) = 0.693 hr. The population standard deviation for clearance, ω_{Cl} , was varied (1, 2, ..., 5 l/hr), but the standard deviation for volume, ω_V , was fixed at 1 l. For the sets with random error added to concentration a combination error model was used as described in section 2.2.3, with the proportional error component, σ_1 , set to 0.05, (i.e., 5%) and the additive error component, σ_2 , set to 0.25 mg/l.

The concentration variance was calculated at each time point, using the standard equation for variance (equation 3.17 below), for each simulated population of 5000 subjects and plotted up to 5 hours post-dose and the results compared to those predicted from equation 3.7.

$$\text{Variance} = (SD)^2; SD = \sqrt{\frac{\sum (x - \bar{x})^2}{n - 1}} \quad \text{Equation 3.17}$$

Two-Compartment PK Model

For the two-compartment model, the mean population parameter values were set at 10 l/h and 15 l/h for the total clearance (Cl) and the inter-compartmental clearance (Q), respectively, and 10 l and 20 l for the volumes of the central (V_1) and peripheral (V_2) compartments, respectively, giving a value for the terminal half-life ($t_{1/2\beta}$) = 2.8 hr. As the equations for the two-compartment model were intractable, initially, each parameter was examined for effects on concentration variability by setting the variability on all other parameters to zero. No random error was added to

concentration at this time, and the standard deviation of the parameter being examined was varied from 10 to 50%, in steps of 10%.

Following the initial studies, the simulated populations were further examined for peaks in total concentration variance. The concentration variance was calculated for each population of 5000 subjects and again plotted up to 5 hours post-dose. The observed concentration variance was compared to that predicted by Equation 3.16.

Again for the sets with random error added to concentration the combination error model described in section 2.2.3 was used. The proportional error component, σ_1 , was set to 0.05, (i.e., 5%) and the additive error component, σ_2 , to 0.35 mg/l.



Figure 3.3 Organisation of simulated populations for calculation of observed concentration variance for comparison with that predicted from the equations derived in section 3.2.

3.3.3 Results

3.3.3.1 One-Compartment IV Bolus PK Model

Reproducibility of Simulation Results

To assess the reproducibility of the results of the simulation, ten simulations were carried out for each set of parameter values.

Figure 3.4 shows the concentration variance ($(\text{mg/l})^2$) over time for the ten simulations when $\omega_{Cl} = 30\%$, in the absence of a random intra-individual error. The theoretically derived concentration variance curve (Equation 3.7) is also shown. From the figure it can be seen that the curves for each of the ten simulations are superimposed, but that all diverged from the theoretically derived curve from 0.6h onwards. The results when random error was introduced (Figure 3.5) were similar.

Due to the reproducibility being accurate, the results are presented with only one simulated population being compared to the concentration variance predicted from the equations.

Effect of Increasing Variability of Clearance

Figures 3.6 to 3.10 show the expected variance in concentration in the absence of random intra-individual error on concentration. Each plot shows the variance components due to each parameter: clearance (Var (Cl)), volume of distribution (Var (V)), proportional random error (Var (prop)) and additive random error (Var (add)). The total concentration variance (Var Total) is also plotted along with the observed variance obtained from a simulated population (Var Sim) of 5000 subjects. The SD of clearance (ω_{Cl}) increases from 1 to 5 l/h in Figures 3.5 to 3.9, respectively and Var(add) and Var(prop) are zero in these plots as there was no random error added. The distributions of the parameters *Cl* and *V* within the populations are shown as histograms on each plot.

Each plot shows a peak in both the calculated and simulated total concentration variances at time = 0 hr due to the component from volume of distribution. There was a further peak at 2.0 hr due to volume, corresponding to $t = \frac{2}{k_e}$, but this was not obvious in the total concentration variance profile due to the size of the other peaks.

A maximum in the total concentration variance occurred at 1.0 hr due to the variance component from clearance and was shown to increase in magnitude as ω_{Cl} increased from 1 to 5 l/h. Although, the calculated time of this peak was constant, in the simulated sets it shifted to later times as the variance in clearance increased so that when $\omega_{Cl} = 5$, the concentration variance peak occurred at 1.2 hours (Figure 3.10). When ω_{Cl} was 1-2 l/h for clearance (figures 3.6 and 3.7) the calculated and simulated variance curves were superimposed. Differences between the calculated and simulated curves were obvious when the CV for clearance increased above 30% (Figures 3.8 - 3.10) when the simulations gave rise to higher concentration variance.

Similar results were obtained when a random error was included in the model (Figures 3.11-3.15). The times at which the peaks in variance occurred were unaffected.

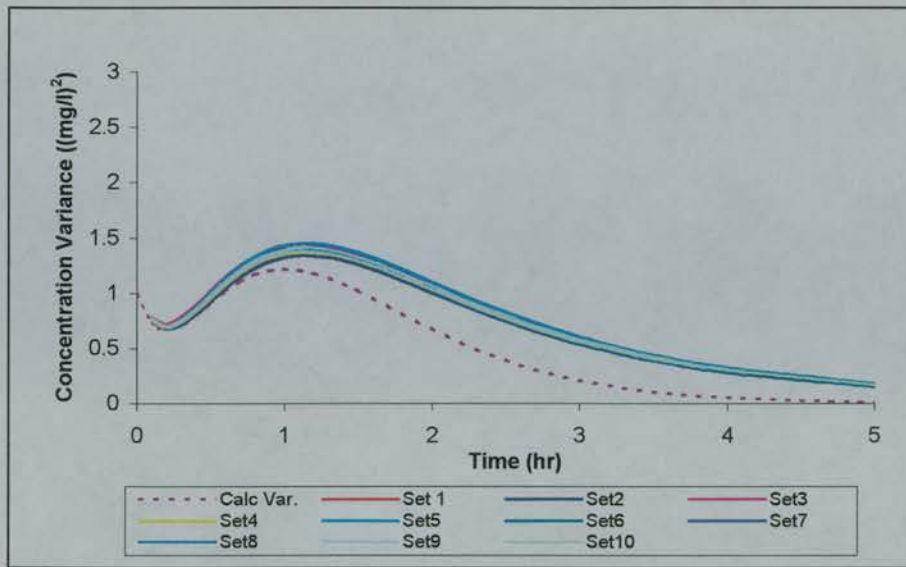


Figure 3.4 Plot of concentration variance over time for ten simulations of 5000 subjects and the derived concentration variance when $\omega_{Cl} = 3$ l/h (no random error).

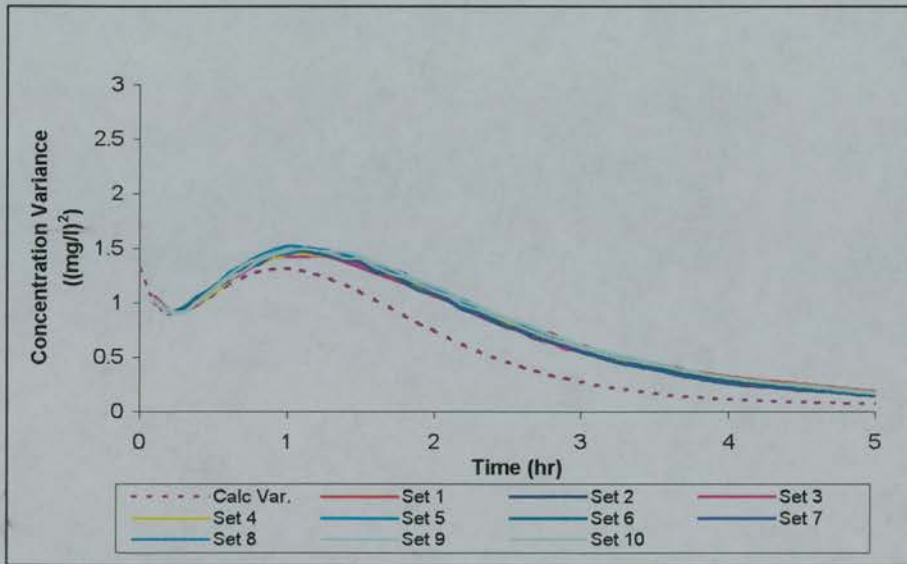


Figure 3.5 Plot of concentration variance over time for ten simulations of 5000 subjects and the derived concentration variance when $\omega_{Cl} = 3$ l/h (random error).

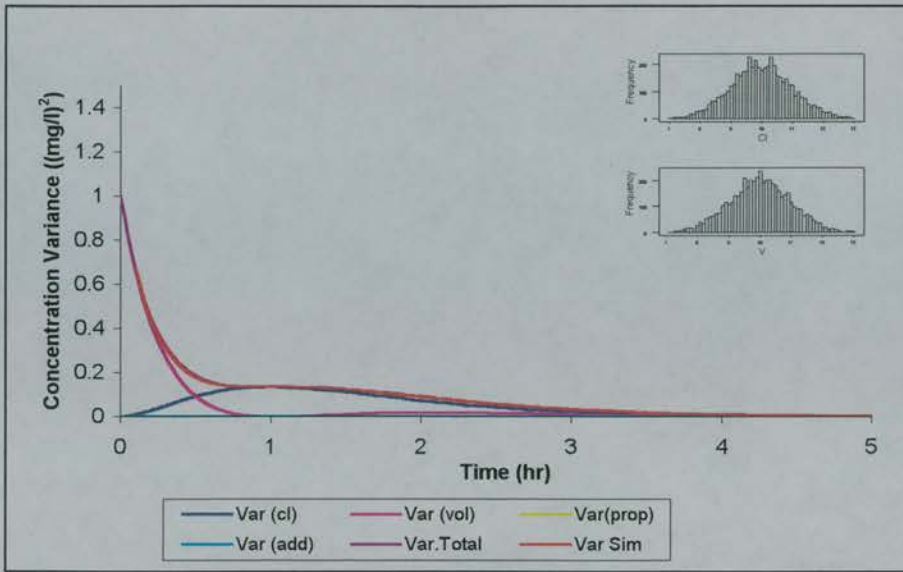


Figure 3.6 Concentration variance across time for $\omega_{Cl} = 1$ l/h (no random error).

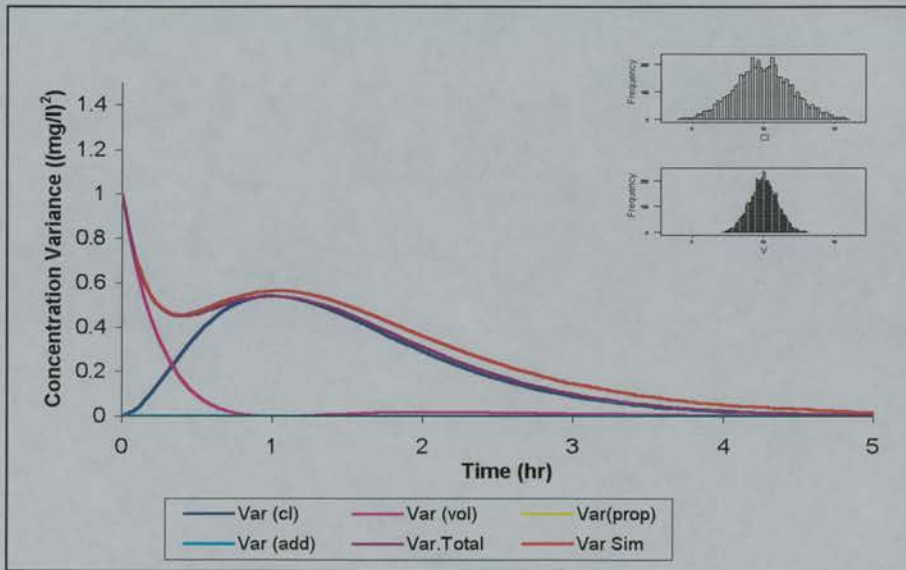


Figure 3.7 Concentration variance across time for $\omega_{Cl} = 2$ l/h (no random error).

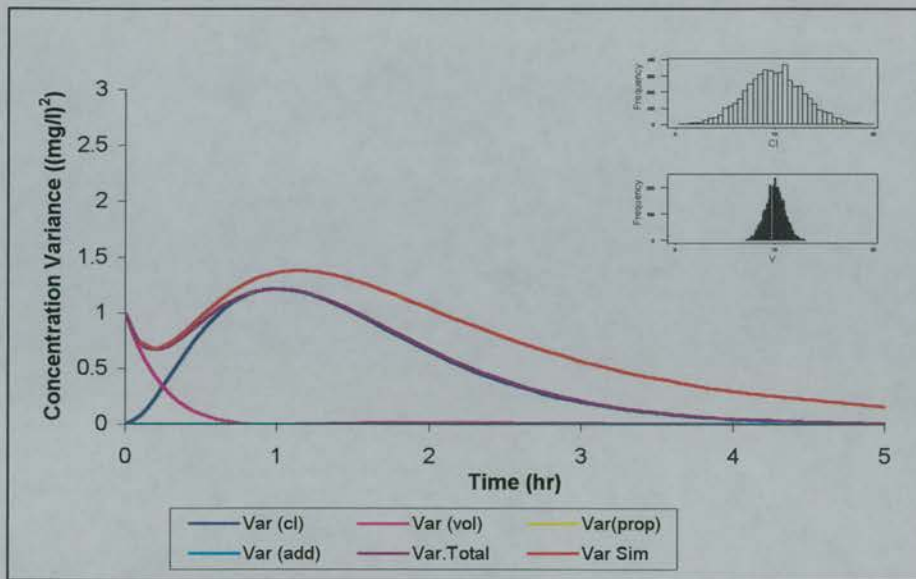


Figure 3.8 Concentration variance across time for $\omega_{Cl} = 3$ 1/h (no random error).

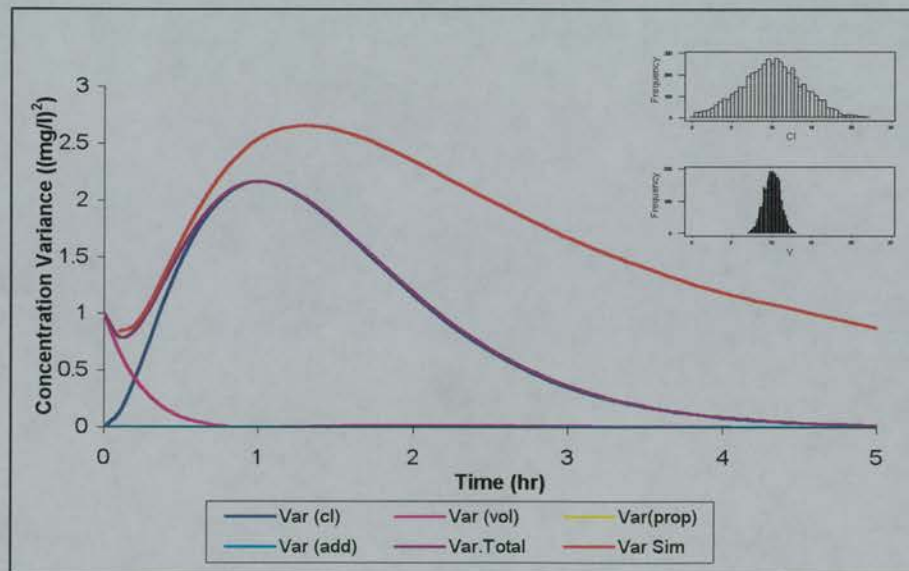


Figure 3.9 Concentration variance across time for $\omega_{Cl} = 4$ 1/h (no random error).

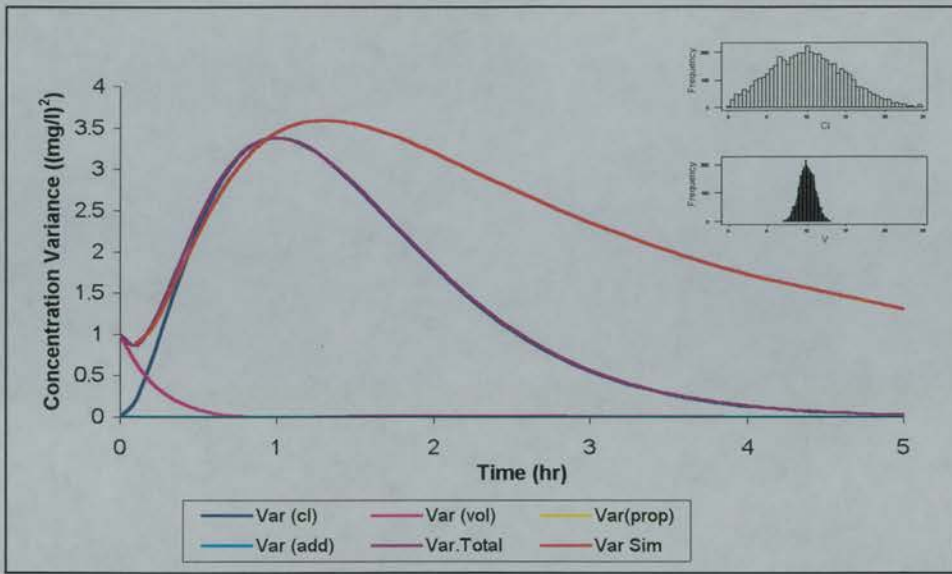


Figure 3.10 Concentration variance across time for $\omega_{Cl} = 5$ l/h (no random error).

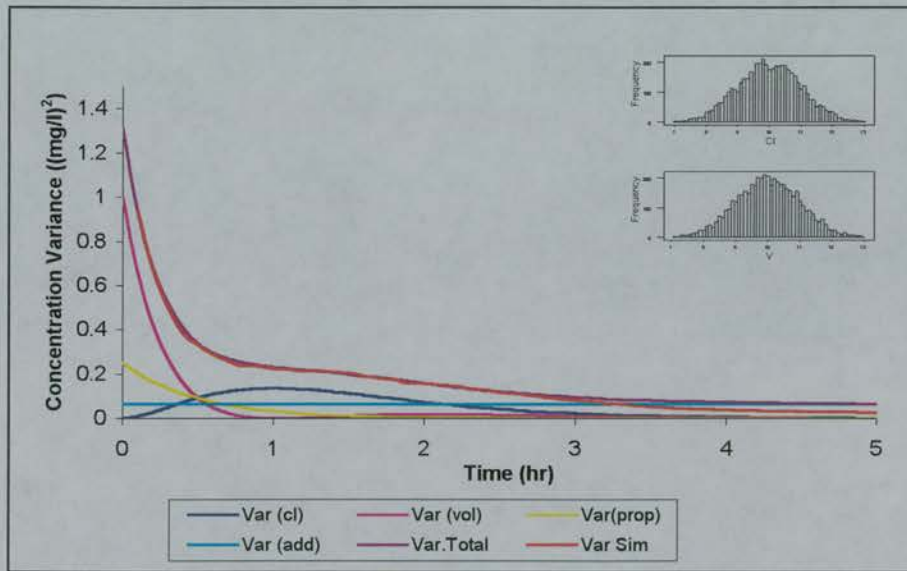


Figure 3.11 Concentration variance across time for $\omega_{Cl} = 1$ l/h (random error).

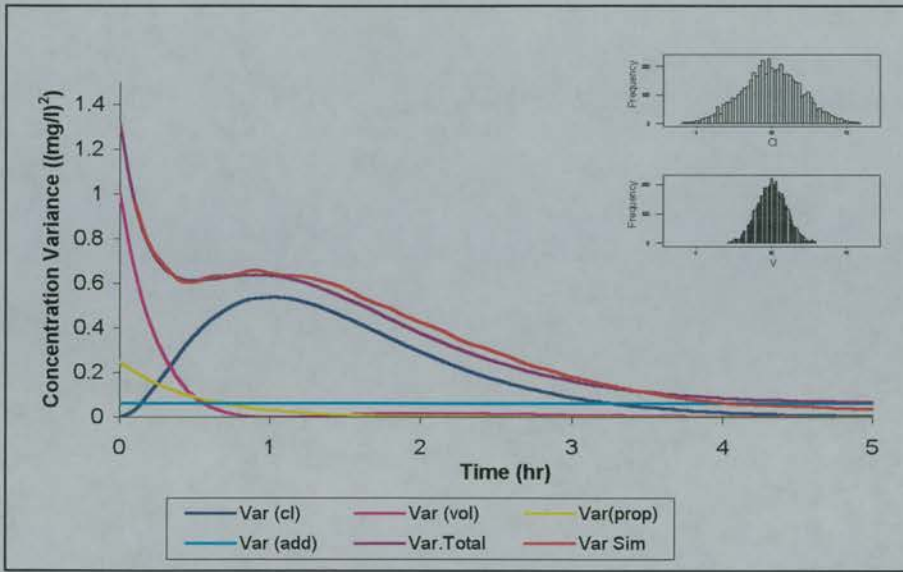


Figure 3.12 Concentration variance across time for $\omega_{Cl} = 2$ l/h (random error).

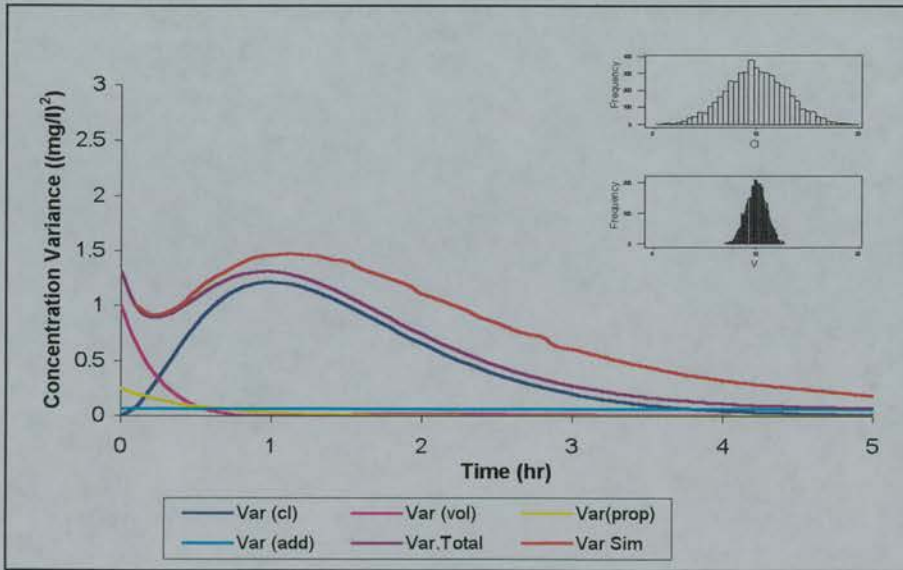


Figure 3.13 Concentration variance across time for $\omega_{Cl} = 3$ l/h (random error).

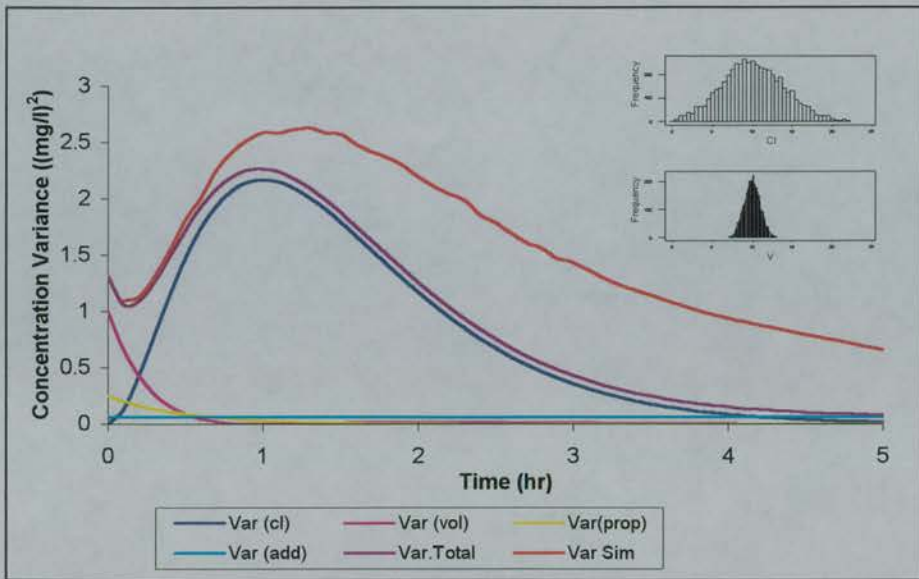


Figure 3.14 Concentration variance across time for $\omega_{Cl} = 4$ l/h (random error).

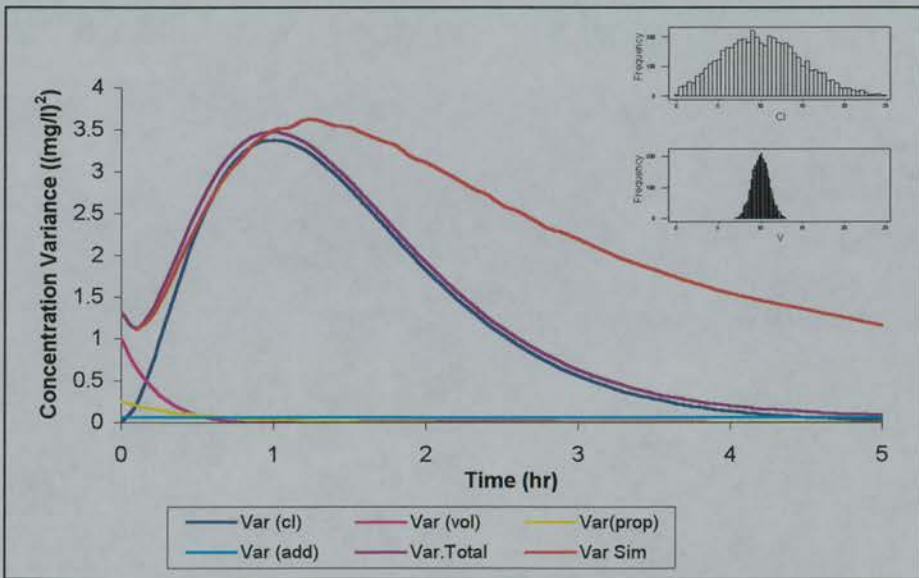


Figure 3.15 Concentration variance across time for $\omega_{Cl} = 5$ l/h (random error).

Effect of High Concentrations on Total Concentration Variance Within a Population

Figure 3.16 shows frequency histograms of the concentrations at 1.0 hr and 5.0 hr, for the populations with $\omega_{CI} = 3$ and Figure 3.17 showed the same for $\omega_{CI} = 5$. As ω_{CI} increased from 3 to 5, the distributions became skew and this was more apparent at the later times.

The effect of the high concentrations observed in simulated populations on the standard deviations is shown in Table 3.1. The variance in the simulated population was artificially inflated at 5.0 hr by a small number of concentrations that were greater than 0.5 mg/l. Concentrations greater than 2.0mg/l increased the standard deviation of the population when random error was added to concentration. Removal of these concentrations from the distribution reduced the standard deviation of the remaining population to a value that was similar to the value predicted for the equations.

As the ω_{CI} increased to 5 l/h (Table 3.2), a greater number of concentration measurements had to be removed in order to decrease the standard deviation of the remaining population to a value similar to that predicted. However, in the absence of random error on concentration, the higher variability in clearance allowed a higher range on concentrations to be accepted (0.8 mg/l compared to 0.5 mg/l), whereas in the presence of random error the range was reduced from 2 mg/l to 1.6 mg/l.

This indicated that at times where the concentrations were generally small in relation to the dose, and at higher levels of variation in the parameters, the mean and standard deviation were not appropriate to describe the distribution of concentration. Hence, divergence of the observed concentration variance from the predicted values was noted.

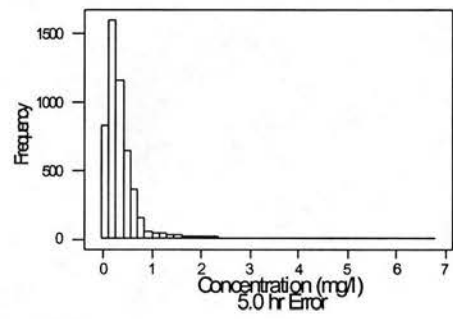
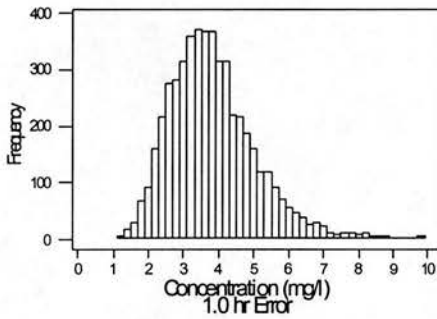
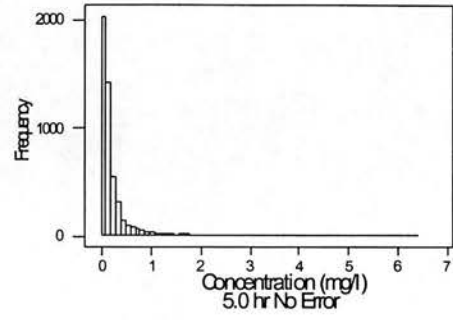
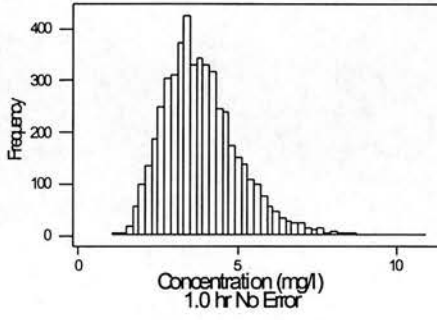


Figure 3.16 Histograms of concentration at 1.0 hr and 5.0 hr when $\omega_{Cl} = 3$, with the one-compartment model ($n=5000$).

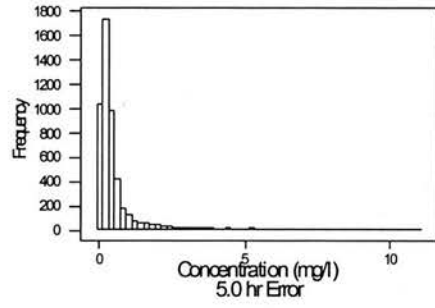
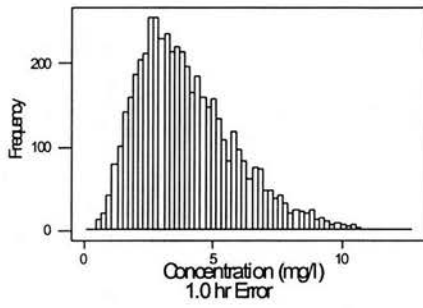
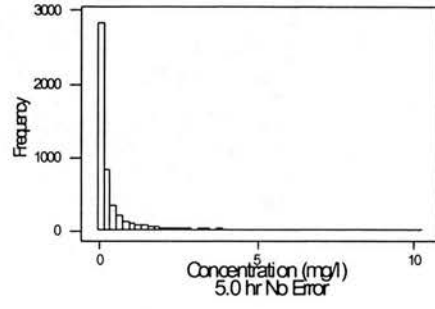
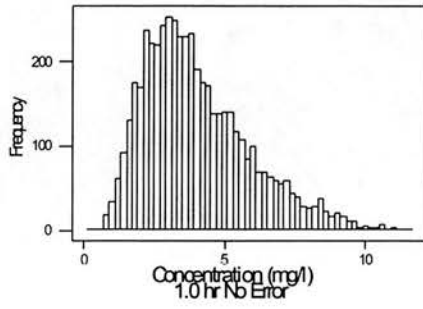


Figure 3.17 Histograms of concentration at 1.0 hr and 5.0 hr when $\omega_{Cl} = 5$, with the one-compartment model ($n=5000$).

Table 3.1 Effect of High Concentrations on Population Standard Deviation, Using the One-Compartment PK Model ($\omega_{Cl} = 3$ l/h, $t = 5.0$ hr)

	No Random Error on Concentration		Random Error on Concentration	
	Concentration Range Accepted (mg/l)	Concentration Range Accepted (mg/l)	Concentration Range Accepted (mg/l)	Concentration Range Accepted (mg/l)
No. Subjects	0-7	0-1.5	0-0.5	0-1.5
	5000	4908	4522	4906
Population SD	0.403	0.229	0.106	0.244
Predicted SD		0.105		0.271
			5000	4944
			0.433	0.274

Table 3.2 Effect of High Concentrations on Population Standard Deviation, Using the One-Compartment PK Model ($\omega_{Cl} = 5$ l/h, $t = 5.0$ hr)

	No Random Error on Concentration		Random Error on Concentration	
	Concentration Range Accepted (mg/l)	Concentration Range Accepted (mg/l)	Concentration Range Accepted (mg/l)	Concentration Range Accepted (mg/l)
No. Subjects	0-11	0-2.5	0-0.8	0-2.5
	5000	4743	4265	4775
Population SD	1.145	0.450	0.173	0.430
Predicted SD		0.171		0.303
			5000	4609
			1.080	0.298

3.3.3.2 Two-Compartment IV Bolus

Results From Sensitivity Analysis for the Two-Compartment PK Model

As the equations from section 3.22 were intractable, the contribution of each of the parameters Cl , V_1 , V_2 and Q to the total concentration variance was examined graphically, by the substitution of different values in Equation 3.16. The variability in each parameter was examined as it was increased from 10 to 50% in steps of 10%. Figures 3.18 to 3.21 show how increasing variability in each of the population mean parameters Cl , V_1 , V_2 and Q , respectively, affected concentration variance, using simulated populations of 5000 subjects.

Figure 3.17 shows one peak in concentration due to the variance in clearance. The peak shifted slightly from 0.5 hr to 0.6 hr as CV increased from 10 to 50% (or as ω_{Cl} increased from 1 to 5 l/h).

Variability in the volume of the central compartment (V_1) caused a high peak immediately after administration of the drug (Figure 3.19) and a small second peak at 0.8 hr when $\omega_V = 1$ l and 0.5 hr when ω_V was 3 l. This peak was not observed when the CV was greater than 30% due to the contribution from the early peak.

A maximum occurred at 1.1 hr due to the variation in volume of distribution of the peripheral compartment (V_2) when CV was 10%. This peak moved gradually to earlier times and occurred at 0.8 hr when CV was 50% (Figure 3.20).

The variability in the inter-compartmental clearance, Q , gave rise to two maxima in concentration variance: one at 0.3-0.4 hr which remained relatively fixed in time and one which shifted from 2.1 hr to 2.7 hr as CV increased from 10 to 50%. See Figure 3.21.

Table 3.3 shows how the peak times shifted for each parameter as the CV of each parameter increased from 10 to 50%.

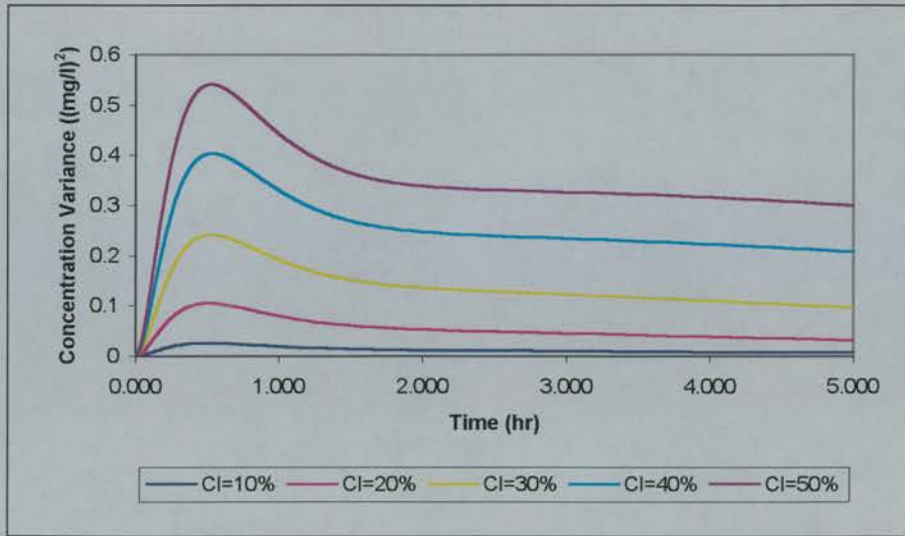


Figure 3.18 Plot of concentration variance over time showing the effect of increasing variance in clearance (CI) from 10 to 50%, with the two-compartment PK model.

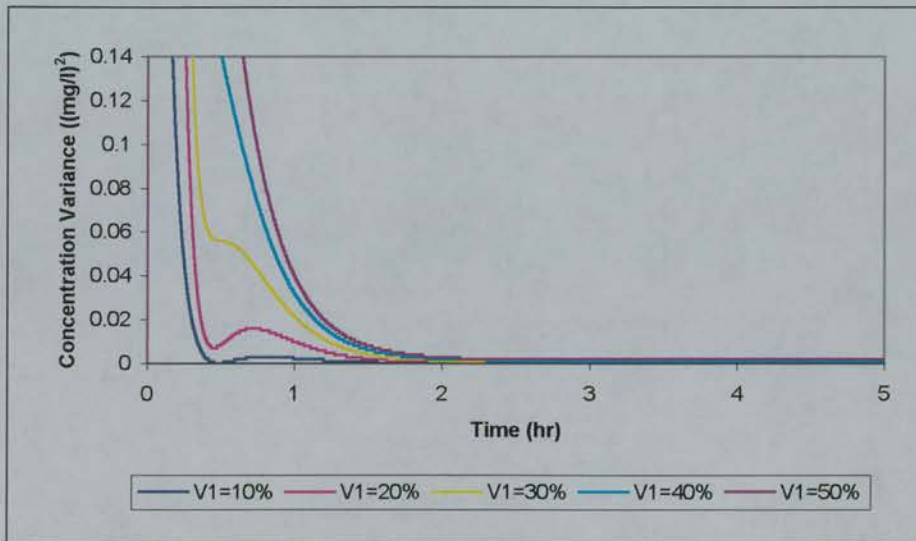


Figure 3.19 Plot of concentration variance over time showing the effect of increasing variance in volume of the central compartment (V_1) from 10 to 50%, with the two-compartment PK model.

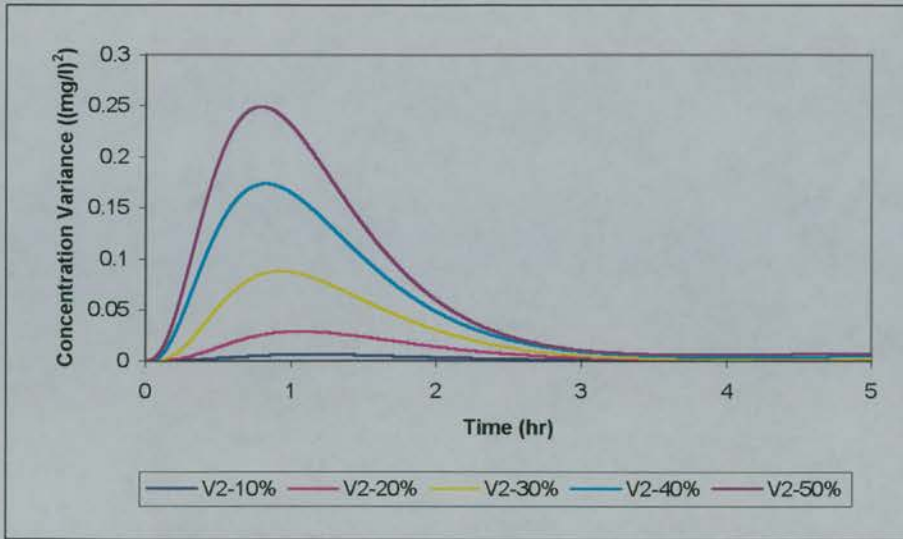


Figure 3.20 Plot of concentration variance over time showing the effect of increasing variance in volume of the peripheral compartment (V_2) from 10 to 50%, with the two-compartment PK model.

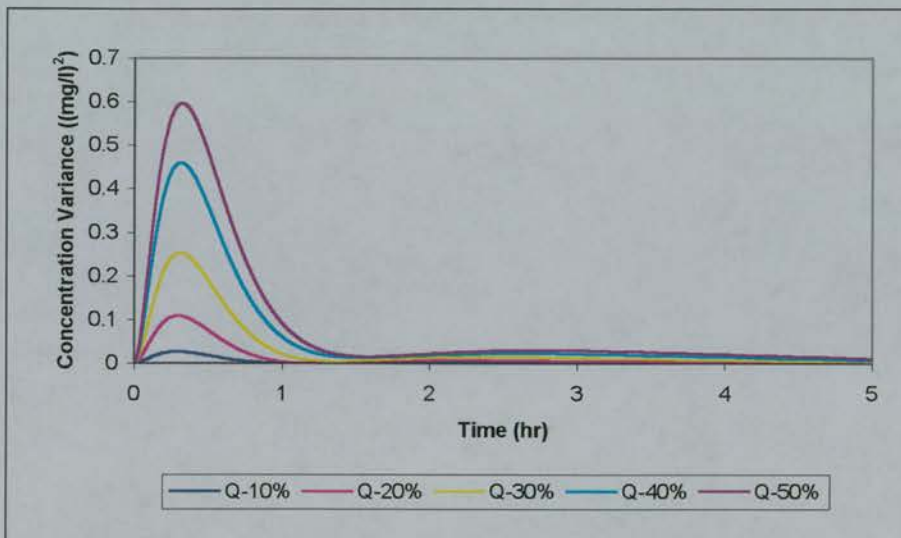


Figure 3.21 Plot of concentration variance over time showing the effect of increasing variance in inter-compartmental clearance (Q) from 10 to 50%, with the two-compartment PK model.

Table 3.3 Times of peak concentration variance due to each parameter (from Figures 3.18-3.21).

Parameter (Peak No.)	Time of Peaks 10% CV	Time of Peaks 20% CV	Time of Peaks 30% CV	Time of Peaks 40% CV	Time of Peaks 50% CV
<i>Cl</i>	0.5 hr	0.5 hr	0.5 hr	0.6 hr	0.6 hr
<i>V₁ (1)</i>	Early as Possible	Early as Possible	Early as Possible	Early as Possible	Early as Possible
<i>V₁ (2)</i>	0.8 hr	0.7 hr	0.5 hr	None	None
<i>V₂</i>	1.1 hr	1.1 hr	0.9 hr	0.8 hr	0.8 hr
<i>Q (1)</i>	0.3 hr	0.3 hr	0.3 hr	0.3 hr	0.4 hr
<i>Q (2)</i>	2.1 hr	2.2 hr	2.4 hr	2.5 hr	2.7 hr

Reproducibility of Simulation Results

As in the one-compartment situation, Figures 3.22 and 3.23 show examples of the reproducibility of the concentration variability within ten simulated populations of 5000 subjects when $\omega_{Cl} = 3$ l/h, in the absence and presence of random error on concentration, respectively. In Figure 3.22 the simulated curves were all superimposed and when compared to the predicted concentration variance, there was a slight divergence of the curves at all times. However, this was less apparent than with the one-compartment model (see Figures 3.6-3.15). The addition of random error did not affect these results (Figure 3.23).

Similar to the one-compartment results, the remaining results in this section only show concentration variance of one simulated population along with the predicted concentration variance curve.

Effect of Increasing Variability of Clearance

Figures 3.24 to 3.28 show the concentration variance components from each parameter as shown in Equation 3.16 (Cl comp, V_1 comp, V_2 comp and Q comp on figures), for different values of ω_{Cl} . The total observed variance in simulated populations of 5000 subjects when no random error was added to concentration (Total) is also shown along with the concentration variance predicted from the equations (Sim Var). Histograms of the distributions of the parameters are also included in the plots, confirming them all to be Normally distributed. Variability in clearance increased from a CV of 10 up to 50% in plots 3.24 to 3.28, respectively.

In each plot (Figures 3.24-3.28), the only visible peaks in total concentration variance (simulated and calculated) occurred at $t = 0$ hr and at around 0.5 hr due to variability in V_1 and Cl , respectively. The peak at 0.5 hr shifted to progressively later times as the variability in Cl increased from 10 to 50%. When the CV of clearance was 10% (Figure 3.24) the simulated and calculated total concentration variance curves were superimposed. The two curves diverged after the peak in total concentration variance seen at 0.5 hr when CV on clearance was greater than 20%.

However, the time of the peak variability in both the simulated and calculated curves remained the same (Figures 3.26 to 3.28).

Figures 3.29 to 3.33 show how increasing the CV on clearance from 10 to 50% affected concentration variance when a combined random error model was added to concentration (proportional component = 5% and additive component = 0.35 mg/l). Adding intra-individual random error to concentration caused the simulated and calculated total curves to diverge slightly at times later than 3.5 hr, when CV on clearance was 10-30%. When $\omega_{Cl} = 4-5$ l/h the lines were slightly separated at all times, with the greatest separation being when $\omega_{Cl} = 5$ l/h. However, the peak in concentration variance which occurred at approximately 0.5 hr was observed at the same time in both the simulated and predicted curves.

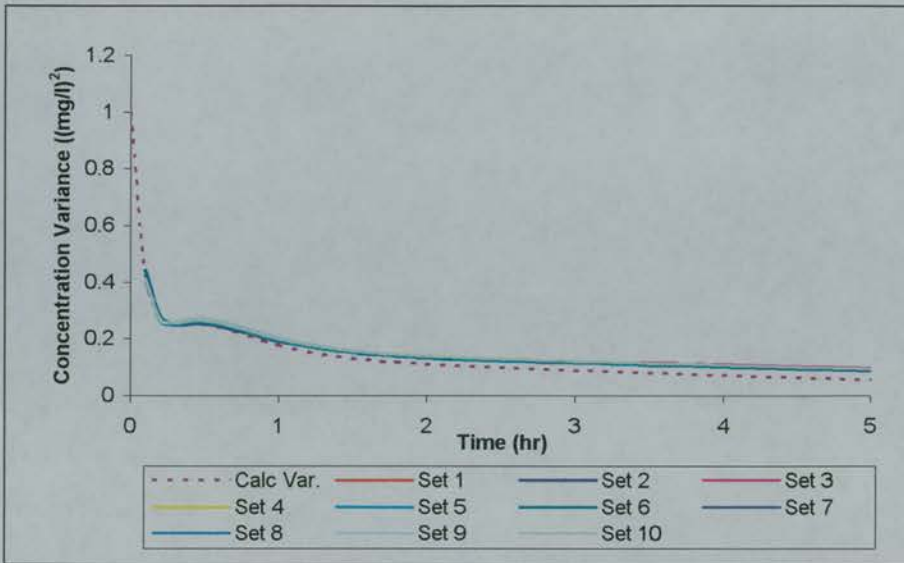


Figure 3.22 Plot of concentration variance over time for ten simulations of 5000 subjects and the derived concentration variance when $\omega_{Cl} = 3$ l/h (no random error).

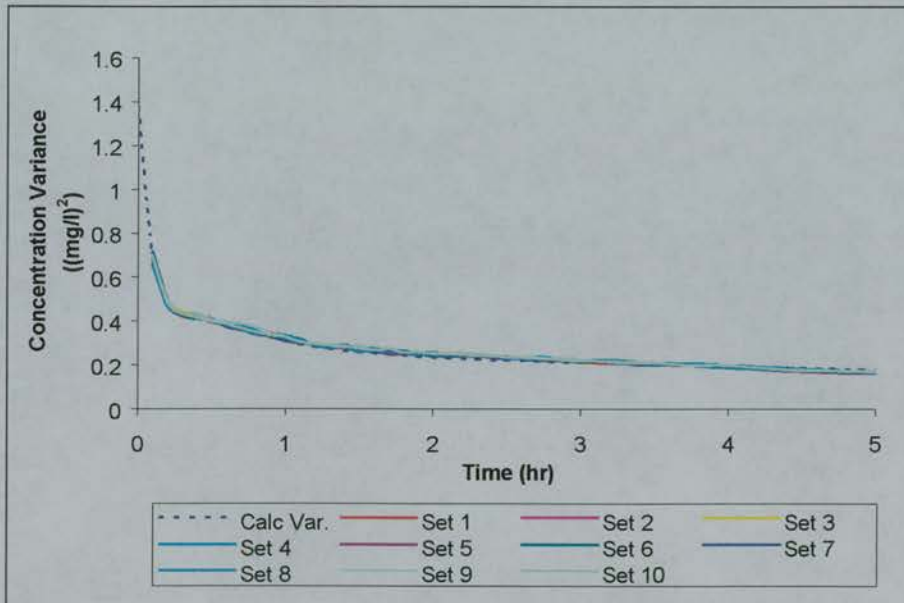


Figure 3.23 Plot of concentration variance over time for ten simulations of 5000 subjects and the derived concentration variance when $\omega_{Cl} = 3$ l/h (random error).

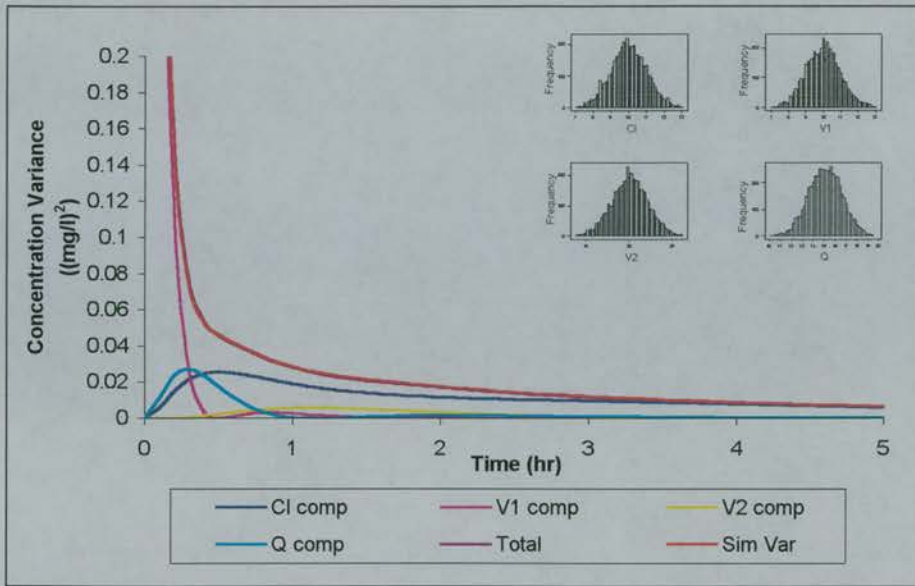


Figure 3.24 Concentration variance across time for $\omega_{Cl} = 1$ l/h (no random error).

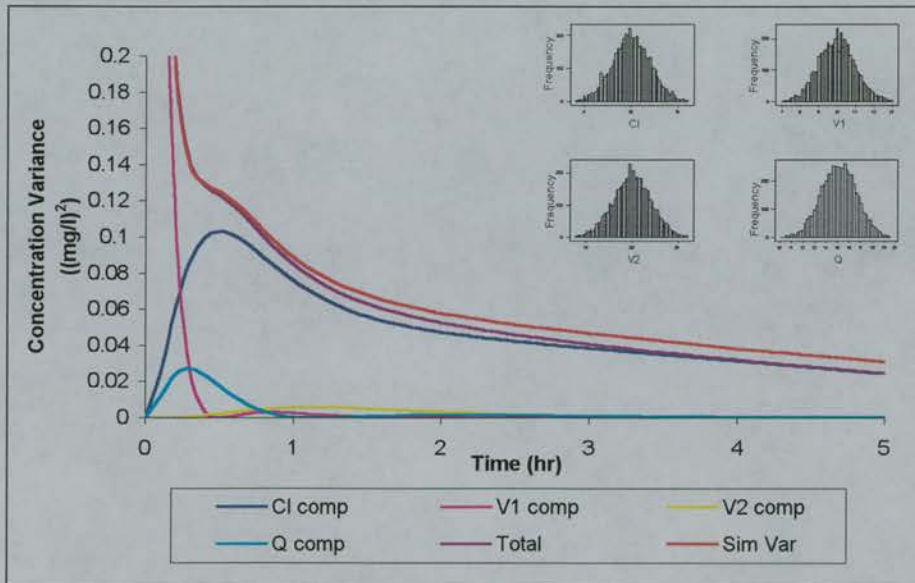


Figure 3.25 Concentration variance across time for $\omega_{Cl} = 2$ l/h (no random error).

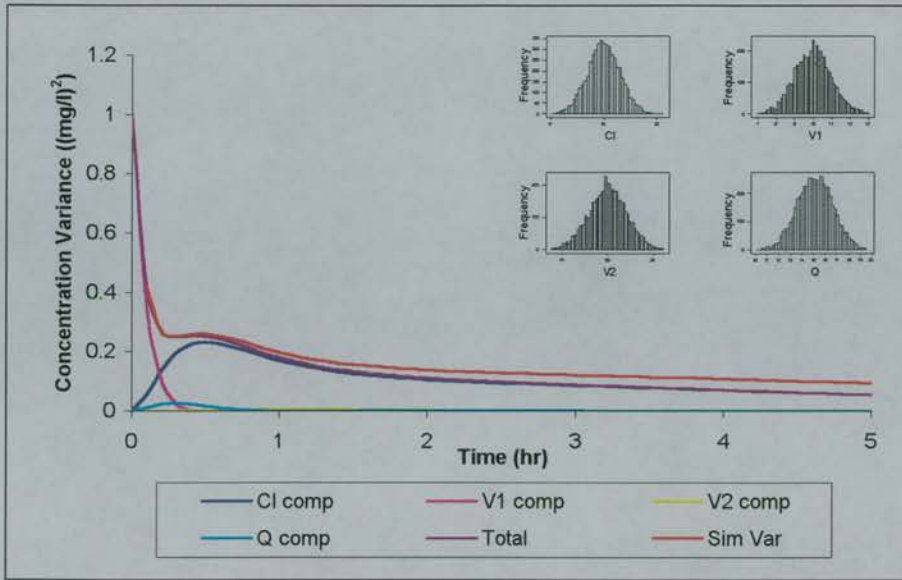


Figure 3.26 Concentration variance across time for $\omega_{Cl} = 3$ l/h (no random error).

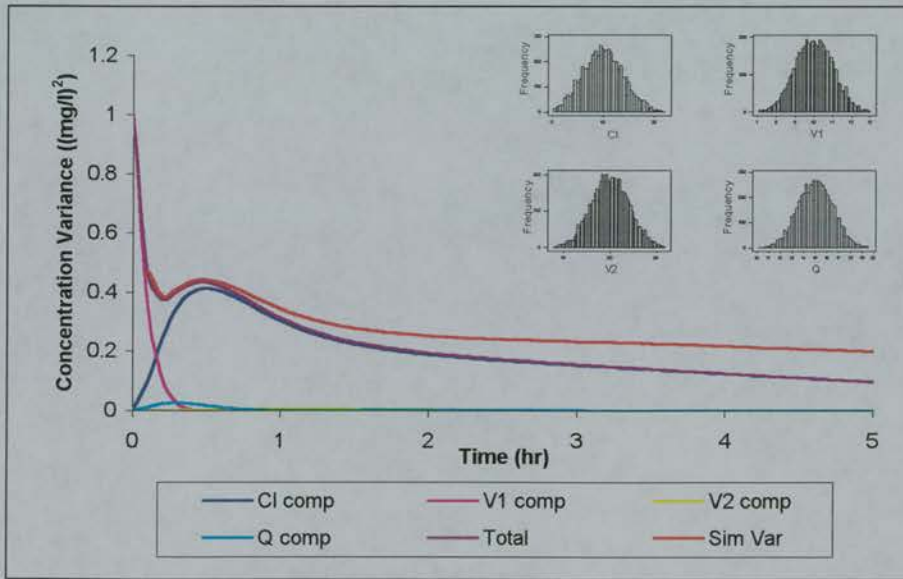


Figure 3.27 Concentration variance across time for $\omega_{Cl} = 4$ l/h (no random error).

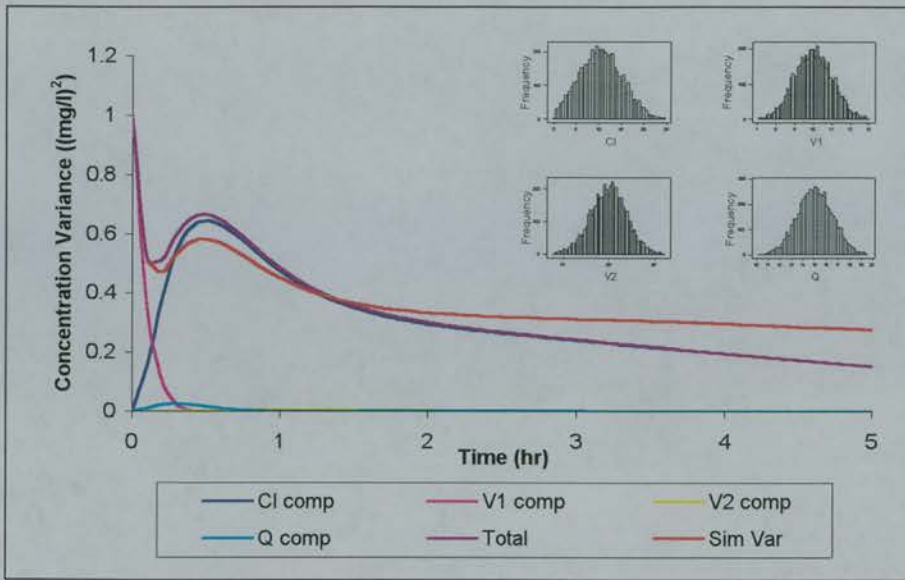


Figure 3.28 Concentration variance across time for $\omega_{CI} = 5$ l/h (no random error).

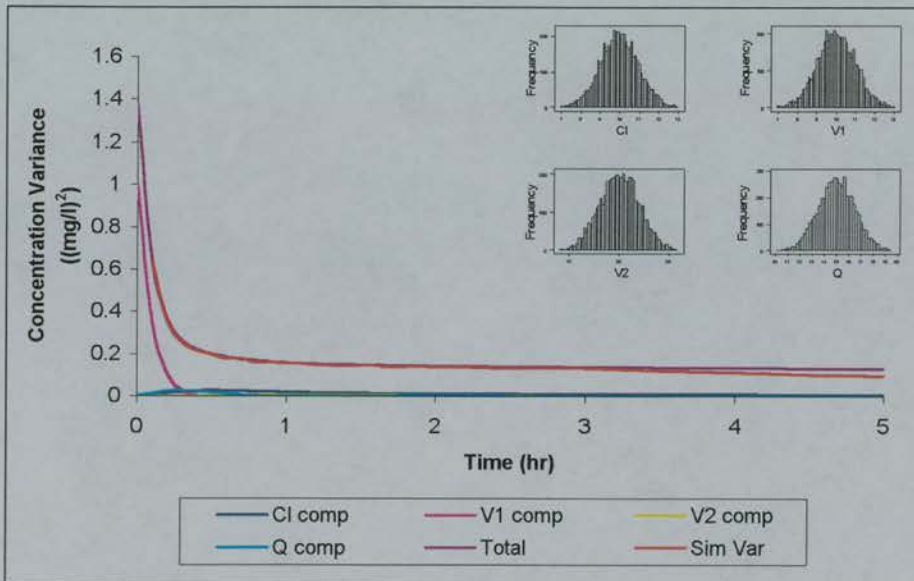


Figure 3.29 Concentration variance across time for $\omega_{CI} = 1$ l/h (random error).

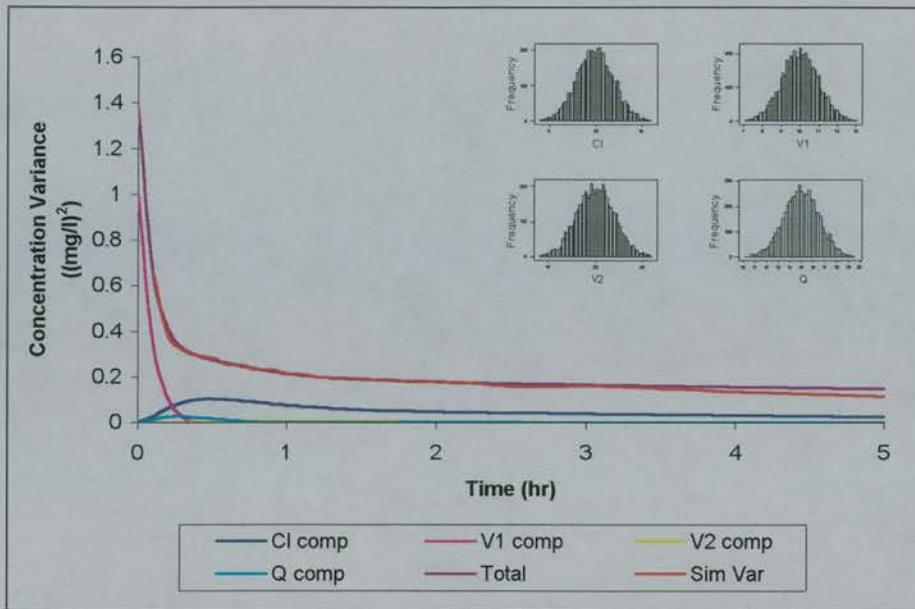


Figure 3.30 Concentration variance across time for $\omega_{Cl} = 2$ l/h (random error).

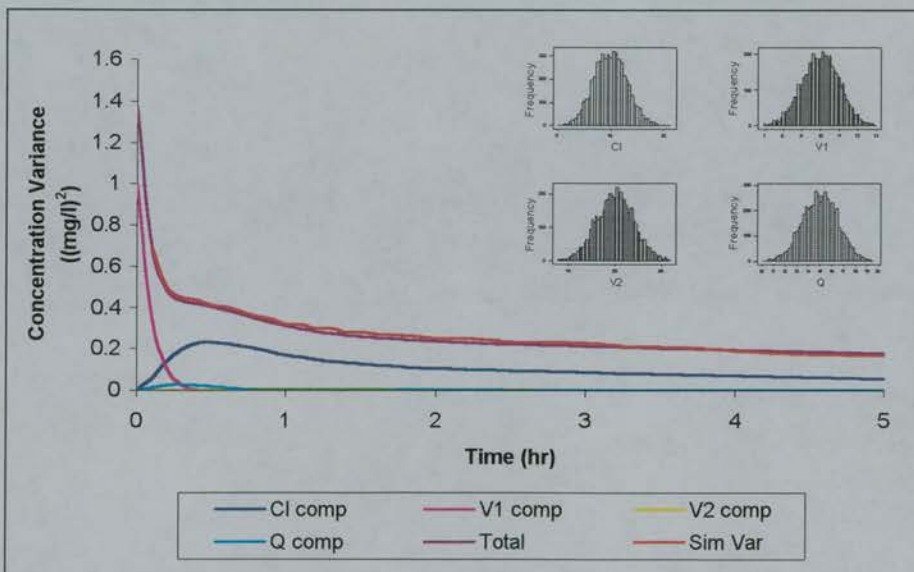


Figure 3.31 Concentration variance across time for $\omega_{Cl} = 3$ l/h (random error).

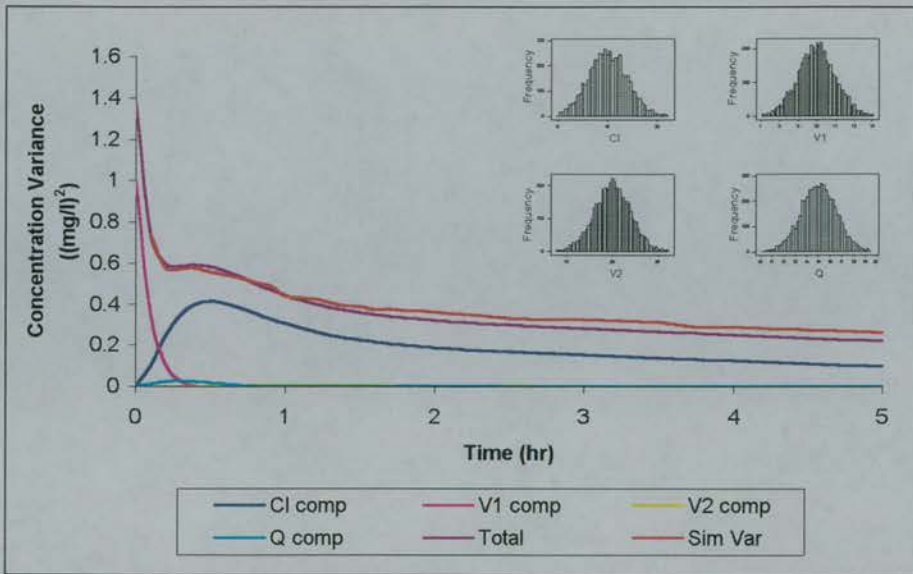


Figure 3.32 Concentration variance across time for $\omega_{CI} = 4$ l/h (random error).

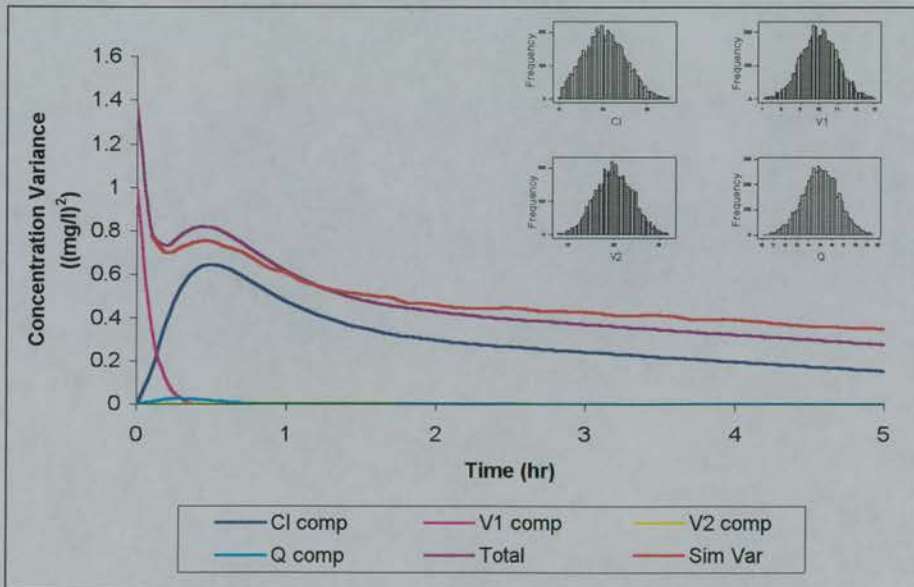


Figure 3.33 Concentration variance across time for $\omega_{CI} = 5$ l/h (random error).

Effect of High Concentrations on Total Concentration Variance Within a Population

Figures 3.34 and 3.35 show frequency histograms of the concentration distributions at 0.5 hr and 5.0 hr when $\omega_{Cl} = 3$ and 5 l/hr, respectively. The distribution at 0.5 hr is that obtained when concentration variance was maximal, and that at 5.0 hr corresponds to the last sampling time.

When $\omega_{Cl} = 3$ (Figure 3.34), the concentrations were Normally distributed at $t = 0.5$ hr, regardless of whether random error was added. As ω_{Cl} increased to 5 the concentration distribution remained Normal (Figure 3.35).

The concentration distribution at 5.0 hr was skew regardless of the amount of variability in clearance or whether random error had been added, again suggesting that at later times when concentrations are small in relation to the dose, the mean and standard deviation are not appropriate for describing the distribution.

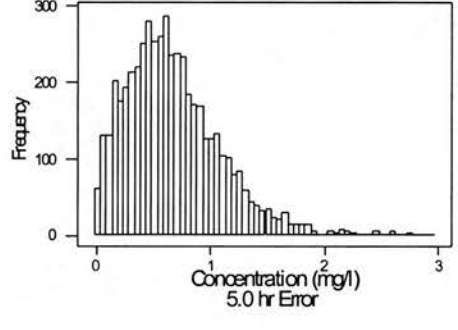
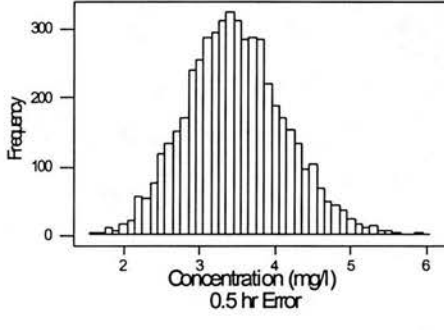
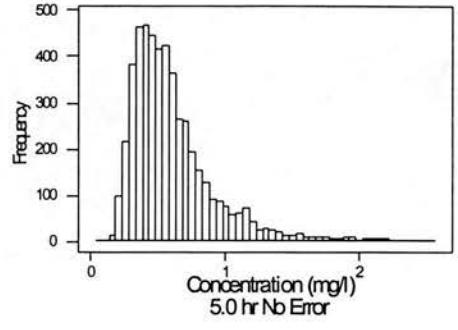
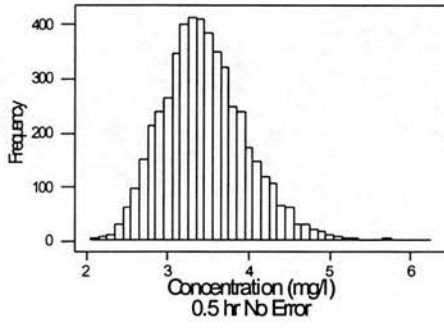


Figure 3.34 Histograms of Concentration at 0.5 hr and 5.0 hr when $\omega_{Cl} = 3$, with the Two-Compartment Model.

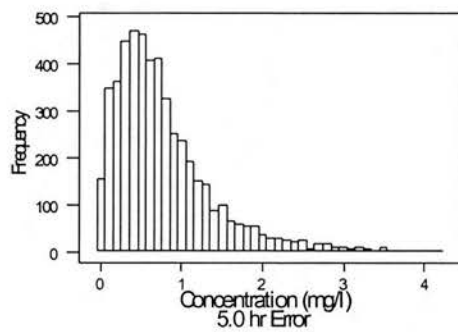
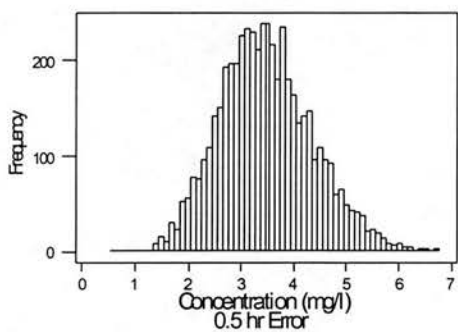
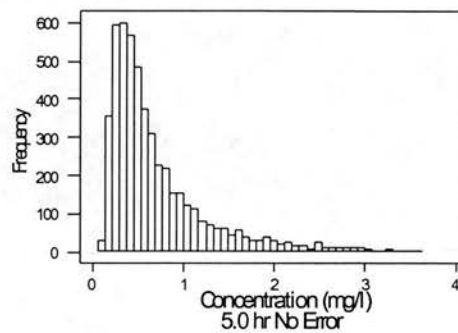
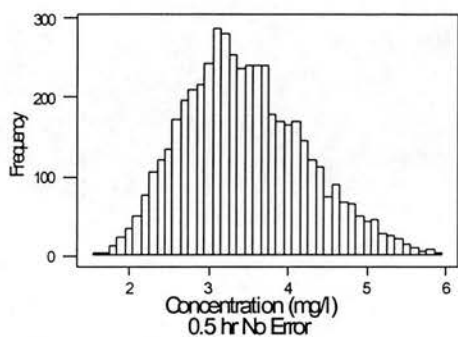


Figure 3.35 Histograms of Concentration at 0.5 hr and 5.0 hr when $\omega_{CI} = 5$, with the Two-Compartment Model.

3.3.4 Discussion

3.3.4.1 One-Compartment Model

Sensitivity analysis predicted that peaks in concentration variance would occur at the times $\frac{1}{k_e}$, due to the component from the variance in clearance and at 0 hr and $\frac{2}{k_e}$, due to the component from the variance in volume of distribution. The time of $\frac{1}{k_e}$ has also been identified as that which would produce estimates of clearance with a minimum variance (Døssing et al. 1983).

Using a simulated population of 5000 subjects showed that the peaks at $t = 0$ hr and $\frac{1}{k_e}$ were clearly visible, although the predicted one at $\frac{2}{k_e}$ was not, due to the magnitude of the other peaks.

When the variability for clearance was less than 20%, curves showing the simulated total concentration variance and the total calculated from the equations were superimposed. However, when the variability of clearance was greater than 30% the two curves diverged and the simulated concentration variance was greater than that calculated from the equations. The peak which occurred at exactly $\frac{1}{k_e}$ (1.0 hr) in the calculated variance curve moved slightly in the curve from the simulated population, to 1.1 hr, when the variability of clearance was 30% and to 1.2 hr when CV was 40-50%.

The mathematical proofs in Appendix 1 predicted that when random error was added to concentration, the times of maximal concentration variance became more dependent on the amount of variance for the clearance and volume parameters. However, as the divergence was noted regardless of whether random error was added, this result could not be attributed to its inclusion.

Examination of the concentration distributions at 1.0 hr and 5.0 hr showed that as the variability in clearance increased, the concentration distributions at 1.0 hr became skewed and at 5.0 hr they were highly skewed. This implied that at later times and higher parameter variability the SD, and hence the variance, was greater than expected due to a small number of high concentrations within the population. This accounted for the divergence between the simulated and predicted concentration variance curves at the later times.

When CV of clearance was 50% the separation of the curves began at around 1.0 hr (1.4 half lives). Sensitivity analysis in this study suggested that there was no advantage in sampling after 1.4 half-lives (peak in concentration variance at $\frac{1}{k_e} = 1.4$ half lives) and in theory this effect could be ignored if the last sampling time occurred at 1.4 half lives. However, most PK studies will sample to around 3-5 half-lives to verify that the PK model is appropriate. Hence, the occurrence of curve divergence and shifts in peak time in the one-compartment model could not be excluded on the basis of half-life. These results indicated that at high variability population simulations should be carried out in order to define the sampling times.

The effect was possibly due to the magnitude of the concentrations at later times in relation to the dose administered rather than number of half-lives that had passed. In particular the small number of high concentrations that artificially inflated the variance across the population. In addition another measure of the spread of concentrations rather than mean and standard deviation requires investigation. For example, the upper 95% limit of the distributions may provide values within the simulated populations that are the same as those predicted.

3.3.4.2 Two-Compartment Model

Initially, concentration variance was plotted over time, for simulated populations of 5000 subjects to define the times of peaks in concentration variance due to variability in each of the PK parameters Cl , V_1 , V_2 and Q . The effect on the times of peak

concentration variance in response to increasing variability of the parameters was also examined. This showed that any observed peaks tended to move slightly as the CV of each parameter was increased from 10-50%. For the parameter values used, the component due to variability in clearance gave rise to one peak in concentration variance at 0.5 hr. The component due to variability in V_1 gave rise to one at $t = 0$ hr and a second at 0.7 hr when CV of clearance was 10-30%; V_2 gave rise to one at 1.0 hr and Q gave rise to one at 0.3 hr and a second between 2.1 and 2.7 hr, depending on the variability of Q .

Populations of 5000 subjects were then simulated for the same parameter values, with and without random error on concentration. The concentration variance from these populations was compared to the total concentration variance predicted using Equation 3.16. In this set of simulations, the CV was fixed at 10% on all parameters except clearance, where it was varied from 10 to 50%.

The simulated and calculated concentration variance profiles for a two-compartment IV bolus PK model show that Equation 3.16 predicted peaks in concentration variance in close agreement to those seen in simulated populations of 5000 subjects, regardless of whether or not random error was added. The only peaks seen in the total variance curves were due to V_1 at $t = 0$ hr and Cl at 0.5 hr. This was because the contribution from these components was much larger than the contribution from the other components at the levels of variability examined.

Some divergence between the simulated and predicted curves was noted, but there were no shifts in the times at which the peaks in concentration variance were observed when the variability in clearance was 30-50%, unlike the one-compartment case.

Again, the concentration distributions were examined at the time of the maximum concentration variance in the simulated populations and at the last sampling time. These showed that the distribution of concentration at the peak in variance (0.5 hr) was Normal, regardless of the variance of clearance and whether random error was

added. The distributions at 5.0 hr were all skew, but not to the same degree as for the one-compartment model. However, the lack of divergence of the predicted and calculated concentration variance curves in the two-compartment model can be attributed to the fact that 5.0 hr is only $1.8 \cdot t_{1/2\beta}$. At this time the concentrations were not as small as they were at the same time in the one-compartment model and the distributions were less skew and less sensitive to a small number of large concentrations. Hence, later sampling times in this model may show the same effect as with the one-compartment model.

3.4 Conclusion

In the field of risk assessment sensitivity analysis has often been used to define physiologically based pharmacokinetic (PBPK) models which allow the determination of the effects of toxic chemicals and drugs on different organs and tissues of the body over time. The times at which the model output (concentration in an organ or tissue) is most sensitive to changes in each model input parameter (dose, blood flow rates into specific organs, organ/tissue weights) can be defined. The method involves examination of the partial derivatives of the output with respect to each of the input parameters and the total variability in the output parameter can be related to factors from each of the input parameters.

Sensitivity analysis of concentration variance with respect to each of the PK parameters included in the one-compartment IV bolus PK model showed that two peaks in concentration variance in addition to an initial peak at $t = 0$ hr should be present. In general, the predicted times corresponding to the peaks were in close agreement with those seen in simulated populations of 5000 subjects. However, the predictions of concentration variance from the derived equations were less accurate at high levels of variability on clearance when compared to the simulated concentration variance. This was shown to be due to the concentration distribution in the simulated populations becoming more skew at later times, as the variability on clearance increased. Hence, the calculation of concentration variance in the simulated populations was higher than that predicted from the equations derived from the sensitivity analysis. The use of simulated populations in conjunction with sensitivity analysis would overcome this discrepancy as the divergence of the two curves began as early as 1.4 half lives.

The two-compartment model proved to be more stable than the one-compartment model, in that there was greater agreement between the predicted and simulated concentration variance, even at high levels of variability in clearance. The concentration distributions were less skew at the later times used in these simulations, than the one-compartment model. Hence, the divergence observed with

the one-compartment model was not seen with the two-compartment model. However, the last sampling time of 5.0 hr in the two-compartment model corresponded to only $1.8 * t_{1/2\beta}$, whereas 5.0 hr in the one-compartment model corresponded to $7.2 * t_{1/2}$ and the divergence of the curves may perhaps be more apparent at this time on the two-compartment model. The divergence effect relates to the magnitude of the concentrations at the later times and would also depend on the dose given and the amount of random error present. The addition of random error reduced the divergence slightly, in that a smaller number of concentrations had to be removed in order to reduce the standard deviation of the remaining population to a value that was similar to that predicted.

In conclusion, in this chapter it has been shown that the times of peak concentration variance observed in simulated populations generally corresponded to the times of peak concentration variance obtained from sensitivity analysis. Hence, sensitivity analysis proved a useful tool for use in the design of limited sampling strategies for PK studies in conjunction with simulated populations where the parameter variability may be greater than 30% CV. The sampling times would correspond to the times of peak concentration variance and an 'optimal' sampling design may exist. These times should offer the most information about the parameters in question, in terms of accurate estimation, and designs based on these times are investigated in later chapters of this thesis.

Chapter 4

4 Limited Sampling in a One-Compartment IV Bolus Pharmacokinetic Model (Two Sampling Times)

4.1 Introduction

In chapter 3 sensitivity analysis of a one-compartment PK model suggested two sampling times that may offer improved parameter estimates over other sampling times, in a limited-sampling strategy. These were a sample taken as early as possible in order to estimate volume of distribution and a sample taken at $1.44 * t_{1/2}$ to estimate clearance. For the parameter values investigated in this section the sampling times corresponded to 0.1 hr and 1.0 hr, respectively. The concept of using sensitivity analysis to define sampling times is investigated in this chapter by the use of a simulation study.

Two study designs were compared: one based on the times defined by the sensitivity analysis and a second which used the same first time and a second chosen from a different point on the concentration variance curve. The comparisons related to the accuracy with which each of the PK parameters were estimated with each design and also to examine whether there were any benefits to using sensitivity analysis to define sampling times, over the use of other times.

Before continuing the investigation into study designs, two of the NONMEM estimation methods (first-order (FO) and first-order conditional (FOCE)) were examined as to which would provide the least biased and imprecise PK parameter estimates. The reason being that although the FOCE method is not the first choice for analysis of sparse data sets, some authors have suggested that estimation bias may be reduced with it's use (Al-Banna et al. 1990; Vozeh et al. 1990; White et al. 1991; Jonsson et al. 1996). Although this has been suggested in these studies, few studies have been published with comparison of the same data sets, using both methods of analysis. During simulations carried out in this chapter, it was noted that estimation bias increased as the variability in clearance increased and hence a direct

comparison of the NONMEM FO and FOCE methods in the analysis of sparse data was carried out.

Finally, the estimates of bias and imprecision obtained from ten sets of 500 subjects were compared to those obtained from 100 sets of 500 subjects, in order to define if the ten sets were a representative sample of the population. Generally only ten results would be considered a small number to make statistical comparisons from (the results are presented as the mean bias \pm 95% confidence interval from ten NONMEM estimates). However, in the simulations used in this thesis these ten results represent $10 \times 500 = 5000$ subject's data. The distribution of the ten results were compared to the distribution of 100 similar results to define whether only using 10×500 subjects was adequate for comparing different study designs.

In summary, this chapter examines three aspects designing PK studies: when to take samples, which method of analysis is best and how many sets of data require to be analysed.

4.2 Comparison of Two Sampling Designs based on Sensitivity Analysis

4.2.1 Methods

4.2.1.1 Data Simulation

Concentration-time data were simulated according to a one-compartment model, following a single IV bolus dose of 100mg of drug, as described in Chapter 2.

The values of the parameters used to simulate data for comparison of the two study designs are summarised in table 4.1. One hundred sets of 500 patients were simulated using an additive inter-individual error model on the PK parameters and a proportional intra-individual residual error model.

4.2.1.2 Sampling Designs

Sampling design 1 was based upon the times where maximum concentration variance occurred (chapter 3) and design 2 used one of these peaks combined with a second time which corresponded to the intersect of the concentration variance curves that were due to volume of distribution and clearance. This time was chosen to examine the effects of using a time where the both clearance and volume of distribution contributed the same to the total concentration variance.

Design 1. Two fixed sampling times corresponding to the two peaks in concentration variance (0.1 and 1.0 hr).

Design 2. Two fixed sampling times using the early peak and the time where the concentration variance curves due to each of the parameters intersected (0.1 and 0.5 hr).

The concentration variance curve is shown in Figure 4.1 and the sampling designs are summarised in Table 4.2.

4.2.1.3 Data Analysis

In the comparison of the two study designs, the parameters \bar{Cl} , \bar{V} , ω_{Cl} , ω_V and σ_1 were estimated using NONMEM First Order (FO) estimation with the posthoc option for calculating individual values of the η_i . The successful termination of the NONMEM runs was defined as completion of both the estimation and covariance steps along with accurate parameter estimates.

Calculation of the percentage bias and imprecision of the NONMEM population estimates, as described in Chapter 2, was used to compare the designs.

Table 4.1 Mean pharmacokinetic parameter values used to simulate data for comparison of Designs 1 and 2 (table 4.2) ^a

Parameter	Value
\overline{Cl}	10.0 l/h
\overline{V}	10.0 l
ω_{Cl}	1.0 l/h
ω_V	1.0 l
σ_l	0.1

^aIt was assumed that there was no covariance between Cl and V .

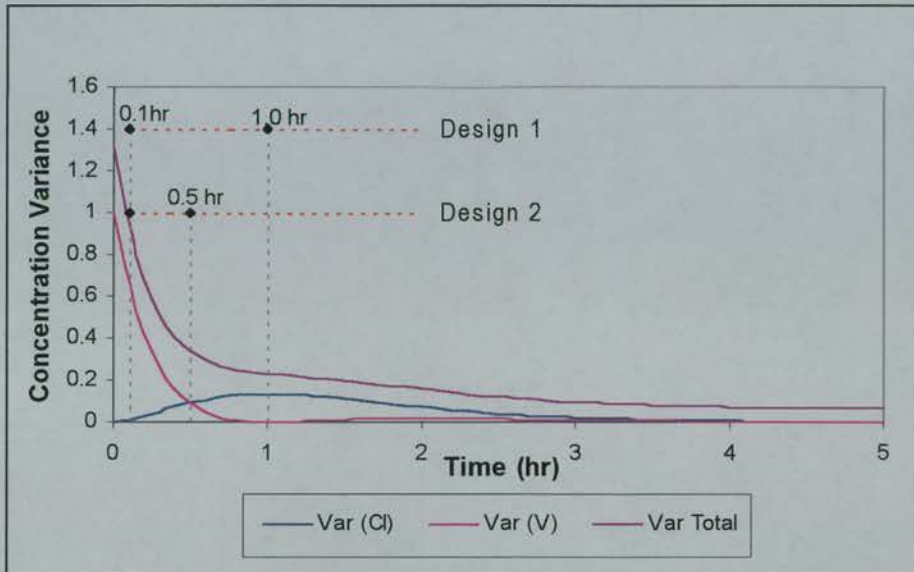


Figure 4.1 Sampling times for Designs 1 and 2 shown on the concentration variance curve. The curves show the contribution of each parameter (Var (Cl) and Var (V)) to the total concentration variance curve (Var Total).

Table 4.2 Sampling designs for a one-compartment IV bolus PK model using two fixed sampling times.

Design No.	Description	Time t_1 (h)	Time t_2 (h)
1	Two Peaks	0.1	1.0
2	Early Peak, Intersect	0.1	0.5

4.2.2 Results

During estimation of the PK parameters for comparison of designs 1 and 2, all data sets minimised successfully. Hence for each design and each PK parameter, there were 100 estimates available for analysis.

Figures 4.2, 4.4 and 4.6 to 4.8 show the percentage bias and precision for each parameter (\overline{Cl} , \overline{V} , ω_{Cl} , ω_V and σ_I) as estimated by NONMEM. Figures 4.3 and 4.5 show the comparison between the mean simulated values of clearance and volume of distribution and the mean NONMEM posthoc estimates of clearance and volume. These mean values were calculated for the 500 subjects in each of the 100 data sets for both sampling designs.

The average bias and imprecision for the population estimates of clearance are shown in figure 4.2. The values for design 1 were -0.87% and 0.52%, respectively, and 0.5% and 1.14%, respectively, for design 2. Figure 4.3 shows that design 1 consistently underestimated clearance, but that the estimates were close to the line of identity, when compared to the simulated value. Design 2 tended to overestimate clearance, but had a greater spread of results across the line of identity. Although generally, the best design would be the one with the least imprecision and bias, in this case no distinction could be made between designs 1 and 2 on this basis as the amount was so small.

Figure 4.4 shows the average bias and imprecision of the population estimates of volume of distribution, using both sampling designs. The mean values for design 1 were -0.78% and 0.75%, respectively and -0.94% and 0.83%, respectively, for design 2. Figure 4.5 shows that there was little difference between the designs in the posthoc estimation of volume of distribution and both designs 1 and 2 consistently underestimated the mean value of V within the populations.

The results for the estimation of the bias and imprecision of the standard deviation of clearance (ω_{Cl}) are shown in figure 4.6. ω_{Cl} was estimated accurately using design

1 with a mean bias and imprecision of -1.37% and 4.64%, respectively. However, design 2 was more inaccurate in estimating ω_{Cl} , shown by a wider 95% confidence interval for the bias (mean = -3.81%) and an unacceptable value of 28.8% for the imprecision.

The estimation of the standard deviation of volume of distribution (ω_V) was improved when design 2 was used, compared to design 1, as shown in figure 4.7. The values of mean bias and imprecision were -2.37% & 9.09% and -0.25% & 7.26% for designs 1 and 2, respectively. In addition, the 95% confidence interval for design 2 covered zero, suggesting that there may be no bias in estimating ω_V with this design.

Figure 4.8 illustrates the bias and imprecision for the estimation of the proportional random error on concentration (σ_I) and design 2 was more precise than design 1, although the mean bias was larger. The values of the mean bias and imprecision were -0.28 & 7.84% for design 1 and -1.62% & 5.0% for design 2.

Table 4.3 summarises the bias and precision estimates for designs 1 and 2 for all NONMEM population estimates of the PK parameters.

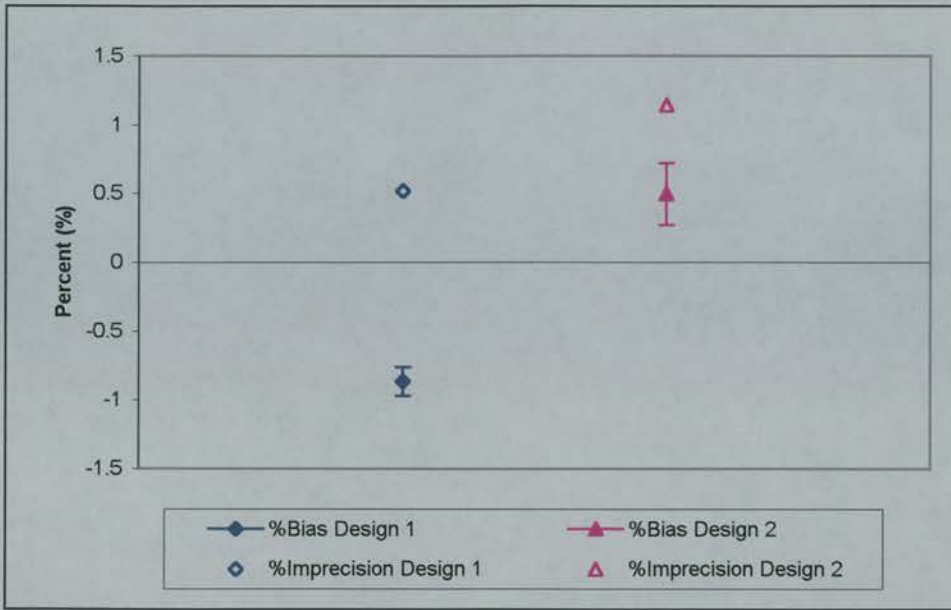


Figure 4.2 Bias ($\pm 95\%$ CI) and imprecision of the NONMEM population estimates of clearance (\overline{Cl}), using Designs 1 and 2.

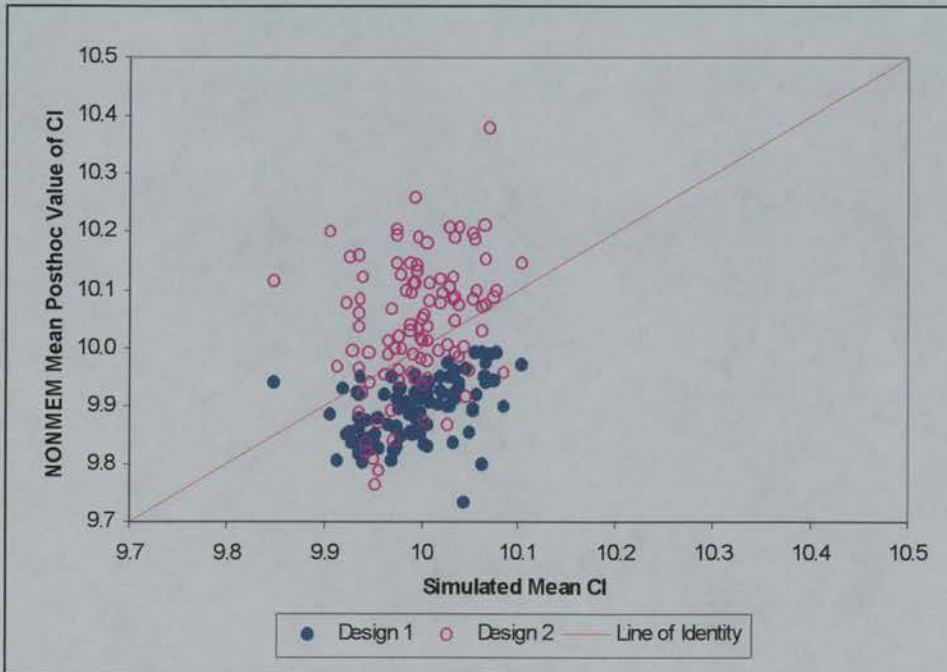


Figure 4.3 Comparison of mean individual simulated values of clearance with the mean NONMEM posthoc values

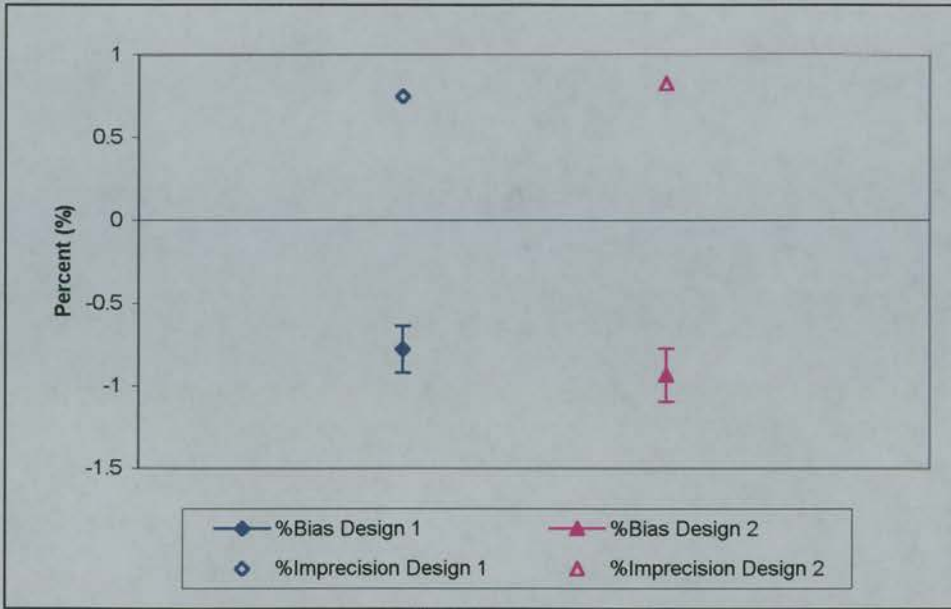


Figure 4.4 Bias ($\pm 95\%$ CI) and imprecision of the NONMEM population estimates of volume of distribution (\bar{V}), using Designs 1 and 2

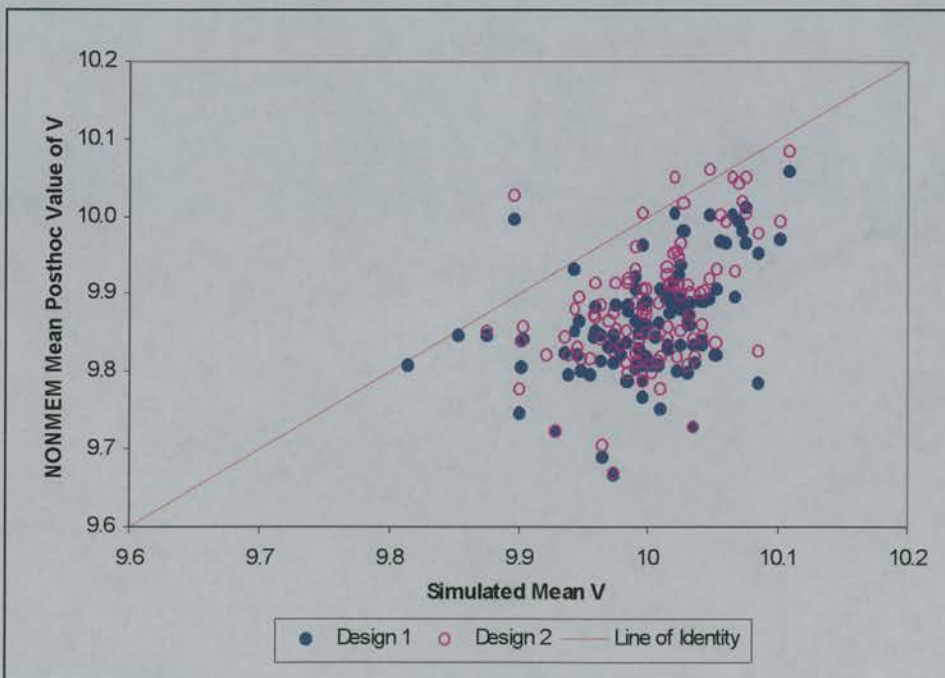


Figure 4.5 Comparison of mean individual simulated values of volume of distribution with the mean NONMEM posthoc values

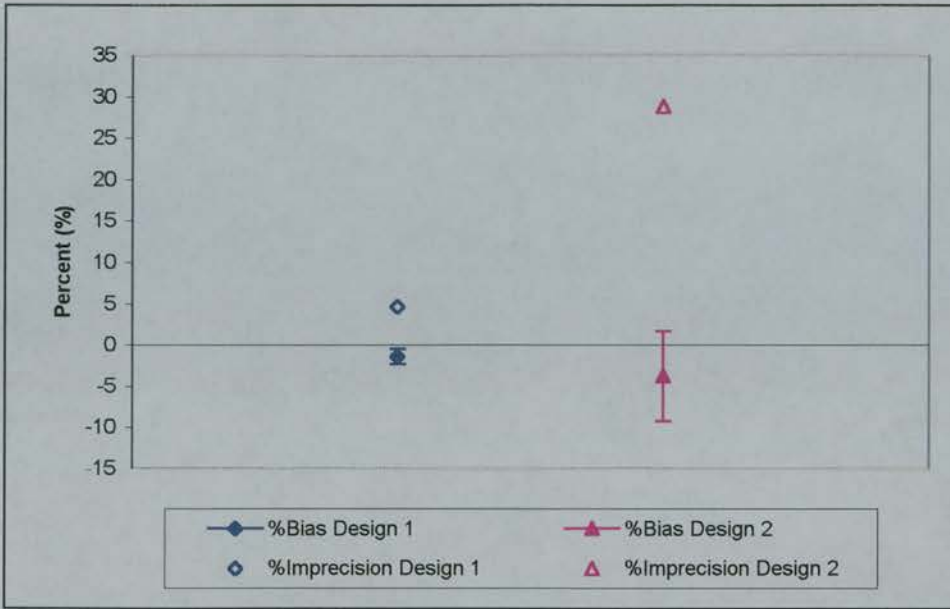


Figure 4.6 Bias ($\pm 95\%$ CI) and imprecision of the NONMEM population estimates of standard deviation in clearance (ω_{cl}), using Designs 1 and 2.

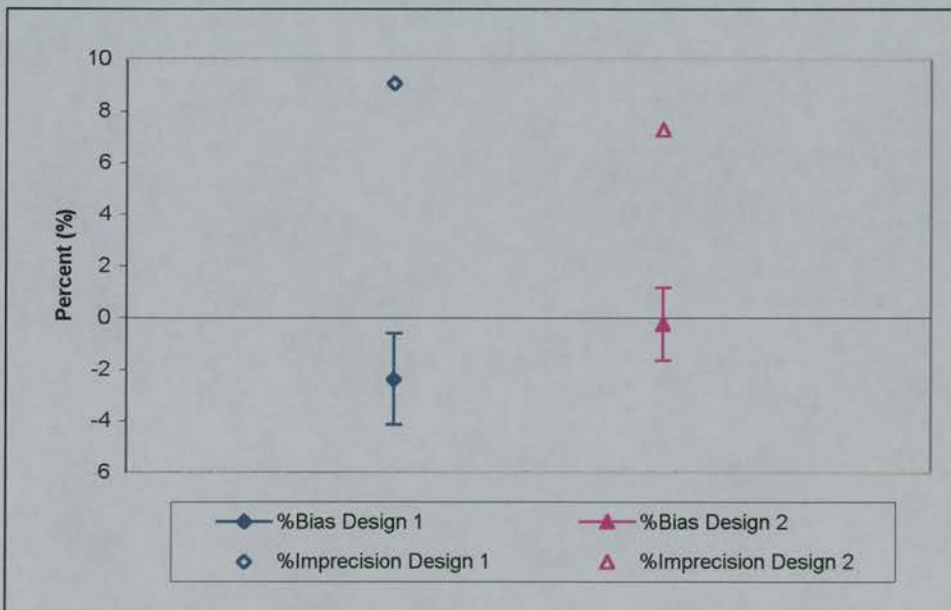


Figure 4.7 Bias ($\pm 95\%$ CI) and imprecision of the NONMEM population estimates of standard deviation in volume of distribution (ω_v), using Designs 1 and 2.

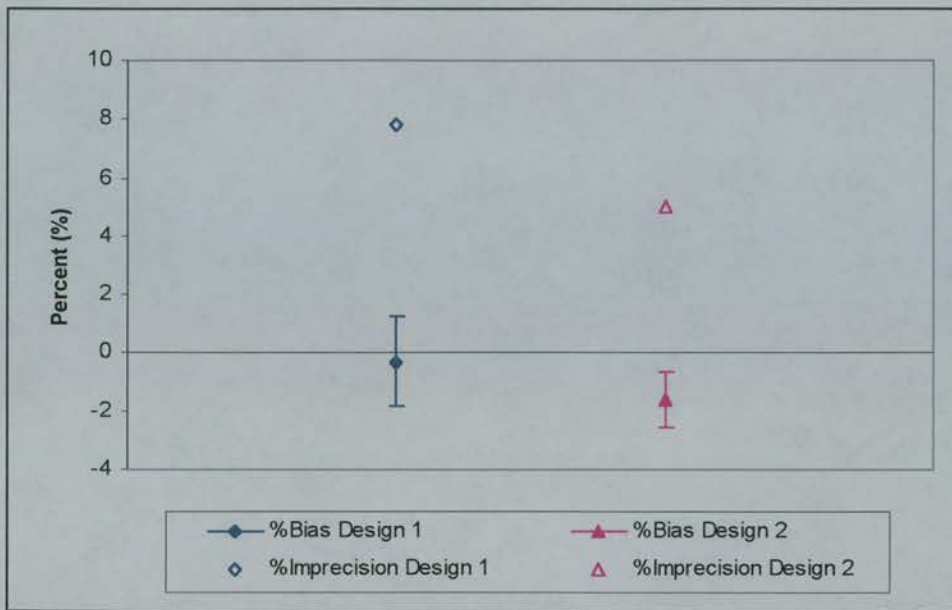


Figure 4.8 Bias ($\pm 95\%$ CI) and imprecision of the NONMEM population estimates of proportional intra-subject random error in concentration (σ_1), using Designs 1 and 2.

Table 4.3 Summary of bias and imprecision results using Designs 1 and 2 with NONMEM for estimation of PK parameters.

	Mean Bias (SE) (%)				
	\bar{C}_I	\bar{V}	ω_{C_I}	ω_V	σ_1
Design 1	-0.87 (0.05)	-0.78 (0.07)	-1.37 (0.46)	-2.37 (0.9)	-0.28 (0.79)
	0.52	0.75	4.64	9.09	7.84
Design 2	0.5 (0.11)	-0.94 (0.08)	-3.81 (2.77)	-0.25 (0.72)	1.62 (0.49)
	1.14	0.83	28.8	7.26	5.0

4.2.3 Discussion

Designs 1 and 2 showed little difference in the estimation of clearance (Cl), volume of distribution (V), standard deviation of volume (ω_V) and the proportional random error on concentration (σ_I). For these parameters the mean bias was less than 3% and the imprecision was within an acceptable limit of 10%. However, although standard deviation of clearance (ω_{Cl}), was estimated accurately with both designs in terms of having acceptable values of bias (less than 4%), design 2 was very imprecise with a value of 28.8%.

Examination of the posthoc estimates of Cl showed that there was a difference in the estimation of the clearance parameter, when compared to the true, simulated value. Design 1 underestimated clearance, but the estimates were closer to the true values than the estimates produced using design 2. This was also evident in the larger value for standard deviation of clearance using design 2. The poorer performance of design 2 in the estimation of clearance was as expected as the sampling time that had corresponded to the peak in concentration variance due to clearance was not included. Design 1 had sampled at the times that corresponded to the peaks in concentration variance that were due to both clearance and volume, whereas design 2 only included the peak due to volume. The times of peak concentration variance were those which were expected to contain the most information about the parameters that were attributed to them, from the results of the sensitivity analysis. Hence, it was expected that design 1 would estimate both clearance and volume accurately and that design 2 would only estimate volume accurately and this was evident in the results.

Overall, design 1 was the better of the two designs as it estimated all of the parameters with acceptable levels of imprecision and bias, whereas design 2 had a very imprecise estimate of ω_{Cl} at almost 30%. The large variability in estimation of this parameter made design 2 inappropriate for further investigation. The ultimate consideration of these designs is their usefulness in a clinical situation and an imprecision in estimation of 30% may translate into a higher imprecision when used

for prediction. Design 1 was the sampling design that was used for comparison with some empirical sampling designs in subsequent experiments.

4.3 Comparison of NONMEM FO and FOCE Methods

4.3.1 Methods

4.3.1.1 Data Simulation

Again, concentration-time data for this chapter were simulated according to a one-compartment PK model, following a single IV bolus dose of 100mg of drug, as described in Chapter 2.

The NONMEM FO and FOCE methods were compared using design 1, as described in table 4.2 with a population mean clearance (\overline{Cl}) of 10 l/h and the standard deviation of clearance (ω_{Cl}) was varied in different simulations from 1, 2, ..., 5 l/h, i.e., 10%, 20%, ..., 50% of the population mean. The population mean volume (\overline{V}) was fixed at 10 l with a standard deviation (ω_V) of 1 l.

The random intra-individual error model was changed to the combined one as described in Chapter 2, where ε_{1ij} and ε_{2ij} were sampled from $\varepsilon_1 \sim N(0, \sigma_1^2)$ and $\varepsilon_2 \sim N(0, \sigma_2^2)$. σ_1 and σ_2 were set to 0.05 and 0.25 mg/l, respectively. This represented a more realistic error model when compared to those used for analysis of real clinical data. The mean PK parameters used in the simulations to compare the NONMEM FO and FOCE methods are summarised in table 4.4. Ten sets of 500 subjects were simulated for each level of variability of clearance.

4.3.1.2 Data Analysis

In order to compare the FO and the FOCE methods directly, the parameters \overline{Cl} , \overline{V} , ω_{Cl}^2 , ω_V^2 , σ_1^2 and σ_2^2 were estimated by NONMEM, firstly using the FO method and secondly using FOCE with interaction. These methods are described in more detail in Chapter 2 and calculation of the percentage bias and imprecision of the NONMEM population estimates, was used to compare the designs.

Table 4.4 Mean pharmacokinetic parameter values used to simulate data for comparison of NONMEM FO and FOCE methods ^a

Parameter	Value
\overline{Cl}	10.0 l/h
\overline{V}	10.0 l
ω_{Cl}	Varied from 1.0, 2.0, ..., 5.0 l/h
ω_V	1.0 l
σ_1	0.05
σ_2	0.25 mg/l

^aIt was assumed that there was no covariance between Cl and V .

4.3.2 Results

Several runs failed to terminate successfully due either to NONMEM not completing the covariance step of the estimation following a successful minimisation of the objective function, or to NONMEM rejecting the data from one or more individuals. When the standard deviation for clearance (ω_{Cl}) was 4 and 5 l/h (i.e. 40 and 50%), NONMEM failed to terminate successfully at all using both FO and FOCE methods, apparently due to several individuals with particularly low clearance values. Removal of these individuals reduced the overall variance of the sample, but the data sets would still not terminate successfully. Hence the results with ω_{Cl} equal to 4 and 5 l/h were excluded from the analysis for both methods. In two out of the ten runs, with $\omega_{Cl} = 1$ l/h, NONMEM was unable to complete the covariance estimation step using the FO method, and these sets were removed from the results presented. Hence for these sets the mean and 95% confidence interval calculations were based on eight runs.

Estimation of Clearance

Figure 4.9 summarises the results for the estimates of the population average clearance. Using the FO method, there was no significant bias when the population $\omega_{Cl} = 1$ l/h (10%). However, as ω_{Cl} increased to 3 l/h (30%) a negative bias of -3.7% was introduced. The estimates of imprecision were small when $\omega_{Cl} = 1$ l/h, but became gradually more imprecise (ranging from 0.74% to 1.6%) as ω_{Cl} increased to 3 l/h.

FOCE resulted in a small bias (0.42%) in the average estimate of population mean clearance, but this was approximately constant for all values of ω_{Cl} up to 30% CV. The estimates became gradually more imprecise (ranging from 0.76% to 1.5%) as ω_{Cl} increased, similar to the FO method.

Estimation of Volume of Distribution

Using FO, the estimation bias for the volume of distribution (Figure 4.10) decreased in absolute magnitude from -0.96% to -0.53% as ω_{Cl} increased from 1 to 3 l/h. The degree of imprecision remained relatively constant at approximately 0.5% . The bias and the precision across all models for ω_{Cl} remained constant using FOCE.

Estimation of Standard Deviation of Clearance (ω_{Cl})

Figure 4.11 shows the results for the estimation of ω_{Cl} , the standard deviation of the population clearance distribution. Using FO, when $\omega_{Cl} = 1$ l/h, the estimated bias was -26.5% and this decreased in magnitude to -6.5% for $\omega_{Cl} = 2$ l/h and -1.1% for $\omega_{Cl} = 3$ l/h. Similarly, the imprecision improved as ω_{Cl} increased from 1 to 3 l/h (18.7% improving to 5.4%). In this case FOCE resulted in a decrease in estimation bias from -11.7% for $\omega_{Cl} = 1$ l/h to -3.6% when $\omega_{Cl} = 3$ l/h with a similar improvement in precision (11.6% to 4.4%).

Estimation of Standard Deviation of Volume of Distribution (ω_V)

No obvious pattern in bias and imprecision was determined in the estimation of ω_V , the standard deviation of the population distribution for volume of distribution, using the FO method (Figure 4.12). However, using FOCE, the confidence intervals for ω_V were reduced compared to those obtained when using the FO method, for all values of ω_{Cl} and the negative bias changed from -4.7% to -7.2% as ω_{Cl} increased from 1 to 3 l/h. The estimates became slightly less precise, when FOCE was used, as ω_{Cl} increased (5.3% to 7.0%).

Estimation of Intra-Subject Error (σ_1 & σ_2)

The results for the intra-subject variability components are shown in figures 4.13 and 4.14. The confidence intervals for the bias estimates for both the proportional component, σ_1 (figure 4.13) and the additive component, σ_2 (figure 4.14) were greatly reduced using the FOCE method. Figure 4.13 shows that the proportional

component was estimated with a positive bias, with the FOCE method, which remained relatively constant (8-9.5%). Figure 4.14 shows that, using FOCE, the bias in the additive component increased from 13.5% to 26.5% as ω_{Cl} increased. Imprecise average estimates for both the proportional component and the additive component resulting from the FO method improved with FOCE

Summary

In summary, in the estimation of the fixed effect parameters, clearance and volume, the FOCE method removed patterns in bias introduced as ω_{Cl} increased. In the cases of the random effects, inter and intra-individual error, the mean bias was reduced and the precision improved. In general, the results were more stable using the FOCE method.

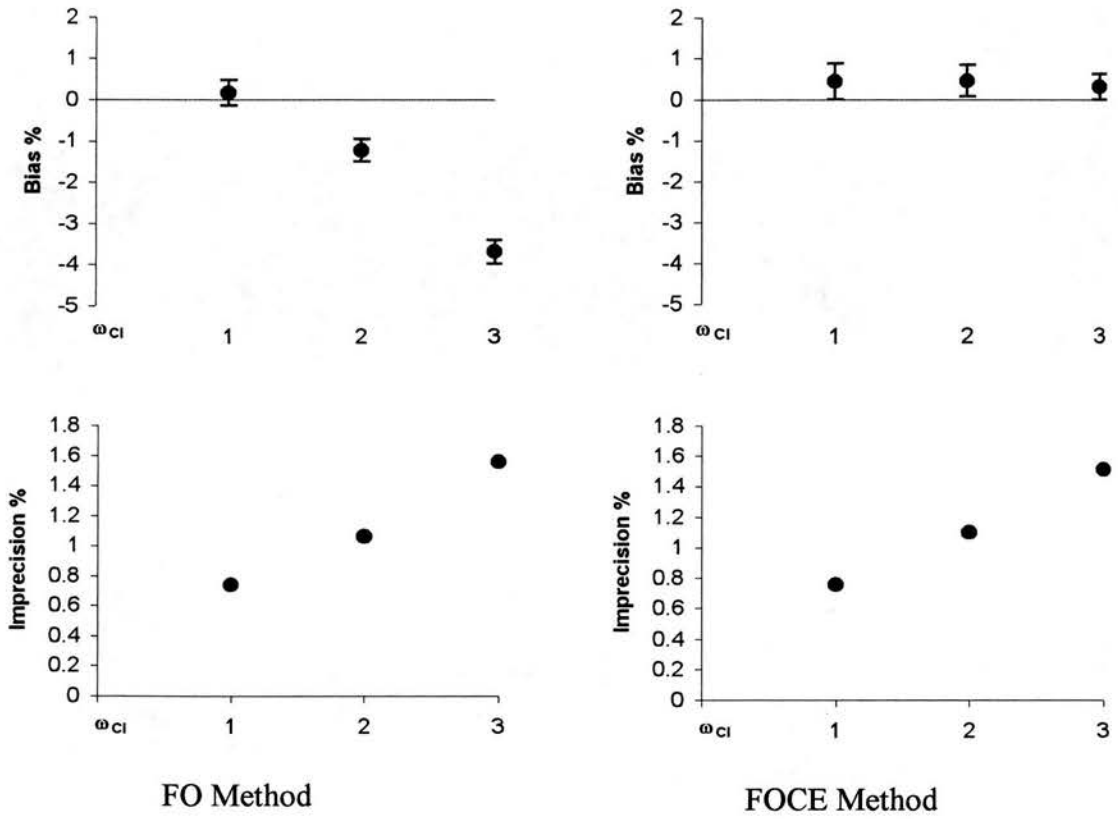


Figure 4.9 Bias (mean and 95% CI) and imprecision results for the estimates of population mean clearance.

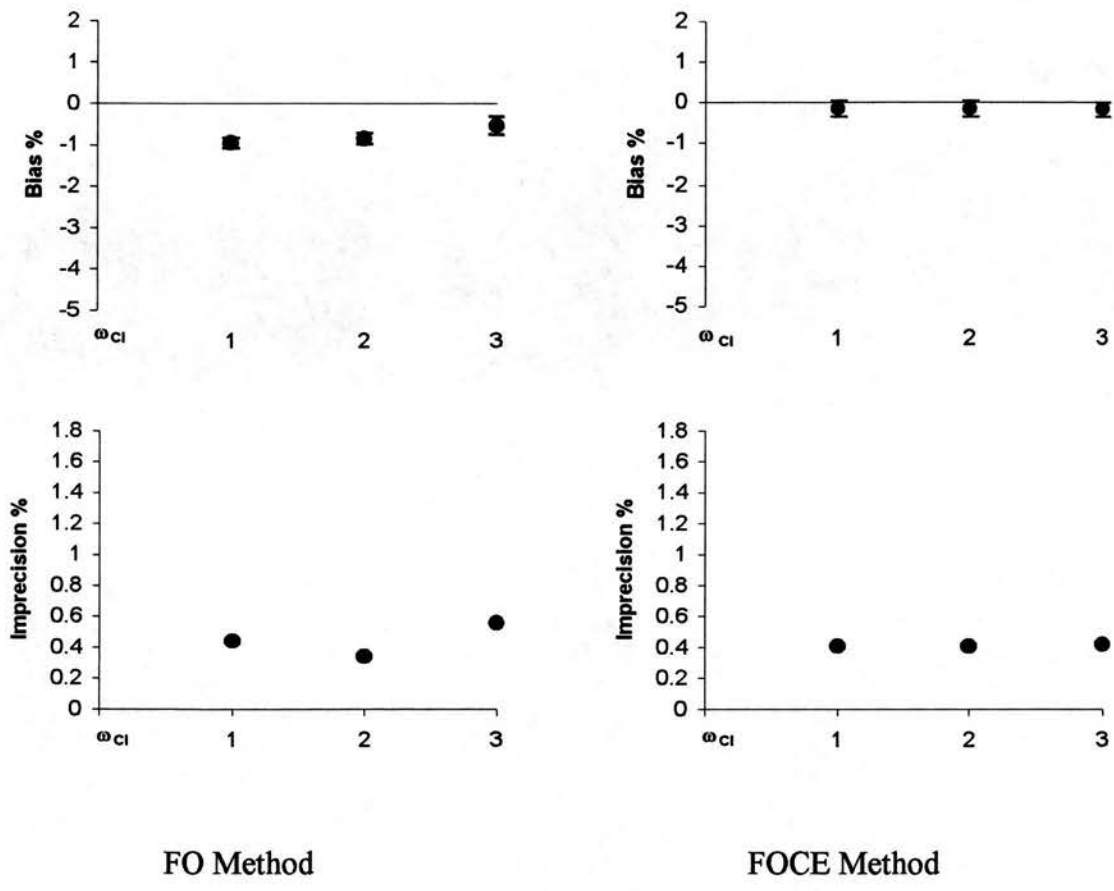


Figure 4.10 Bias (mean and 95% CI) and imprecision results for the estimates of population mean volume of distribution.

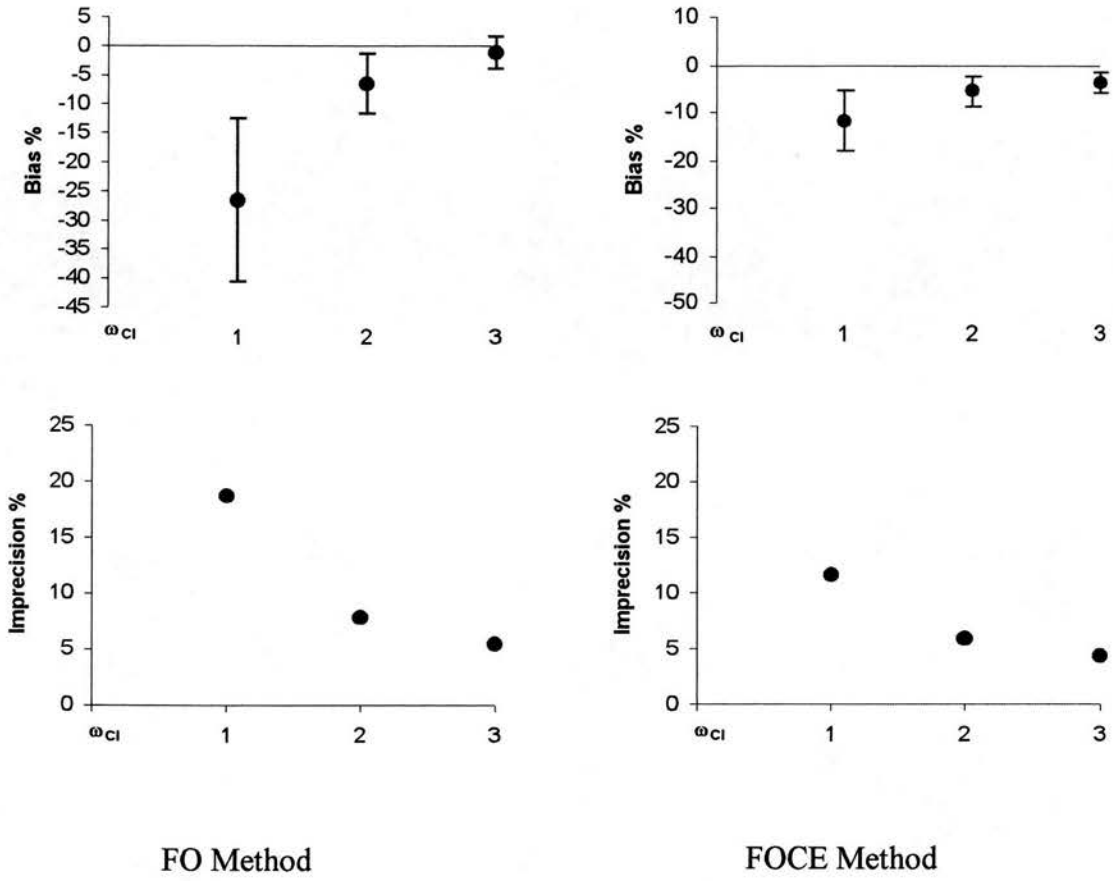


Figure 4.11 Bias (mean and 95% CI) and imprecision results for the estimates of the standard deviation of the population clearance distribution (ω_{Cl}).

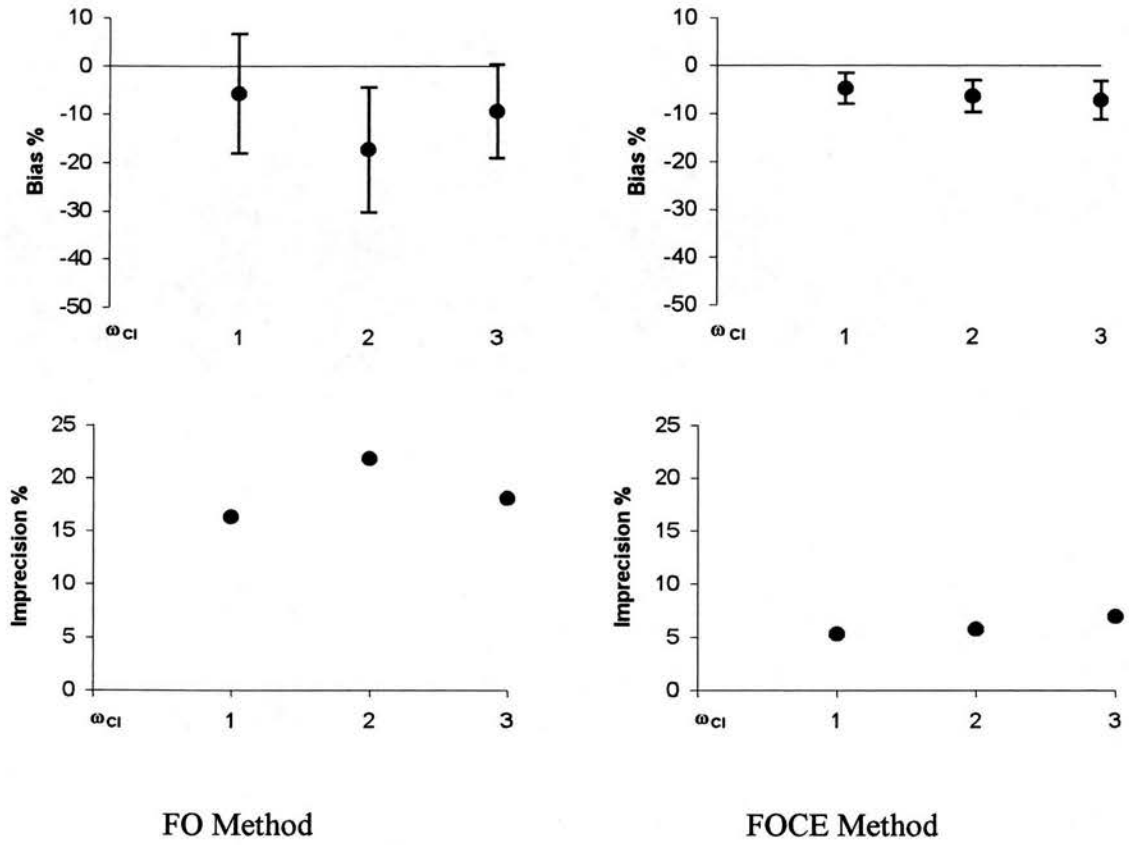


Figure 4.12 Bias (mean and 95% CI) and imprecision results for the estimates of the standard deviation of the distribution of the population volume of distribution (ω_V).

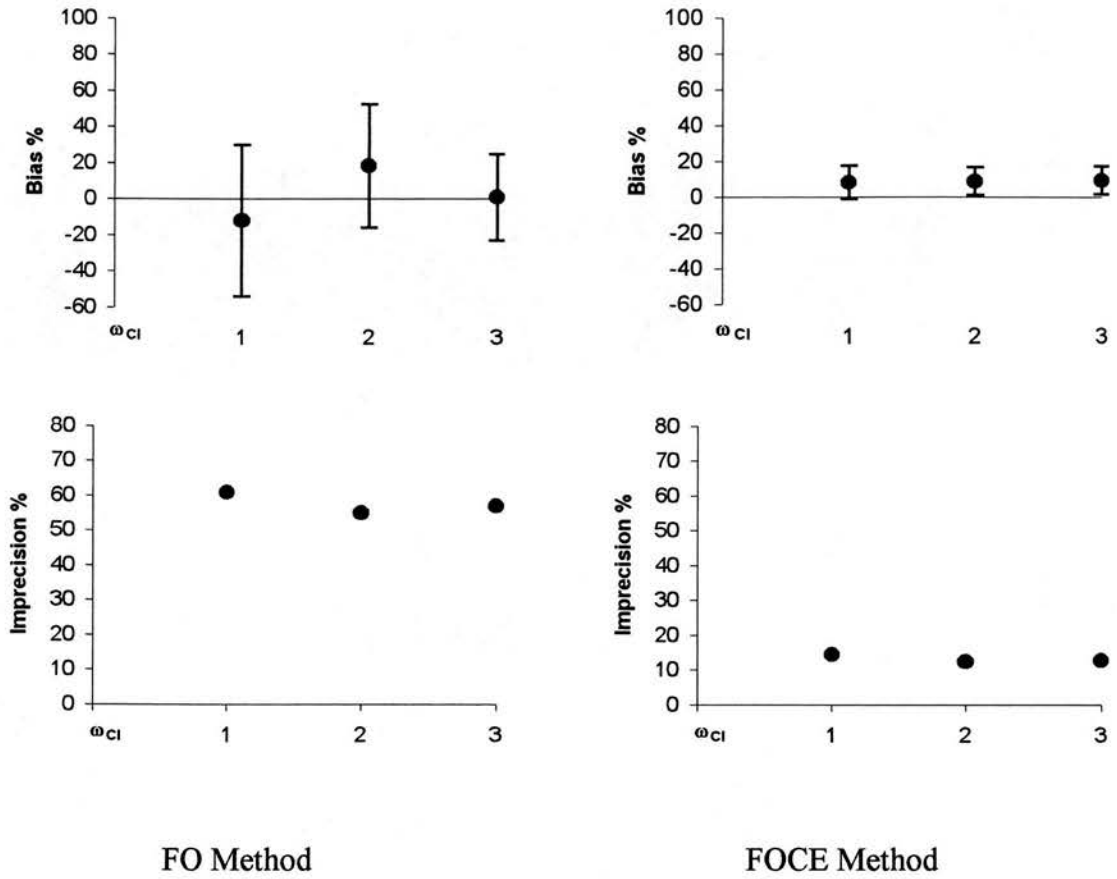


Figure 4.13 Bias (mean and 95% CI) and imprecision results for the estimates of the proportional error component (σ_I).

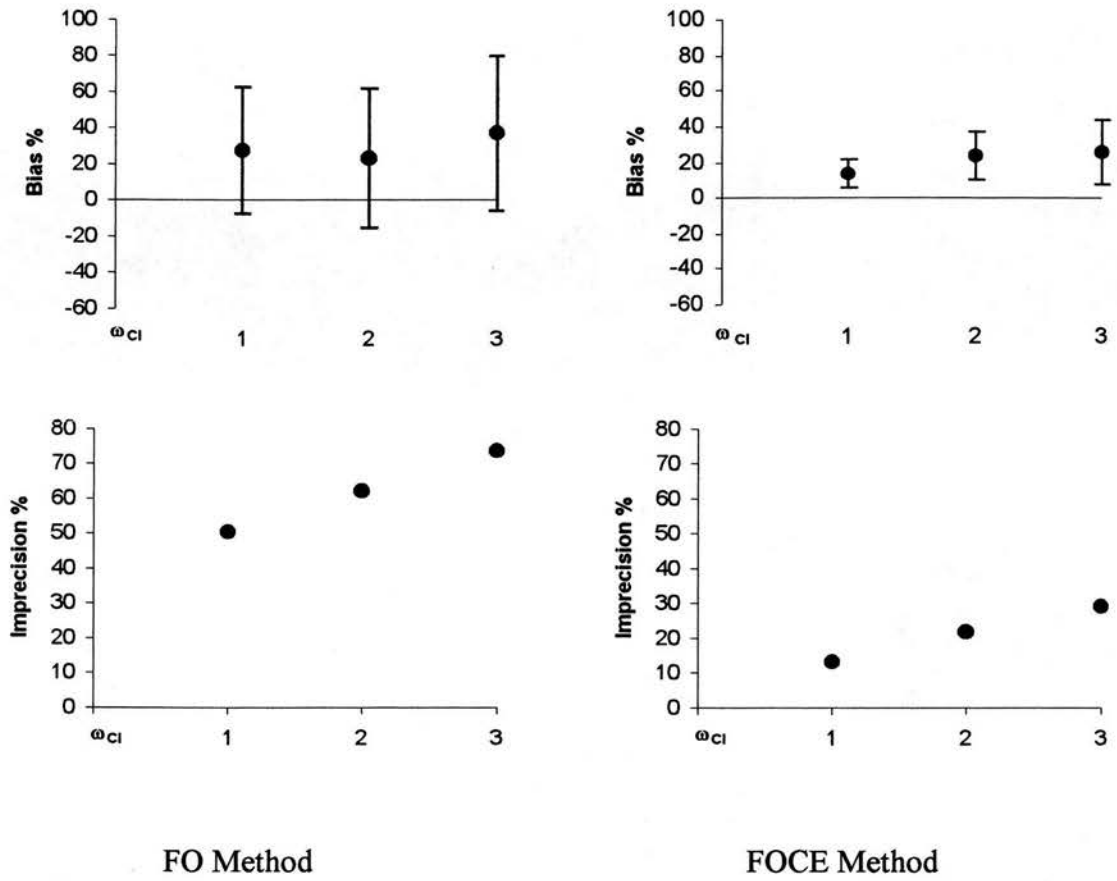


Figure 4.14 Bias (mean and 95% CI) and imprecision results for the estimates of the additive error component (σ_2).

4.3.3 Discussion

The First-Order (FO) and the First-Order Conditional Estimation (FOCE) methods implemented in NONMEM were investigated in this simulation study, in which the effect of altering the standard deviation (ω_{Cl}) of the population distribution for clearance was examined while all other factors remained constant.

The negative bias in the population estimates of clearance as ω_{Cl} increased confirmed the results reported by Al-Banna et al (1990) using FO. There was also a small negative bias in the estimation of volume of distribution. However, both of these effects were virtually eliminated using FOCE.

There was no difference between FO and FOCE in the degree of precision with which the mean values for clearance and volume were estimated.

The bias and precision for volume remained relatively constant across the range of clearance variability investigated. This was probably due to the population variability in volume being fixed at only 10% and also to the first sampling time being shortly after administration.

Other authors have noted similar results. White et al (1991) reported increasing bias in the estimates of clearance, and ω_V as the variability in the clearance and volume of distribution or random intra-subject error increased. The bias in clearance was negative, similar to the current study, but the absolute values cannot be compared as the variability in the population parameter distributions was different. Vozech et al (1990) showed that although the bias in parameter estimates was significant, it was also relatively small. However, using the anaesthetic agent alfentanil as an example, they also showed that small biases could translate into prediction intervals with clinically significant implications. In another simulation study comparing some practical sampling designs with sparse data, Jonsson et al (1996) noted that the FOCE method reduced the bias and improved the precision with which clearance and ω_{Cl} were estimated.

Satisfactory parameter estimation has been defined as estimates of fixed effects having little (less than 15%) or no bias and imprecision of less than 25% (Ette et al. 1998). Using these criteria the fixed effect parameters, clearance and volume, were satisfactorily estimated using the FO method. However, when examined closely, a negative bias was introduced as the standard deviation (ω_{Cl}) on clearance increased.

Both FO and FOCE produced biased estimates for the population parameters, ω_{Cl} and ω_V . In the case of ω_{Cl} , bias was approximately -30% when the true standard deviation was 1 l/h (10% CV) and decreased as the true variability increased. The precision also improved as the variability increased. Although the FOCE method did not remove the bias, it was considerably reduced. The degree of precision was similar using both estimation methods. Thus, it appeared that the parameter estimates were less biased when there was greater inter patient variability in clearance.

The results for ω_V were less consistent, but for all values of ω_{Cl} , the bias for ω_V was less and the results more precise using FOCE.

FOCE also produced more accurate and precise estimates for the intra-individual error components than FO, but these still showed a significant positive bias of 10-30%, presumably reflecting the sparse nature of the data.

Comparisons of NONMEM in the scientific literature are often with the 'standard two-stage' method of analysis which relies on linear regression techniques for estimation of PK parameters. NONMEM has been shown to result in similar estimates of fixed effects even when the number of samples included in the NONMEM analysis was reduced to three from the twelve used in the standard two-stage analysis (Grasela et al. 1986). In addition, the use of NONMEM resulted in reduced estimates of the inter-subject variability by the inclusion or exclusion of covariates and the partitioning of errors into that due to inter and intra-subject error (Yu et al. 1994; Vadiee et al. 1997).

NONMEM has been compared to other population pharmacokinetic analysis computer programs and the NONMEM FO method was shown to give similar parameter estimates to other first-order estimation programs (Roe 1997). In addition, the FOCE method has resulted in parameter estimates that were similar to other conditional and Bayesian estimation methods using both simulated (Roe 1997) and clinical (Racine-Poon et al. 1998) data. The FO method has also been shown to give improved parameter estimates over a computer program which incorporates a two-stage type of algorithm, but inferior estimates to the Bayesian algorithm (Bennett et al. 1996).

There is a lack of published direct comparisons of the FO and FOCE methods on the same data set. However, in a comparison with a Bayesian two-step algorithm from another computer program, P-PHARM, the FOCE method was noted to result in similar parameter estimates, using a three-sample, one-compartment PK model, for simulation (Mentré et al. 1995b). This study also included a comparison to the FO method which resulted in greater bias and imprecision than either of the other two methods of analysis.

In the particularly sparse design examined in this section, FOCE largely removed the bias in the population estimates noted using the FO method. CPU time was not an issue with these data sets, although it may become one with larger, more complex data sets or when using more complex models, perhaps including covariates. However, this study has demonstrated the importance of using the FOCE method either throughout an analysis, or at least as a check of the final results, as recommended in the NONMEM manuals (Beal et al. 1998).

4.4 Comparison of Results from 10 Sets of 500 subjects with those from 100 sets of 500 Subjects

4.4.1 Methods

4.4.1.1 Data Simulation

Similar to the other sections in this chapter, the concentration-time data were simulated according to a one-compartment model, following a single IV bolus dose of 100mg of drug, as described in chapter 2.

Data for one hundred sets of 500 subjects were simulated using design 1 from table 4.2 and the parameter values described in table 4.4. The PK parameters were estimated using the NONMEM FOCE method and the bias of the 100 parameter estimates was calculated as described in chapter 2. The distributions of the 100 parameter estimates obtained in this section were compared to the distributions of the ten parameter estimates obtained in section 4.3, to establish if the initial ten sets of 500 were representative of the population.

4.4.1.2 Data Analysis

The distributions of the parameter estimates from 100 runs were compared to those obtained from 10 runs by the use of box and whisker plots. The bottom line of the box in each figure represents the first quartile (Q1) and the top line the third quartile (Q3). The median value of the data is represented by a line across the middle of the box. The whiskers are the lines that extend from the top and bottom of the box and define the upper and lower limits $[Q3 + 1.5 (Q3 - Q1)]$ and $[Q1 - 1.5 (Q3 - Q1)]$, respectively. Outliers are defined as data points which lie outwith the limits and are plotted with asterisks (*).

4.4.2 Results

All data in this section were analysed using the NONMEM FOCE method and the distribution of parameter estimates across 100 sets of 500 subjects was compared to those obtained from 10 sets of 500 subjects. Figures 4.15 to 4.20 show the comparisons of the spread of estimates of the PK parameters \overline{Cl} , \overline{V} , ω_{Cl} , ω_V , σ_1 and σ_2 , respectively.

In all figures the median value of bias was greater when only ten runs were used instead of 100. The distributions of ten runs overlap those of 100 runs in the estimation of all parameters. No line is evident for the median of 100 runs for the estimation of volume of distribution as the upper quartile (Q3) value was equal to the median value of 0%. In the estimation of the fixed effect parameters, Cl and V , the difference in the median bias was less than 0.4% and this increased to 7% for the inter-subject variability parameters ω_{Cl}^2 and ω_V^2 . The average difference for the bias in the estimation of the proportional error component was 9% in absolute terms, although this was in the opposite direction, i.e., positive bias for the ten runs and negative bias for the 100 runs. However, the difference in median bias was greatest for the estimation of the additive random error component where the difference between 100 and 10 runs was approximately 30%.

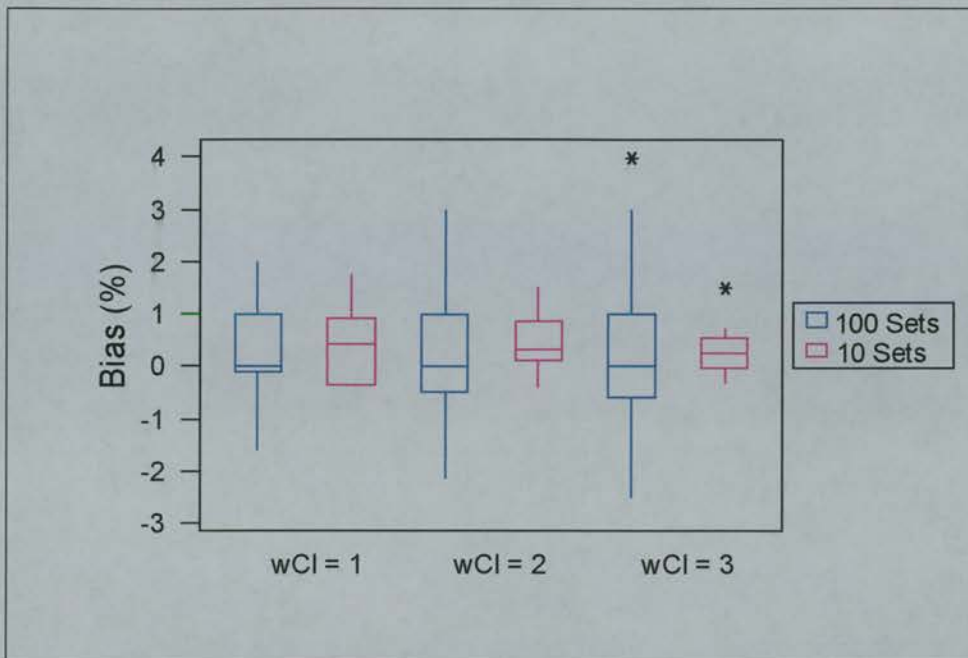


Figure 4.15 Comparison of average bias and imprecision in the estimation of clearance (CI), using either 100 or 10 sets of 500 subjects.

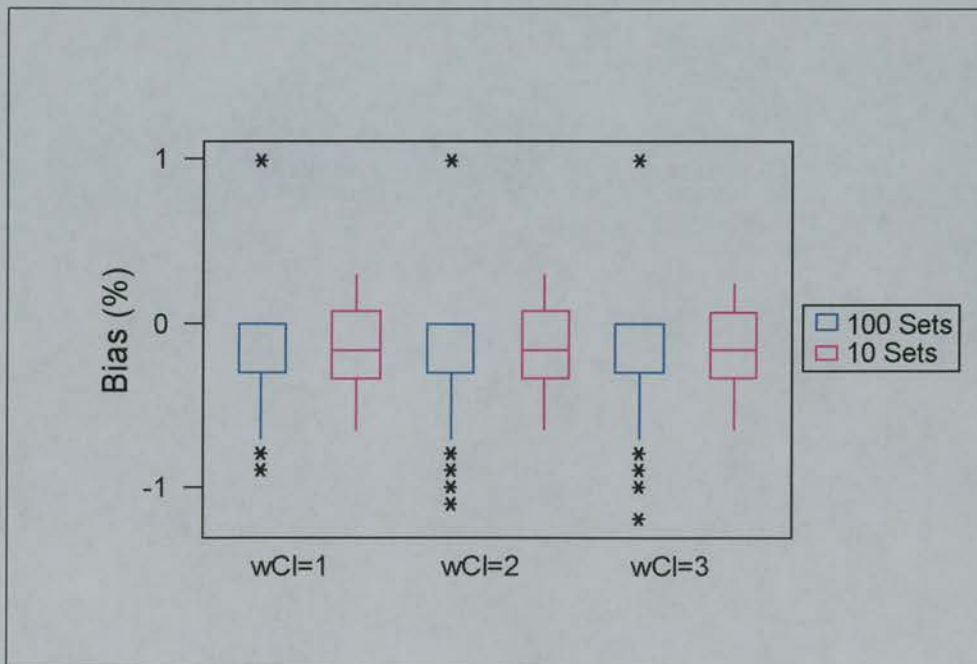


Figure 4.16 Comparison of average bias and imprecision in the estimation of volume of distribution (V), using either 100 or 10 sets of 500 subjects.

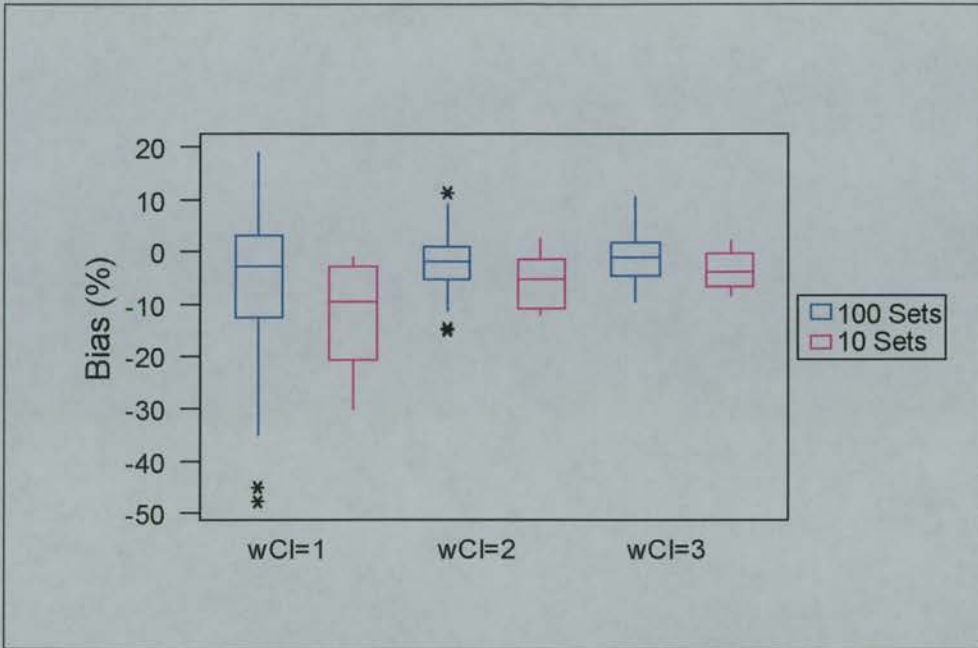


Figure 4.17 Comparison of average bias and imprecision in the estimation of standard deviation of clearance (ω_{Cl}), using either 100 or 10 sets of 500 subjects.

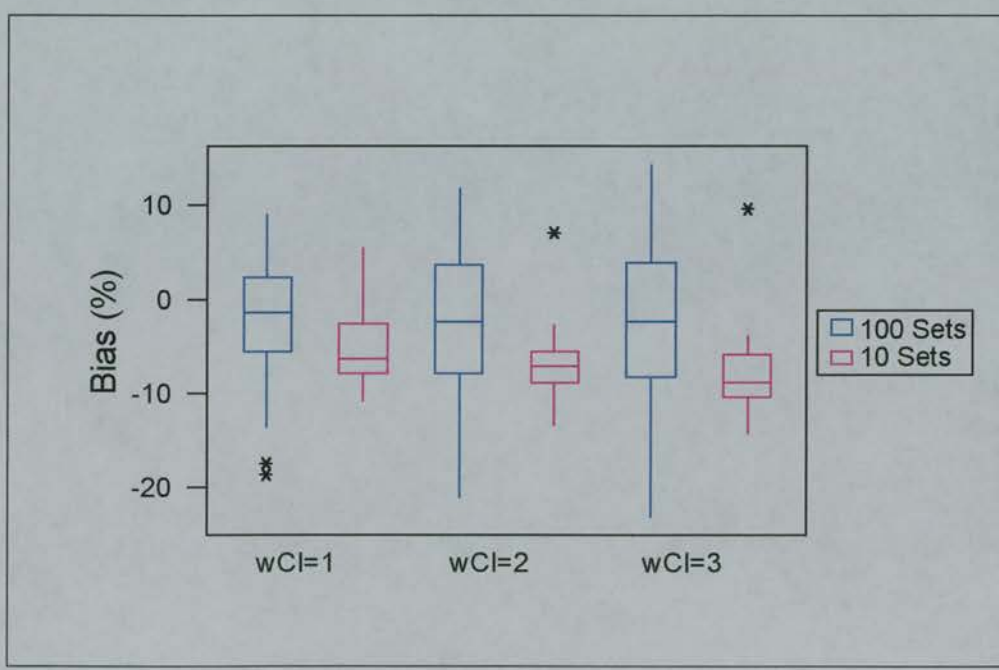


Figure 4.18 Comparison of average bias and imprecision in the estimation of standard deviation of volume of distribution (ω_V), using either 100 or 10 sets of 500 subjects.

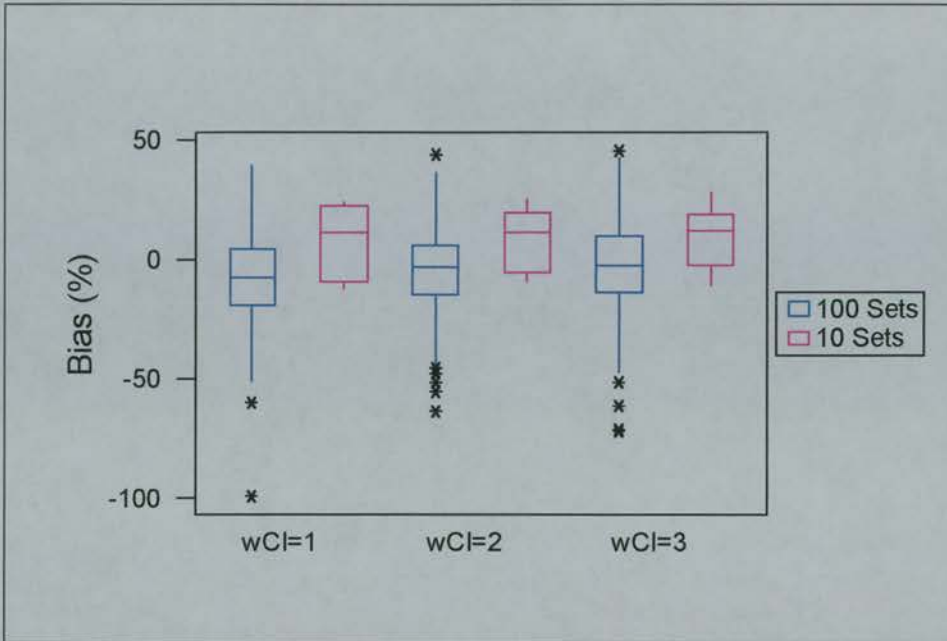


Figure 4.19 Comparison of average bias and imprecision in the estimation of the proportional random error component (σ_1), using either 100 or 10 sets of 500 subjects.

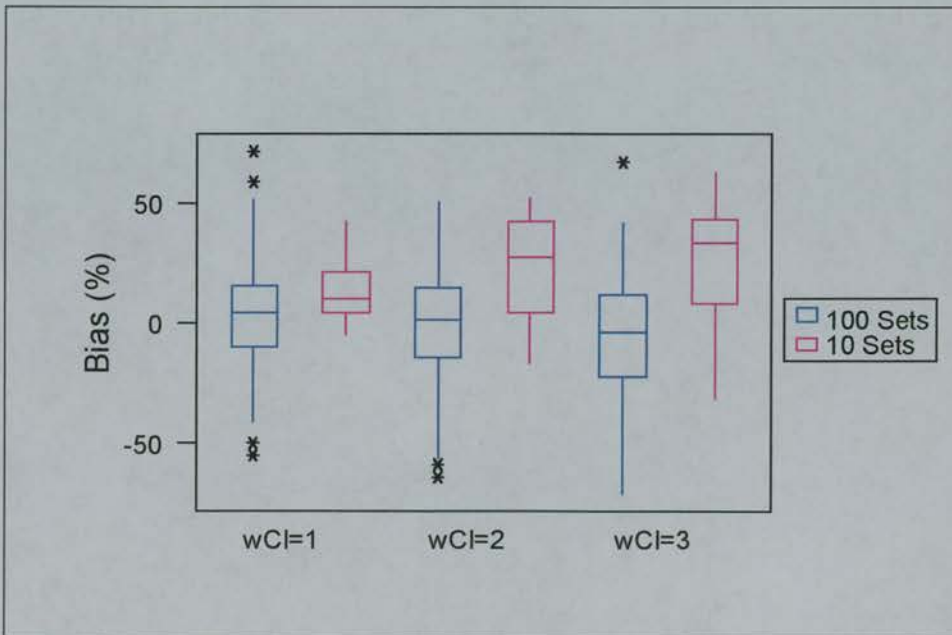


Figure 4.20 Comparison of average bias and imprecision in the estimation of the additive random error component (σ_2), using either 100 or 10 sets of 500 subjects.

4.4.3 Discussion

The third section of this chapter examined the effect of the number of NONMEM runs on the estimates of bias. This was carried out to examine whether ten population estimates of the PK parameters was representative of the whole population. In general, an n of 10 would be considered small, but overall these estimates were from $10 \times 500 = 5000$ subject, which is a large sample size. However, a comparison was made with 100 population estimates of PK parameters which represented $100 \times 500 = 50,000$ subject's data.

The results were satisfactory for the fixed effects (Cl and V), the random inter-subject effects (ω_{Cl} and ω_V) and the random proportional component of intra-subject error (σ_1) in that although the median bias over 100 runs was slightly different to that obtained with ten runs, the distributions of results overlapped. The median bias results for the estimation of the additive component of the random intra-subject error (σ_2) showed greater deviation, but the distributions for both sets of results remained overlapped due to the large variability in the estimation of this parameter. The poor estimation of this parameter can be attributed to the sampling design. Additive random errors are best estimated with later sampling times when an additive component affects low concentrations to a greater extent.

Hence, it was considered that the 10 sets of 500 subjects was representative of the results that would be obtained from 100 sets of 500 subjects. For this reason 10×500 subject's data were simulated and analysed in the remaining PK designs in this thesis. The main reason being that although the time factor was not an issue in using FOCE method of analysis for ten sets of data, it would become one for the analysis of 100 sets of data for each design.

4.5 Conclusion

Sensitivity analysis carried out in chapter 3 suggested two sampling times that would offer accurate parameter estimation of the parameters Cl and V for a one-compartment PK model. These were a sample taken as early as possible to estimate volume of distribution and a sample taken at $1.44*t_{1/2}$ to estimate clearance.

Sampling design 1 utilised both of these times and was compared to design 2 which used the first of these times and a second time chosen from the concentration variance curve where the curves due to each parameter intersected. Comparison of these designs showed that sampling at the times suggested by sensitivity analysis gave more precise parameter estimates for all of the parameters, rather than only a few of them, when the samples were taken at times that hold less information about the parameters. The main drawback of design 2 was that it had an unacceptably high level of imprecision in the estimation of ω_{Cl} , which in a clinical situation may lead to errors in predicting doses for individuals. This preliminary experiment showed that sensitivity analysis was a useful tool for defining sampling times and further comparisons with 'empirically' chosen designs were carried out later in this thesis to investigate this.

Before further experiments were carried out, two intermediate simulations were undertaken: comparison of the NONMEM FO and FOCE estimation methods and comparison of the estimation results from two different sample sizes.

It was shown in this chapter that the FOCE method removed bias introduced by the FO method, even though the data in these simulations were sparse. These results were consistent with similar results in the scientific literature. In the past the major drawback to using the FOCE method of analysis was the increase in computer time required to undertake the analysis. However, this is less of a problem with higher performance computers that are available. Time to analyse the data sets was not an issue in this study and hence due to the results in section 4.3, the FOCE method was used to analyse the data in all other chapters of this thesis.

While comparing the FO and FOCE methods data from only ten sets of 500 subjects were analysed for each PK study design where previously in section 4.2 100 sets of 500 subject's data had been analysed. If 100*500 subjects data had to be analysed for each design, then time for analysis would have become a drawback. Hence the distributions of the results from ten sets of 500 subject's data were compared to those from 100 sets of 500 subjects. It was shown that the distributions overlapped and that ten sets of 500 subjects was a large enough sample size to be representative of the whole population.

In conclusion, this chapter set out the following details for the remainder of this thesis: design 1 (based on sensitivity analysis) should be compared to other study designs by simulation of 10* 500 subject's data for each design and analysed using the NONMEM FOCE method.

Chapter 5

5 Limited Sampling in a One-Compartment IV Bolus Pharmacokinetic Model

5.1 Introduction

An important aspect in the design of population PK studies is the timing of the samples as only sparse data are collected for each subject within the study. Optimal design strategies exist where sampling times are selected on the basis of design criteria that identify which times should offer the most information about the parameters of the PK model. The most frequently used design criterion for selecting optimal sampling times is D-optimality (Box et al. 1959). D-optimality uses the population mean values of the parameters to minimise the determinant of the inverse of Fisher Information Matrix, which effectively selects sampling times that are equivalent to the times where concentration variance would be maximal with respect to the PK parameters (Silvey 1980). This is similar to the sensitivity analysis carried out in chapter 3. However, the D-optimality design criterion does not incorporate information about the PK parameter variance, but the use of sensitivity analysis allowed investigation of the effects of increasing variability in the parameters.

Results presented in chapter 3 showed that when variability in clearance increased, the 'optimal' sampling time from the simulated population moved to a higher time point, similar to that demonstrated by Tod et al (Tod et al. 1998). Within a Bayesian context increased variance on the parameters has also been shown to result in D-optimal times that were different to those obtained at lower variance, with lower variability giving the expected D-optimal times (Merlé et al. 1995).

Another important issue regarding the sparse nature of the data collected for population PK analyses is the minimum number of samples to collect. At least two sampling times are required in order to be able to estimate the fixed effect parameters clearance (Cl) and volume of distribution (V) for a one-compartment PK model (Sheiner et al. 1983). A two-sample design derived from D-optimality would give the first sampling time to be the earliest possible and the second as the first time plus

$1.44*t_{1/2}$, for an additive random-error model. For a proportional random-error model the second time would be the latest time possible (Endrenyi 1981). The sampling design based on sensitivity analysis in chapter 3 identified two sampling times that were similar to those from D-optimality for the additive intra-individual error model (as early as possible and $1.44*t_{1/2}$). However, when the proportional intra-individual error model was used, the sampling times were also as early as possible and $1.44*t_{1/2}$ and hence these times were used in the study.

Increasing the number of samples from two to three has been shown to improve the estimation of variance in parameters, regardless of where it was inserted when the two other times were as early and as late as possible (Al-Banna et al. 1990). Another study, which allowed the collection of only one sample in some individuals demonstrated that the addition of a second sample to some subjects improved the parameter estimates, also regardless of where the second time occurred within a specified time window (Jonsson et al. 1996).

The use of sampling windows is another aspect of population study design that is investigated in this chapter. Jonsson et al (1996) investigated a clinical situation involving two morning and afternoon out-patient clinics, each lasting two hours. If all individuals attending the clinic could only have one sample taken per visit, within either the morning or afternoon sampling window, then it was beneficial to obtain both a morning and an afternoon sample on different occasions rather than both within one sampling window. Two simulation studies have also demonstrated that the use of random sampling at a range of times around optimal sampling times defined by D-optimality improved the precision and accuracy of the parameter estimates. However, sampling around non-optimal times gave inferior parameter estimates (Hashimoto et al. 1991; Mentré et al. 1995a).

This chapter further investigates some aspects raised in the literature, regarding designing PK studies. Limited sampling designs based on the one-compartment PK model were used to examine the issues relating to the use of sampling windows and the effect of adding a third sample to the minimum number of two already defined.

The designs examined in this chapter were based around the design derived from sensitivity analysis in chapter 3 (design 1 in this thesis). The first set of simulations involved examining the effect of adding sampling windows of varying size to the second time point used in design 1, to mimic variability in sampling that can occur in a clinical situation. The second set of simulations examined the effect of adding a third sampling time to the two already defined, at different times, and also included the use of sampling windows.

Firstly this chapter aimed to investigate whether strict guidelines on when blood samples should be taken during clinically-based PK studies could be relaxed by the use of sampling windows. The second objective was that if the 'optimal' times of sampling have been defined as only two, using sensitivity analysis, would the addition of a third sample improve parameter estimation, and if so, should it be taken at a particular time.

5.2 Methods

5.2.1 Data Simulation

Concentration-time data for this chapter were simulated according to a one-compartment PK model, following a single IV bolus dose of 100mg of drug, as described in Chapter 2.

The values of the parameters used were the same as those used in chapter 4 for the comparison of the FO and FOCE methods and table 4.2 is reproduced as table 5.1. Each population sample consisted of 500 subjects (2 observations/subject) and each design was repeated 10 times.

5.2.2 Two-Sample Designs

The sampling times were defined from design 1, described in chapter 4, and the initial investigations in this chapter examined the effect of adding a sampling window to the second sampling time. The size of the sampling window varied from 10% to 50% of the half-life of the drug ($t_{1/2} = 0.69$ hr) and the samples were uniformly distributed within the window. These designs were compared to the fixed sampling times used in design 1 (reproduced as design 3 in this chapter). The second sampling time in design 1 was $1.44 * t_{1/2}$ for the population average parameter values. The six designs described above were also compared to a further design in which the second sample was taken at $1.44 * t_{1/2}$ where the $t_{1/2}$ was calculated for each individual. In this design each individual had the same first sampling time, but a different second sampling time dependent on the value of their own parameters.

Hence, the three different sampling designs described above resulted in seven different sampling schedules being evaluated.

Design 3. $t_1 = 0.1$ hr, $t_2 = 1.0$ hr, where 1hr was $1.44 * t_{1/2}$ for the population average parameter values.

Design 4. $t_1 = 0.1$ hr, $t_2 =$ randomly sampled from a window equal to 1 hr \pm 10% of the drug $t_{1/2}$. i.e., 1.0 hr \pm 0.07hr.

- Design 5. $t_1 = 0.1\text{hr}$, $t_2 =$ randomly sampled from a window equal to $1\text{hr} \pm 20\%$ of the drug $t_{1/2}$. i.e., $1.0\text{hr} \pm 0.14\text{hr}$.
- Design 6. $t_1 = 0.1\text{hr}$, $t_2 =$ randomly sampled from a window equal to $1\text{hr} \pm 30\%$ of the drug $t_{1/2}$. i.e., $1.0\text{hr} \pm 0.21\text{hr}$.
- Design 7. $t_1 = 0.1\text{hr}$, $t_2 =$ randomly sampled from a window equal to $1\text{hr} \pm 40\%$ of the drug $t_{1/2}$. i.e., $1.0\text{hr} \pm 0.28\text{hr}$.
- Design 8. $t_1 = 0.1\text{hr}$, $t_2 =$ randomly sampled from a window equal to $1\text{hr} \pm 50\%$ of the drug $t_{1/2}$. i.e., $1.0\text{hr} \pm 0.35\text{hr}$.
- Design 9. $t_1 = 0.1\text{hr}$, $t_2 = 1.44 * t_{1/2}$ for each individual.

These designs are also summarised in table 5.2. Designs 3-8 are shown in figure 5.1 which shows the concentration variance curves derived from sensitivity analysis in chapter 3.

5.2.3 Three-Sample Designs

The second investigation in this chapter considered the effect of adding a third sample to the two fixed samples defined from sensitivity analysis in chapter 3 and used in design 1. The third time was either added in between the two original times or after them at two different times, one close to the last sample time and one later at $3 * t_{1/2}$. The first sampling time was fixed at 0.1hr but the second and third times incorporated sampling windows. Three different schedules were simulated:

- Design 10. Third sample between the two already defined, i.e., at the time where the curves of concentration variance due to the clearance and volume parameters intersected (0.5 hr, see chapters 3 and 4).
- Design 11. The third sample after the two already defined, at the same time interval as the 'intersect' time was from the second peak at 1.0hr (i.e., 1.5 hr).
- Design 12. The third sample at $3 * t_{1/2}$ (2.0 hr).

Each schedule was simulated with sampling windows on the second and third times. The windows were set as 10% and 50% of the half-life, respectively, and again, the samples were uniformly distributed within the window. The sampling times were

restricted to be at least 5 minutes apart, as the windows overlapped in some cases, see figure 5.2. Six simulations were carried out in total. The sampling schedules are summarised in table 5.3 and figure 5.2.

5.2.4 Data Analysis

The parameters \overline{Cl} , \overline{V} , ω_{Cl}^2 , ω_V^2 , σ_1^2 and σ_2^2 were estimated by NONMEM, version V, using FOCE with interaction, which accounts for interactions between the η and the ε due to the proportional intra-individual error model.

Calculation of the percentage bias and imprecision of the NONMEM population estimates for each data set, as described in chapter 2, was used for all comparisons.

Table 5.1 Mean pharmacokinetic parameter values used to simulate data^a.

Parameter	Value
\overline{Cl}	10.0 l/h
\overline{V}	10.0 l
ω_{Cl}	Varied from 1.0, 2.0, 3.0 l/h
ω_V	1.0 l
σ_1	0.05
σ_2	0.25 mg/l

^aIt was assumed that there was no covariance between Cl and V .

Table 5.2 Sampling designs for evaluation of sampling windows with two sampling times.

Design Number	First Sampling Time (t_1) (hr)	Second Sampling Time (t_2) (hr)
3	0.1	1.0
4	0.1	1.0 ± 0.07
5	0.1	1.0 ± 0.14
6	0.1	1.0 ± 0.21
7	0.1	1.0 ± 0.28
8	0.1	1.0 ± 0.35
9	0.1	1.44*individual $t_{1/2}$

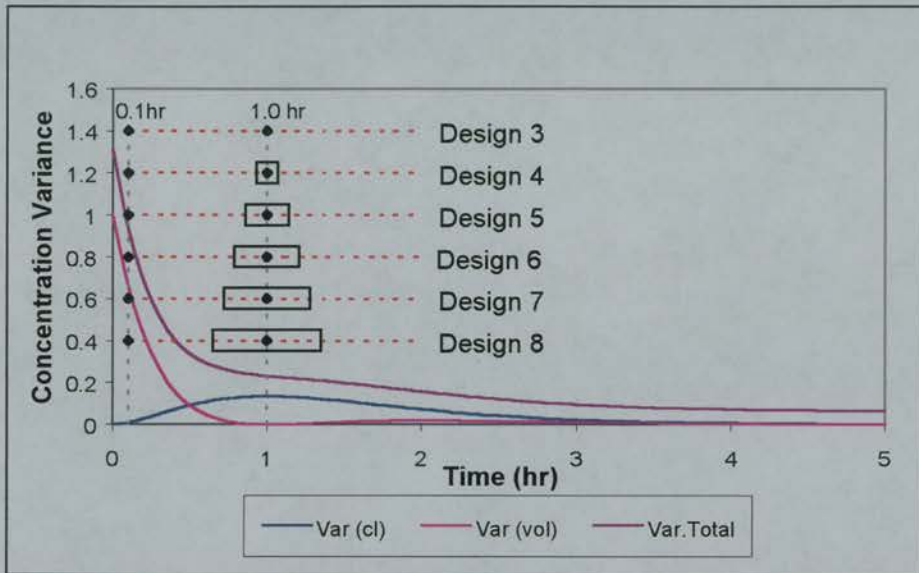


Figure 5.1 Sampling times for designs 3 to 8 shown on the concentration variance curve. The boxes represent the distribution of the sampling window around the 1.0hr sample.

Table 5.3 Sampling schedules for three sampling times on a one-compartment IV bolus PK model ($t_{1/2} = 0.69$ hr).

Design Number	Sampling Window	First Sampling Time (t_1) (hr)	Second Sampling Time (t_2) (hr)	Third Sampling Time (t_3) (hr)
10a	10% * $t_{1/2}$	0.1	0.5±0.07	1.0±0.07
10b	50% * $t_{1/2}$	0.1	0.5±0.35	1.0±0.35
11a	10% * $t_{1/2}$	0.1	1.0±0.07	1.5±0.07
11b	50% * $t_{1/2}$	0.1	1.0±0.35	1.5±0.35
12a	10% * $t_{1/2}$	0.1	1.0±0.07	2.0±0.07
12b	50% * $t_{1/2}$	0.1	1.0±0.35	2.0±0.35

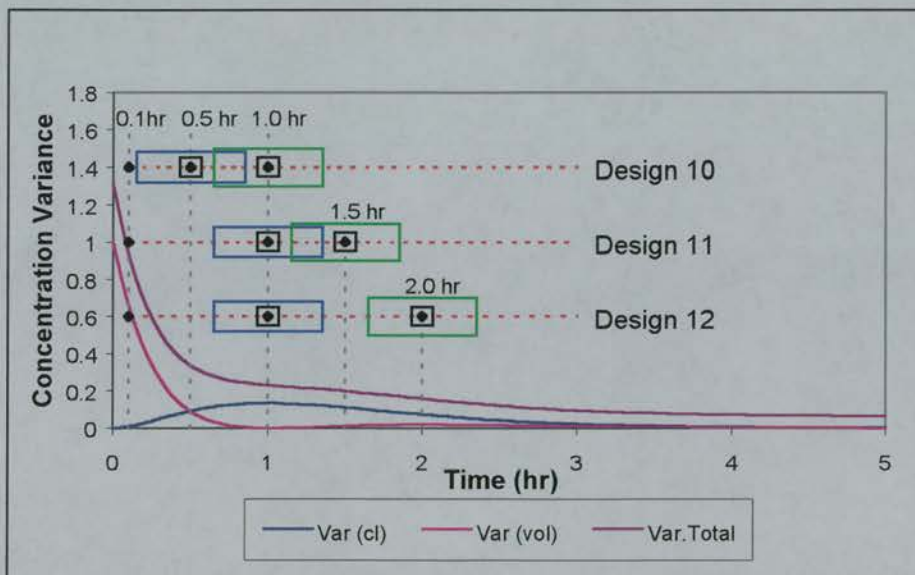


Figure 5.2 Concentration variance components and the sampling times for designs 10 to 12 shown on the concentration variance curve. The boxes represent the distribution of the sampling window around the second and third samples. The black boxes represent the 10% * $t_{1/2}$ sampling window and the blue and green boxes represent the 50% * $t_{1/2}$ sampling windows on the second and third time, respectively.

5.3 Results

5.3.1 Two-Sample Designs

The simulations in this section were performed using the sampling times derived from sensitivity analysis in chapter 3, for the one-compartment IV bolus model (i.e., 0.1 and 1.0 hr). The first design (3) was design 1 in chapter 4 and further designs (4-8) had sampling windows of varying size arranged around the 1.0 hr time-point. These six designs were also compared to the situation where each individual had a second sampling time of $1.44 * t_{1/2}$, which varied dependent on the individual's parameter values. The results for each design are shown as ω_{Cl} increased from 1 to 3, i.e., from left to right for each design within the plots.

Estimation of Population Mean Clearance (\overline{Cl}).

Figures 5.3 and 5.4 show the bias and imprecision, respectively for the estimation of population average clearance, from all of the two-sample designs.

The design containing fixed samples based on each individual (design 9) had a similar mean bias to the design with fixed samples based on the population parameter values (design 3), and the sampling window designs (4-8). However, design 9 underestimated \overline{Cl} , whereas designs 3-8 overestimated it, and also had the narrowest 95% confidence intervals. There were no major differences in the bias estimates, for any of the designs, as ω_{Cl} increased from 1 to 3, although there was a trend for the results to be more imprecise as ω_{Cl} increased from 1 to 3 (figure 5.4). The individual-based design was the most precise and design 8 with the sampling window equal to 50% of $t_{1/2}$ performed better than the population design with the fixed times and the rest of the sampling window designs.

Overall, the population average Clearance was estimated accurately with all designs, with bias less than 1% and imprecision less than 1.5% and no distinction could be made between the designs on this basis as the values were so small.

Estimation of Population Mean Volume of Distribution (\bar{V}).

The results for the estimation of the population average volume of distribution are shown in figures 5.5 and 5.6. Similar to Cl , V was estimated accurately across all designs, with bias less than 1.0% and imprecision less than 0.6%.

The bias was shown in figure 5.5 and this shows that the results from design 8, with a sampling window equal to 50% of $t_{1/2}$ were similar to the results observed with the individual-based design 9. However, the population-based fixed-sample (design 3) and the designs with sampling windows equal to 10% - 40% of $t_{1/2}$ (designs 4-7) had the smallest means and narrowest confidence intervals. Designs 8 and 9 were also slightly more imprecise than the other designs (figure 5.6), although similar to Cl , the values were so small that no difference could be established between the designs in the estimation of V . There were also no patterns in bias or imprecision as ω_{Cl} increased from 1 to 3.

Estimation of Standard Deviation of Population Mean Clearance (ω_{Cl}).

Figures 5.7 and 5.8 summarise the results for the estimation of ω_{Cl} , the standard deviation of the population clearance distribution.

The pattern of results was broadly similar across all designs, apart, perhaps for design 9.

When $\omega_{Cl} = 1$ (10%) the average bias for ω_{Cl} was between -5% to -12% for designs 3-8 with wide confidence intervals. However, when the value of ω_{Cl} was increased to 20 and 30%, the mean bias reduced to -1.3 to -6%, with much narrower confidence intervals. The imprecision also decreased substantially as ω_{Cl} increased from 1 to 3 (figure 5.8).

The pattern for bias was slightly different for design 9 in that the mean bias was positive for this design (3.6% when $\omega_{CI} = 1$ decreasing to 0.84% when $\omega_{CI} = 2-3$) and negative for all of the others. However, the pattern for imprecision was similar to that obtained for designs 3-8.

Estimation of Standard Deviation of Population Mean Volume of Distribution (ω_V).

Figures 5.9 and 5.10 show the bias and imprecision, respectively, for the estimation of ω_V , the standard deviation of the population distribution for volume of distribution.

The population-based fixed-sample design (3) and all of the sampling window designs (4-8) were less biased than the individual-based design (9) in the estimation of ω_V (figure 5.9). Design 9 had the largest mean bias (9%) and the widest 95% confidence intervals and there was a progressive increase in bias as ω_{CI} increased from 1 to 3 for designs 3-7 by 2.5 - 4.2%). Design 8 with a sampling window equal to 50% of $t_{1/2}$ and design 9 had a slight increase and then a decrease in bias as ω_{CI} increased from 1 to 3. Designs 3-8 all had bias within 9%.

The most precise design was design 7 with the sampling window equal to 40% of $t_{1/2}$. However, all designs were precise in the estimation of ω_V , with imprecision of less than 14% (figure 5.10), although all designs became more imprecise as ω_{CI} increased from 1 to 3.

Estimation of the Proportional Intra-Individual Random Error Component (σ_1).

The results for the estimation of the proportional error component of intra-subject variability, σ_1 , are shown in figure 5.11. Designs 3-8 produced less biased results than design 9, which had the largest mean bias (-57.5%) and the widest 95% confidence intervals. There were slight patterns in the bias as ω_{CI} increased from 1 to

3 for designs 4-8. The pattern was the same for each design in that as ω_{CI} increased, the mean absolute value of bias increased by 4-20%. In designs 4-6 this represented an increase in bias and in design 8 a decrease, but neither in the case of design 7 as the direction of the bias changed from negative to positive. However, as the confidence intervals for the different values of ω_{CI} overlapped within each design this observation may be irrelevant.

Imprecision decreased from 16% to 12% as ω_{CI} increased from 10 to 30% for designs 3-7 (figure 5.12). Design 8 had imprecision in excess of 15% at $\omega_{CI}=1-3$, and the imprecision for design 9 was the poorest of all designs with the value increasing from 40 to 50% as ω_{CI} increased from 10 to 30%.

Estimation of the Additive Intra-Individual Random Error Component (σ_2).

Figure 5.13 shows that in the estimation of σ_2 , the additive component of intra-subject variability, designs 3-7 performed equally well. The mean bias increased from 15% to 24.6% as ω_{CI} increased from 1 to 3 and the confidence intervals also got progressively wider for these designs. The bias for design 8 decreased as ω_{CI} increased from 1 to 3 and design 9 gave the most biased estimates, which increased as ω_{CI} increased. Again, similar to the observation made for the estimation of σ_1 , these patterns may not be important as the confidence intervals for the different values of ω_{CI} overlap within each design.

The imprecision for designs 3-8 increased from 12-22% to 26-30% as ω_{CI} increased from 1 to 3. However, the increase for design 9, the most inaccurate design in the estimation of σ_2 , was greater - from 32% to 60% (figure 6.14).

Summary of Results for Two-Sample Designs.

Overall the designs including sampling windows (designs 4-8) estimated as well as, if not better than the population-based fixed-sample design (3).

Design 8 with the sampling window equal to 50% of $t_{1/2}$ was slightly different from designs 4-7 with the sampling window equal to 10%-40% of $t_{1/2}$. The mean bias values were more similar to the values obtained from design 9, the individually-based fixed-sample design, although the 95% confidence intervals could be quite different.

The fixed effects, clearance and volume of distribution, were estimated accurately with all designs. The random inter-individual effects were estimated with acceptable accuracy by both the population-based fixed-sample design and the designs with sampling windows, but less so by the individually-based fixed-sample design. The intra-individual effects were estimated inaccurately by all designs, but the individually-based design performed worst.

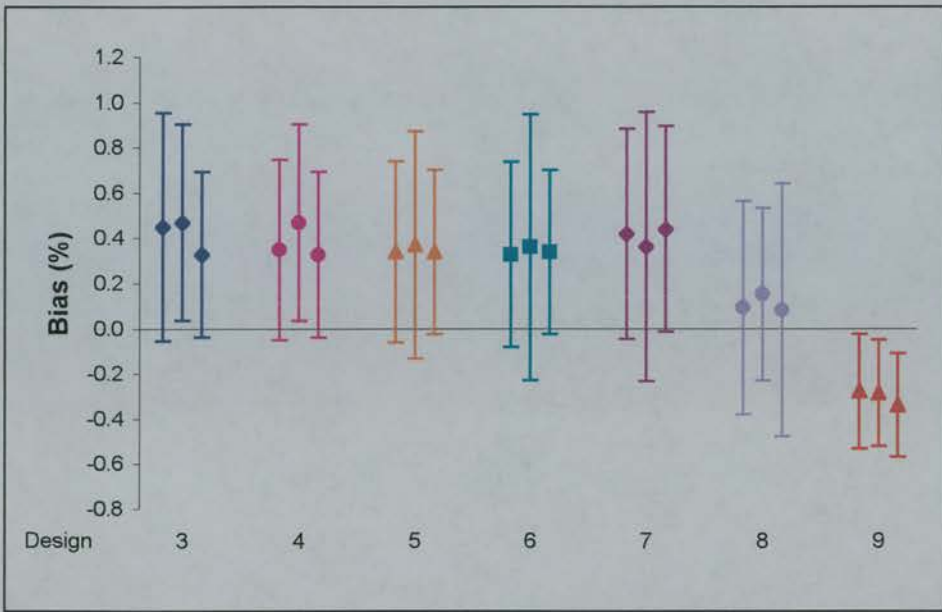


Figure 5.3 Bias (mean \pm 95% CI) results for the estimates of population mean clearance. The results for designs 3-9 are shown as the simulated ω_{CI} increased from 1 to 3, from left to right.



Figure 5.4 Imprecision results for the estimates of population mean clearance. The results for designs 3-9 are shown as the simulated ω_{CI} increased from 1 to 3, from left to right.

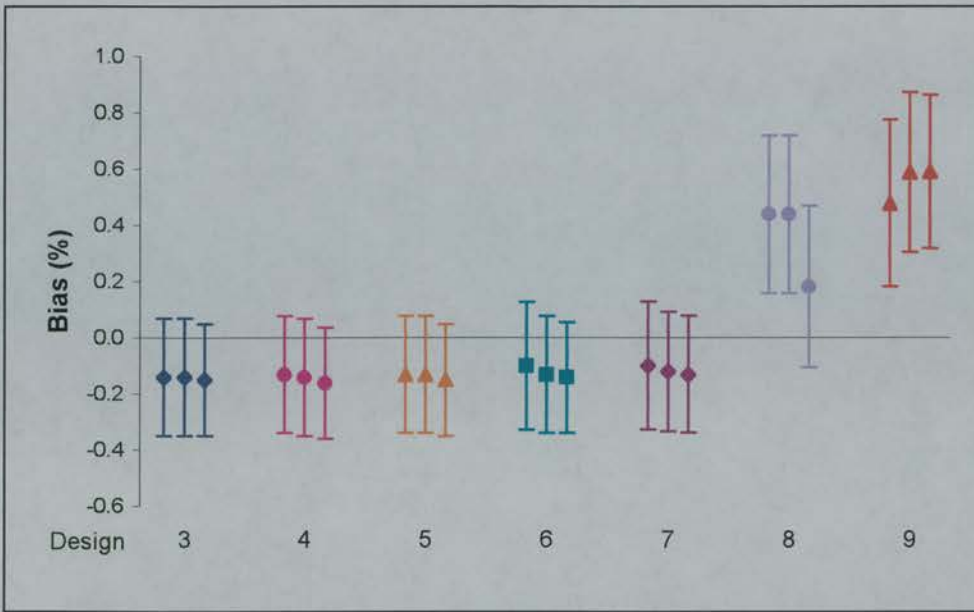


Figure 5.5 Bias (mean \pm 95% CI) results for the estimates of population mean volume of distribution. The results for designs 3-9 are shown as the simulated ω_{CI} increased from 1 to 3, from left to right.

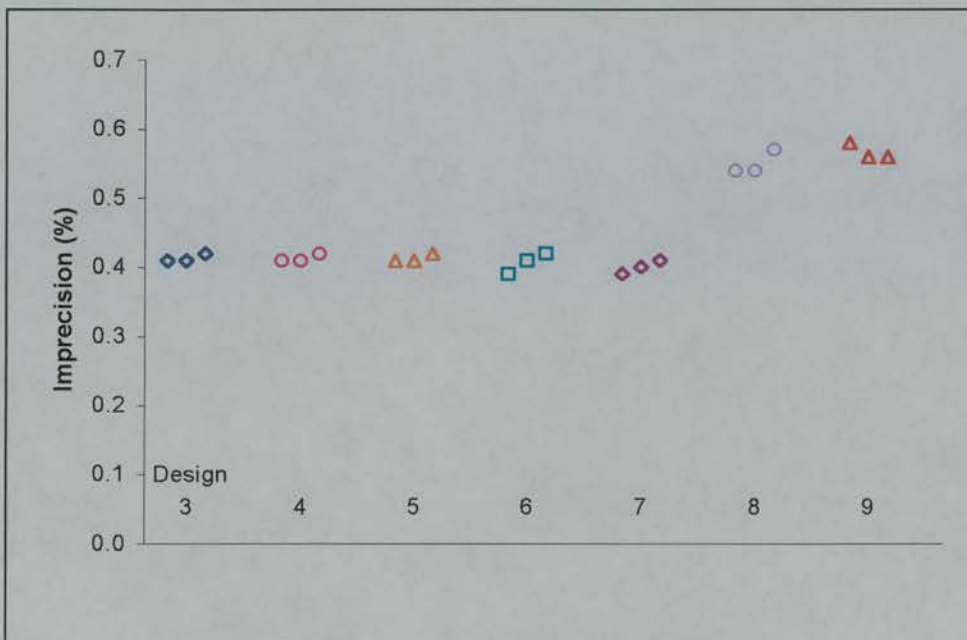


Figure 5.6 Imprecision results for the estimates of population mean volume of distribution. The results for designs 3-9 are shown as the simulated ω_{CI} increased from 1 to 3, from left to right.

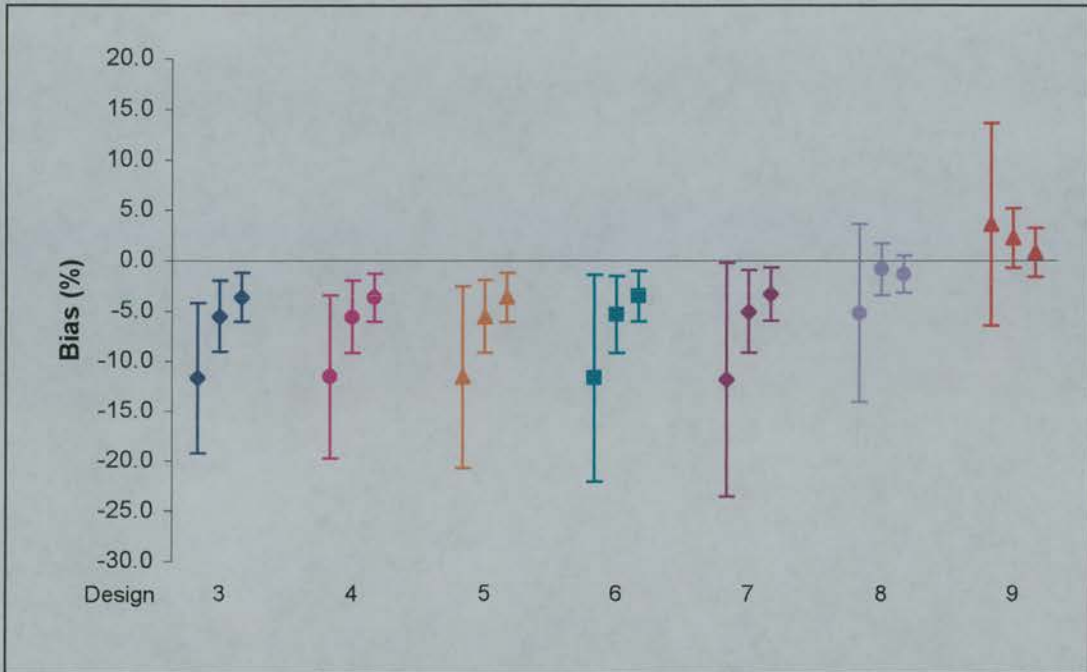


Figure 5.7 Bias (mean \pm 95% CI) results for the estimates of standard deviation of the population clearance distribution (ω_{Cl}). The results for designs 3-9 are shown as the simulated ω_{Cl} increased from 1 to 3, from left to right.

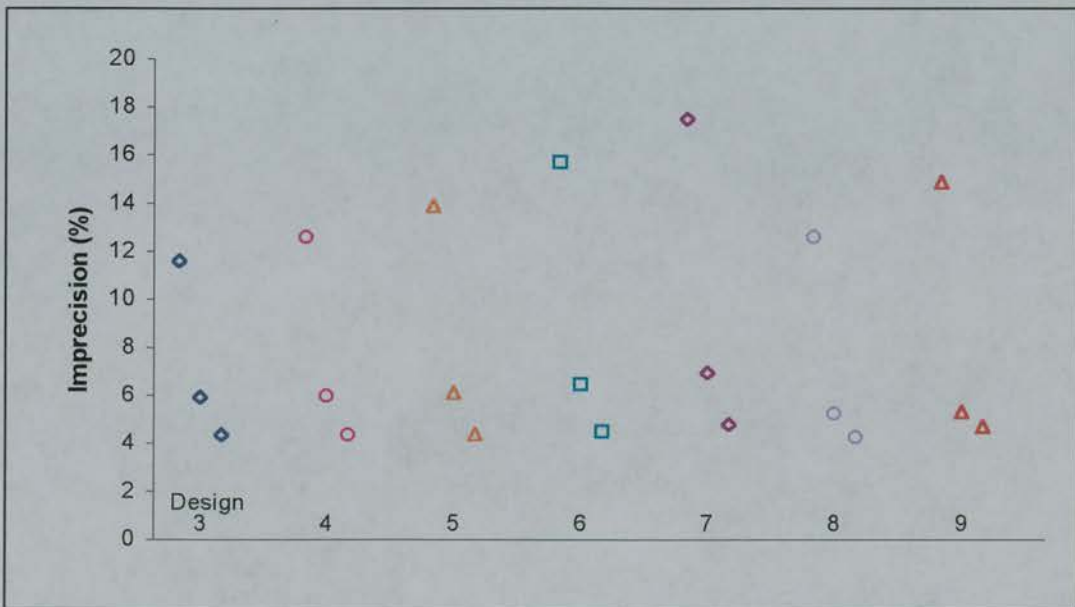


Figure 5.8 Imprecision results for the estimates of the standard deviation of the population clearance distribution (ω_{Cl}). The results for designs 3-9 are shown as the simulated ω_{Cl} increased from 1 to 3, from left to right.

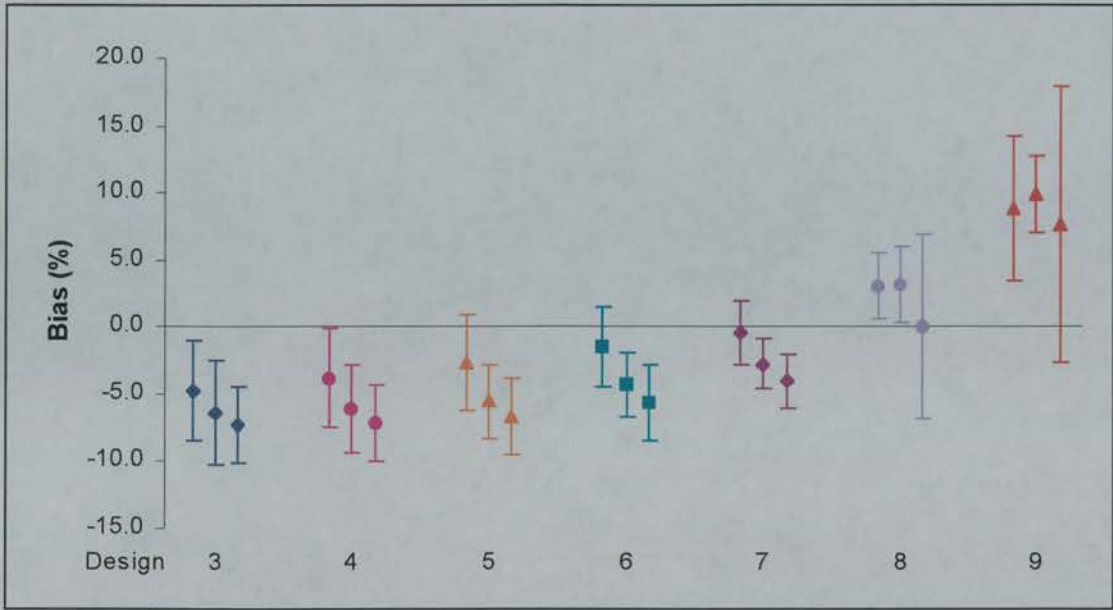


Figure 5.9 Bias (mean \pm 95% CI) results for the estimates of standard deviation of the population volume distribution (ω_V). The results for designs 3-9 are shown as the simulated ω_{CI} increased from 1 to 3, from left to right.

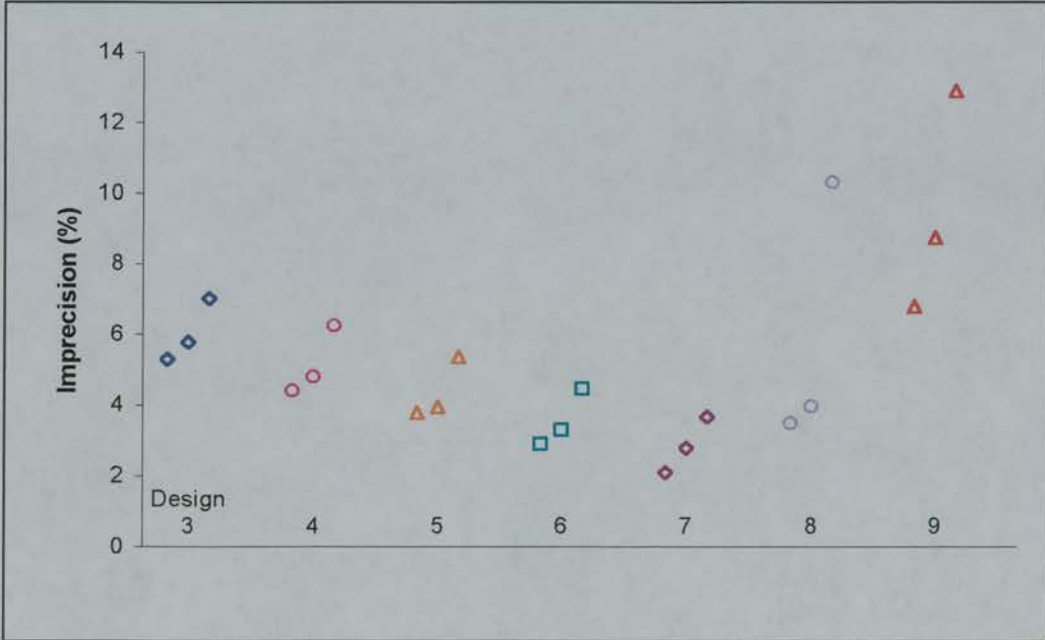


Figure 5.10 Imprecision results for the estimates of the standard deviation of the population volume distribution (ω_V). The results for designs 3-9 are shown as the simulated ω_{CI} increased from 1 to 3, from left to right.

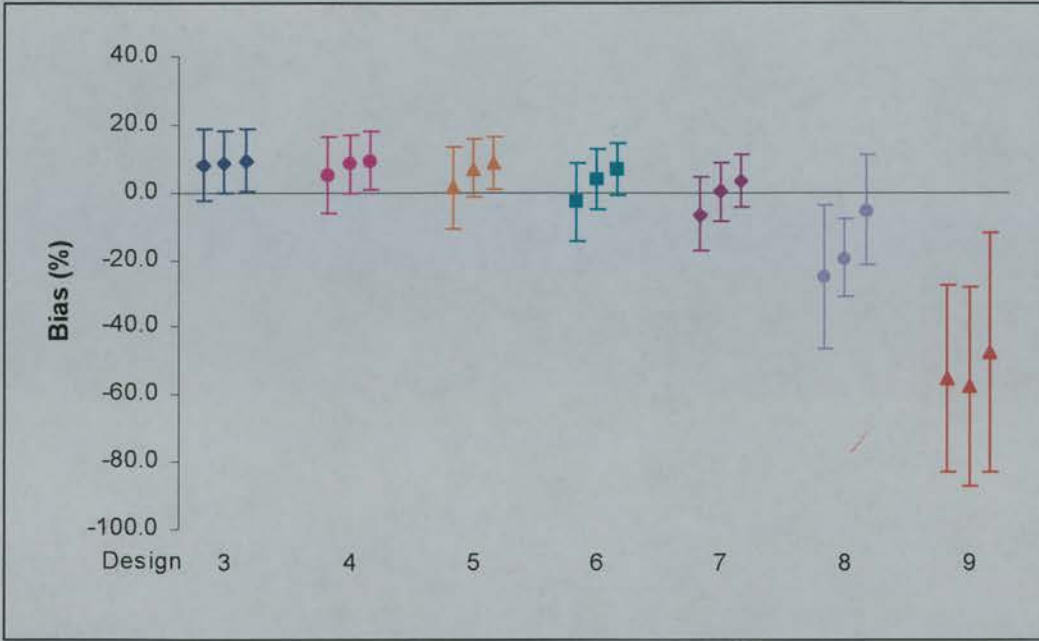


Figure 5.11 Bias (mean \pm 95% CI) results for the estimates of the proportional error component (σ_I). The results for designs 3-9 are shown as the simulated ω_{CI} increased from 1 to 3, from left to right.

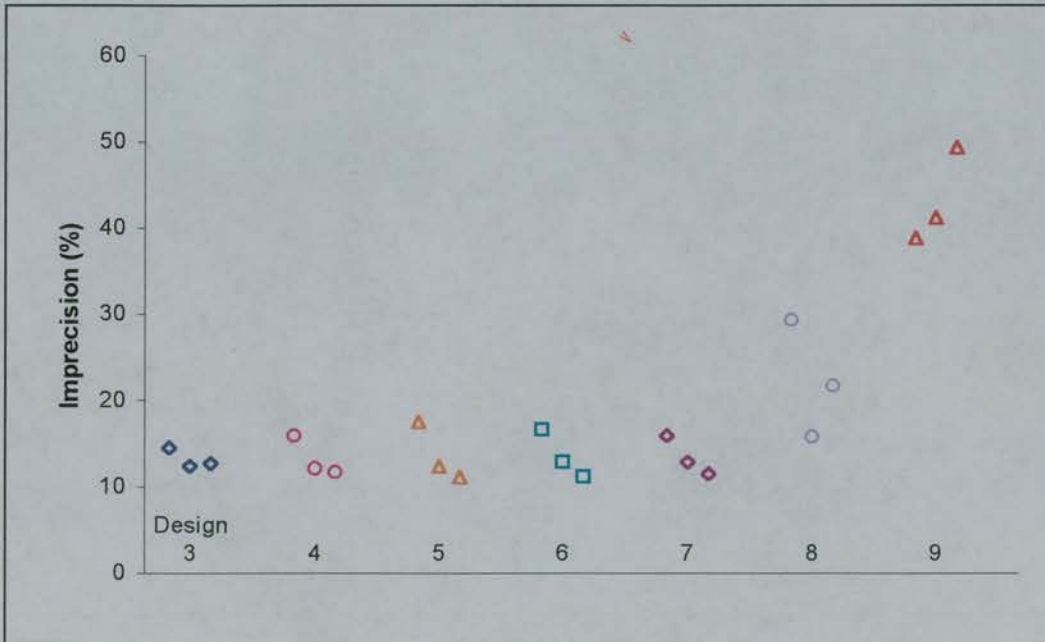


Figure 5.12 Imprecision results for the estimates of the proportional error component (σ_I). The results for designs 3-9 are shown as the simulated ω_{CI} increased from 1 to 3, from left to right.

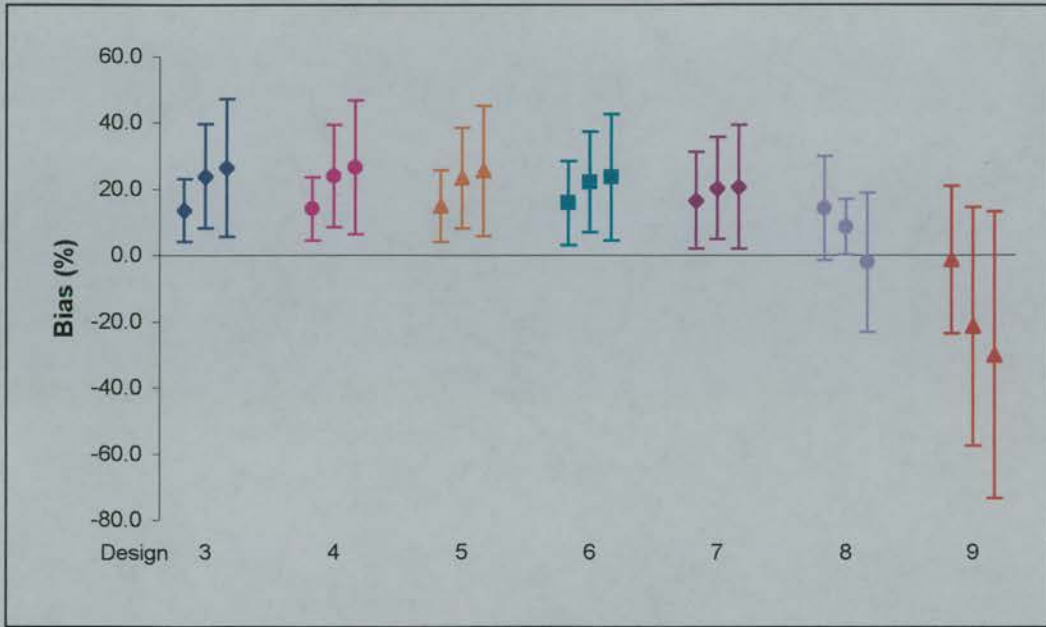


Figure 5.13 Bias (mean \pm 95% CI) results for the estimates of the additive error component (σ_2). The results for designs 3-9 are shown as the simulated ω_{CI} increased from 1 to 3, from left to right.

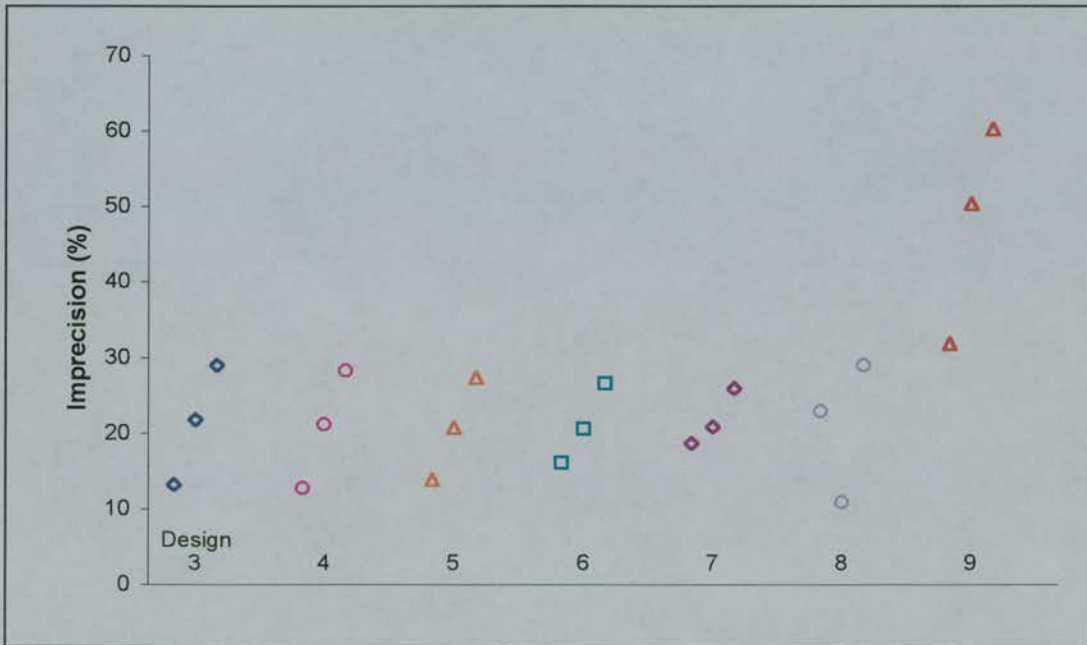


Figure 5.14 Imprecision results for the estimates of the additive error component (σ_2). The results for designs 3-9 are shown as the simulated ω_{CI} increased from 1 to 3, from left to right.

5.3.2 Three-Sample Designs

Design 1, with sampling times at 0.1 and 1.0 hr was augmented to include a third sample time. A sampling window was also included around the 1.0hr sampling time.

In designs 10a and 10b, the additional sample was taken between the other samples from a window centred around 0.5 hr and with windows of 10% and 50% of $t_{1/2}$, respectively. For designs 11a and b, the third sample was taken within a sampling window centred around 1.5hr and for 12a and b the third point was sampled around 2.0 hr. Again the windows were 10% and 50% of $t_{1/2}$, i.e., 0.07hr and 0.35 hr, respectively. Samples were uniformly distributed in the sampling window, but were constrained to be at least 5 minutes apart.

Estimation of Population Mean Clearance (\overline{CI}).

The bias and imprecision for the estimation of the population mean clearance using $10\%*t_{1/2}$ and $50\%*t_{1/2}$ sampling windows are shown in figures 5.15 and 5.16, respectively. Within each design the population standard deviation for clearance (ω_{CI}) increases from 10 - 30% from left to right.

Increasing the size of the sampling windows from 10 to $50\%*t_{1/2}$ caused a slight increase in mean bias (0.1% to 0.3%) and imprecision (0.5% to 0.6%) for design 10. With design 11, the use of a 50% window eliminated the pattern in the bias seen with the 10% window, where it decreased as ω_{CI} increased from 1 to 3 (0.22% to -0.03%). The imprecision of the estimation of clearance was also slightly improved when design 11 used the 50% windows (0.4% compared with 0.3%). Design 12 also had a slight improvement in the imprecision when the sampling windows were increased from 10% to 50% (0.44% compared with 0.39%), but a pattern in the mean bias emerged where the mean bias increased as ω_{CI} increased from 1 to 3 (0% to -0.3%).

Overall, clearance was estimated accurately with each of the three 3-sample schedules, regardless of the size of the sampling window. The bias and the imprecision levels for all schedules were within 0.8%.

Estimation of Population Mean Volume of Distribution (\bar{V}).

The mean bias for designs 10a, 11a and 12a was almost zero (0.01, -0.01 and 0.09%, respectively). However, the designs using sampling windows equal to 50%* $t_{1/2}$ were more imprecise (+0.2-0.3%) and although the mean bias was also increased compared to the 10% windows, it was still very small (-0.1%, 0.2%, 0.1% for designs 10b, 11b and 12b, respectively).

Similar to clearance, volume of distribution was also estimated accurately with all of the three-sample designs (see figures 5.17 and 5.18). The 95% confidence interval for the mean bias and the imprecision levels were within 0.6%, for both sizes of sampling window. No patterns in the mean bias were observed with increasing ω_{CI} .

Estimation of Standard Deviation of Population Mean Clearance (ω_{CI}).

Figure 5.19 shows the results for the 10%* $t_{1/2}$ sampling windows, for each of the three-sample designs. The mean biases were less than 2% and design 12 had the largest mean biases of the three designs. The imprecision improved when ω_{CI} increased from 1 to 3 for designs 10a, 11a and 12a.

Using the 50% windows reduced the imprecision for designs 10 (4.6% to 2.8%) and 12 (3.4% to 2%) when $\omega_{CI} = 1$. When $\omega_{CI} = 2-3$ the imprecision was slightly poorer using the 50% windows compared to the 10% windows for all designs (increased by 0.1 to 0.5%). However, the imprecision for design 11 was slightly increased when the 50% windows were used (increased by 0.3-1.0%). See figure 5.20.

Overall, the 95% confidence intervals for the bias and the imprecision for all designs were less than 5%, which was an acceptable level for estimation.

Estimation of Standard Deviation of Population Mean Volume (ω_V).

Of the designs incorporating the $10\% \cdot t^{1/2}$ sampling windows, design 10a had the least imprecision and the narrowest 95% confidence intervals (Figure 5.21). Design 11a had the largest mean bias and imprecision and design 12a had a pattern in mean bias in that it decreased as ω_{CI} increased from 1 to 3 (from -2.7% to 1.1%).

Figure 5.22 shows the results from estimating ω_V using the 50% sampling windows. All designs had similar mean biases and imprecision and there were no significant differences between the designs.

The estimates of ω_V were within $\pm 7\%$ bias and imprecision for all sampling designs, although the designs with the $50\% \cdot t^{1/2}$ windows were improved over the $10\% \cdot t^{1/2}$ windows in all designs.

Estimation of the Proportional Intra-Individual Random Error Component (σ_I).

When using designs 10a, 11a and 12a, the bias and imprecision of the estimates of σ_I were within 22%, i.e., an unacceptably high value (see figure 6.23). The mean values of bias ranged from $\pm 1\%$ to $\pm 6\%$, but the 95% confidence intervals were wide, extending to 22% for design 12 when $\omega_{CI} = 2$. The imprecision varied from 13% to 22% across all designs.

The results obtained when designs 10b, 11b and 12b were used improved the estimation of σ_I (figure 5.24). All bias and imprecision estimates were within $\pm 11\%$. The mean biases were generally improved (range $\pm 0.4\%$ to $\pm 3.5\%$) except for design 12 when $\omega_{CI} = 3$. Design 11 had the smallest mean bias, while design 10 had the smallest imprecision.

Estimation of Random Additive Error on Concentration (σ_2).

Figure 5.25 shows the bias and imprecision estimates for σ_2 when using the 10% windows (designs 10a, 11a and 12a). Design 12a had the most accurate estimates, with the mean bias close to zero and the imprecision less than 7%. Design 11a performed similarly to 12a with imprecision of 7-10% and mean estimates of bias of less than 2%. Although design 10a also had mean biases of less than 3%, the 95% confidence interval was $\pm 16\%$ and the imprecision was almost 19%, giving the poorest estimates of σ_2 in this instance.

Using the 50% sampling windows (figure 5.26) the imprecision of the estimates of σ_2 improved with all of the sampling designs and also made the mean bias closer to zero. Design 12b still performed best (imprecision 5.5%) and design 10b poorest (imprecision 8%) of the three, but all of these designs produced acceptable estimates of σ_2 .

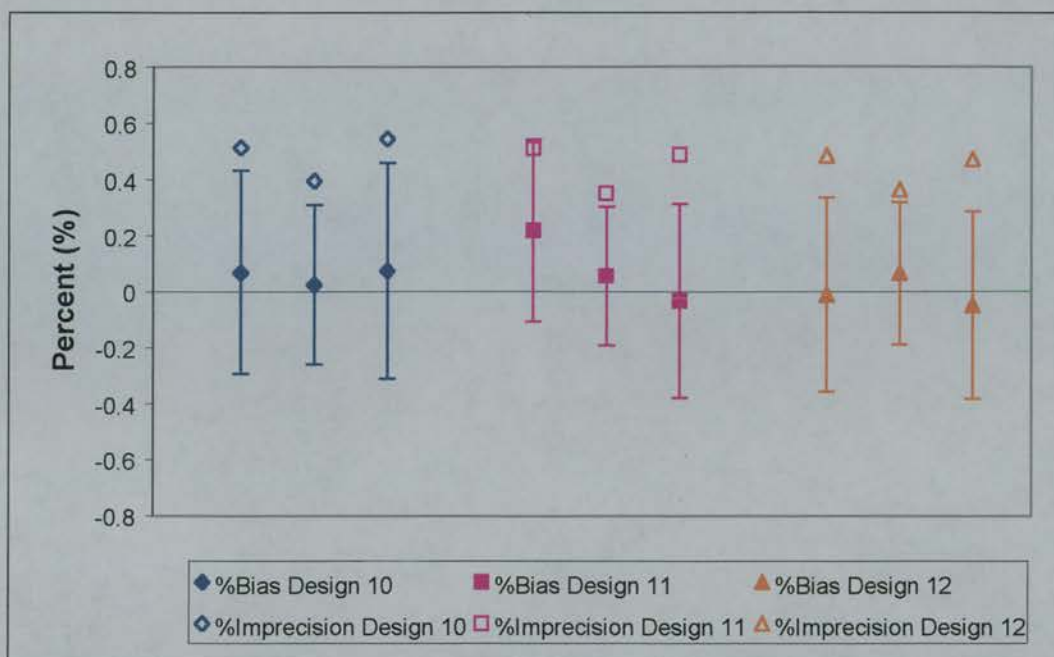


Figure 5.15 %Bias and %Imprecision of the estimation of clearance (\overline{Cl}) with windows of 10% of the half life around the second two sampling times.

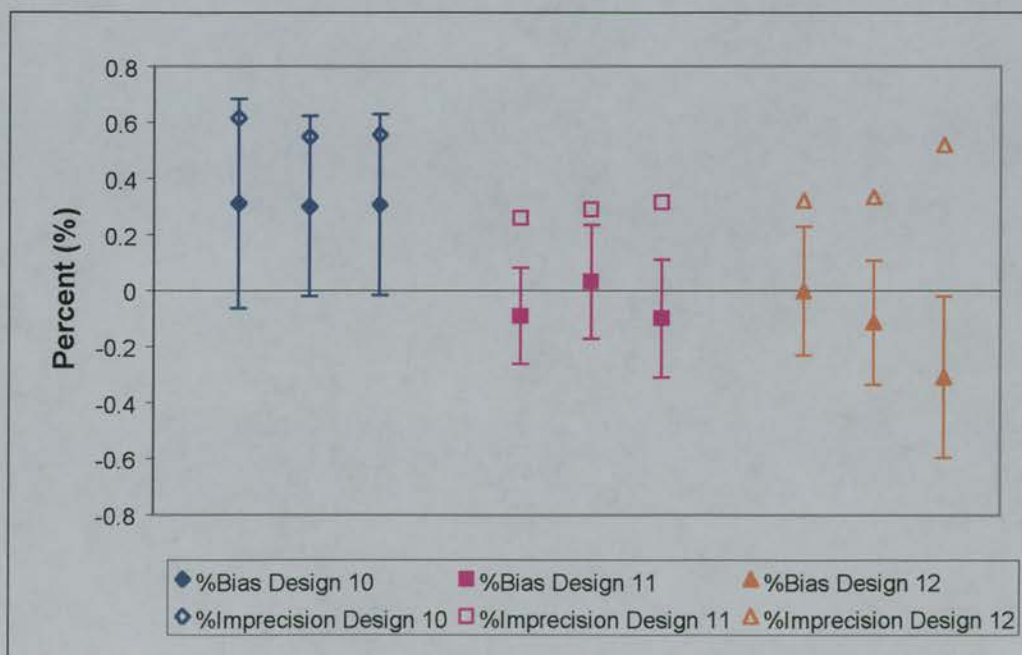


Figure 5.16 %Bias and %Imprecision of the estimation of clearance (\overline{Cl}) with windows of 50% of the half life around the second two sampling times.

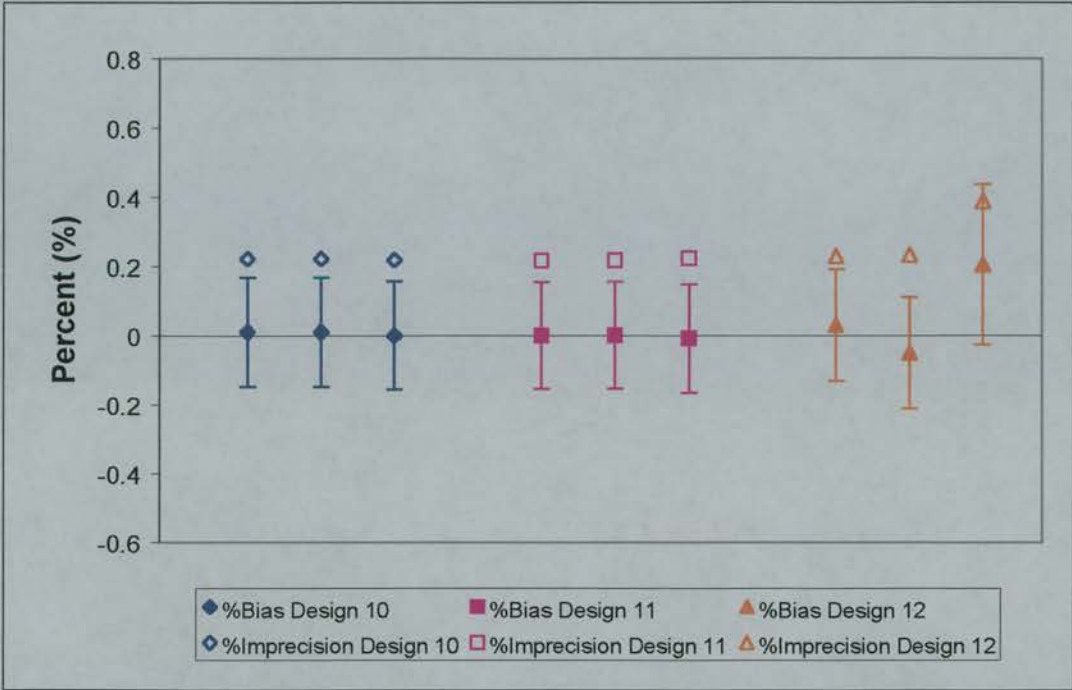


Figure 5.17 %Bias and %Imprecision of the estimation of volume (\bar{V}) with windows of 10% of the half life around the second two sampling times.

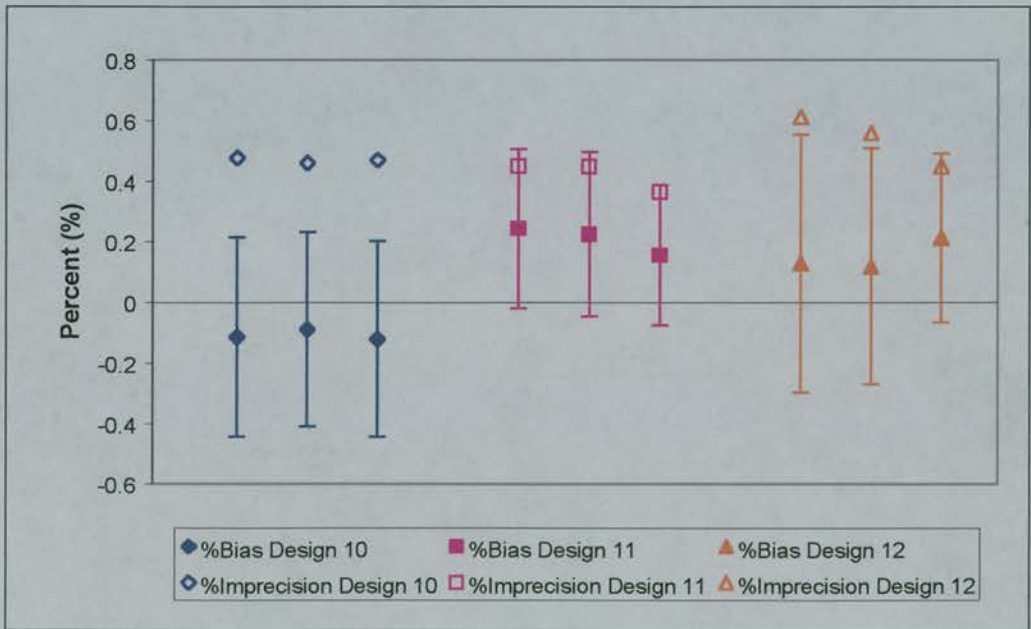


Figure 5.18 %Bias and %Imprecision of the estimation of volume (\bar{V}) with windows of 50% of the half life around the second two sampling times.

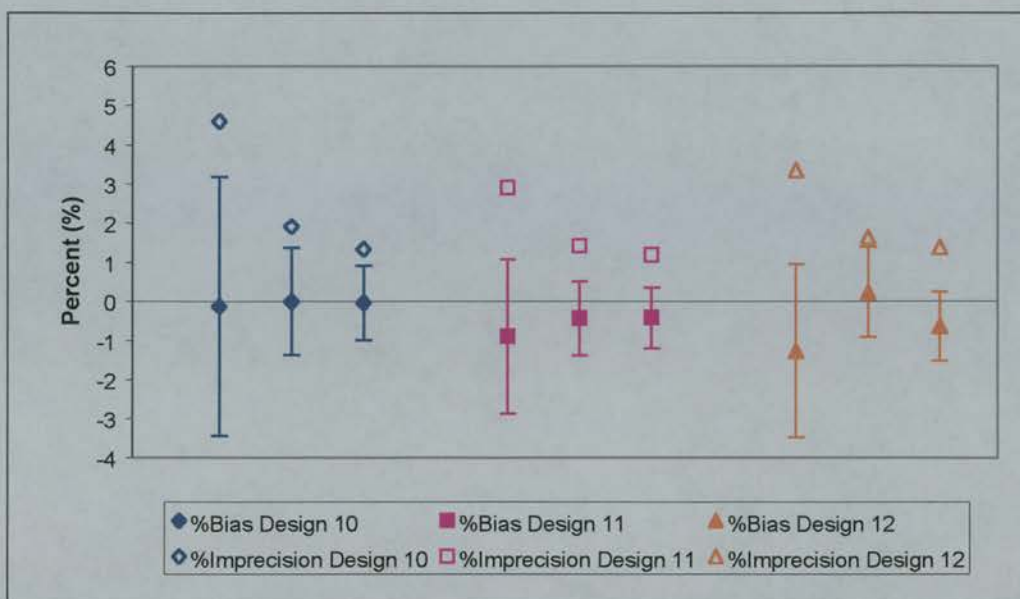


Figure 5.19 %Bias and %Imprecision of the estimation of standard deviation of clearance (ω_{Cl}) with windows of 10% of the half life around the second two sampling times.

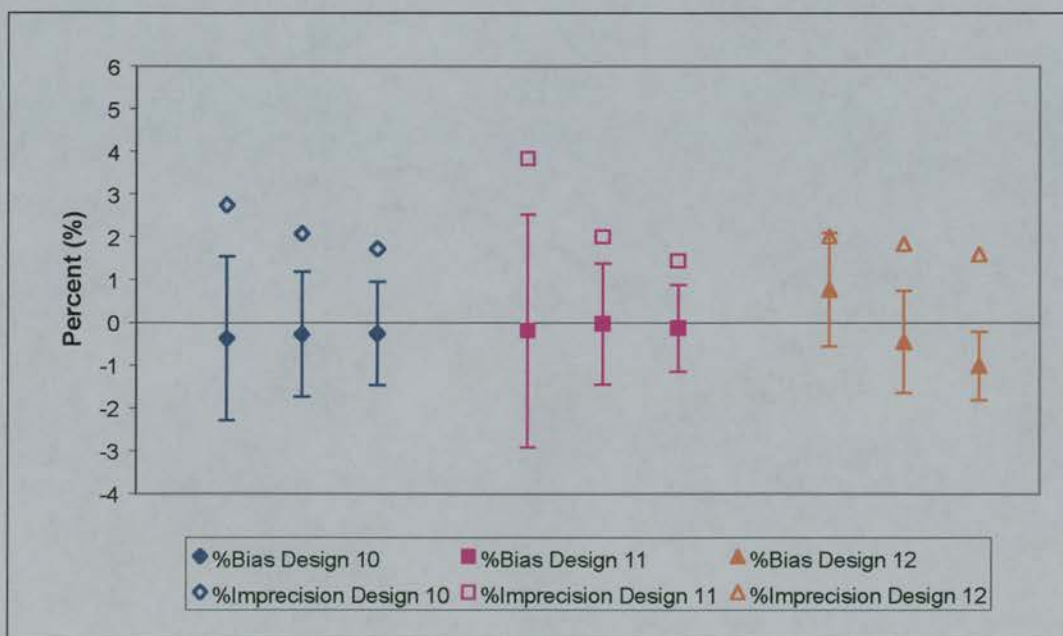


Figure 5.20 %Bias and %Imprecision of the estimation of standard deviation of clearance (ω_{Cl}) with windows of 50% of the half life around the second two sampling times.

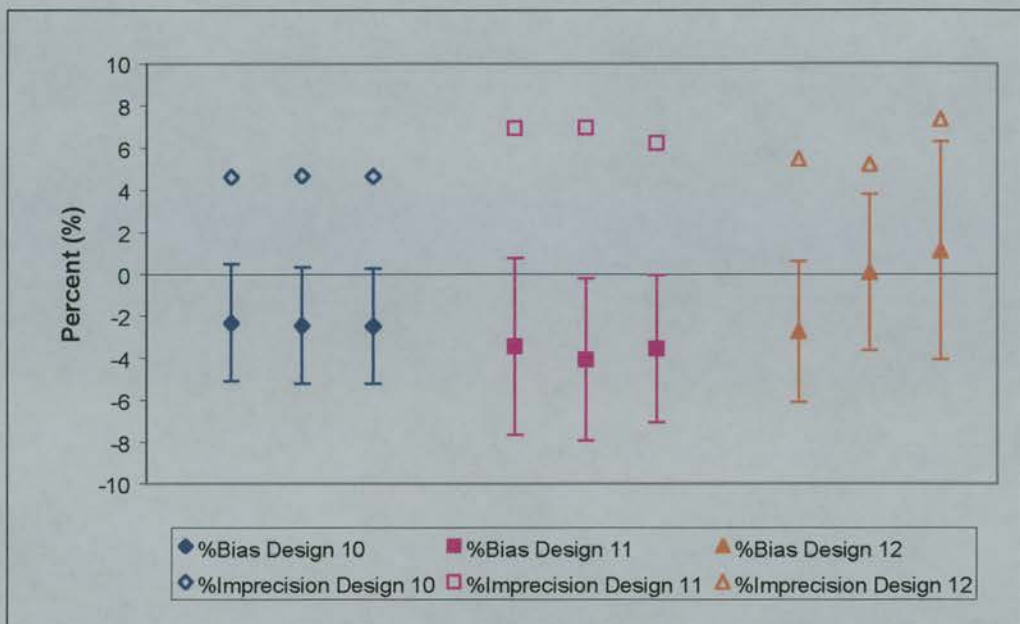


Figure 5.21 %Bias and %Imprecision of the estimation of standard deviation of volume (ω_V) with windows of 10% of the half life around the second two sampling times.

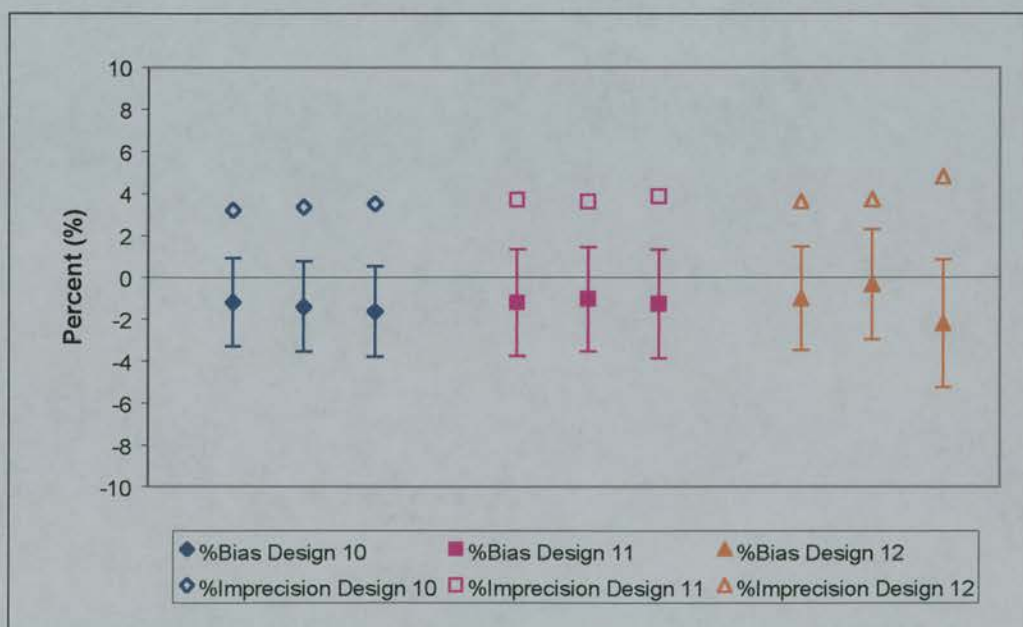


Figure 5.22 %Bias and %Imprecision of the estimation of standard deviation of volume (ω_V) with windows of 50% of the half life around the second two sampling times.

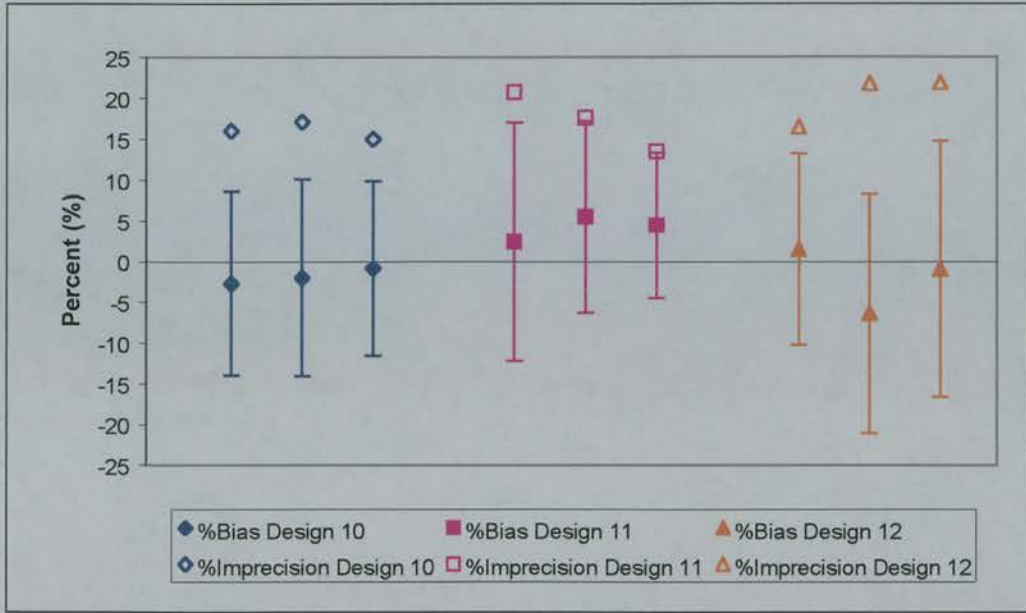


Figure 5.23 %Bias and %Imprecision of the estimation of random proportional error on concentration (σ_I) with windows of 10% of the half life around the second two sampling times.

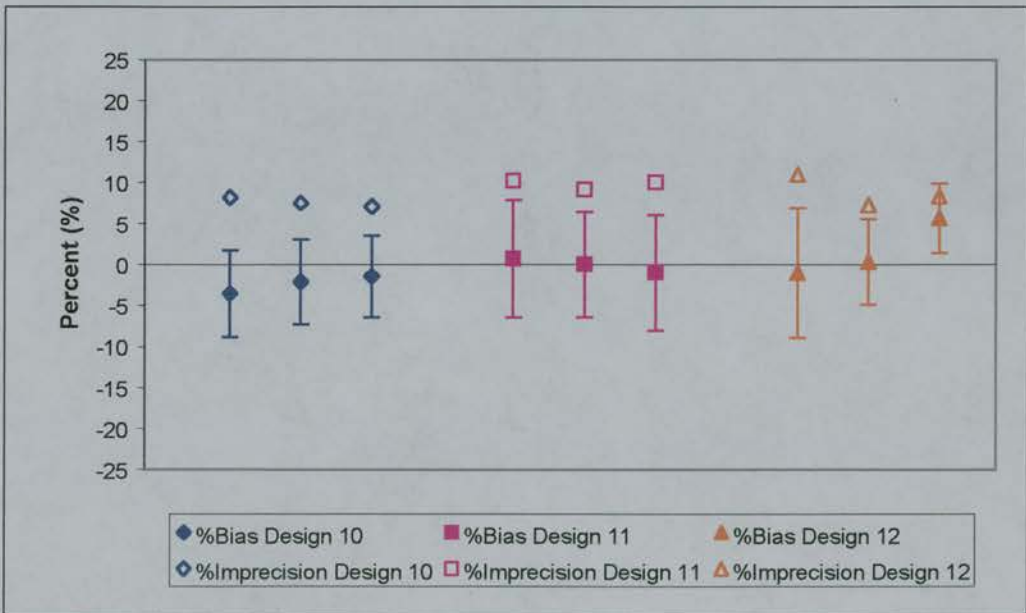


Figure 5.24 %Bias and %Imprecision of the estimation of random proportional error on concentration (σ_I) with windows of 50% of the half life around the second two sampling times.

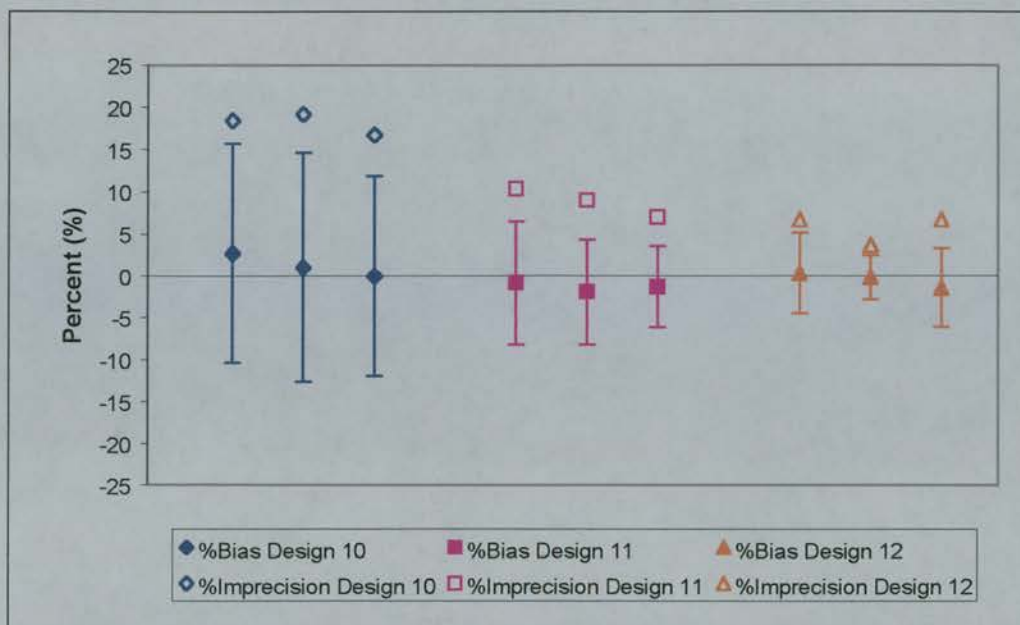


Figure 5.25 %Bias and %Imprecision of the estimation of additive random error on concentration (σ_2) with windows of 10% of the half life around the second two sampling times.

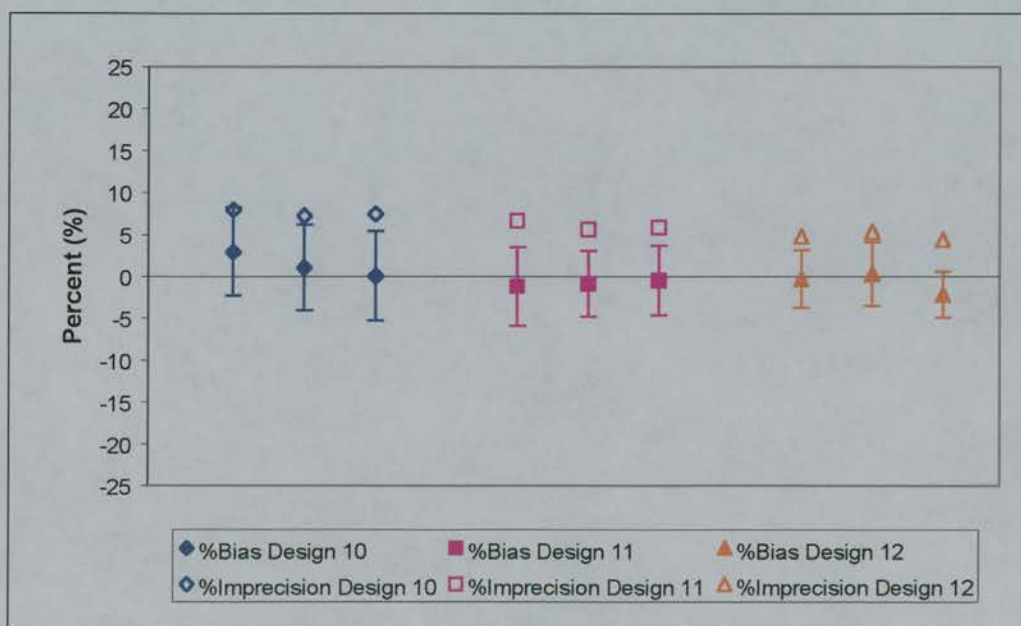


Figure 5.26 %Bias and %Imprecision of the estimation of additive random error on concentration (σ_2) with windows of 50% of the half life around the second two sampling times.

Comparison of Three-Sample Designs to a Two-Sample Design

Table 5.4 compares the three-sample designs (10b, 11b and 12b) to design 8, the two-sample design using a $50\% * t_{1/2}$ sampling window, for $\omega_{Cl} = 3$.

Although the mean biases of the three-sample designs were not always better than those observed in the two-sample design, the imprecision for all parameter estimates was reduced when three samples were used. Each of designs 10, 11 and 12 estimated some parameters better than the designs, but overall there was no distinction to be made between the three-sample designs. The timing of the third sample was not as important as it's inclusion.

Table 5.4 Comparing mean %Bias and %Imprecision for two-sample design 8 with a $50\%*t_{1/2}$ sampling window and the three-sample runs with $50\%*t_{1/2}$ sampling windows (designs 10b, 11b and 12b). Results shown for a standard deviation of clearance = 3 l/h.

Parameter	Design 8		Design 10b		Design 11b		Design 12b	
	Mean %Bias	%Imprecision	Mean %Bias	%Imprecision	Mean %Bias	%Imprecision	Mean %Bias	%Imprecision
\bar{C}_I	0.08	0.97	0.31	0.56	-0.10	0.31	-0.31	0.52
\bar{V}	0.18	0.57	-0.12	0.47	0.16	0.36	0.21	0.45
ω_{CI}	-1.31	4.25	-0.27	1.72	-0.15	1.43	-1.01	1.59
ω_V	0.06	10.34	-1.63	3.50	-1.28	3.83	-2.19	4.82
σ_I	-5.24	21.70	-1.44	7.09	-1.05	9.93	5.66	8.36
σ_2	-2.14	28.96	0.09	7.43	-0.52	5.81	-2.14	4.41

5.4 Discussion

The aim of this chapter was to examine two aspects of limited sampling strategies with a one-compartment PK model. These were (i) the use of sampling windows rather than fixed sampling times and (ii) when to add additional samples to improve parameter estimation.

Two-Sample Designs

In the first section, seven two-sample designs were compared. The first utilised fixed sampling times, as defined by sensitivity analysis in chapter 3 which identified two possible sampling times to be 'as early as possible' and $1.44 * t_{1/2}$. The fixed-sample design (3) was based on the population average PK parameter values. Five other designs (4-8) utilised a sampling window of varying size around the second time defined from sensitivity analysis. The last design (9) also created a spread of second sampling times by basing the second sampling time on each individual's parameter values.

Estimation of Population Mean Clearance (\overline{Cl}) and Volume of Distribution (\overline{V}).

The results from the two-sample designs showed that the fixed effect parameters, clearance and volume of distribution had the smallest mean bias when the designs with sampling windows equal to $40\% * t_{1/2}$ or $50\% * t_{1/2}$ (designs 7-8) were used. In the case of clearance this may be due to these designs allowing later samples to be collected which also aid in the estimation of this parameter when coupled to early sampling times. This is derived from early regression approaches to estimating PK parameters (Endrenyi 1981). Volume of distribution may have also been estimated accurately with these designs as there was a second peak in concentration variance, shown in chapter 3, that occurred at $\frac{2}{k_e}$ (2.0hr) and the designs with the larger sampling windows would have allowed more samples to be taken close to this time.

The most precise estimates for clearance were obtained with the individual-based design (design 9), which is what would be expected if each individual was sampled at their own 'optimal' time of $1.44*t_{1/2}$, defined by the sensitivity analysis. The most precise estimates of volume were obtained with designs 3-7, mainly due to all having a fixed early sample, but the designs with sampling windows may also have had samples taken close to the 2.0 hr time-point as described previously.

However, overall the bias and imprecision in the estimation of the fixed effects was less than 1.6% and so in practice, there was little difference between the designs. Using design 3, based on the average population PK parameter values, or a random sampling window (designs 4-8) provided results that were equally as good as design 9 which could be considered the theoretical best if, in reality, each individual could be sampled optimally.

Estimation of Inter-Individual Variability (ω_{Cl} and ω_V).

Increasing the spread of times around those in design 3 (designs 4-8) resulted in comparable estimates of inter-subject variability in clearance (ω_{Cl}) to those obtained when the fixed-sample design (3) was used. The results from design 9, where a spread of times was obtained by sampling each individual at their own 'optimal' time of $1.44*t_{1/2}$, were also similar. The results for all designs would be considered acceptable in terms of the mean bias and imprecision being less than 15%, however, the 95% confidence intervals for the bias were as much as $\pm 20\%$ for some sets when $\omega_{Cl} = 1$ and this would be unacceptable. However, this may be a factor of presenting these data as percentages.

Inter-subject variability in volume of distribution (ω_V) was best estimated by designs in which there was a sampling window of 40-50% of the drug half-life on the second sample (designs 7 and 8). Again, allowing more samples to be closer to the later time of 2.0 hr may have improved estimation of ω_V with these designs.

In the estimation of ω_{Cl} and ω_V there was little difference between designs 3-8, but the most biased and imprecise estimates were obtained with design 9, the individual-based design.

Estimation of Intra-Individual Variability (σ_1 and σ_2).

The intra-individual variability was estimated poorest using design 9, perhaps because the second times were fixed at the time of $1.44 \cdot t_{1/2}$, when the concentrations were not the lowest observed and hence this result for the additive error component is not unexpected. In general, lower concentrations are more susceptible to additive error and hence hold more information about the parameter. Likewise, that the higher concentrations are more affected by the proportional component, but in this design the timing of the samples was not adequate for defining the residual error model.

The most accurate results for both the proportional and additive components were obtained with designs 3-8 and there was little benefit in using fixed samples based on the population mean parameters or using a spread of times around the optimal time. Although design 3 had fixed sampling times, the results were not as poor as with design 9, presumably because the times were based on the population average PK parameters and not their individual parameters. Hence, at the fixed times, there would have been both high and low concentration measurements and information about the residual error model.

The estimates of intra-subject variability were poorest of the all of the parameters in terms of having the largest mean bias and imprecision. The imprecision across designs 3-8 varied from 15-30% and up to 60% with design 9. This increase in imprecision was most likely a factor of the two-sample designs. However, the designs with sampling windows again performed as well as the fixed-sample design.

Summary of Two-Sample Designs

The use of random sampling within a window around an 'optimal' sampling time gave parameter estimates that were comparable to, if not better than those obtained using either fixed population optimal sampling times or each individual's optimal sampling time. The designs with the larger sampling windows - designs 7 and 8 in which the sampling window was 40 and $50\%*t_{1/2}$ respectively, showed consistently accurate estimates. This confirms the data presented by Hashimoto et al (1991) and Jonsson et al (1996) who both showed that more information is gained about the PK model and the parameters when the sampling window is longer in comparison to the half-life of the drug. This allows more information to be gained about the drop in concentration over time and hence more accurate parameter estimates.

Although the individual-based design (design 9) also resulted in a spread of times, the same information would not be gained in the population sense as the designs above, as each individual is effectively being sampled at the same point in the sampling window ($1.44*t_{1/2}$). Sampling around the 'optimal' sampling times has been shown to protect against model misspecification with simulated data (Hashimoto et al. 1991) and allow a reduction in the number of sampling times with clinical data (Baille et al. 1997). Baille et al allowed random sampling to occur around D-optimal sampling times specified for a 1 hr docetaxel infusion with minimal loss in bias and imprecision in the estimation of the clearance. Thus, perhaps the poor performance of design 9 is not surprising.

Three-Sample Designs.

The second part of this chapter examined the effect of adding a third sample to the two defined from sensitivity analysis. The third sample was placed at different points in relation to the two already defined and three different designs were investigated. Sampling windows were also incorporated for the second and third samples.

The results showed that in general, all pharmacokinetic parameters were well estimated with all of the three-sample designs. The exception to this was the intra-subject variability when estimated using $10\%*t_{1/2}$ windows around the second two sampling times. However, this improved when the $50\%*t_{1/2}$ windows were used.

Estimation of Population Mean Clearance (\bar{Cl}) and Volume of Distribution (\bar{V}).

Clearance and volume of distribution were accurately estimated with all designs and the bias and imprecision were less than 1% on average. This was the case for both the 10% and 50% windows. There was little difference in the estimation of clearance using any of the designs with the $10\%*t_{1/2}$ windows. However, designs 11 and 12, where the third time was added after the two existing times, estimated clearance better than design 10 when the sampling windows were $50\%*t_{1/2}$. This was as expected as later times give better estimates of clearance than earlier ones, as mentioned previously (Endrenyi 1981). Design 10 may not have estimated clearance as well with the 50% window as more of the sampling times may have tended towards earlier times, rather than later, so giving less information about the parameter. Design 11 would have had more sampling times around the 'optimal time' for estimating clearance, of 1.0hr (according to sensitivity analysis), from the window at 1.5hr and design 12 would have had more later times from the window at 2.0 hr giving more information about clearance, as mentioned previously.

Volume of distribution tended to be better estimated when the sampling windows were $10\%*t_{1/2}$ rather than 50%. This may be a factor of the wider sampling times

allowing more times to be later and hence further away from the 'optimal' time for volume of 'as early as possible'.

There was no difference between any of the designs in terms of the imprecision and bias for the fixed effect as all were less than 1%.

Estimation of Inter-Individual Variability (ω_{Cl} and ω_V).

The inter-individual error on clearance, ω_{Cl} , was estimated similarly with all sampling designs and with both sampling window sizes. The inter-individual error of volume of distribution, ω_V , was better estimated when the sampling window was $50\%*t_{1/2}$ rather than 10%. No design offered an overall advantage over the others in the estimation of these parameters.

Estimation of Intra-Individual Variability (σ_1 and σ_2).

The random errors on concentration benefited most from the increase in sampling window size from 10% to $50\%*t_{1/2}$. The estimation of the proportional error component (σ_1) improved from $\pm 22\%$ to $\pm 10\%$ and the estimation of the additional error component (σ_2) improved from $\pm 19\%$ to $\pm 8\%$. Of the three designs, design 10 had the least biased estimates of the proportional error and design 12 performed most accurately in estimating the additive error. In design 10 the three early sampling times give rise to higher concentrations, which will be more affected by the proportional error component than by the small, additive part. The sampling times in design 12 were later and hence resulted in lower concentrations which were more affected by an additive error component. Thus these results are what would be expected.

Summary of Three-Sample Designs

When the three-sample designs were compared to a similar two-sample design, it was obvious that the mean bias may not always be less with three samples over two, but the imprecision was less. These improvements were observed regardless of where the third sample was placed, similar to the results observed by Al Banna et al (1990). The finding of improved parameter estimates with the increased number of samples per subject is not surprising, but it is interesting that the timing of the sample is not important, once the 'optimal' sampling times have been defined.

5.5 Conclusion

In conclusion, the first section of this chapter demonstrated that the use of random sampling within a window around an 'optimal' sampling time gave parameter estimates that were comparable to, if not better than those obtained using either fixed population optimal sampling times or each individual's optimal sampling time. The inter and intra-subject variability showed greatest benefit from the designs using sampling windows and this would allow the use of less stringent sampling schedules when carrying out PK studies in a clinical situation.

The second section of this chapter showed that the addition of a third sample and a larger sampling window offered the advantage of more accurate estimation of random intra-subject errors on concentration over the smaller sampling windows, while no real advantages or disadvantages were seen for the other PK parameters. It was also shown that the timing of the third sample was not as important as its inclusion.

The results presented in this chapter show that sensitivity analysis is a useful tool for defining the initial times for designing a pharmacokinetic study. Using these to build on by the use of sampling windows and additional sampling times should provide flexibility in clinical situations, but also accurate population parameter estimates.

Chapter 6

6 Limited Sampling in a Two-Compartment IV Bolus Pharmacokinetic Model

6.1 Introduction

In this chapter, study designs based on sensitivity analysis were compared to some empirical designs in the estimation of the parameters of a two-compartment PK model following IV bolus administration.

The first set of designs, based on sensitivity analysis, were considered to offer the most information about each of the parameters. The magnitude and also the amount of variability in each parameter affected the time at which peaks in concentration variance occurred. The parameters clearance (Cl), volume of distribution of the central compartment (V_1), volume of distribution of the peripheral compartment (V_2) and the inter-compartmental clearance (Q) were examined for their contributions to peaks in concentration variance. The parameters used in this simulation resulted in a design consisting of five samples - one for each peak in concentration variance due to Cl and V_2 , two due to Q and a fifth corresponding to the peak in concentration variance attributable to V_1 at 0h. This last sampling time was set to be as 'early as possible'. The sampling times were 0.1, 0.3, 0.5, 1.0 and 2.5 hours after administration of an IV bolus dose (see section 3.3.3.2).

Three further designs were based on modifications to the above schedule. The inter-compartmental clearance, Q , resulted in two peaks in concentration variance, namely at 0.3 hr and 2.5 hr. The magnitude of the 2.5 hr peak was small in comparison to all other peaks, and it was unclear how much information about the parameters would be gained by including a sample at this time. In order to investigate this aspect, a four sample schedule was also included with the sampling times fixed at 0.1, 0.3, 0.5 and 1.0 hours.

The influence of variability in sampling times was investigated by the addition of sampling windows. A four-sample schedule with a fixed point at 0.1 hr and three

sampling windows at 0.4, 1.0 and 2.5 hr was examined. The sampling window around 0.4 hr was included to capture information about the points at 0.3 and 0.5 hr, present in the other designs. The inclusion of sampling windows around sampling times mimics variability in sampling times in a real clinical situation.

The fourth design included five samples with sampling windows added only to the 1.0 and 2.5 hr samples. It was considered that in a clinical situation patients could easily be monitored during the period of 0.1, 0.3 and 0.5 hr after administration, so three fixed samples in this period was not unreasonable.

The previous designs were compared to designs in which the sampling times were selected empirically. Conventionally, it might be considered that the minimum number of samples required to define a biexponential curve would be four with two points situated on each component of the curve. Thus designs incorporating sampling times at 0.25, 0.5, 1.25 and 2.5 hours were investigated. In the first design the sampling times were fixed. Two further designs examined the effect of including sampling windows. One consisted of a fixed time at 0.25 hr, and three sampling windows based at 0.5, 1.25 and 2.5 hr. In the other schedule, sampling windows were only included around the times of 1.0 and 2.5 hr. Note that the point at 0.1 hr was deliberately omitted in this set of designs, in order to examine the effect of excluding a very early sample time.

The efficiency of parameter estimation resulting from these designs was examined using the methodology discussed previously (Chapter 2).

6.2 Methods

6.2.1 Data Simulation

Concentration-time data were simulated according to a two-compartment model following a single IV bolus dose of a drug. The methods used were as discussed for the one-compartment case except that the parameters were clearance (Cl), volume of distribution of the central compartment (V_1), volume of distribution of the peripheral compartment (V_2) and the inter-compartmental clearance (Q), with the expected concentration being calculated from:

$$C_{ij}^* = A_i e^{-\alpha_i t_{ij}} + B_i e^{-\beta_i t_{ij}} \quad \text{Equation 6.1}$$

Appendix 1 details the relationships between A , α , B , β and Cl , V_1 , V_2 , Q .

The single IV bolus dose was 100mg and all parameters were assumed to be Normally distributed. The population distribution for Cl had a mean value of 10 l/h and the SD was set at 1, 2 and 3 l/h. The population distributions for the other parameters were mean values of 10 l, 20 l and 15 l/h for V_1 , V_2 and Q , respectively, with standard deviations of 1 l, 2 l, and 1.5 l/h respectively. (Table 6.1).

As in the previous experiments, concentration-time data were simulated for ten sets of 500 individuals using each sampling design.

Each expected concentration, C_{ij}^* , was subject to error by the addition of a random proportional and additive error component as previously described, i.e.,

$$C_{ij} = C_{ij}^* (1 + \varepsilon_{1ij}) + \varepsilon_{2ij} \quad \text{Equation 6.2}$$

where ε_{1ij} and ε_{2ij} were sampled from $\varepsilon_{1ij} \sim N(0, \sigma_1^2)$ and $\varepsilon_{2ij} \sim N(0, \sigma_2^2)$. (Table 6.1).

Table 6.1 Pharmacokinetic parameter values for designs 13 to 19^a (Table 6.2)

Parameter	Value
\bar{Cl}	10 l/h
\bar{V}_1	10 l
\bar{V}_2	20 l
\bar{Q}	15 l/h
ω_{Cl}	1.0, 2.0, 3.0 l/h
ω_{V_1}	1.0 l
ω_{V_2}	2.0 l
ω_Q	1.5 l/h
σ_1	0.05
σ_2	0.35 mg/l

^aIt was assumed that there was no covariance between Cl , V_1 , V_2 , and Q .

6.2.2 Sampling Schedules

As indicated in Chapter 3 (section 3.3.3.2 and table 3.3), the peak times shifted as the variability of each parameter increased from 10% to 50%. The times marked in Figure 6.1 are the means of those obtained in the earlier study and indicate the sampling times used in the initial designs described in this chapter. The components of the total concentration variance due to variability in each parameter are shown in Figure 6.1 for $\omega_{Cl} = 10\%$.

The designs were as follows:

- Design 13. Five sampling times, fixed at the peaks in concentration variance (0.1, 0.3, 0.5, 1.0 and 2.5 hr).
- Design 14. Four fixed samples at the times of the peaks in concentration variance, i.e., as (i), but excluding the time of the second peak due to Q (2.5 hr) as this was small in comparison to the other peaks.
- Design 15. Four samples where the first time was fixed (0.1 hr) and the other three had sampling windows (0.4, 1.0 and 2.5 hr).
- Design 16. Five samples where the first three times were fixed (0.1, 0.3, 0.5 hr) and the other two included sampling windows, (1.0 and 2.5 hr).

The additional three designs selected empirically were:

- Design 17. Four fixed samples (0.25, 0.5, 1.25, 2.5 hr).
- Design 18. Four samples where the first time was fixed (0.25 hr) and three included sampling windows (0.5, 1.25, 2.5 hr).
- Design 19. Four samples where the first two times were fixed (0.25 & 0.5 hr) and the other two incorporated sampling windows (1.25 & 2.5 hr).

Table 6.2 summarises the sampling schedules. The sampling windows were based on the terminal half-life of the hypothetical drug ($t_{1/2\beta}$), i.e., 2.8 hours, and were 10%, 30% or 50% of the $t_{1/2\beta}$, with the larger sampling windows being used for the later time points. Samples were uniformly distributed within each window and figure 6.2 shows the sampling times on a log concentration-time profile.

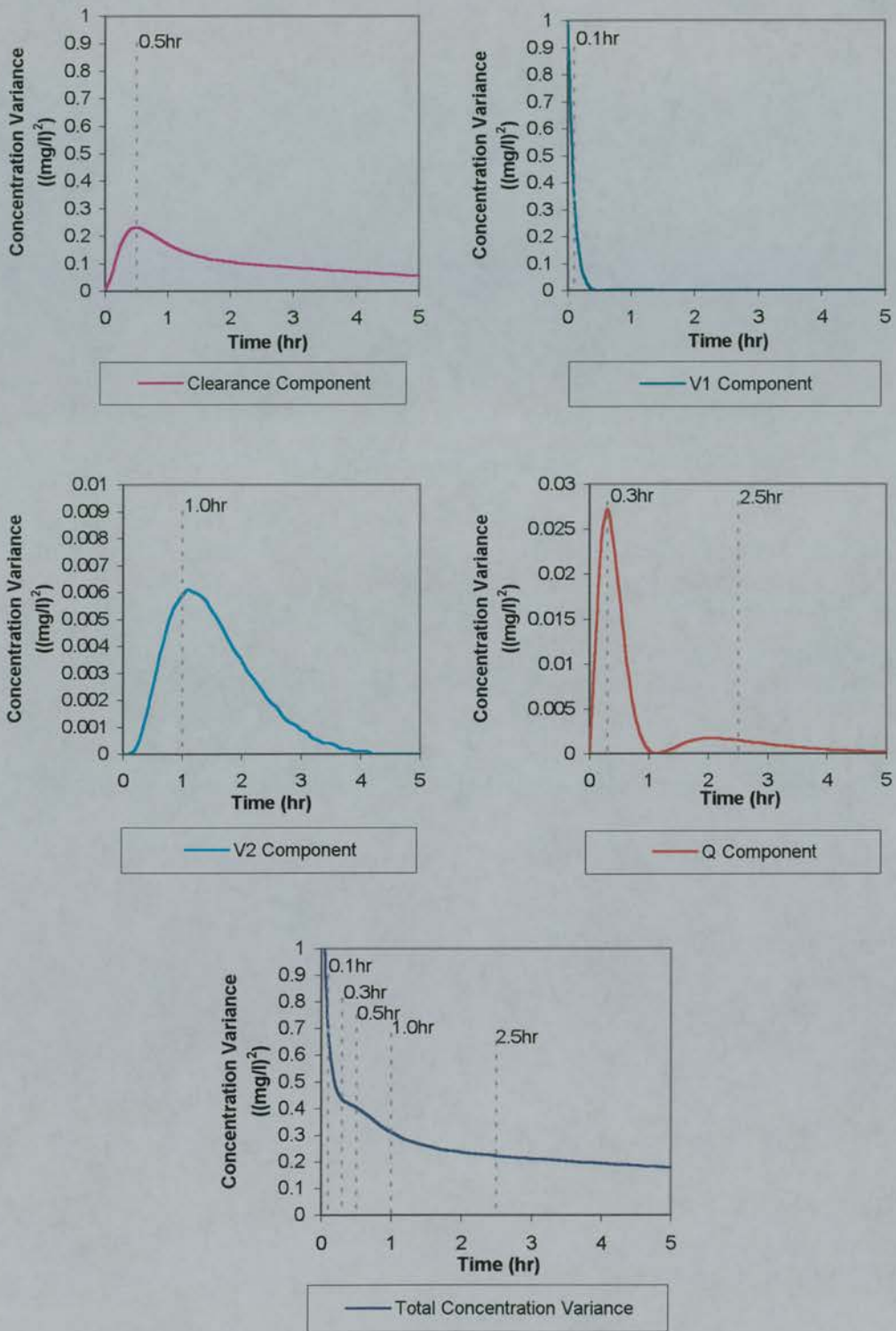


Figure 6.1 Sampling times based on sensitivity analysis for the two-compartment IV bolus PK model.

Table 6.2 Sampling schedules for simulation of the two-compartment IV bolus PK model.

Design No.	Description	Time t_1 (h)	Time t_2 (h)	Time t_3 (h)	Time t_4 (h)	Time t_5 (h)
13	Five Fixed Times	0.1	0.3	0.5	1.0	2.5
14	Four Fixed Times	0.1	0.3	0.5	1.0	-
15	Four Times: One fixed, Three Windows	0.1	0.4 ± 0.28	-	1.0 ± 0.84	2.5 ± 1.4
16	Five Times: Three fixed, Two Windows	0.1	0.3	0.5	1.0 ± 0.84	2.5 ± 1.4
17	Four Fixed Times	-	0.25	0.5	1.25	2.5
18	Four Times: One fixed, Three Windows	-	0.25	0.5 ± 0.28	1.25 ± 0.84	2.5 ± 1.4
19	Four Times: Two fixed, Two Windows	-	0.25	0.5	1.25 ± 0.84	2.5 ± 1.4

Size of sampling windows: 0.28 hr = 10% of $t_{1/2\beta}$, 0.84 hr = 30% of $t_{1/2\beta}$, 1.4 hr = 50% of $t_{1/2\beta}$.

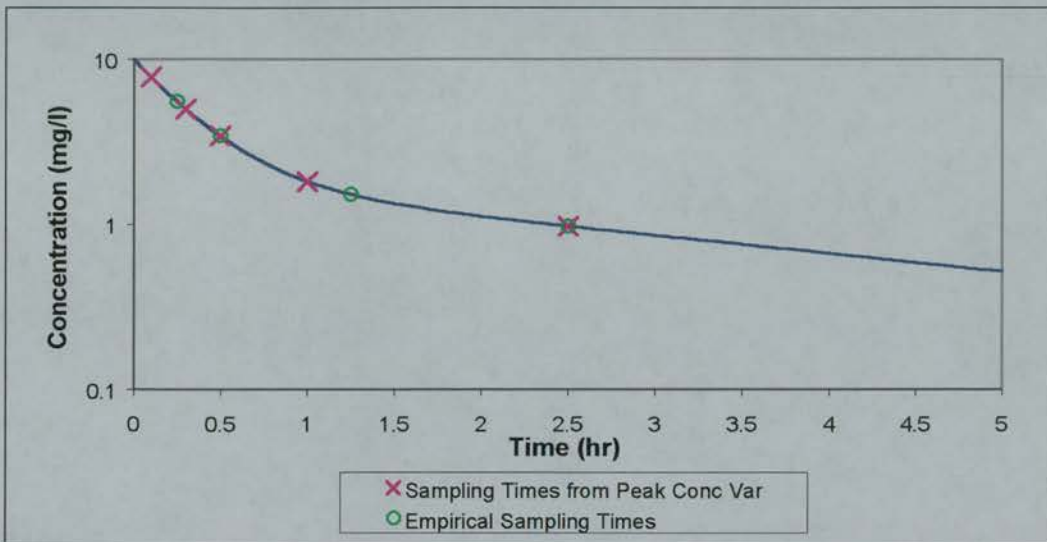


Figure 6.2 Plot of log concentration against time, using the population average parameter values from table 6.1, showing the sampling times according to peaks in concentration variance from each parameter (X) and the empirical sampling times (O).

6.3 Results

Figures 6.3 to 6.13 summarise the average bias and imprecision for the estimates of \overline{CI} , \overline{V}_1 , \overline{V}_2 , \overline{Q} , ω_{CI}^2 , $\omega_{V_1}^2$, $\omega_{V_2}^2$, ω_Q^2 , σ_1^2 and σ_2^2 . Each plot consists of seven sets of results, one for each design, i.e., designs 13 to 19, showing the effect of increasing the population standard deviation for clearance, (ω_{CI}), from 10% to 30%.

Estimation of Population Mean Clearance (\overline{CI})

Figure 6.3 shows the results for clearance. No pattern in either bias or imprecision was evident for any design as ω_{CI} increased from 1 l/h (10%) to 3 l/h (30%).

However, design 13 appeared to perform best of all the designs studied with the average bias being -1% and ranging from -8.4% to 6.0% over all levels of ω_{CI} .

Design 14, four points with the 2.5 hr sample omitted, performed worst and the comparison between designs 13 and 14 indicated the importance of the additional sample at 2.5 hr. Comparing design 14 with designs 15-19 suggests that the importance of the 2.5 hr sample is in the timing rather than the increase in the number of samples from four to five.

The other designs, 15-19, performed similarly, with average bias being less than 6%. Average imprecision was also less than 6% for these designs. The empirical designs 17-19, which included a sample at 2.5 hr, performed almost as well as design 13 in the estimation of clearance.

The inclusion of variability in sampling times in some of the designs had no significant effect, although the standard error of the mean was reduced and hence designs 15, 16, 18 and 19 had improved precision over designs that had fixed sampling times.

Direct comparison of designs 13 & 17 and 15 & 18 showed that there was little difference between schedules based on the peaks in concentration variance or the empirical designs. All results for bias and imprecision for these designs were within

6% for estimating clearance. This was as expected, as all of these designs included data at or around 0.5 hr, which corresponded to the most sensitive time for Cl .

Estimation of Population Mean Volume of Distribution of the Central Compartment (\bar{V}_1)

The volume of distribution of the central compartment (V_1) was estimated accurately for all designs (Figure 6.4) with all estimates of imprecision and bias being within 2.5%. However, design 14 performed worst of the group 13-16, but all designs which included the 0.1 hr point performed better than the empirical designs 17-19 where the first sample was at 0.25 hr.

Designs 15 and 16, which incorporated sampling windows, performed as well as the five-point design with fixed times (design 13).

Estimation of Population Mean Volume of Distribution of the Peripheral Compartment (\bar{V}_2)

The mean bias for the estimation of V_2 for each design, apart from 14, was less than 15%. Design 13 (bias 1-2%, imprecision 8-11%) was comparable to design 17 (bias 2-4%, imprecision 8-12%) indicating that the 0.1 hr time-point contained little information about V_2 . However, designs 15, 16, 18 & 19 which incorporated windows appeared to perform slightly better than the fixed-point designs (13 & 17). Design 14 again performed very poorly in comparison to all of the designs investigated.

Estimation of Population Mean Inter-Compartmental Clearance (\bar{Q})

Similarly, the poorest results for estimating Q were obtained using design 14 (Figure 6.6), with the 95% confidence intervals for the mean bias extending to $\pm 17\%$. The three remaining schedules derived from sensitivity analysis (13, 15 and 16) had similar results with mean biases less than 4%. The imprecision was reduced by using sampling windows rather than fixed times. Design 17 had the smallest mean bias of the empirical schedules, but the largest 95% confidence interval. Again, the imprecision was reduced by the use of sampling windows in the case of designs 18 and 19 compared to 17.

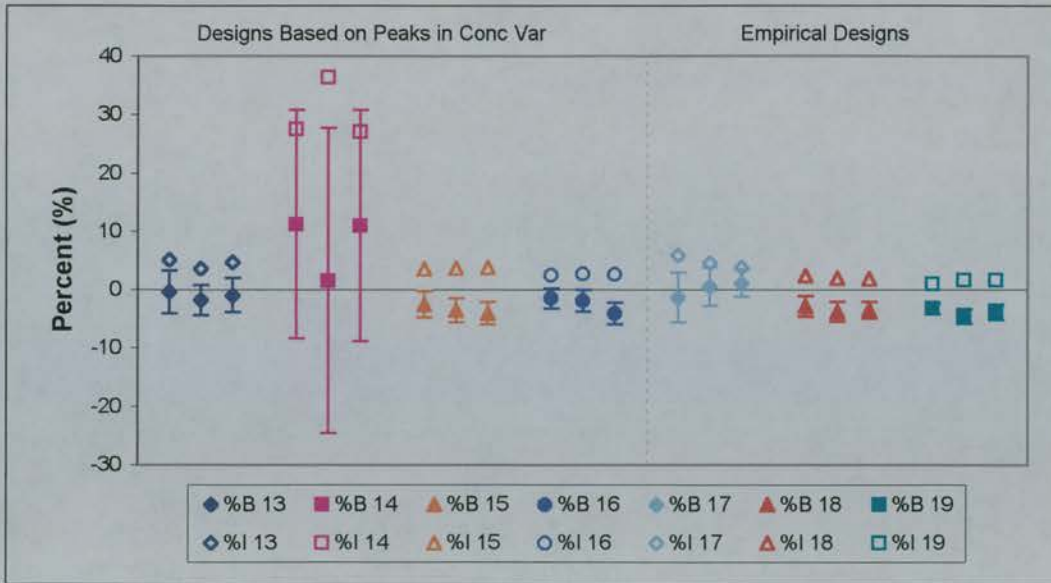


Figure 6.3 Bias (%B) and imprecision (%I) in the estimation of clearance (Cl) using designs 13 to 19. The set of three results for each design represents increasing variability in clearance, i.e., from left to right represents ω_{Cl} increasing from 1 l/h to 3 l/h.

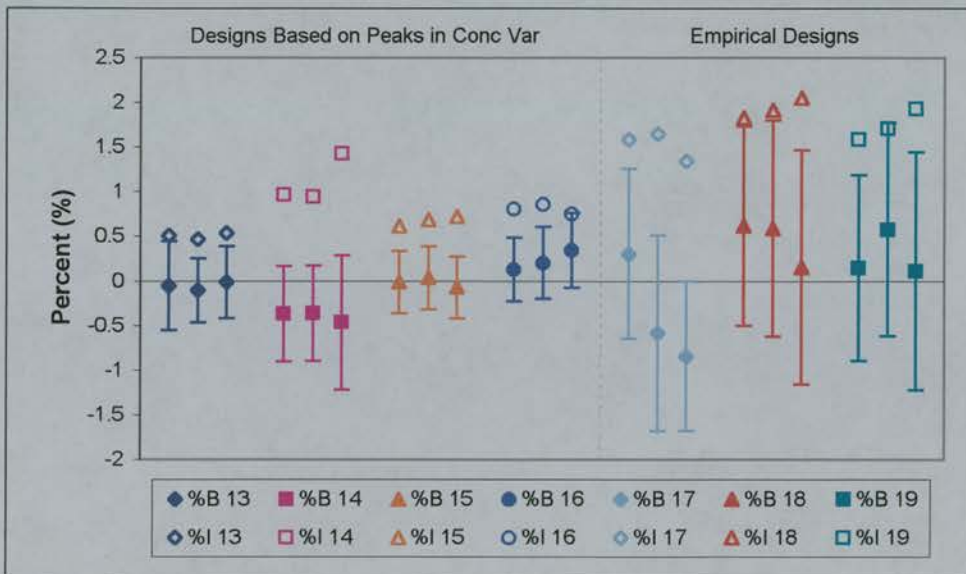


Figure 6.4 Bias (%B) and imprecision (%I) in the estimation of the volume of distribution of the central compartment (V_1) using designs 13 to 19. The set of three results for each design represents increasing variability in clearance, i.e., from left to right represents ω_{Cl} increasing from 1 l/h to 3 l/h.

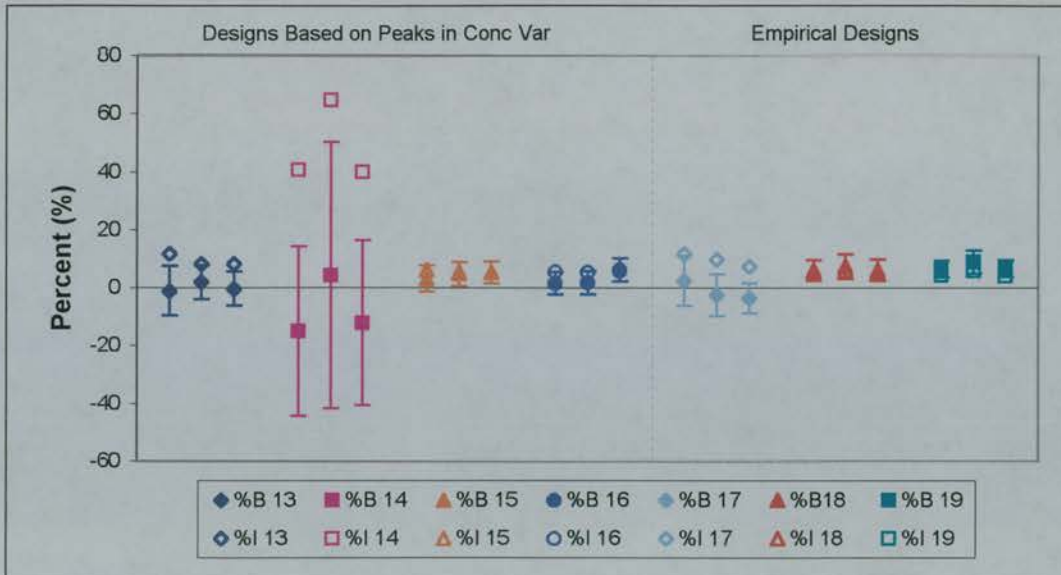


Figure 6.5 Bias (%B) and imprecision (%I) in the estimation of the volume of distribution of the peripheral compartment (V_2) using designs 13 to 19. The set of three results for each design represents increasing variability in clearance, i.e., from left to right represents ω_{Cl} increasing from 1 l/h to 3 l/h.

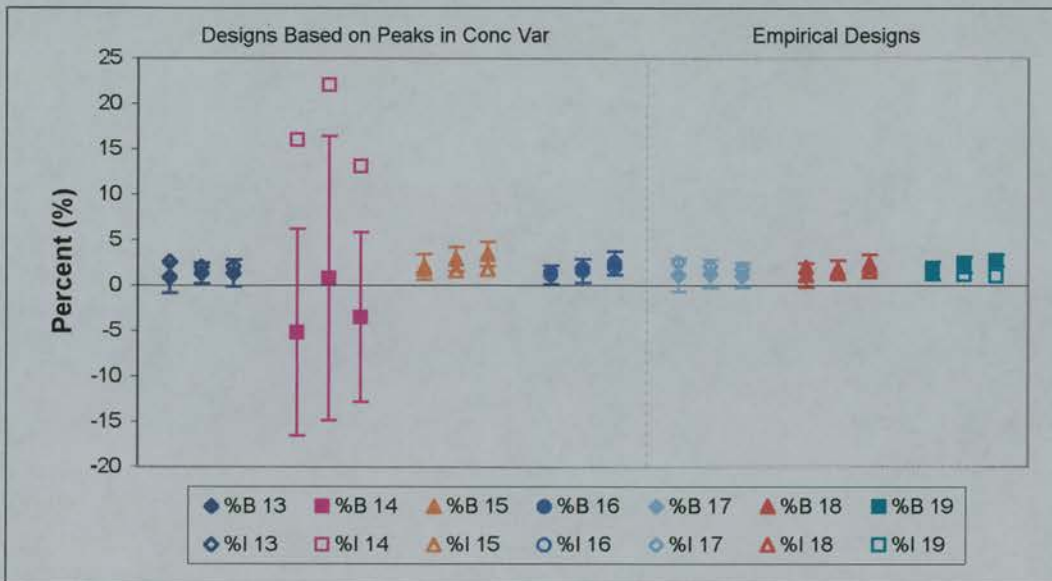


Figure 6.6 Bias (%B) and imprecision (%I) in the estimation of the inter-compartmental clearance (Q) using designs 13 to 19. The set of three results for each design represents increasing variability in clearance, i.e., from left to right represents ω_{Cl} increasing from 1 l/h to 3 l/h.

Estimation of Population Standard Deviation of Clearance (ω_{Cl})

Figure 6.7 shows the bias and imprecision for the estimation of population standard deviation in clearance (ω_{Cl}). The poorest estimation of ω_{Cl} was when the true value was 1 l/h (10%), regardless of the design, and a consistent improvement was evident as ω_{Cl} increased to 20% and 30%. The ten individual estimates of bias are shown in Figure 6.8, where it was clear that the results for ω_{Cl} 10% were due to a greater spread in the estimates than when ω_{Cl} was 20-30%. As ω_{Cl} increased to greater than 20%, all designs performed similarly with mean biases less than 11% and imprecision between 4 and 17%.

Smaller mean biases were found with the fixed sampling designs 13 and 17 when ω_{Cl} was 20-30%, but the smallest imprecision was seen with the designs which incorporated sampling windows (15, 16, 18 & 19).

There was little difference between the schedules based on sensitivity analysis and the empirical designs.

Estimation of Population Standard Deviation of the Volume of Distribution of the Central Compartment (ω_{V_1})

The results for estimating the population standard deviation in the volume of the central compartment (ω_{V_1}) are presented in Figure 6.9. Design 15, which did not include a sample at 0.5 hr, did not perform as well as 13, 14 and 16, for which the bias and imprecision were less than 3% and 11%, respectively. However, the estimation of ω_{V_1} was not influenced by the value of ω_{Cl} in designs 13-16 and these designs performed better than all of the empirical designs, 17-19, which omitted the sample at 0.1 hr. For the latter designs, the mean biases were in excess of 20% and imprecision ranged from 16 to 38%.

Estimation of Population Standard Deviation of the Volume of Distribution of the Peripheral Compartment (ω_{V_2})

The variability of V_2 was estimated poorest of all the fixed and random effect parameters, with the imprecision ranging from 51 to 160% for all designs. The mean biases ranged from -4% to 107%, and most were greater than 15%.

Estimation of Population Standard Deviation of the Inter-Compartmental Clearance (ω_Q)

The variability of Q was also poorly estimated. The mean biases were less than 19%, but the confidence intervals extended to 37 - 45% in the case of designs 14 and 15. The imprecision ranged from 18% to 50% across all schedules.

There was little difference between the sampling designs in the estimation of ω_{V_2} and ω_Q .

Estimation of the Proportional Component of Random Intra-Subject Error (σ_I)

Figure 6.12 summarise the results for the estimation of the proportional random error parameter, σ_I . This was estimated fairly consistently within each design, irrespective of the value of ω_{Cl} . Design 15 performed worse than designs 13, 14 and 16, with a mean bias of 18%, but this varied from 0.5 - 60%. The mean imprecision was also 18% with this design. For designs 13, 14 and 16 the mean bias was consistently approximately 5% with imprecision varying between 10 and 15%. The empirical designs, 17 - 19, performed similarly to design 15 and no design performed consistently well within this group.

Estimation of the Additive Component of Random Intra-Subject Error (σ_2)

In the case of the additive random error, σ_2 (Figure 6.13) all estimates of bias and imprecision were less than 7%. However, design 14 which omitted the 2.5 hr sample, apparently performed poorest of all the designs in terms of imprecision. There were no significant differences between the sampling schedules in terms of magnitude of the bias and imprecision.

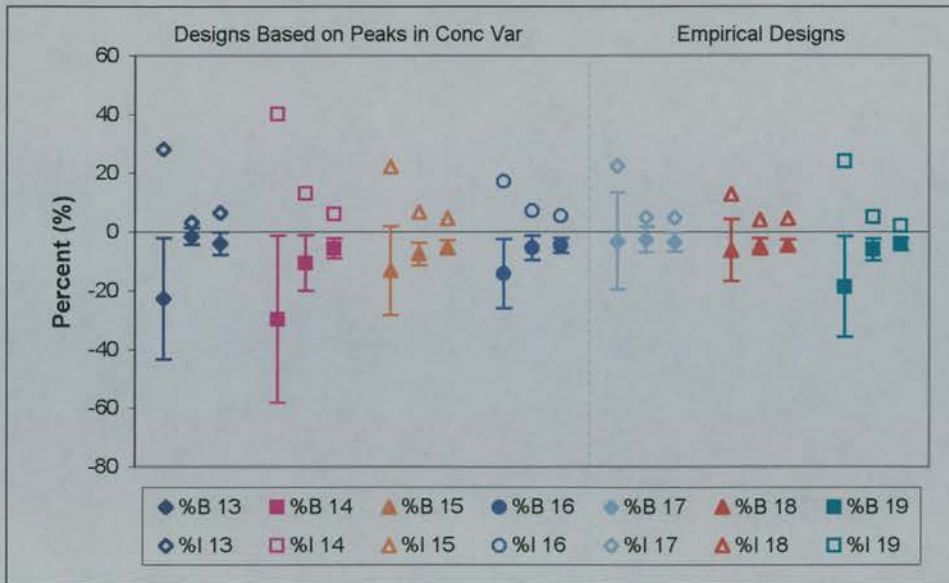


Figure 6.7 Bias (%B) and imprecision (%I) in the estimation of the standard deviation of clearance (ω_{CI}) using designs 13 to 19. The set of three results for each design represents increasing variability in clearance, i.e., from left to right represents ω_{CI} increasing from 1 l/h to 3 l/h.

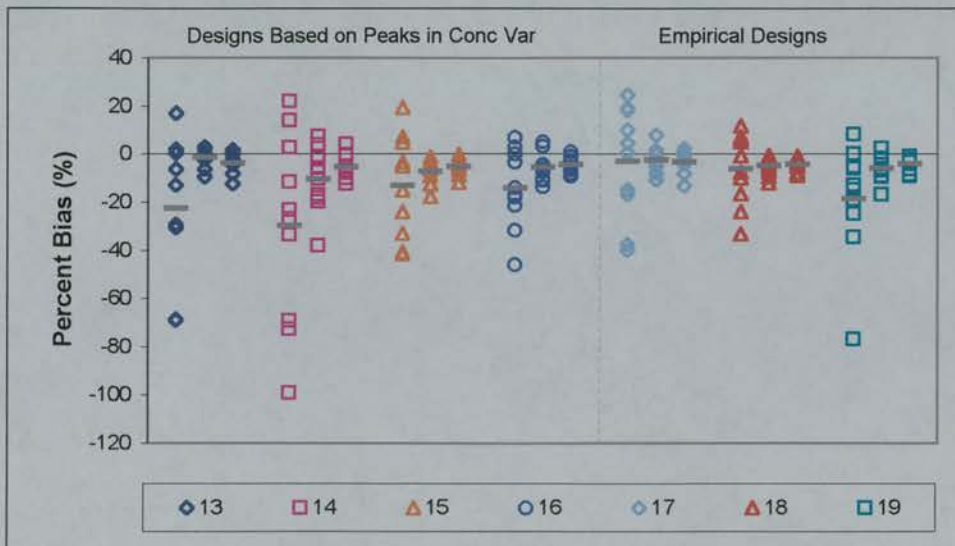


Figure 6.8 Spread of the bias estimates for the standard deviation of clearance (ω_{CI}) using designs 13 to 19. (–) is the mean of the ten bias values. The set of three results for each design represents increasing variability in clearance, i.e., from left to right represents ω_{CI} increasing from 1 l/h to 3 l/h.

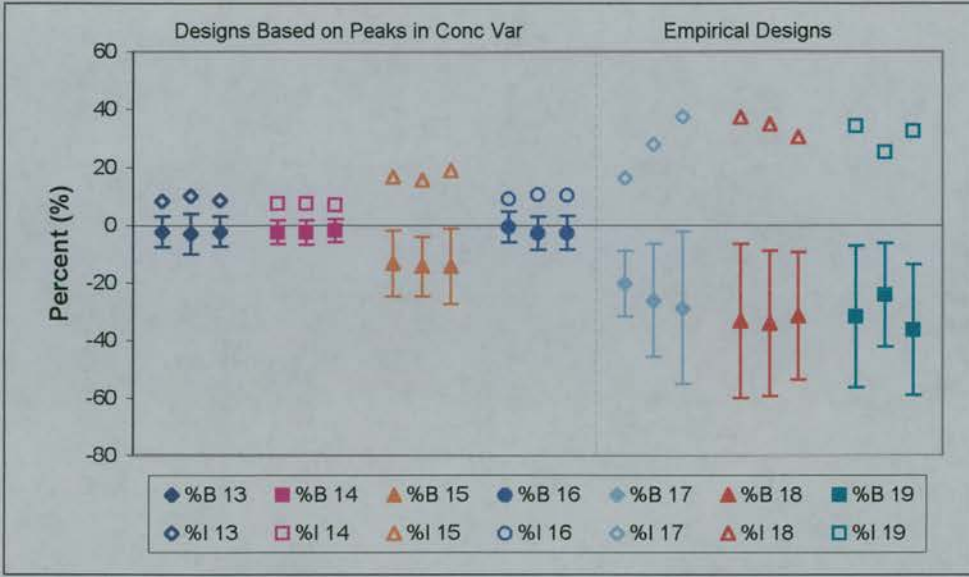


Figure 6.9 Bias (%B) and imprecision (%I) in the estimation of the standard deviation of the volume of the central compartment (ω_{V_1}) using designs 13 to 19. The set of three results for each design represents increasing variability in clearance, i.e., from left to right represents ω_{Cl} increasing from 1 l/h to 3 l/h.

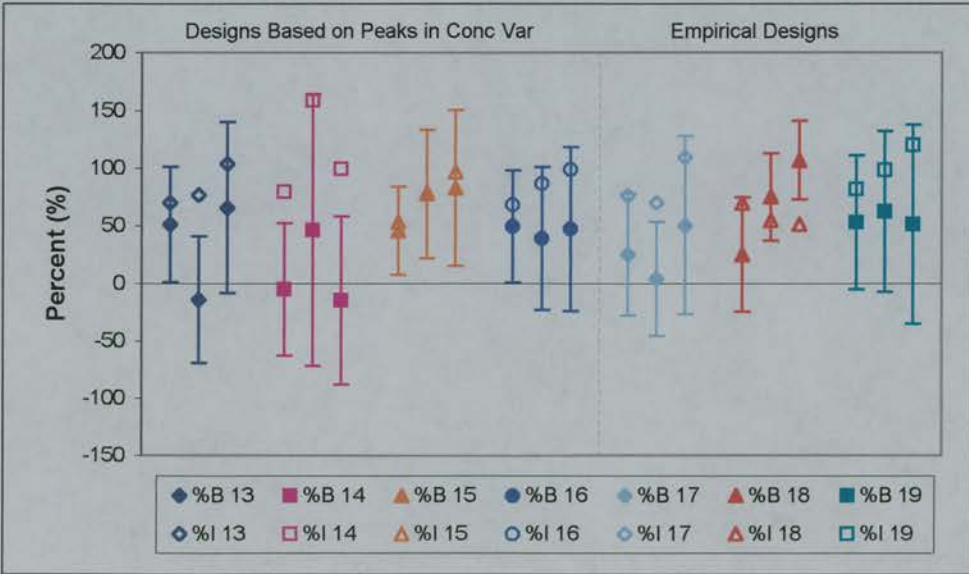


Figure 6.10 Bias (%B) and imprecision (%I) in the estimation of the standard deviation of the volume of the peripheral compartment (ω_{V_2}) using designs 13 to 19. The set of three results for each design represents increasing variability in clearance, i.e., from left to right represents ω_{Cl} increasing from 1 l/h to 3 l/h.

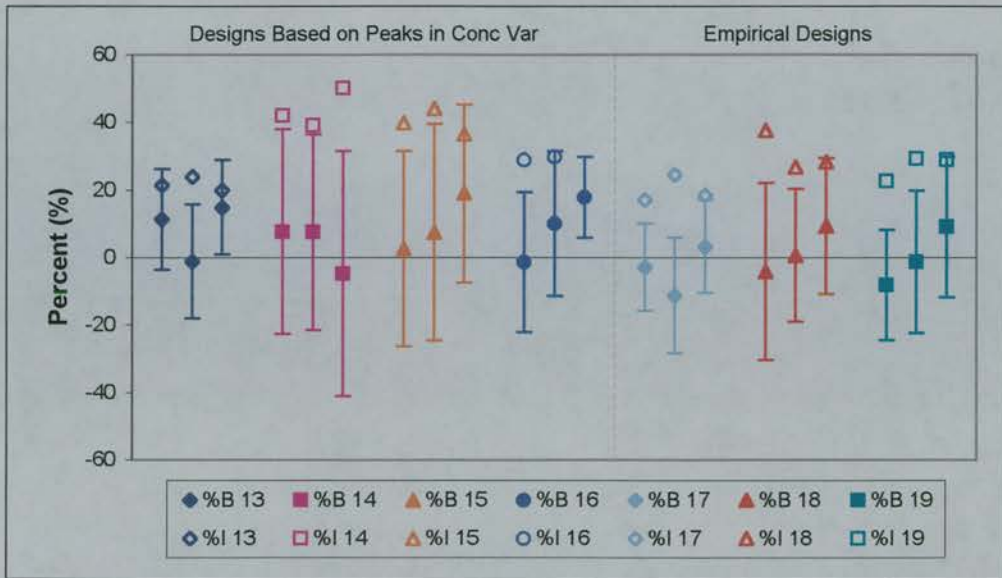


Figure 6.11 Bias (%B) and imprecision (%I) in the estimation of the standard deviation of the inter-compartmental clearance (ω_{Cl}) using designs 13 to 19. The set of three results for each design represents increasing variability in clearance, i.e., from left to right represents ω_{Cl} increasing from 1 l/h to 3 l/h.

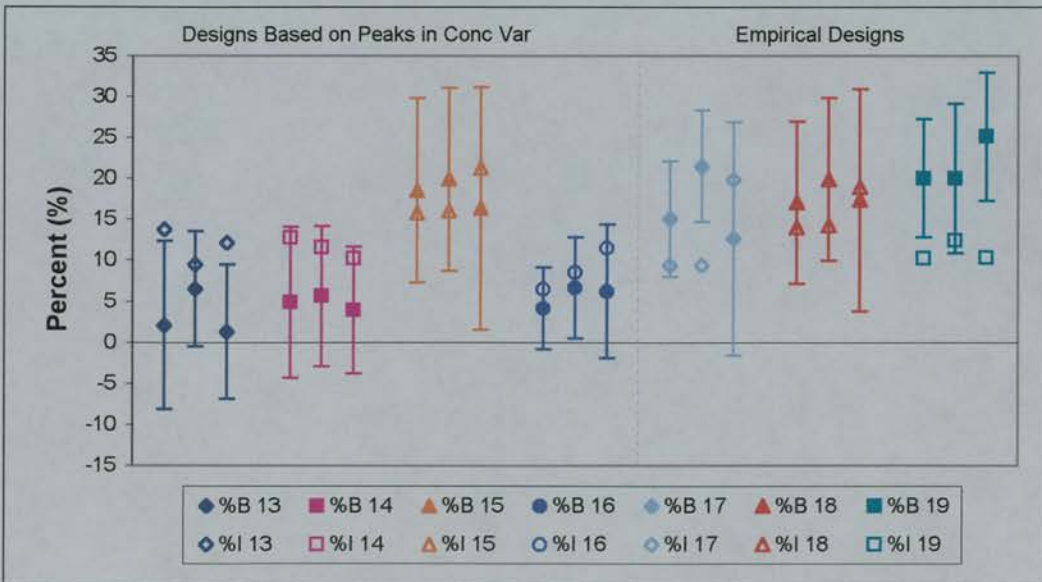


Figure 6.12 Bias (%B) and imprecision (%I) in the estimation of proportional random error on concentration (σ_l) using designs 13 to 19. The set of three results for each design represents increasing variability in clearance, i.e., from left to right represents ω_{Cl} increasing from 1 l/h to 3 l/h.

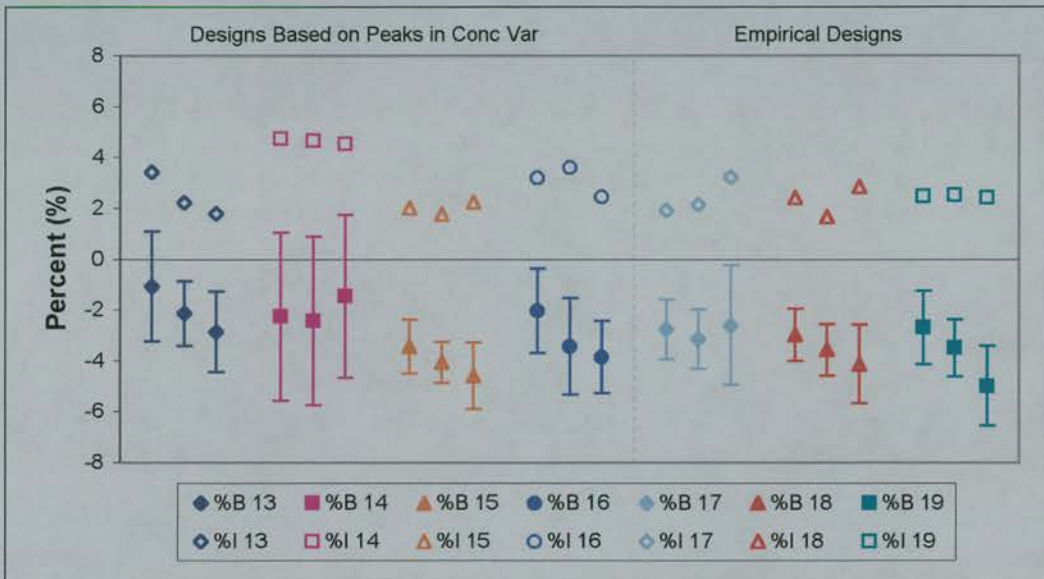


Figure 6.13 Bias (%B) and imprecision (%I) in the estimation of additive random error on concentration (σ_2) using designs 13 to 19. The set of three results for each design represents increasing variability in clearance, i.e., from left to right represents ω_{CI} increasing from 1 l/h to 3 l/h.

6.4 Discussion

The efficiency with which population PK parameters were estimated when the study design was based on sensitivity analysis was compared to that resulting from empirical design.

The initial design consisted of five sampling times at 0.1, 0.3, 0.5, 1.0 and 2.5 hours post dose (design 13). This design was unusual for two reasons: the minimum number of samples for identification of a two-compartment model is considered to be four and also the last sample was taken before one terminal half life ($t_{1/2\beta}$) had elapsed ($t_{1/2\beta} = 2.8$ hr).

Three other designs were based on modifications to schedule 13: a four fixed point design (design 14) consisted of sampling at 0.1, 0.3, 0.5 and 1.0 hours; a four-sample schedule with a fixed 0.1 hr sample and three sampling windows centred at 0.4, 1.0 and 2.5 hr (design 15) and a five-sample schedule, incorporating sampling windows at the 1.0 and 2.5 hr samples (design 16).

The initial empirical designs consisted of a four sample design with samples at 0.25, 0.5, 1.25 and 2.5 hours (design 17). Two further designs were based on this design: four samples with three sampling windows (design 18) and four samples with two sampling windows (design 19).

Overall, each of the fixed effect parameters Cl , V_1 , V_2 and Q were estimated with reasonable accuracy (bias and imprecision within 15%), with all of the designs except design 14. The estimates of V_1 and Q were particularly good with bias and imprecision of less than 5%.

The results show that incorporating sampling windows in the design may not improve parameter estimation in terms of mean bias, but in general imprecision was reduced. This was consistent for all parameters and all designs investigated. It was shown that design 15 (four sampling times with three windows, based on sensitivity

analysis) often performed as well as, if not better than design 13 (five fixed samples), i.e., the 0.4 hr sample with a sampling window was as informative as two fixed samples at 0.3 hr and 0.5 hr, respectively.

Of the designs based on sensitivity analysis, design 14 (four fixed times) performed poorest for the estimation of the fixed effect parameters Cl , V_1 , V_2 and Q , although the bias for V_1 was only 2%. Designs 13 and 14 differed in that the 2.5 hr time point corresponding to the second peak in concentration variability due to Q was removed in design 14. Thus, the result that design 14 estimated Q less accurately was not unexpected. However, the similar effect for Cl , V_1 , and V_2 was not expected. In the case of clearance it is likely that although the 'optimal' time of 0.5 hr was included, later samples also improve estimation of clearance (Endrenyi 1981). Also, figure 6.1 shows that at 2.5 hr the concentration variance due to clearance is still approximately half the value at the peak. Hence, there is still information about clearance to be gained using this sampling time. This is also true for V_2 where the concentration variance at 2.5 hr is approximately a third of the value at the peak. Although no covariance between the parameters was simulated, the estimation process may introduce correlations (see equations in Appendix 1). Hence inter-relationships with Q may also cause V_2 to be inaccurately estimated when Q is poorly estimated. This could explain the fact that V_1 was poorest estimated with this design, although the bias was less than 2% and unlikely to be clinically relevant. Comparison of designs 14 and 15 showed that the timing of the 2.5 hr sample was more important than the increase in the number of samples from four to five.

Schedule 17, four fixed samples chosen empirically, produced the most biased and imprecise estimates of Cl , V_2 and Q of the empirical designs. However, since all imprecision results were less than 15%, this would be unlikely to have clinical relevance. There was little difference between designs 17 to 19 in the estimation of V_1 and all estimates were less than 2.5%.

The sample at 0.5 hr was included in all designs except 15, in which the window around 0.4 hr incorporated similar information. This time should be important for

the estimation of clearance. In general, there was no difference between designs 13, 15, 16, 17, 18 and 19 in the estimation of clearance and all results were within 10%. The results for design 14 implied that the 2.5 hr sample was also important in improving the estimates of clearance as discussed previously.

The volume of distribution of the central compartment (V_1) was estimated well using all designs, and all estimates of bias and imprecision were less than 2.5%. The peak in concentration variance due to V_1 occurred at $t = 0$ hr and the sampling time defined as 'as early as possible', i.e., 0.1 hr, and was included in designs 13 - 16. The empirical designs also included an early sampling time, but this was deliberately selected to be later than 0.1 hr, and the fixed sampling time at 0.25 hr was used in designs 17 - 19. No differences were found within each design. However, it was clear that, although all designs estimated V_1 with minimum bias and imprecision, the designs which included 0.1 hr performed better than those in which the first sample was 0.25 hr.

Of the fixed effect parameters, V_2 was the poorest estimated, although all designs except 14 had bias and imprecision less than 15%. The inclusion of sampling windows increased the mean bias, but reduced the imprecision. Examination of designs 17 to 19 showed that the sampling window at 1.25 hr (designs 18 and 19) improved the estimation of V_2 compared to the fixed sampling time design (17). This may have been due to more samples being closer to 1.0 hr, the time suggested by sensitivity analysis for V_2 . Apart from design 14, there was little difference between the other designs in terms of bias and imprecision in the estimation of V_2 .

Similarly, the inter-compartmental clearance, Q , was estimated accurately, regardless of the design, except for design 14. All parameter estimates from designs 13 and 15 to 19 were within 5% of the true value. Sensitivity analysis suggested two design points with respect to Q , i.e., at 0.3 hr and 2.5 hr. The 2.5 hr sample was removed in design 14 and was shown to be important in the estimation of all of the fixed effect parameters. Although the empirical designs did not include the 0.3 hr sample, the

sample at 0.25 hr may have been close enough to 0.3 hr to allow accurate estimation of Q .

Regardless of the design, the random effect parameters were less accurately estimated than the fixed effect parameters.

The estimation of ω_{CI} depended on the true value, and for all designs performance improved as ω_{CI} increased from 10% to 30%. When $\omega_{CI}=1$ l/h the estimation was highly variable within each design and up to three outliers were present in some sets of results, causing high values of imprecision. However, when $\omega_{CI}=2-3$ l/h, there was little difference between the designs in terms of either bias or imprecision. The four-sample designs incorporating windows (15, 18 and 19) performed as well as the five-sample designs (13 and 16), and indicated that these designs might require fewer samples for similar performance.

In estimating the variability of V_I , (ω_{V_I}), design 15 performed poorest of the designs based on the sensitivity analysis, probably due to having only two early times compared to the three early times in designs 13, 14 and 16. The sampling window at 0.4 hr also allowed more of the second samples to be taken later, i.e., instead of two early samples at 0.1 and 0.3 hr, the second time could be at 0.9 hr. The concentration variance due to V_I falls rapidly, suggesting that at 0.3 hr there would be much more information than at 0.9 hr.

Designs 17 - 19 showed similar results for the estimation of ω_{V_I} as for V_I , i.e., there was little difference between the designs as all had the early time at 0.25 hr. However, all empirical designs performed poorer than those which included the 0.1 hr point. Imprecision was poor, up to 51% with designs 18 and 19, and the mean bias varied from 20-36%. This showed that while the 0.25 hr sample was adequate for estimating the fixed effect, V_I , ω_{V_I} was better estimated using the earlier sampling time.

Similar to the fixed effect parameter V_2 , the variability ω_{V_2} was the poorest estimated of the random effect parameters, regardless of the sampling design. Overall, the empirical designs had slightly better results than the other designs. Table 3.3 showed that as the variability in V_2 increased from 10 to 30%, the peak in concentration variance moved from 1.1 to 0.9 hr. Over all designs, those incorporating three windows (15 and 18) had the lowest imprecision showing that increasing the variability in sampling times improved estimation of ω_{V_2} . In particular the windows on the 0.4 and 0.5 hr sampling times appeared to improve estimation of ω_{V_2} . This could be due to more samples being closer to the peak in concentration variance.

In estimating the variability in Q (ω_Q), including sampling windows did not improve the bias or imprecision compared to fixed sampling time designs. Similar to ω_{V_2} , the empirical designs showed slightly better results for ω_Q than the designs based on the sensitivity analysis, although three sampling window designs offered no improvement over those with two sampling windows. However, using sampling windows would be more convenient in clinical practice.

The proportional random error component, σ_1 , was estimated less accurately than the additive component, σ_2 , regardless of the design. In particular, design 15 estimated σ_1 less accurately than the other three designs based on the sensitivity analysis, probably due to designs 13, 14 and 16 having three early samples compared to two in design 15. Higher concentrations at earlier times are more susceptible to proportional error and hence have most information about σ_1 . The results obtained using the other designs (17 to 19) were similar to those from design 15 in terms of bias and imprecision, also indicating that early sampling times appear to hold more information about σ_1 .

Later concentrations, being lower, were more affected by additive error, and all results for σ_2 were accurate. The most notable result from this aspect was that design

14, which did not include the late 2.5 hr sample, had the highest imprecision. Designs 15, 16, 18 and 19, including sampling windows, showed greater precision, possibly by allowing samples to be taken even later than 2.5 hr. However, overall there was little difference between the designs.

In conclusion, these results showed that while incorporating sampling windows may not have improved the mean bias, the imprecision was generally reduced for all designs. Sampling windows, mimicking variability in sampling in a clinical situation, performed no worse than the fixed times, although in a real clinical situation, the sampling times would have to be recorded accurately to make the data reliable. The inclusion of sampling windows may also allow a reduction in the number of samples from five to four, without an increase in bias and imprecision. This is similar to results presented by Baille et al (Baille et al. 1997) where random sampling occurred around D-optimal sampling times specified for a 1 hr docetaxel infusion. This resulted in a six-sample model as the pharmacokinetics of docetaxel are described by a three-compartment model. D-optimality does not allow less samples than there are parameters to be estimated (Silvey 1980). When coupled to a Bayesian estimation algorithm this allowed a reduction from six samples to four with minimal loss in bias and imprecision. In addition a two fixed-sample design was selected as being acceptable for use in an outpatient setting.

The most obvious result of using the designs based on sensitivity analysis in these simulations was that while the estimates of the fixed effects were similar to those obtained with empirical designs, the estimates of the random effects were generally improved. This would confirm the suggestion from chapter 3 that basing sampling schedules on sensitivity analysis is worthwhile and that the use of these times allows accurate estimation of both the fixed and random effect PK parameters. In addition, these sampling times provide an initial design that extra samples could be added to when there are doubts about the identification of the PK model and the true population parameter values.

Chapter 7

7 Application of Limited Sampling Design to Two Anticancer Drugs

7.1 One-Compartment PK Model - Carboplatin (Simulated Data)

7.1.1 Introduction

In chapter 3 a sensitivity analysis was described in which the analysis was used to define the times at which the model output was most sensitive to changes in each model parameter. In that chapter arbitrary values of the parameters were chosen and the variability in each was small.

In this section of chapter 7 the one-compartment PK model described in chapter three was re-examined, using PK parameter values for an existing anticancer drug, carboplatin. As carboplatin pharmacokinetics are best described by a two-compartment model, it was necessary to modify the parameter values. Carboplatin was chosen as the pharmacokinetics are well established (van der Vijgh 1991; Duffull et al. 1997). The two-compartment data from several studies was modified by averaging the values published for the parameters volume at steady state (V_{SS}) and total clearance (CL). These were then treated as the parameters for the one-compartment model (V and Cl) with the variability in V 26% and Cl 30% (van der Vijgh 1991).

The sampling schedules derived from sensitivity analysis were compared to sampling designs derived from two published carboplatin limited sampling strategies from the Biomed2 project (Personal Communication, D.I. Jodrell, L.S. Murray). The Biomed2 project compared two therapeutic protocols for ovarian cancer:

- Carboplatin given as a single agent by 30 minute IV infusion.
- Carboplatin given as a 1 hour IV infusion following a 3 hour IV infusion of taxol.

Nine sampling designs in total were examined for their accuracy in estimating the PK parameters and the random variability associated with them.

7.1.2 Methods

7.1.2.1 Data Simulation

Concentration-time data for this section were simulated according to a one-compartment PK model, following a single IV bolus dose of 400mg of carboplatin and were derived as described previously in Chapter 2.

The population mean values of the parameters used in the simulations are summarised in table 7.1, along with the standard deviations. The values used in this thesis were taken from the publication by van der Vijgh (van der Vijgh 1991) where the population parameter estimates of carboplatin in plasma from several PK studies were listed. The values for the total clearance (CL (ml/min/m²)) and the volume of distribution at steady state (V_{SS} (l/m²)) of the six studies listed were averaged to give values of 4.6 l/h/m² and 15.4 l/m², respectively. These average values were rounded to give the values of 5.0 l/h and 15.0 l, which were used in the simulations, along with an IV bolus dose of 400mg. The dose was obtained from a regimen of 400mg/m², which was used prior to the dosing of carboplatin being based on AUC values. A combination error model was used and the values used are also listed in table 7.1.

7.1.2.2 Sampling Schedules

The sampling schedules based upon the sensitivity analysis described in chapter 3 were defined for the carboplatin parameter values listed in table 7.1. As in section 3.3, the concentration variance was examined using simulated populations of 5000 subjects and compared to that calculated from the equations derived in chapter 3. This was to ensure that predicted peaks in concentration variance were similar to those observed in simulated populations, in order to select the sampling times. Both the total calculated and simulated concentration variances over time are shown in figure 7.1, along with the separate, calculated, components due to clearance and volume of distribution. The choice of sampling times is also shown in relation to the peaks in concentration variance.

Table 7.1 Mean pharmacokinetic parameter values for Carboplatin simulations^a.

Parameter	Value
\overline{Cl}	5 l/h
\overline{V}	15 l
ω_{Cl}	1.5 l/h
ω_V	4 l
σ_l	0.05
σ_2	0.67 mg/l

^aIt was assumed that there was no covariance between Cl and V .

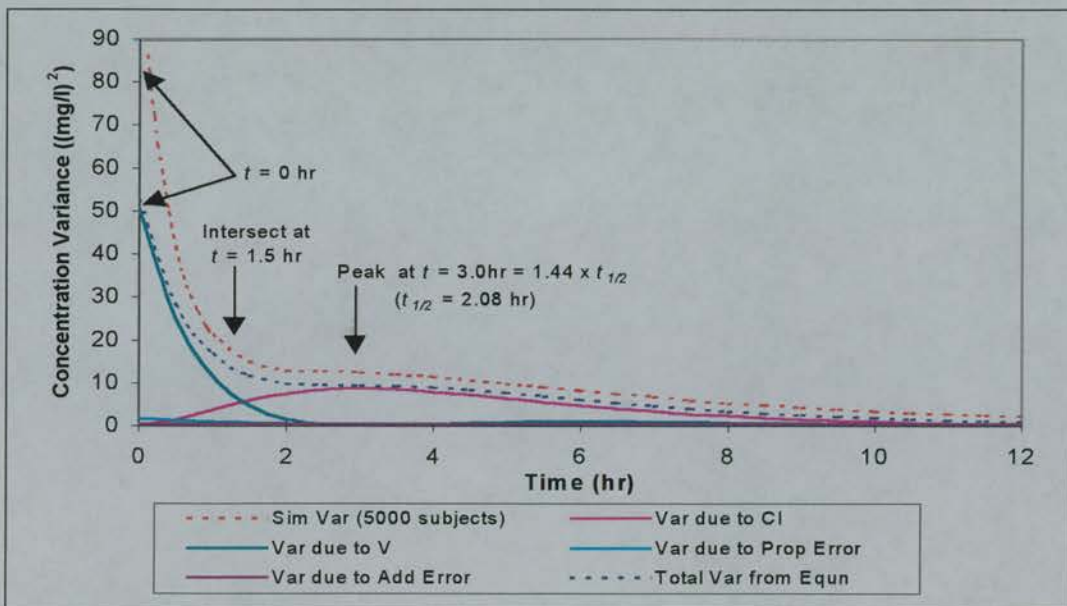


Figure 7.1 Sensitivity analysis of concentration variance using carboplatin parameter values. The variance in concentration from a simulated population of 5000 subjects was compared to that predicted. Two sampling times were based on the peaks in concentration variance due to the components clearance and volume of distribution. A third sampling time was selected from the intersect of the variance curves due to these components.

Figure 7.1 shows that the derived equations produced two peaks in concentration variance - one at $t = 0$ hr due to the volume of distribution component and one at 3.0hrs due to the clearance component. As in chapter 4, these two sampling times were examined along with the time at which the two curves intersected - 1.5hr. The first sample time was set to 0.1hr, rather than 0hr. The total variability in concentration within the simulated population was slightly higher than the total predicted from the equations, although the two peaks occurred at the same times.

Three different designs based on the sensitivity analysis using carboplatin parameter values were investigated:

- Design 20. Two fixed sampling times using the early peak and the time of the intersection of the curves due to the clearance and volume components (0.1 & 1.5 hr).
- Design 21. Two fixed sampling times at the times of the two peaks in concentration variance (0.1 & 3.0 hr).
- Design 22. Three fixed sampling times at each of the above times (0.1, 1.5 & 3.0 hr).

The above sampling schedules were also compared to two further designs, with sampling times from the Biomed2 project. Only the sampling times were taken from these schedules and the simulation was carried out using an IV bolus and one-compartment PK model as previously described.

- Design 23. Based on the Biomed2 schedule (where carboplatin was given as a single agent by a 30 minute IV infusion). Sampling was taken 1, 4 and 6 hours after the end of the infusion.
- Design 24. Based on the Biomed2 schedule (where carboplatin was given as a 1 hour IV infusion in combination with a 3 hour IV infusion of taxol). Taxol was given first and the sampling times were at 0, 1, 3, 4, 6, 8 and 12 hours after starting taxol. For the purpose of this simulation the sampling times of interest were those following administration of carboplatin, i.e., 4, 6, 8 and 12 hours which correspond to 1, 3, 5 and 9 hours after starting the carboplatin infusion.

A further four three-sample designs were simulated based on design 24 above. All combinations of three sampling times out of the four were examined.

Design 25. 1.0, 3.0 & 5.0 hr from the start of the 1 hr infusion.

Design 26. 1.0, 5.0 & 9.0 hr from the start of the 1 hr infusion.

Design 27. 1.0, 3.0 & 9.0 hr from the start of the 1 hr infusion.

Design 28. 3.0, 5.0 & 9.0 hr from the start of the 1 hr infusion.

Thus nine designs were investigated in total with ten data sets of 500 subjects simulated for each design. The sampling schedules for carboplatin are summarised in table 7.2 and illustrated on a mean concentration-time curve in figure 7.2. Figure 7.3 shows how the sampling designs relate to the concentration variance-time curves.

7.1.2.3 Data Analysis

The parameters \overline{Cl} , \overline{V} , ω_{Cl}^2 , ω_V^2 , σ_1^2 and σ_2^2 were estimated by NONMEM, version V, using FOCE with interaction, and calculation of the percentage bias and imprecision of the NONMEM population estimates for each data set were as described in chapter 2.

NONMEM estimates were compared to the true (simulated) value by subtracting the simulated value from the NONMEM value and plotting this difference, ideally zero. The magnitude of the deviations from zero were used to compare the different designs.

Table 7.2 Sampling Schedules for Carboplatin using a One-Compartment IV Bolus PK Model.

Design No.	Time t₁ (h)	Time t₂ (h)	Time t₃ (h)	Time t₄ (h)
20	0.1	1.5	-	-
Times based on Sensitivity Analysis				
21	0.1	3.0	-	-
22	0.1	1.5	3.0	-
Times based on the Biomed2 Project				
23	1.0	4.0	6.0	-
24	1.0	3.0	5.0	9.0
Times Modified from Design 24				
25	1.0	3.0	5.0	-
26	1.0	-	5.0	9.0
27	1.0	3.0	-	9.0
28	-	3.0	5.0	9.0

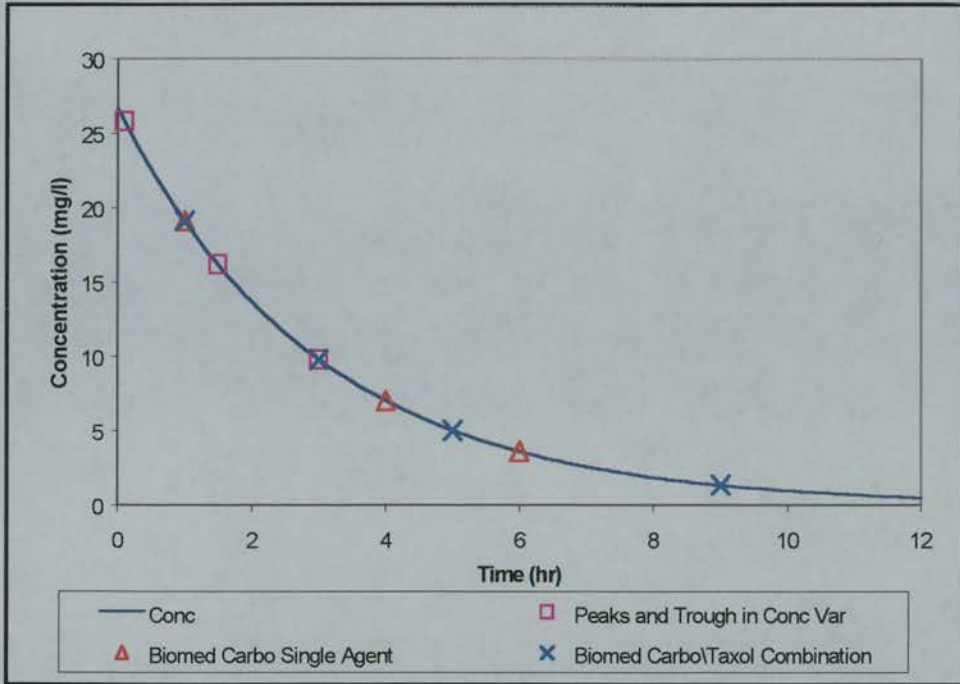


Figure 7.2 Plot of concentration vs time for the mean values of clearance and volume, with the sampling times.

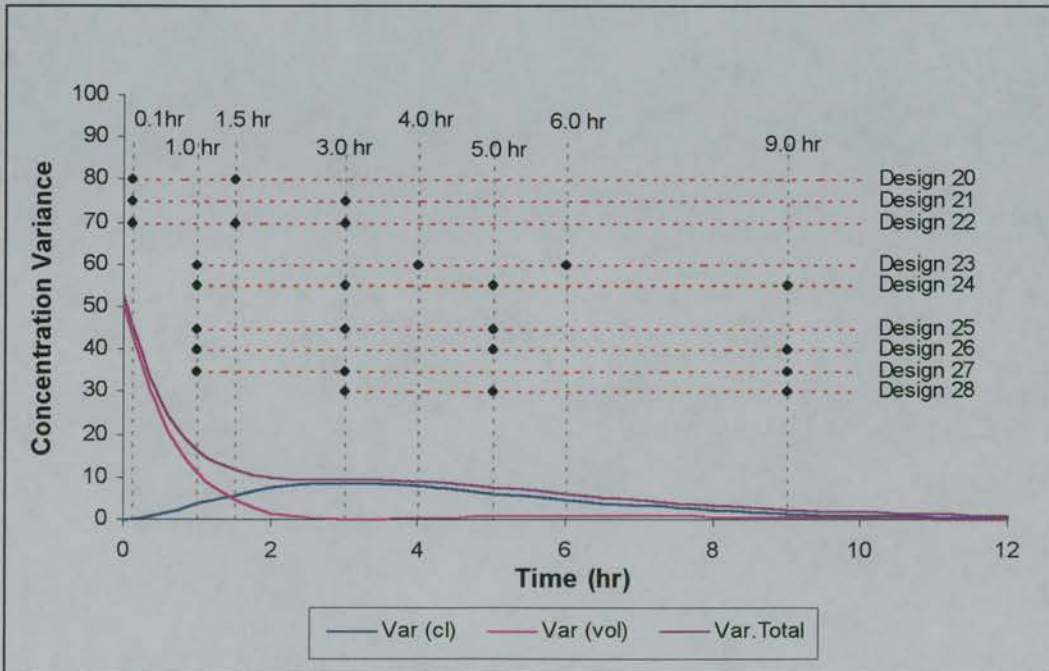


Figure 7.3 Carboplatin sampling designs shown on the concentration variance curve.

7.1.3 Results

Estimation of Population Mean Clearance.

Figure 7.4 shows the bias and imprecision results for the estimation of carboplatin clearance using the nine sampling schedules. All designs except design 28 had bias and imprecision of less than 1%. The results for design 28 were less than 3.5%.

Design 24 had the smallest degree of imprecision and the narrowest confidence interval for the bias. This was to be expected as it also had the most sampling times (four). Five of the three-sample schedules (designs 22, 23, 25, 26 and 27) had similar values for bias and imprecision and performed as well as design 24. Of the two-sample schedules, design 21 performed better than design 20, with a narrower 95% confidence interval and smaller amount of imprecision. Design 21 also performed comparably with the following three-sample schedules: designs 22, 23, 25, 26 and 27.

Figure 7.5 shows how each of the ten NONMEM estimates of clearance within each sampling schedule compared to the simulated mean value, by subtracting the simulated value from the NONMEM estimate. Design 28 showed the greatest deviation from zero and all values were positive, showing that NONMEM consistently over-estimated clearance with design 28. All other sampling designs had distributions which included zero. However, as stated previously, all designs had bias and imprecision within 3.5%, showing no difference between the designs.

Estimation of Population Mean Volume of Distribution.

Bias and imprecision in the estimation of volume of distribution is shown in figure 7.6. The results were similar to those for clearance in that all sets except design 28 had results for bias and imprecision of less than 1%.

Design 24, with four sampling times had the narrowest 95% confidence interval, but not the smallest mean bias or imprecision of the designs. Both of the two-sample

schedules (designs 20 & 21) performed equally with similar values of bias and imprecision. In fact, the two-sample schedules performed best in terms of the smallest mean bias and imprecision. Designs 22 and 25 with three samples had similar values for bias and imprecision as designs 20 and 21.

The ten NONMEM estimates of volume of distribution are compared to the simulated values in figure 7.7. As in the estimation of clearance, design 28 was most biased and the distribution of estimates for all other sampling schedules included zero, with small differences between the simulated and estimated population values for volume of distribution.

Estimation of Standard Deviation of Clearance (ω_{Cl})

In the estimation of ω_{Cl} , all sets had mean bias and imprecision of less than 8% and all sets except design 26 and design 28 had mean bias of less than 1% (figure 7.8). Design 24 with four sampling times had the narrowest confidence interval for bias, but was comparable to that of designs 22, 26 and 27 with three sampling times. The two-sample designs 20 and 21 had the widest confidence intervals, but the value of mean bias is comparable to the other schedules. Of the three-sample schedules, design 28 had the widest confidence interval.

The schedule which proved most precise in the estimation of ω_{Cl} was design 24, with four sampling times. However, designs 22 and 27, with three sampling times had comparable precision. The imprecision for all sampling schedules was less than 7%, with the two-sample schedule, design 20, performing poorest.

Figure 7.9 shows how the ten NONMEM population estimates of ω_{Cl} compared to the simulated values, for each sampling design. When the simulated population values were subtracted from the NONMEM estimates of ω_{Cl} design 28 again had values that were generally positive, indicating that NONMEM consistently overestimated ω_{Cl} with this sampling design. However, the furthest point from zero was one of the estimates from design 20. This corresponded to one data set that had

-14% bias. The estimates from design 20 and design 21 tended to be slightly further from zero than all other sampling schedules, but included zero in the distribution.

Estimation of Standard Deviation of Volume (ω_V)

Figure 7.10 shows the bias and imprecision in the estimation of ω_V . All sampling schedules except designs 26 and 28 had mean bias of less than 2%. Design 22 had the smallest degree of imprecision in the estimation of ω_V and the imprecision was less than 2.7% for all sets except designs 26 and 28.

The two-sample schedules (designs 20 and 21) estimated ω_V as well as the three and four-sample schedules (designs 22-25 and 27).

Figure 7.11 compares the NONMEM estimates of ω_V for each sampling schedule to the original simulated values. The distribution of differences from all sampling schedules, except designs 26 and 28, included zero, after subtraction of the simulated value from the NONMEM estimate.

Estimation of Proportional Random Error on Concentration (σ_I)

The concentration random error terms were poorest estimated of all parameters, probably due the limited number of sampling times.

The bias and imprecision calculated during the estimation of the proportional random error (σ_I) is shown in figure 7.12. The two-sample schedules, designs 20 and 21, had the largest mean bias (-30% and -60%, respectively) and also the widest confidence intervals, although the confidence interval for design 25 was similar to design 21. Designs 22 and 23 (three-sample designs) and 24 (four-sample design) all had similar confidence intervals, with design 22 having the lowest mean bias of the nine sets (5%).

Design 21 was the most imprecise (75%) and design 22 was the least imprecise (12%). In addition to performing better than any of the other three-sample designs, design 22 performed better than design 24 (15% imprecision), which had four sampling times. Although design 20 with two sampling times had poor precision it performed better than design 28 with three sampling times in terms of the precision (42% and 55%, respectively). Design 21 did not estimate a value for σ_1 in three out of ten of the runs and design 25 did not estimate a value for one of the runs. Hence the poor performances in terms of bias and imprecision across ten runs for these sampling schedules.

Figure 7.13 shows how the NONMEM estimated values compared with the simulated values. The spread of bias and imprecision results for designs 21 and 25 was a large compared to the other designs. Designs 22, 23 and 24 were closest to zero and designs 21 and 28 were furthest from zero.

Estimation of Additive Random Error on Concentration (σ_2)

The bias and imprecision in the estimation of the random additive error (σ_2) is shown in figure 7.14. Again, the two-sample sets (designs 20 and 21) and design 25, with three early samples, had the widest confidence intervals. Design 21 had the largest mean bias of -35%. The other three-sample schedules had acceptable results for bias, ranging from -4.6% to -11.4%. Design 22 with three sampling times had a mean bias of -6.2%, compared to design 24, which had four sampling times and a mean bias of -4.6%.

The two-sample schedules also performed poorest in terms of imprecision with values in excess of 35%. Design 25 was the poorest of the three-sample schedules (28%), and design 23 (three samples) estimated σ_2 better than design 24 (four samples with values of 5% and 6% for imprecision, respectively).

The simulated values were subtracted from the NONMEM estimates in figure 7.15. The bias and imprecision results from all designs except 20, 21 and 25 were clustered

close to zero. Design 21 did not estimate a value of σ_2 for three out of the ten runs again, which explained the poor performance in terms of bias and imprecision when calculated across the ten runs.

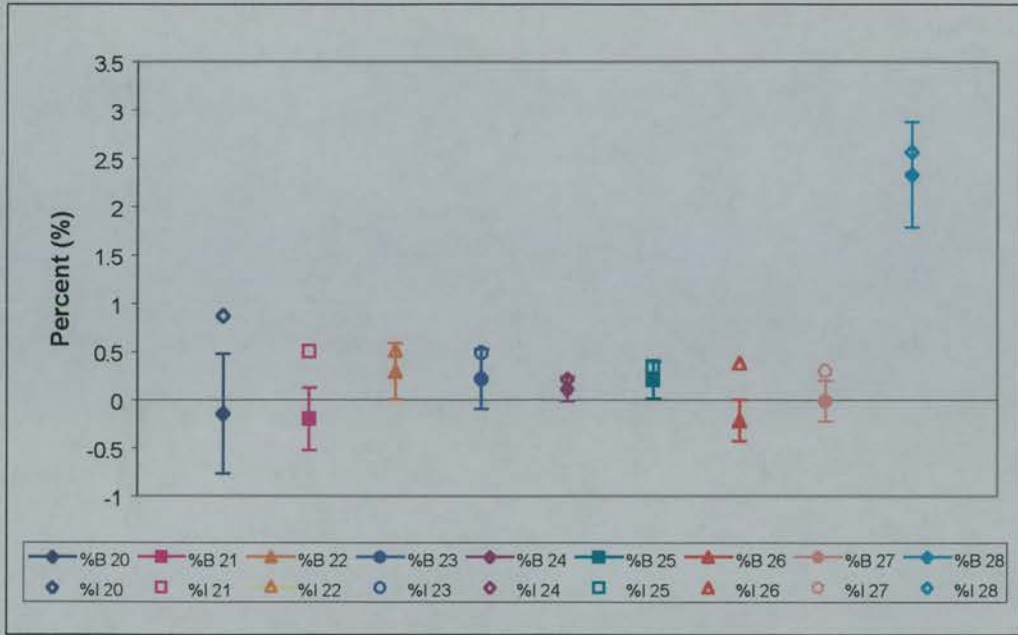


Figure 7.4 Mean percentage bias (%B) \pm 95% confidence interval and imprecision (%I) for the estimation of carboplatin clearance, using designs 20-28.

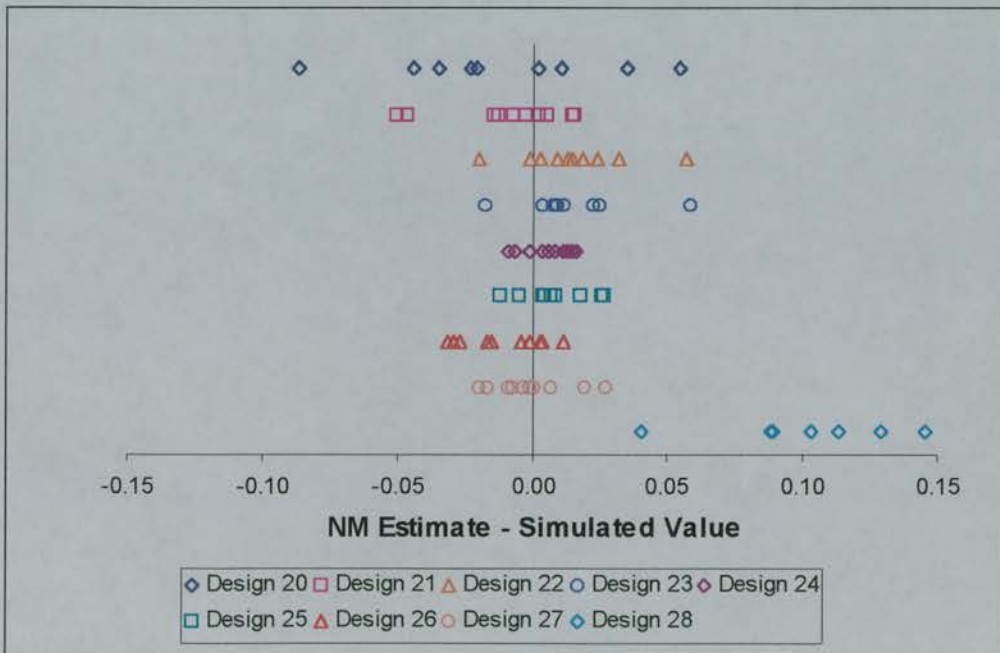


Figure 7.5 Comparison of mean simulated values with NONMEM population estimates of carboplatin clearance.



Figure 7.6 Mean percentage bias (%B) \pm 95% confidence interval and imprecision (%I) for the estimation of carboplatin volume of distribution, using designs 20-28.

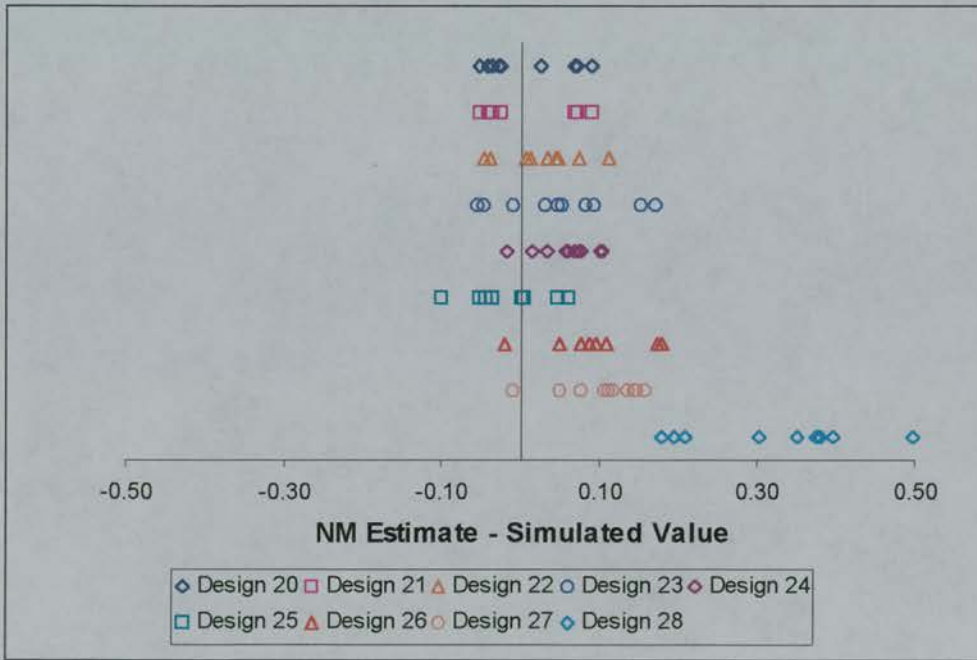


Figure 7.7 Comparison of mean simulated values with NONMEM population estimates of carboplatin volume of distribution.

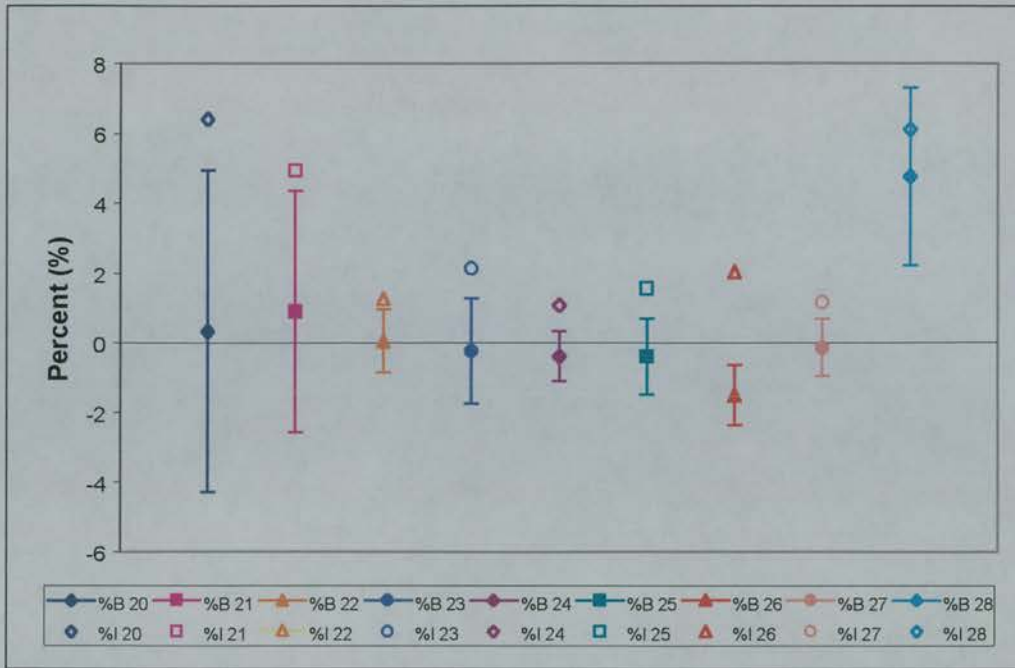


Figure 7.8 Mean percentage bias (%B) \pm 95% confidence interval and imprecision (%I) for the estimation of the standard deviation of carboplatin clearance, using designs 20-28.

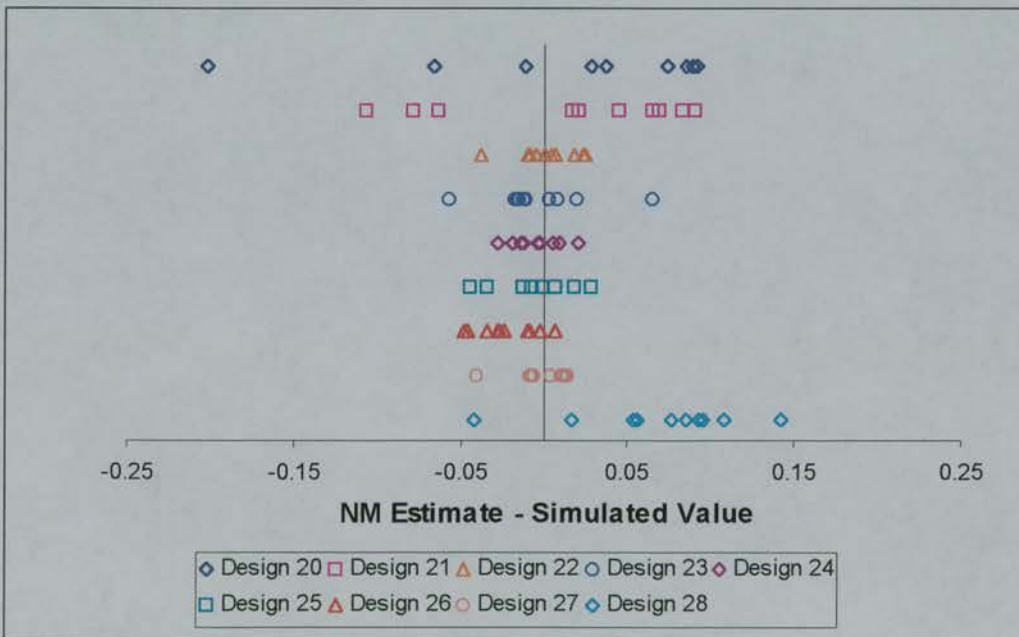


Figure 7.9 Comparison of mean simulated values with NONMEM population estimates of standard deviation of carboplatin clearance.



Figure 7.10 Mean percentage bias (%B) \pm 95% confidence interval and imprecision (%I) for the estimation of the standard deviation of carboplatin volume of distribution, using designs 20-28.

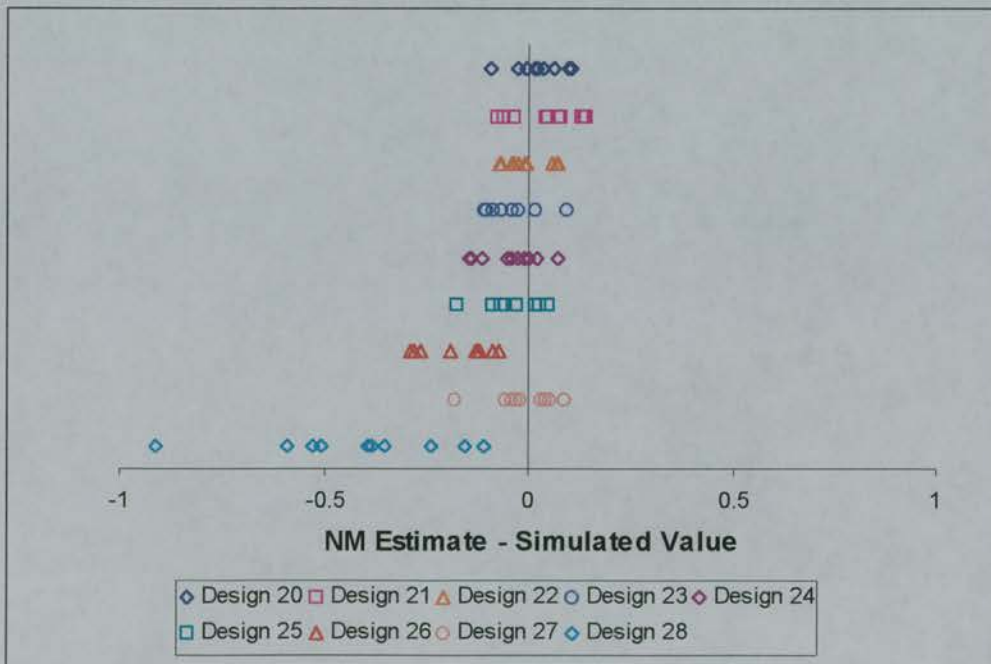


Figure 7.11 Comparison of mean simulated values with NONMEM population estimates of standard deviation of carboplatin volume of distribution.

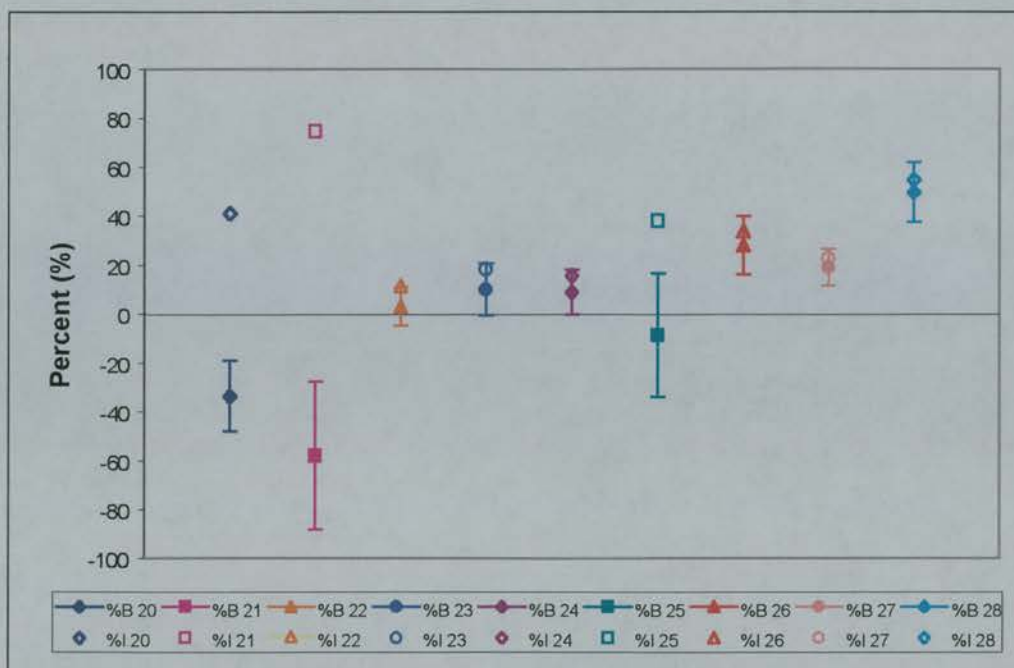


Figure 7.12 Mean percentage bias (%B) \pm 95% confidence interval and imprecision (%I) for the estimation of the proportional random error of carboplatin concentration, using designs 20-28.

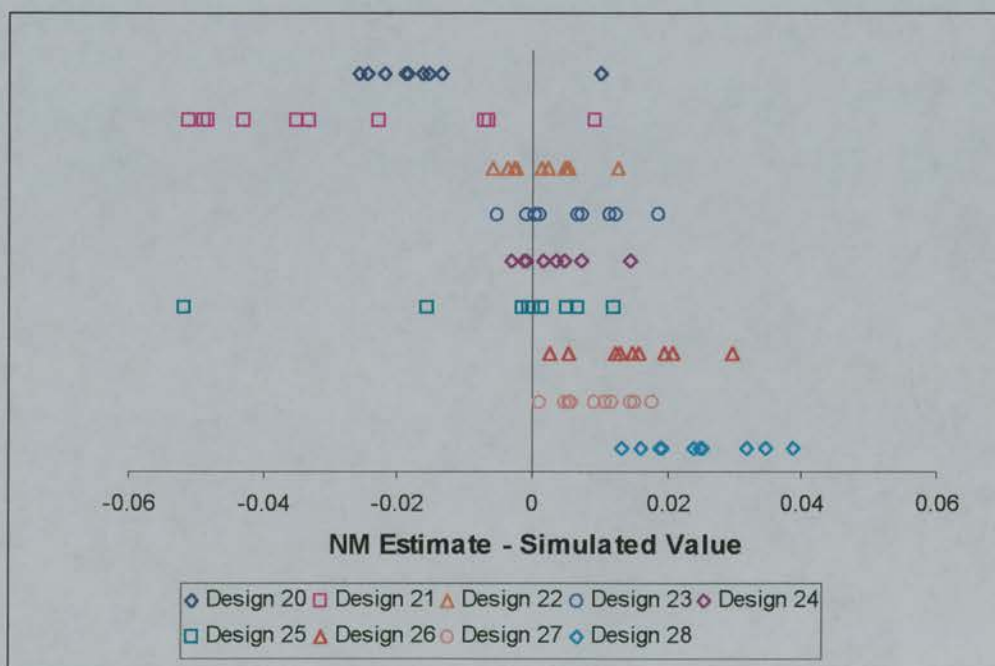


Figure 7.13 Comparison of mean simulated values with NONMEM population estimates of proportional error of carboplatin concentration.

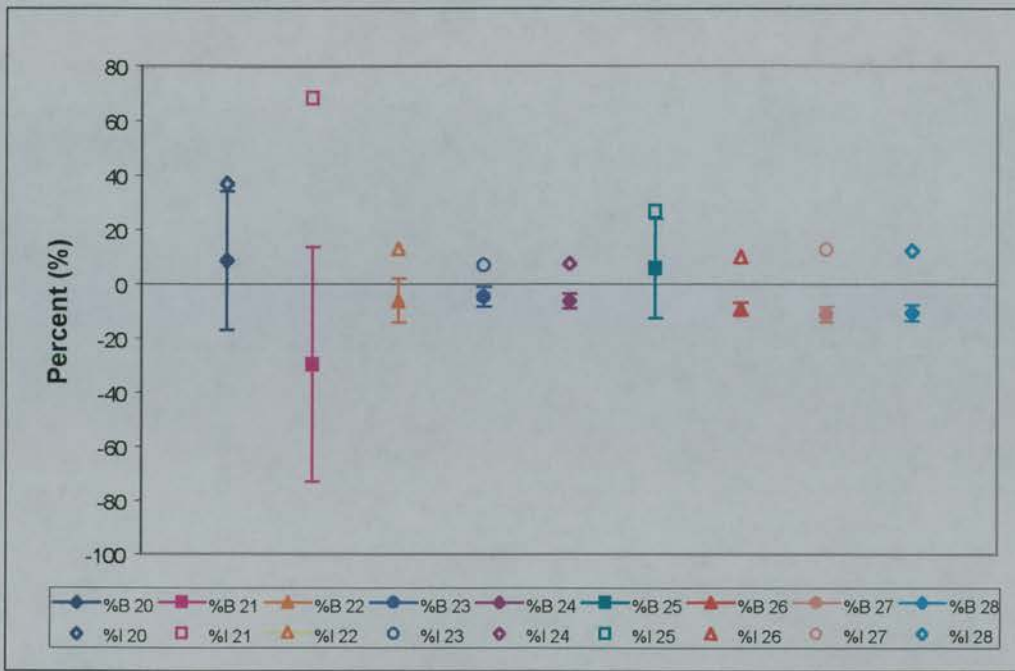


Figure 7.14 Mean percentage bias (%B) \pm 95% confidence interval and imprecision (%I) for the estimation of the additive random error of carboplatin concentration, using designs 20-28.

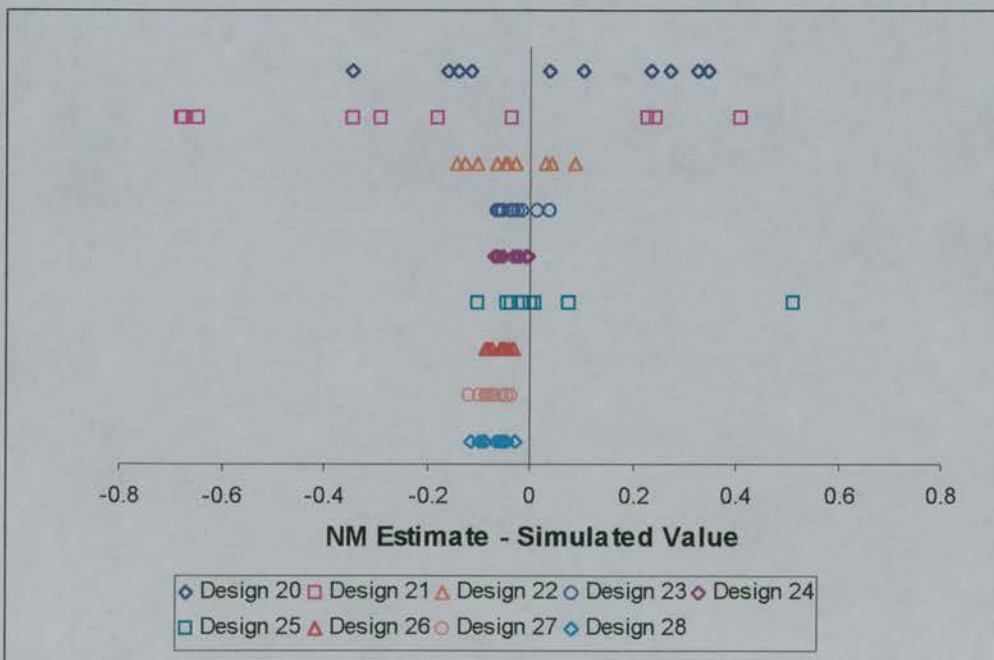


Figure 7.15 Comparison of mean simulated values with NONMEM population estimates of additive error of carboplatin concentration.

7.1.4 Discussion

This simulation was an exercise in testing how the equations for a one-compartment PK model, derived in chapter 3, would perform when applied to ‘real’ values of PK parameters instead of test ones. Carboplatin was the drug of choice as publications exist detailing population values for the PK parameter values (van der Vijgh 1991; Duffull et al. 1997). The values used in this thesis were taken from a review which listed the population parameter estimates of carboplatin in plasma from several PK studies (van der Vijgh 1991). The values for the total clearance (CL (ml/min/m²)) and the volume of distribution at steady state (V_{SS} (l/m²)) of the six studies listed were averaged to give values of 4.6 l/h/m² and 15.4 l/m², respectively. These average values were rounded to give the values of 5.0 l/h and 15.0 l, which were used in the simulations, along with an IV bolus dose of 400mg.

Simulation of concentration-time data for a population of 5000 subjects using the carboplatin PK values described above with variance of 30% on clearance and 26% on volume showed where peaks in concentration variance arose. These were comparable to those predicted from the equations in chapter 3 and showed that the derived equations were ‘scalable’ to other drugs. However, as described previously, care would have to be exercised when extrapolating to actual populations in which parameter variance could be in excess of 30%. In such a case, the peaks in concentration variance observed in the simulated populations shifted slightly when compared to those predicted (chapter 3).

The two-sample schedules derived from concentration variance (designs 20 and 21) performed well compared to the designs based on sampling times taken from two published carboplatin sampling schedules, designs 23(three samples) and 24 (four samples), except in the estimation of the random errors in concentration.

Of the two-sample schedules, design 21 estimated clearance and ω_{Cl} best, which was due to the inclusion of the sampling time at 3.0 hr, which corresponded to the peak in concentration variance due to clearance. Designs 20 and 21 performed equally in the estimation of volume of distribution as both designs included the early 0.1 hr sample

corresponding to the peak in concentration variance due to volume. Also, design 20 estimated ω_V , σ_1 and σ_2 better than design 21. These results were as expected for ω_V and σ_1 as design 20 included two earlier sampling times than design 21. The earlier times were most informative for estimating ω_V as the peak in concentration variance is higher at the 1.5 hr time point than at the 3.0hr time point of design 21 (see figure 7.3). The proportional random error component was best estimated when earlier sampling times were included as earlier concentrations were more susceptible to σ_1 than the later ones. Design 21 would have been expected to estimate σ_2 since the lower concentrations at the later time of 3.0 hr are more affected by the additive error component than the proportional error component. However, design 21 did not estimate the intra-subject random errors in three out of ten simulations and this may account for poorer performance in terms of the higher mean values of bias and the wider confidence intervals.

The three-sample schedules (designs 22, 23, 25-27) performed comparably. Design 28, which had three late sampling times, estimated all PK parameters, excluding the additive intra-subject error (σ_2), poorest of all the schedules. This confirmed that an early sample is essential in IV PK studies.

The four-sample schedule, design 24, estimated clearance, ω_{Cl} and σ_2 (the random additive error) best out of all of the schedules. However, the results from the four 'empirically-chosen' times were often comparable to those obtained with the three-sample design based on the sensitivity analysis (design 22).

In the estimation of clearance, all sampling schedules performed reasonably well with bias and precision within 3.5%. In the estimation of clearance design 21 was better than design 20 (both two-sample schedules) and was comparable to designs 22, 23, 25, 26 and 27 (three-sample schedules). These schedules included a sampling time either close to or at the 3.0 hr time-point, which corresponded to the peak in concentration variance due to clearance from sensitivity analysis. The four-sample design 24 performed best of the nine designs.

Volume of distribution was estimated well with all designs, with imprecision and bias less than 3.5%. It was best estimated by the two-sample schedules (designs 20 and 21) and the three-sample design 22, which had the earliest sampling time of 0.1 hour. This corresponded to the peak in concentration variance due to volume of distribution. Design 24 with four samples had the narrowest 95% confidence interval, but had slightly more imprecision than design 25 with three samples. These two designs had the same three early sampling times, showing that the addition of the fourth sample at 9 hours in design 24 did not add further information for the estimation of volume of distribution. Designs 26 and 27 had similar results and only had the 1.0 hr time in common. The poorer performance of design 28 was due to the lack of the early sampling time where the information about volume of distribution was greatest.

The two-sample schedules performed poorest in estimating the inter-individual variance of clearance (ω_{Cl}) and had the widest 95% confidence intervals, although design 28 (3 samples) had the largest mean bias. However, all bias and imprecision results were less than 8%. Design 22 estimated ω_{Cl} best with designs 24, 25 and 27 being comparable. Similar to clearance, the best results in estimating ω_{Cl} were obtained when there was a sample close to or at 3 hours, which corresponded to the time of peak concentration variance due to clearance. However, design 28 again showed the poorest result, even though the schedule included the 3.0 hr sampling time. Again, this may be due to the late sampling times in design 28. Designs 23 and 26 had sampling times at 4 and 5 hr, respectively, showing that samples which were not at the exact peak in concentration variance, but close to it also resulted in accurate estimation of ω_{Cl} .

The inter-individual variability in volume (ω_V) was estimated well with all designs except designs 26 and 28. It was best estimated by the two-sample schedules (designs 20 and 21) and the three-sample design 22, which had the earliest sample at 0.1 hour. This corresponded to the peak in concentration variance due to volume of distribution. Design 24 which had the same three early sampling times as design 25 performed similarly to it, showing that the addition of the fourth sample at 9 hours

did not add further information for the estimation of the variance of volume of distribution. Designs 23 and 27 also had similar results to designs 24 and 25. The poorer performance of designs 26 and 28 is explained in figure 7.3 where the variance in concentration due to the volume component is illustrated. Both of these designs had later samples at times where the curve due to volume was almost zero and hence there was little information about volume of distribution present at these times. Design 26 showed improved results over design 28 due to the early sample at 1.0 hr where the information about volume was greater. This confirms previous results which showed that early sampling times are important for estimating volume of distribution. At least one early sample gave an accurate estimate with less than 10% imprecision and bias. More than one improved it to less than 5%.

The random intra-individual errors on concentration were estimated least well. The random proportional error (σ_1) was best estimated by design 22. Designs 22, 23 and 24 had precision of less than 20%, showing that schedules with earlier sampling times estimated σ_1 better. This was expected as higher concentrations at earlier times were more affected by the proportional random error than later, smaller concentrations.

The random additive error, (σ_2) was best estimated by sampling schedules with later sampling times. Designs 20, 21 and 25 with only early sampling times performed poorest in the estimation of this parameter. The most noticeable result in this section was that design 28, with only late samples, estimated only this parameter accurately. Random additive errors affect lower, later concentrations more than higher ones, hence, these results were also as expected.

As both toxicity and response to carboplatin have been correlated with the pharmacokinetics, dose modifications are generally made to attain a desired drug exposure as measured by *AUC* (Calvert et al. 1989; Jodrell et al. 1992) and most limited and optimal sampling strategies for carboplatin relate to the estimation of this parameter and not those of clearance or volume of distribution (van Warmerdam et al. 1994a; Ghazal-Aswad et al. 1996; van Warmerdam et al. 1996b; Chatelut et al.

2000). Hence, in addition to the modification to the structural PK model, the simulations carried out in this section cannot be directly compared to published sampling strategies for carboplatin.

In conclusion, this section showed that the equations derived in chapter 3 were scaleable to 'real' values of PK parameters and that sampling schedules derived from the times of peak concentration variance performed as well as published sampling schedules. The two-sample schedules based on the sensitivity analysis performed as well as some of the three-sample schedules and the three-sample schedule from the sensitivity analysis often performed as well as the four-sample schedule derived from the Biomed2 project.

This simulation also showed that although using sampling times from the sensitivity analysis gave accurate estimates of the relevant parameters related to the peaks in concentration variance, sampling schedules with times close to these 'optimal' times also performed well. This was particularly true if these samples were taken at times where the amount of information about the parameter remained high in relation to the total height of the peak.

7.2 Two-Compartment PK Model - Antagonist G 6 hour IV Infusion (Clinical Data).

7.2.1 Introduction

Antagonist G is one of a novel class of compounds being investigated for activity against small cell lung cancer (SCLC). SCLC cells are known to secrete a variety of neuropeptides on which they are dependent to sustain growth. Antagonist G is a broad-spectrum neuropeptide antagonist based on the structure of Substance P and consists of six peptides (H-Arg-D-Trp-NmePhe-D-Trp-Leu-Met-NH₂). The exact mechanism of action is not known, but these compounds are believed to act via competitive inhibition of cell surface receptors to prevent the mitogenic effects of the neuropeptides. Both preclinical and *in vitro* studies have shown Antagonist G to inhibit the proliferation of SCLC cells and a Phase I clinical trial has recently been completed (Jones et al. 1997).

Phase I clinical trials aim to determine the safety and tolerability of a new drug in humans. A secondary aim is to gain information about the drug absorption, distribution and elimination, by the use of pharmacokinetic studies. With non-chemotherapeutic drugs, phase I studies are often carried out on healthy volunteers first and later on patients. In the case of anticancer drugs, patients are used in phase I and hence the drug is being tested in the target population.

This chapter describes the analysis of the pharmacokinetic data collected during the Phase I trial of Antagonist G. Initially, each subject's data were analysed individually and subsequently all data were analysed simultaneously to develop a population PK model for Antagonist G. Using the parameter estimates from the population PK model, the 'optimal' sampling times for Antagonist G were determined using the methods described previously, i.e., examining where times of maximum concentration variance occur.

A simulation study was then carried out to investigate if the 'optimal' sampling times offered any improvement in the population PK parameter estimates compared to

those obtained with the conventional sampling schedule used in the phase I study. Three sampling schedules were examined during the simulation (time zero was not simulated):

- i. The six defined 'optimal' sampling times.
- ii. A modified 'optimal' sampling schedule which was reduced to five samples by the use of a sampling window.
- iii. A simulation using the original sampling times (14 samples).

7.3 Phase I Study

7.3.1 Methods

Antagonist G Administration & PK Sampling Schedule

Antagonist G was administered to patients with cancer for whom no conventional therapy was available. The drug was given in 500ml of 5% dextrose, as a 6 hour IV infusion via a central line every three weeks for up to 12 cycles of treatment. The study had received the approval of the relevant ethical committees in the institution in which it was carried out.

The aim of the first stage of the study was to reach an Antagonist G plasma concentration of $10\mu\text{M}$ at the end of infusion. This concentration was associated with anti-tumour activity pre-clinically. In this part of the study a rapid dose-escalation strategy was employed in the absence of significant toxicity, where the dose was doubled after each patient. The dose escalated from 2 to $300\text{mg}/\text{m}^2$ in 15 patients (12M: 3F, age 36-65 (median59)), using twelve dose levels.

In the second stage of the study, the dose intensity was increased to a weekly infusion. Further dose escalation was guided by the end of infusion concentration and also a pharmacodynamic end-point, forearm bloodflow changes as measured by venous occlusion plethysmography. Nine patients (5M: 4F, age 34-75 (median54)) were entered at three dose levels: 300, 350 and $400\text{mg}/\text{m}^2$.

Full pharmacokinetic data (15 samples) were collected during the first cycle of treatment from each of these 24 patients. Limited pharmacokinetic data were collected from the second (5-10 samples) and subsequent cycles (start and end of infusion samples). Data from the first and second cycles were included in this analysis. For the full profiles plasma samples were collected at the following times, from the start of the infusion: 0, 60, 300, 360, 365, 370, 380, 390, 405, 420, 450, 480, 540, 720, 1440 minutes. For the second cycle data the sampling times were generally selected from 0, 60, 300, 360, 375, 390, 405, 420, 480 minutes from the

start of the infusion, although some earlier samples from 113-224 minutes were occasionally used instead, due to sampling restrictions in the clinic.

Individual PK Analyses

The data from each patient were analysed individually using NONMEM (Version V) and the FO method of analysis described in chapter 2. Previous work had suggested that a two-compartment PK model was the most appropriate for this data (Personal Communication, S. Clive) and the ADVAN 3 and TRANS 4 subroutines were used. As with previous sections in this thesis the parameters Cl , V_1 , V_2 and Q were estimated. The residual error on concentration was described by either an additive or a combination intra-subject error model.

Population PK Analysis

The results from the individual analyses showed that the estimates of clearance were more variable at lower doses, than at higher doses. Hence only the data from patients 13 to 24 was modelled simultaneously in the population PK analysis using NONMEM (Version V). Both the FO and the FOCE with interaction methods of analysis were examined. A two-compartment PK model was used and the parameters \overline{Cl} , \overline{V}_1 , \overline{V}_2 and \overline{Q} were estimated along with estimates of the residual error on concentration. Two models were examined for residual error: an exponential model and a combination model, described below.

$$C_{ij} = C_{ij}^* \times e^{\varepsilon_{ij}} \quad \text{Equation 7.1}$$

$$C_{ij} = C_{ij}^* \times e^{\varepsilon_{1ij}} + \varepsilon_{2ij} \quad \text{Equation 7.2}$$

Different population PK models were compared for:

- i. Successful minimisation.
- ii. Estimation of standard errors of parameters.
- iii. Objective function value.
- iv. Examination of residual plots.

7.3.2 Results

Individual PK Analyses

Concentration data were available from 24 patients (17 male) and 40 cycles of treatment (8 patients had one cycle available only). The doses for each cycle, the total number of concentration measurements available and the parameter estimates from each individual are shown in table 7.3. Figure 7.16 shows the individual concentration-time data along with the NONMEM data predicted from the individual parameter estimates. The higher concentrations are not predicted as well as the lower concentrations, but overall the individual fits were adequate.

The variability in the individual estimates across the population was large, with CV ranging from 58% for clearance to 226% for V_2 and as much as 255% for the additive error on concentration. The high CV for the estimation of V_2 was due to patient 2 being an outlier with a value of 119l. The CV was 45.6% for V_2 with patient 2 removed. The results were not Normally distributed, as shown the box and whisker plots in figure 7.17. Hence median values may be more relevant than mean values to describe the data.

Table 7.3 Summary and results of individual NONMEM analyses.

Subject ID	Dose Cycle 1 (mg)	Dose Cycle 2 (mg)	No. Conc. Measurements	Cl (l/min)	V ₁ (l)	V ₂ (l)	Q (l/min)	Proportional Error (Variance)	Additive Error (Variance) (mg/l) ²
1	4.0	-	11	0.120	0.16	3.35	0.076	-	4.60E-04
2	7.0	-	9	0.086	2.13	119.00	0.069	-	1.52E-04
3	12.0	-	13	0.125	4.26	10.40	0.027	-	4.30E-04
4	21.0	-	14	0.116	0.08	6.41	0.229	-	6.59E-04
5	25.0	-	15	0.223	2.12	5.54	0.442	-	1.58E-04
6	23.0	-	14	0.156	2.72	5.33	0.093	3.87E-03	3.19E-05
7	39.5	39.5	21	0.162	2.64	7.59	0.314	6.49E-03	1.69E-04
8	56.1	56.1	20	0.226	3.91	4.31	0.054	-	1.92E-03
9	85.0	85.0	19	0.275	3.66	4.93	0.039	-	3.88E-03
10	129.0	129.0	21	0.322	2.47	7.80	0.153	1.57E-02	6.55E-05
11	210.0	210.0	21	0.247	1.31	5.19	0.097	2.65E-02	8.85E-03
12	304.0	304.0	21	0.302	3.30	4.87	0.123	2.25E-03	1.14E-02
13	573.0	573.0	22	0.112	8.81	10.60	0.021	-	5.57E+00
14	480.0	-	15	0.111	4.37	3.51	0.023	4.00E-03	2.54E-03
15	636.0	-	15	0.060	5.61	11.50	0.050	-	3.88E-01
16	474.0	474.0	24	0.071	4.38	3.34	0.210	2.17E-02	8.36E-03
17	438.0	438.0	25	0.049	4.15	1.87	0.023	2.33E-02	1.63E-02
18	468.0	468.0	23	0.091	6.75	3.82	0.008	-	2.10E+00
19	735.0	735.0	22	0.104	5.37	2.93	0.023	1.24E-02	4.37E-03
20	791.0	791.0	20	0.136	1.65	5.53	0.150	5.53E-02	6.00E-03
21	658.0	658.0	21	0.063	6.67	5.63	0.022	-	1.16E+00
22	776.0	776.0	22	0.076	1.07	5.78	0.248	9.42E-02	1.26E-02
23	760.0	760.0	25	0.054	4.89	2.76	0.071	2.78E-02	4.13E-02
24	672.0	672.0	25	0.101	0.04	5.29	0.622	-	3.17E+00
Mean	-	-	-	0.141	3.44	10.30	0.133	0.025	0.521
(SD)	-	-	-	(0.081)	(2.25)	(23.29)	(0.151)	(0.03)	(1.33)
Median	-	-	-	0.114	3.48	5.31	0.073	0.019	0.005

Figure 7.16 Individual Antagonist G profiles of measured and predicted concentrations versus time.

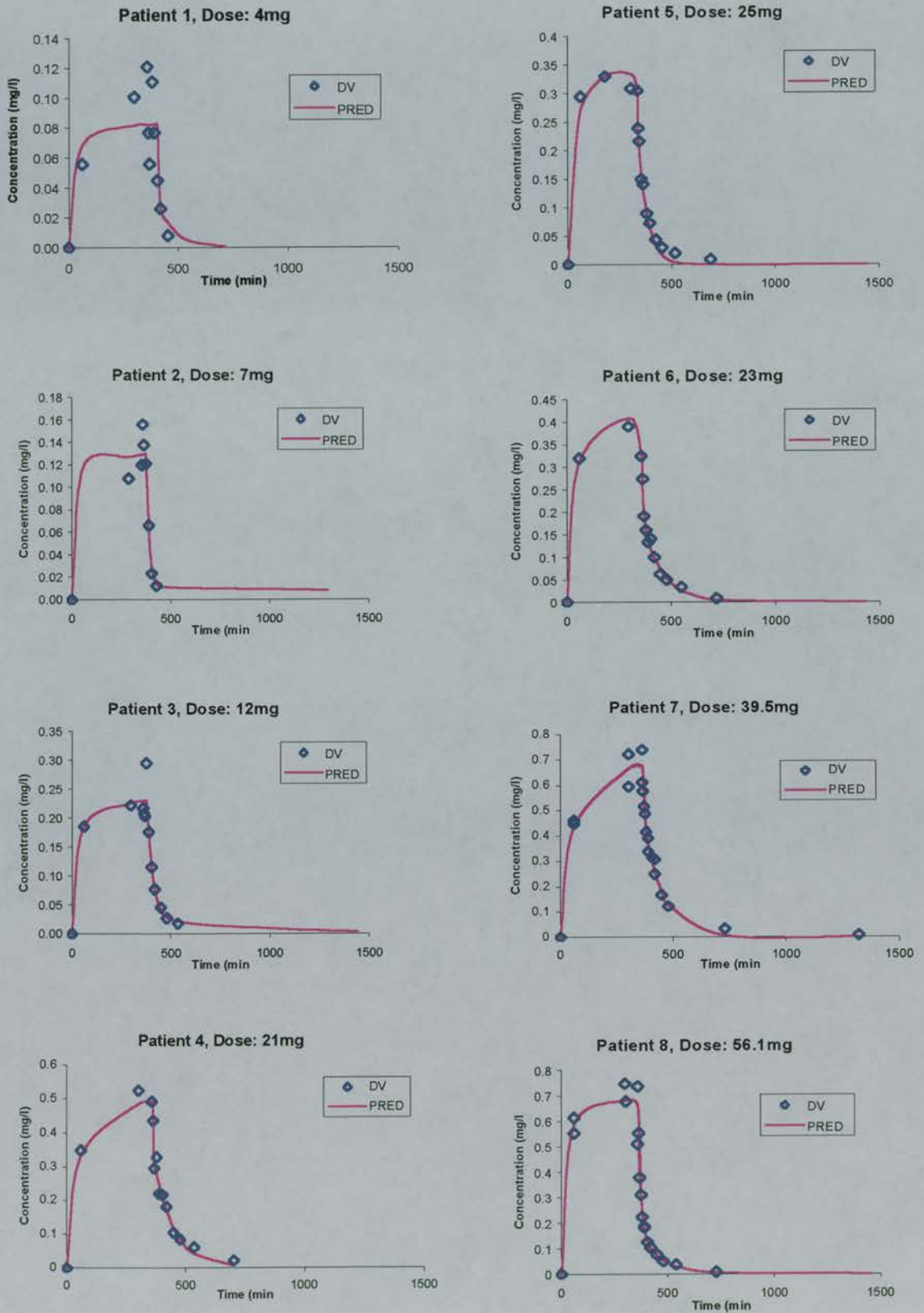


Figure 7.16 Continued

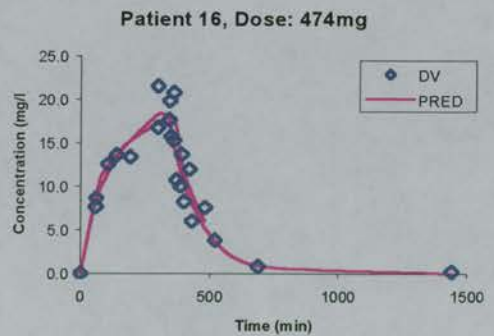
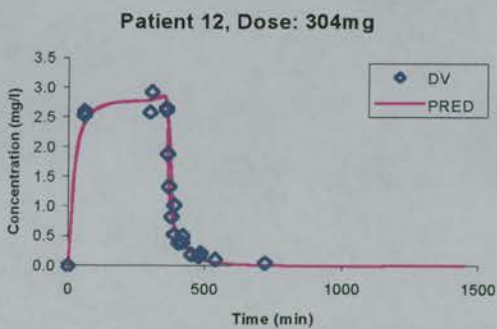
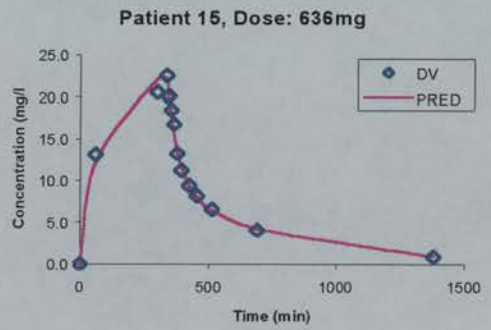
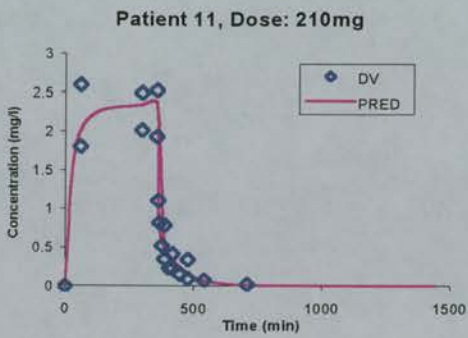
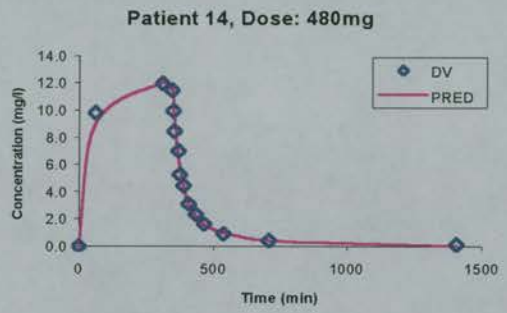
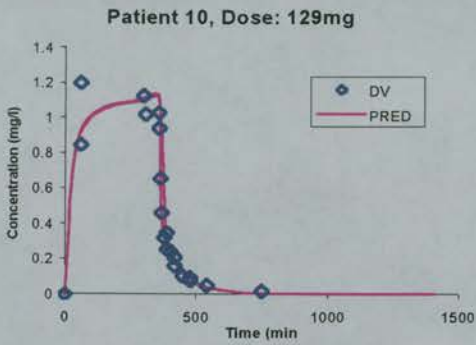
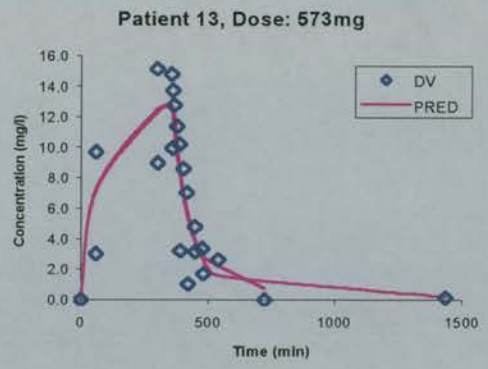
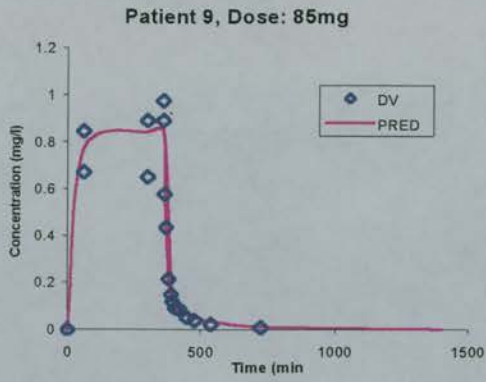


Figure 7.16 Continued

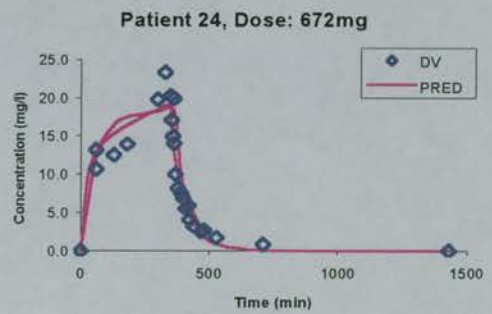
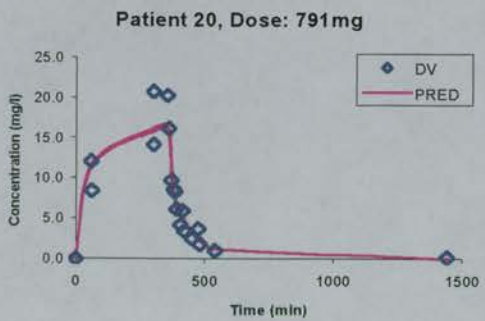
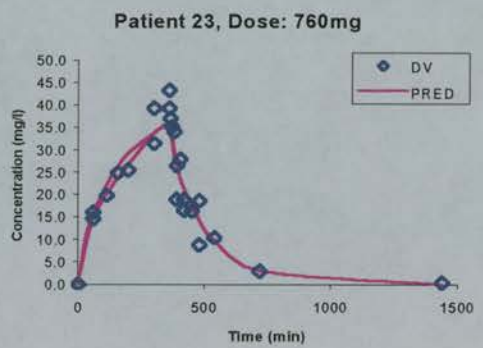
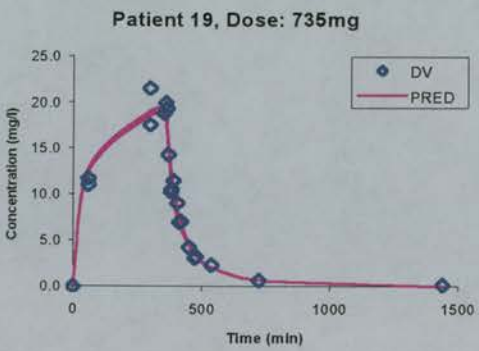
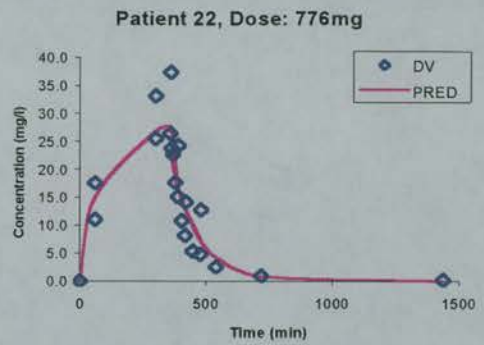
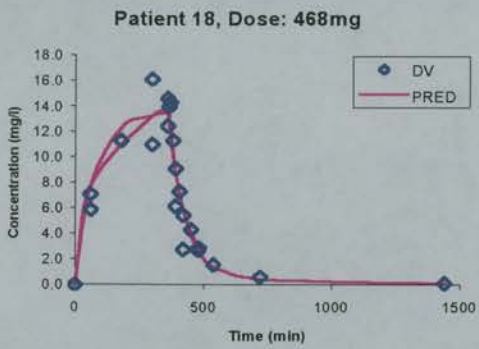
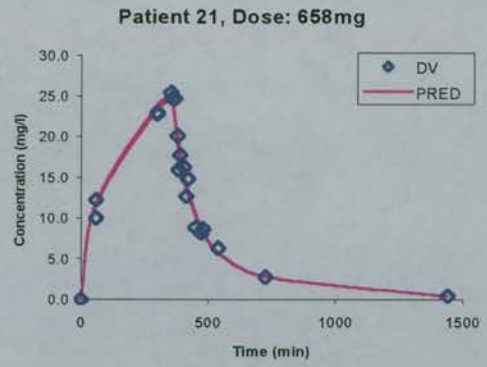
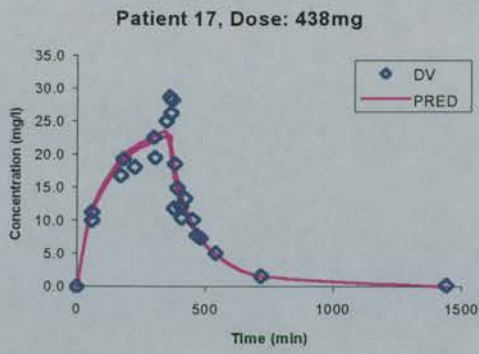
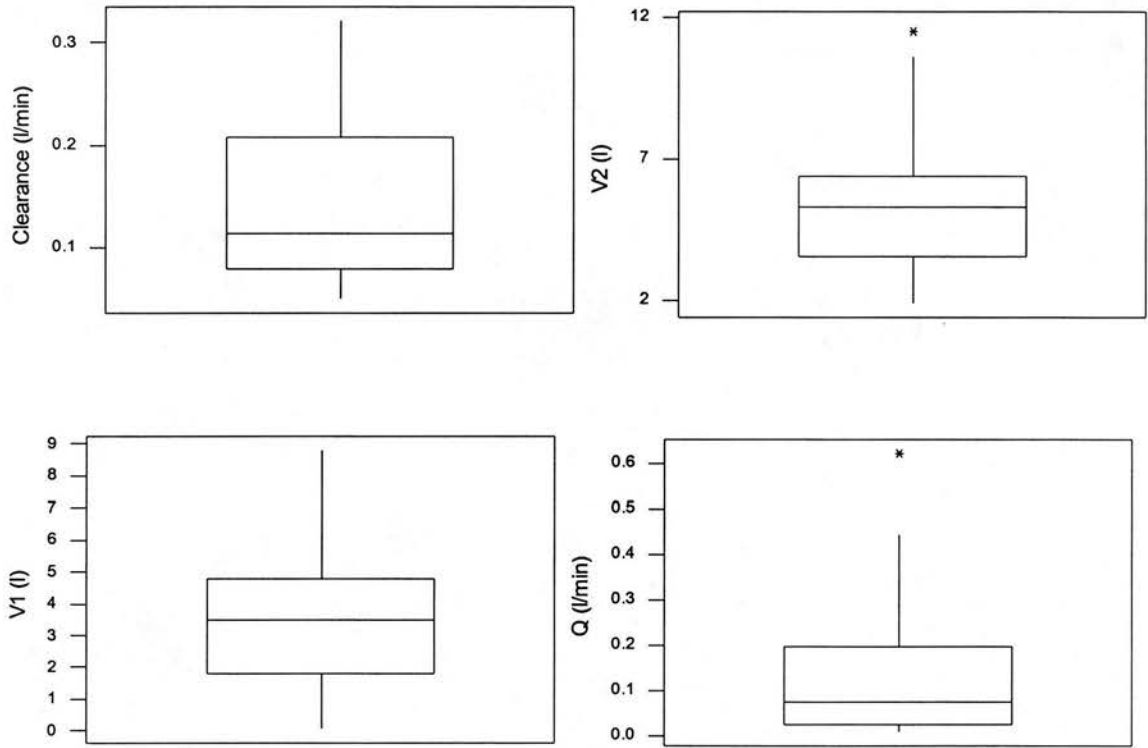


Figure 7.17 Box and whisker plots of individual parameter estimates for Antagonist G. (V_2 is shown without subject 2, value = 1191)



Population PK Analysis

Data from patients 13 to 24 were used to develop the population PK model for Antagonist G as the clearance estimates in patients with doses less than 400mg was variable compared to those obtained at higher doses (see figure 7.18).

The model development for the population model is described in table 7.4 and the parameter estimates obtained from these runs are shown in table 7.5.

Patients 13 to 24 gave rise to two hundred and thirty seven Antagonist G concentration measurements. The model giving the best fit was with the exponential residual error model, combined with a two-compartment PK model. Extending the residual error model by the use of a second, additive, component offered no improvement in the model fit, as shown by no difference in the objective function, standard error estimates or CV. This was the case regardless of whether the FO or FOCE method of estimation was used (see comparison of runs 1 & 2 and 3 & 4).

The FOCE method reduced the variability in the estimation of V_2 to a CV of 18%, from a CV of 63% with the FO method. Although increases in CV were seen for the other parameters (1.5%, 0.6% and 12% respectively for Cl , V_1 and Q), the large reduction (45%) in the estimation of V_2 justifies the choice of the parameter estimates from the FOCE method of estimation for the population model for Antagonist G (Run 3).

Figure 7.19 shows the measured concentration data (DV) for each individual together with the population predicted concentration (PRED) and the individual's predicted concentrations (IPRED) from Run 3. Overall, the individual predicted concentrations were close to the measured concentrations, although the population predicted concentrations were more variable. This is confirmed in figure 7.20 where the population and individual predicted concentrations are plotted against the measured concentrations for patients 13 to 24. It was clear that the individual predictions of concentration were closer to the line of identity than the population

predictions, although the higher concentrations were predicted less accurately than the lower ones.

The final parameter estimates for the population model of Antagonist G were Cl 0.082 l/min (4.92 l/h), V_1 6.9 l, V_2 6.7 l and Q 0.012 l/min (0.72 l/h). These were used to define sampling times for Antagonist G which may offer improved parameter estimation, using sensitivity analysis.

Figure 7.18 Plots of individual parameter estimates for Antagonist G against dose. (V_2 is shown without subject 2, value = 1191)

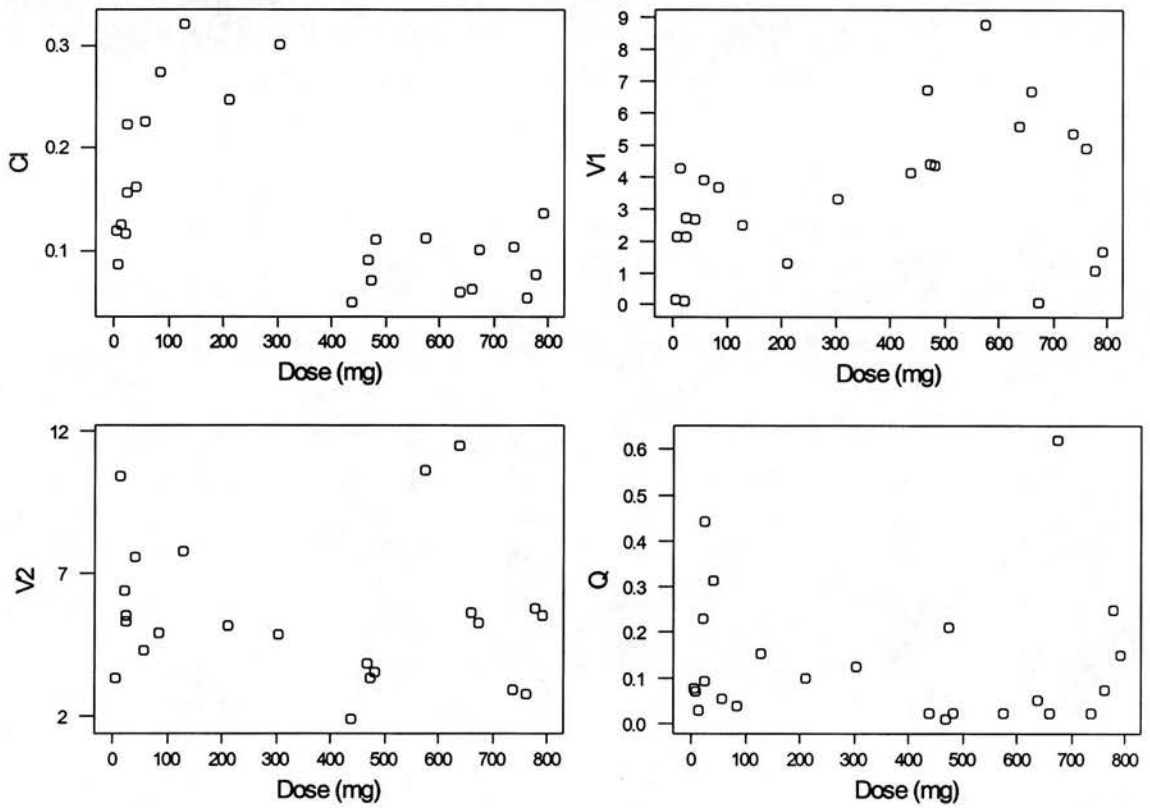


Table 7.4 Summary of the Antagonist G population model development with NONMEM using data from patients 13-24.

Run No.	Estimation Method	Objective Function	Successful Minimisation	No θ Parameters	No ω Parameters	No σ Parameters	No. Significant Figures	Standard Errors Estimated
1	FO	652.479	Yes	4	4	1	3.5	Yes
2	FO	652.479	Yes	4	4	2	4.2	Yes
3	FOCE Interaction	592.975	Yes	4	4	1	3.1	Yes
4	FOCE Interaction	592.974	Yes	4	4	2	3.8	Yes

Table 7.5 Summary of parameter estimates during development of Antagonist G population model using data from patients 13-24.

Run Number.	Successful Minimisation	Parameter Estimates (Standard Error) CV%									
		Cl (l/min)	ω_{Cl}^2	V_1 (l)	$\omega_{V_1}^2$	V_2 (l)	$\omega_{V_2}^2$	Q (l/min)	ω_Q^2	σ_1^2	σ_2^2
1	Yes	0.073 (0.006) 29.8%	0.089 (0.380)	6.620 (1.110) 7.5%	0.006 (0.007)	4.310 (0.023) 63.2%	0.400 (0.009)	0.020 (0.158) 59.7%	0.357 (0.151)	0.039 (0.009)	- -
2	Yes	0.073 (0.006) 29.8%	0.089 (0.380)	6.620 (1.110) 7.5%	0.006 (0.007)	4.310 (0.023) 63.2%	0.400 (0.009)	0.020 (0.158) 59.7%	0.356 (0.151)	0.039 (0.009)	5.10E-13 (3.62E-06)
3	Yes	0.082 (0.008) 31.4%	0.099 (0.409)	6.860 (0.867) 8.1%	0.006 (0.003)	6.700 (0.023) 18.1%	0.033 (0.007)	0.012 (0.037) 71.8%	0.515 (0.172)	0.046 (0.013)	- -
4	Yes	0.082 (0.008) 31.5%	0.099 (0.407)	6.870 (0.870) 8.1%	0.006 (0.003)	6.720 (0.023) 18.1%	0.033 (0.007)	0.012 (0.037) 71.8%	0.515 (0.172)	0.046 (0.013)	2.37E-11 (6.79E-08)

Figure 7.19 Individual Antagonist G profiles of measured, population predicted and individual predicted concentrations versus time.

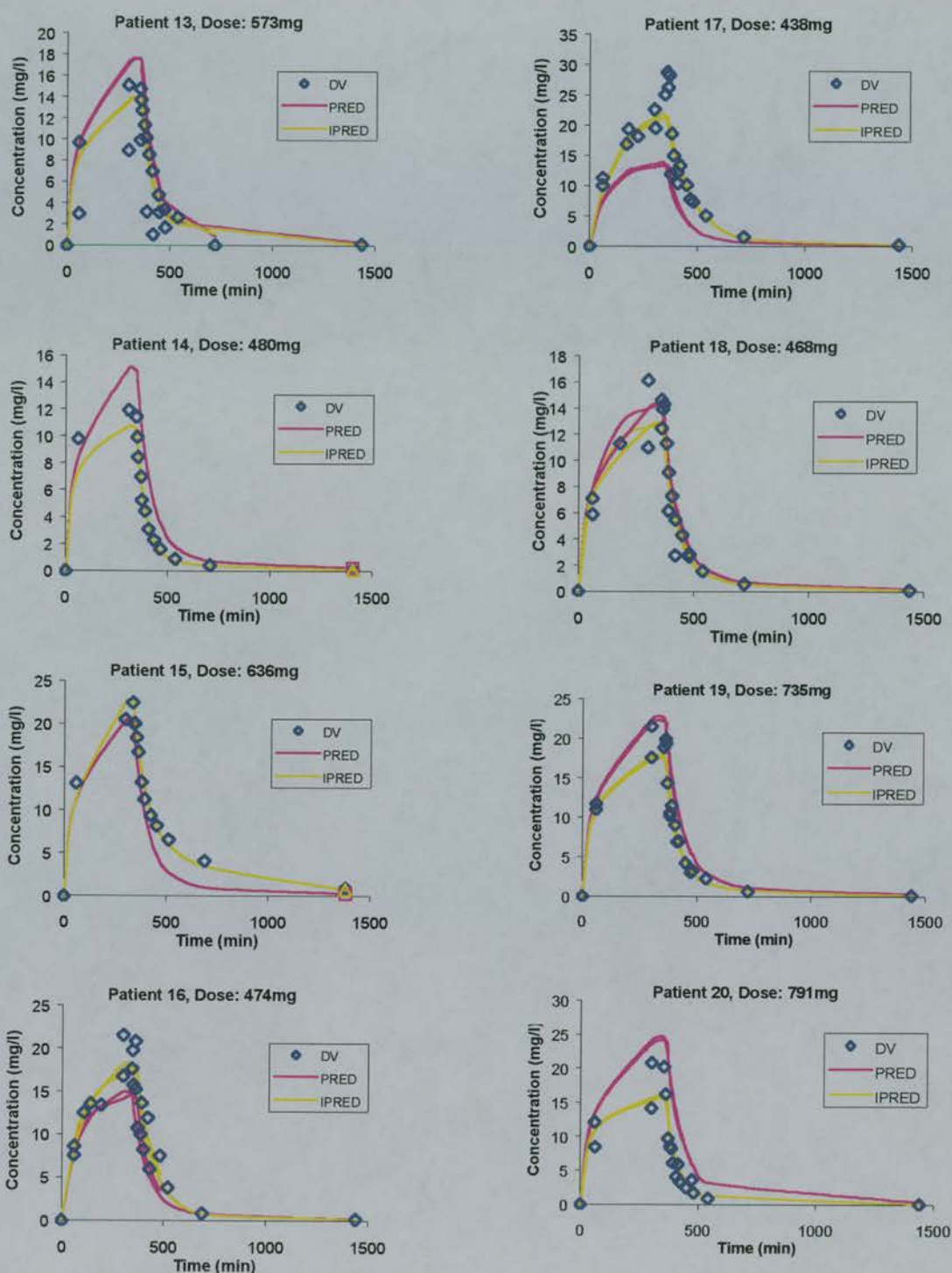


Figure 7.19 Continued

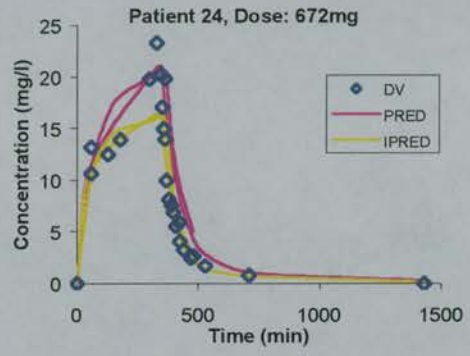
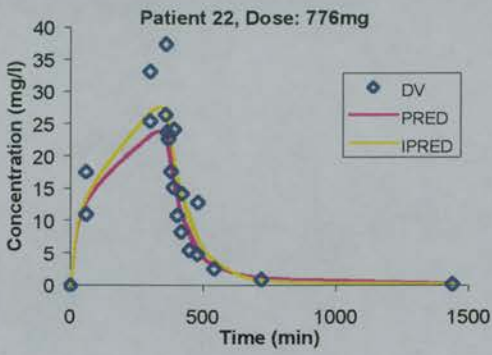
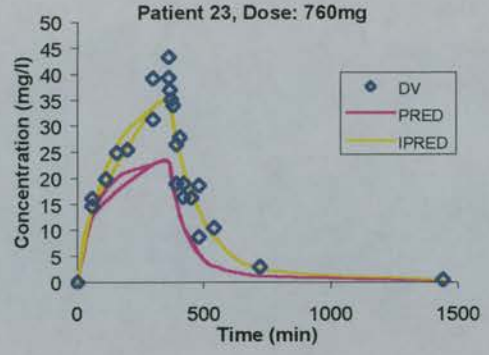
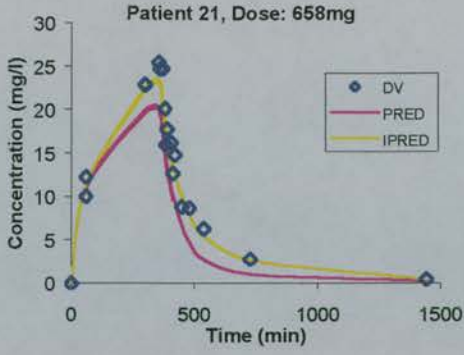
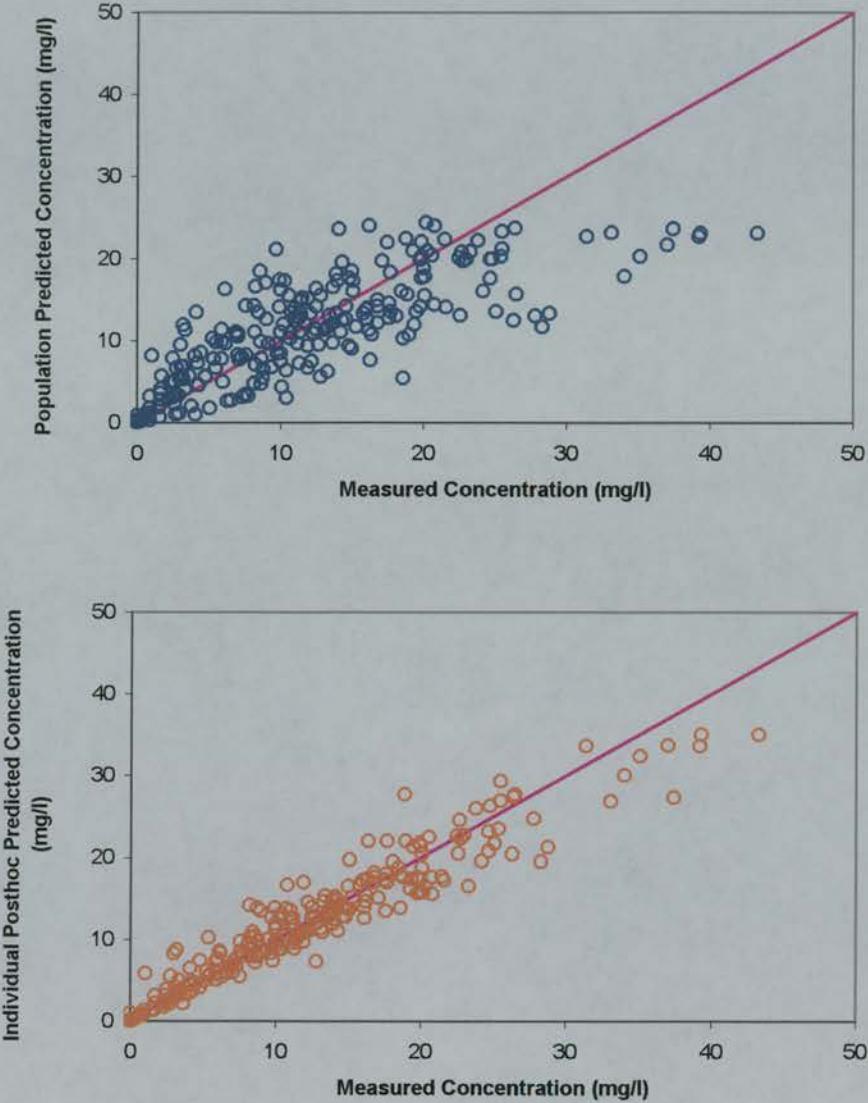


Figure 7.20 Population and individual predicted concentrations versus measured concentrations for patients 13 to 24, with the line of identity shown.



7.4 Optimal Design for Antagonist G

7.4.1 Methods

7.4.1.1 Data Simulation

Sensitivity analysis was carried out to define times of maximum concentration variance attributable to each of the parameters Cl , V_1 , V_2 and Q . The times defined from this may offer improved estimation of the parameters, with fewer sampling times than were used in the phase I study. The 'optimal' sampling times for Antagonist G were defined graphically using the population parameter estimates from Run 3, described previously. The parameters used are summarised below in table 7.6 and the mean dose from the patients who were used to develop the population PK model (patients 13-24) was used (622mg).

Table 7.6 Pharmacokinetic parameter values for optimal sampling design for Antagonist G.

Parameter	Value
\overline{Cl}	4.92 l/h
$\overline{V_1}$	6.86 l
$\overline{V_2}$	6.7 l
\overline{Q}	0.72 l/h
ω_{Cl}	31.5% CV
ω_{V_1}	8.1% CV
ω_{V_2}	18.1% CV
ω_Q	71.8% CV

Changes in the concentration variance were examined with respect to each of the parameters Cl , V_1 , V_2 and Q . This was achieved by setting the variance on all parameters to zero, except the one being examined and the times at which peaks in concentration variance occurred were determined graphically.

7.4.2 Results

Figure 7.21 and table 7.7 detail where the peaks in concentration variance arose for each parameter using the Antagonist G population PK parameter values.

Examination of the range of values of concentration variance for each of the parameters shows that clearance had the largest effect. This was also apparent in the plot of the total concentration variance, which was essentially the same as that for clearance.

Figure 7.22 shows the concentration-time curve for the population average Antagonist G parameters, following a six-hour infusion of 622mg. The sampling times used in the phase I study are plotted along with the optimal sampling times defined in table 7.7. The 'optimal' times were similar to some of those used in the phase I study, although there was no sample in the clinical study at 3.6 hr.

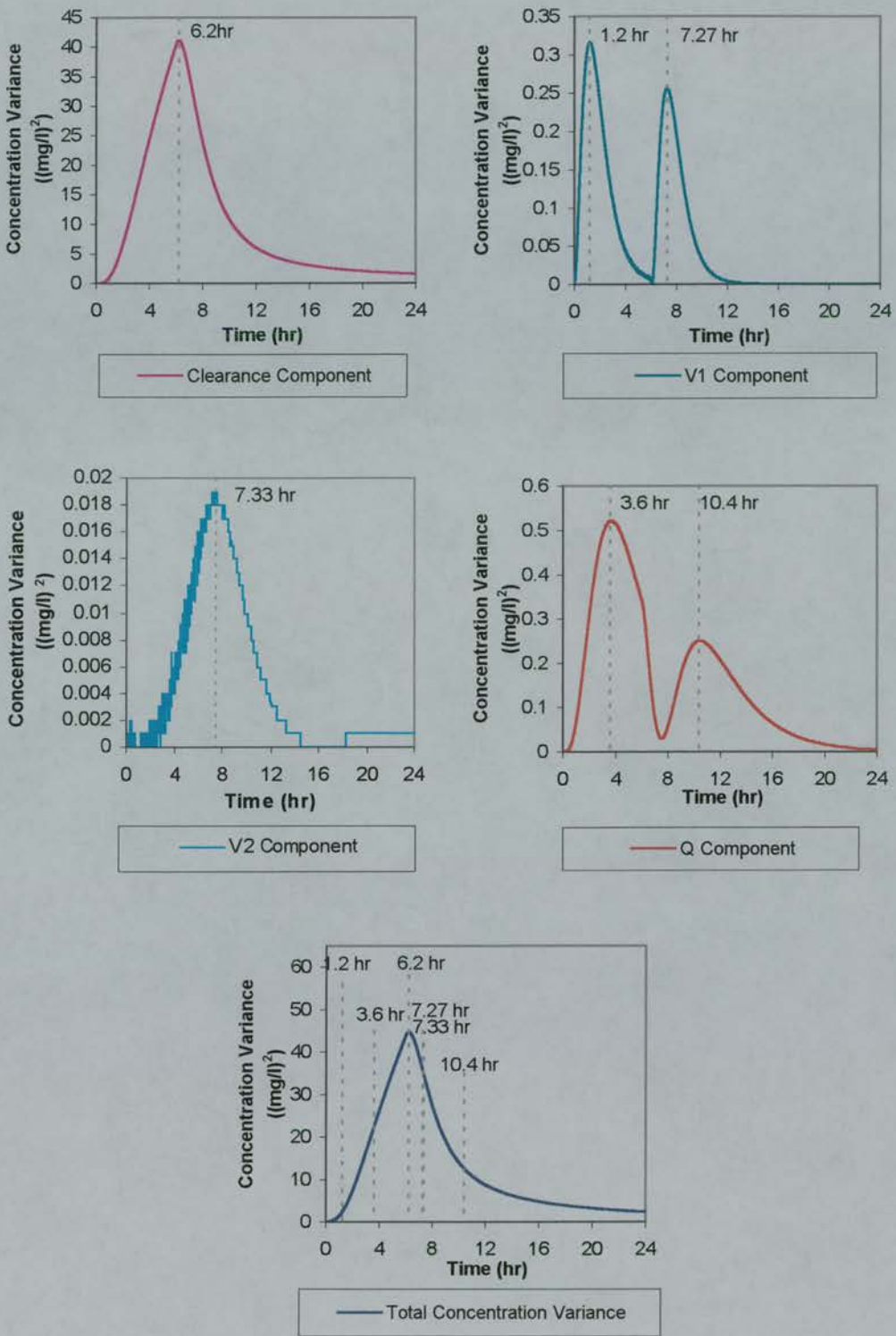


Figure 7.21 Sampling times based on sensitivity analysis for the two-compartment IV infusion of Antagonist G.

Table 7.7 'Optimal' sampling times for Antagonist G.

Parameter	Time
CI	372 min (6.2 h)
V_1 First Peak	72 min (1.2 h)
V_1 Second Peak	436 min (7.27 h)
V_2	440 min (7.33 h)
Q First Peak	216 min (3.6 h)
Q Second Peak	624 min (10.4 h)

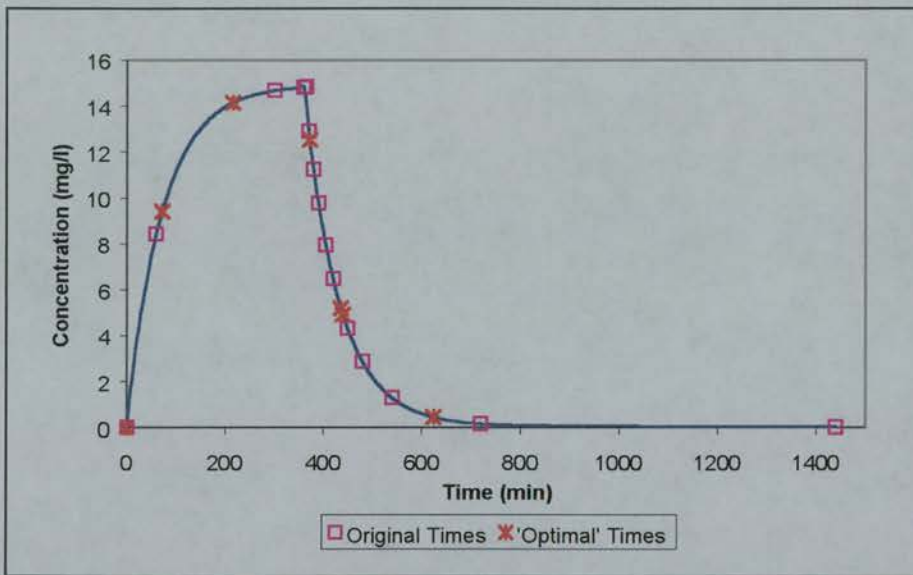


Figure 7.22 'Optimal' sampling times from NONMEM population analysis Run 3 and dose of 622mg. Comparison with sampling times used in phase I study.

7.5 Antagonist G Simulations

7.5.1 Methods

7.5.1.1 Data Simulation

Concentration-time data for Antagonist G were simulated according to a two-compartment PK model following a 6-hour IV infusion of 622mg. The population mean values of the parameters used in the simulations were those obtained from the population analysis of the phase I clinical trial data (table 7.6). The coefficient of variation for Q was reduced to 30% to enable estimation of this parameter. A proportional intra-subject error model was used in which σ_I was set to 10% (0.1).

7.5.1.2 Sampling Schedules

The original sampling design used in the phase I clinical trial was compared to two designs for which the sampling times were based upon sensitivity analysis. Ten sets of 500 subjects were simulated for each of three designs.

- Design 29. Fourteen fixed sampling times at the times used in the phase I clinical trial of Antagonist G (1.0, 5.0, 6.0, 6.08, 6.17, 6.33, 6.5, 6.75, 7.0, 7.5, 8.0, 9.0, 12.0 & 24.0 hr).
- Design 30. Six fixed sampling times selected using sensitivity analysis (1.2, 3.6, 6.2, 7.27, 7.33 & 10.4 hr).
- Design 31. Five fixed sampling times, with windows around each time except the first. (1.2, 3.6 ± 1.5 , 6.2 ± 1.5 , 7.3 ± 1.5 & 10.4 ± 2.25 hr). The samples at 7.27 hr and 7.33 hr were reduced to one sample at 7.3 hr to reduce the number of sample to five. The size of the sampling window corresponded to 20% and 30% of the elimination half-life ($t_{1/2\beta}$), which was 7.5hr (1.5 and 2.25 hr, respectively).

7.5.1.3 Data Analysis

The parameters \overline{Cl} , $\overline{V_1}$, $\overline{V_2}$, \overline{Q} , ω_{Cl}^2 , $\omega_{V_1}^2$, $\omega_{V_2}^2$, ω_Q^2 and σ_1^2 were estimated by NONMEM, version V, using FO with posthoc estimation of each individual's parameters. Calculation of the percentage bias and imprecision of the NONMEM population estimates for each data set were as described in chapter 2.

NONMEM estimates were compared to the true (simulated) value by subtracting the simulated value from the NONMEM value and plotting this difference. Ideally the values would be zero and the magnitude of the deviations from zero were used to compare the different designs.

7.5.2 Results

Figures 7.23 to 7.40 summarise the results for estimating \overline{CI} , \overline{V}_1 , \overline{V}_2 , \overline{Q} , ω_{CI} , ω_{V_1} , ω_{V_2} , ω_Q and σ_I . Plots of the bias and imprecision are shown along with graphical comparisons of the differences between the NONMEM population estimates values and the simulated mean population. Each plot consists of three sets of results, one for each design.

Estimation of Population Mean Clearance (\overline{CI})

The bias and imprecision of the estimated population mean clearance is shown in figure 7.23. All designs had estimates with greater than 30% bias, but were precise.

Figure 7.24 shows how the estimates of clearance compared to the simulated values. Each set of ten results for each design was grouped closely, showing that the error in estimation was constant.

Estimation of Population Mean Volume of Distribution of the Central Compartment (\overline{V}_1)

Figure 7.25 shows that the estimates of the volume of distribution of the central compartment were less biased than those of clearance, but were greater than 27%. The imprecision was again low (less than 5%) and figure 7.26 confirms that the estimation error was constant across the ten sets of data for each design. Design 29 had two results which were more imprecise than the others in the set, resulting in the widest 95% confidence intervals of the three designs.

Estimation of Population Mean Volume of Distribution of the Peripheral Compartment (\overline{V}_2)

The estimates of the volume of distribution of the peripheral compartment were particularly poor with the mean bias greater than 77% for designs 29 and 31. Design 30, with six sampling times selected using sensitivity analysis performed reasonably

with mean bias of 10.3%, although the 95% confidence intervals extended to greater than 20%. Design 30 was also the most imprecise of the three designs with a value of 28% compared to less than 7% for designs 29 and 31. This is confirmed in figure 7.28 where the spread of the ten estimates for each design is shown.

Estimation of Population Mean Inter-Compartmental Clearance (\bar{Q})

The estimation of the inter-compartmental clearance followed a similar pattern to that of V_2 , in that design 30 had the smallest mean bias. However, all designs had bias in excess of 30%, although all were again precise (less than 11% imprecision). (Figures 7.29 and 7.30).

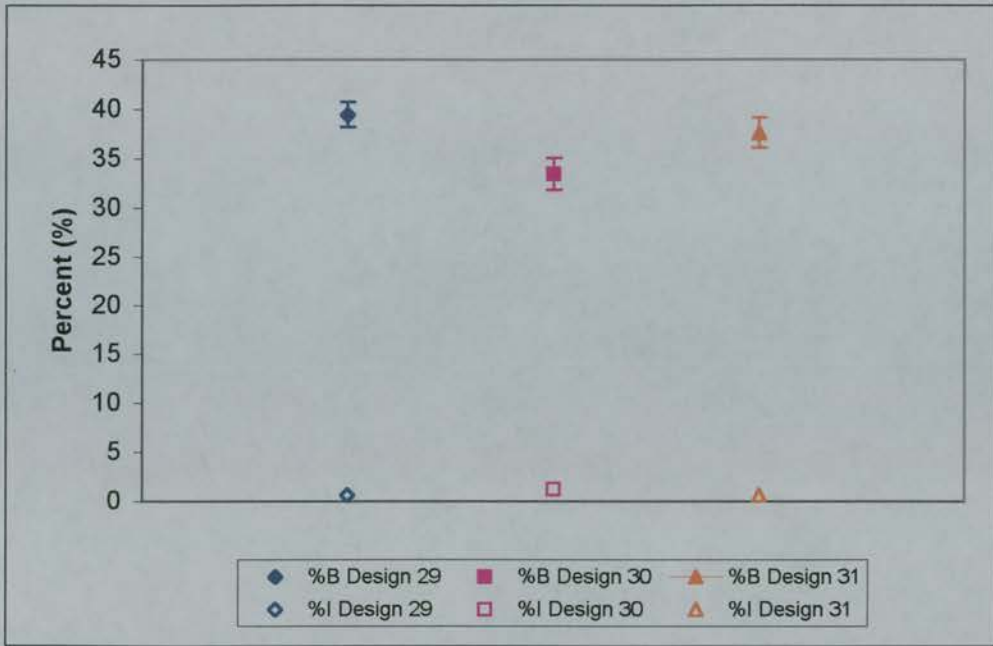


Figure 7.23 Mean percentage bias (%B) \pm 95% confidence interval and imprecision (%I) for the estimation of the clearance (CI) of Antagonist G, using designs 29-31.

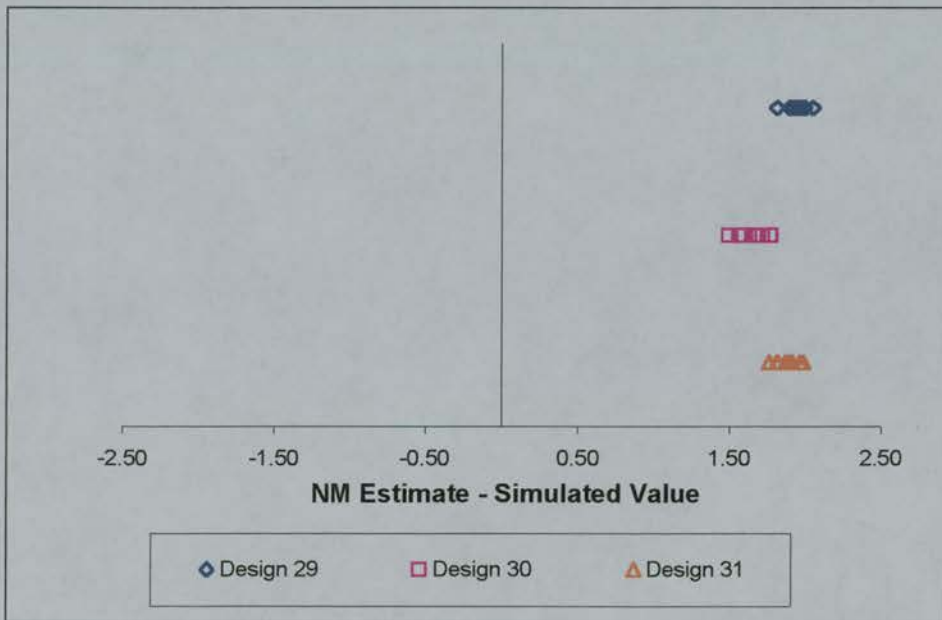


Figure 7.24 Comparison of mean simulated values with NONMEM population estimates of Antagonist G clearance.

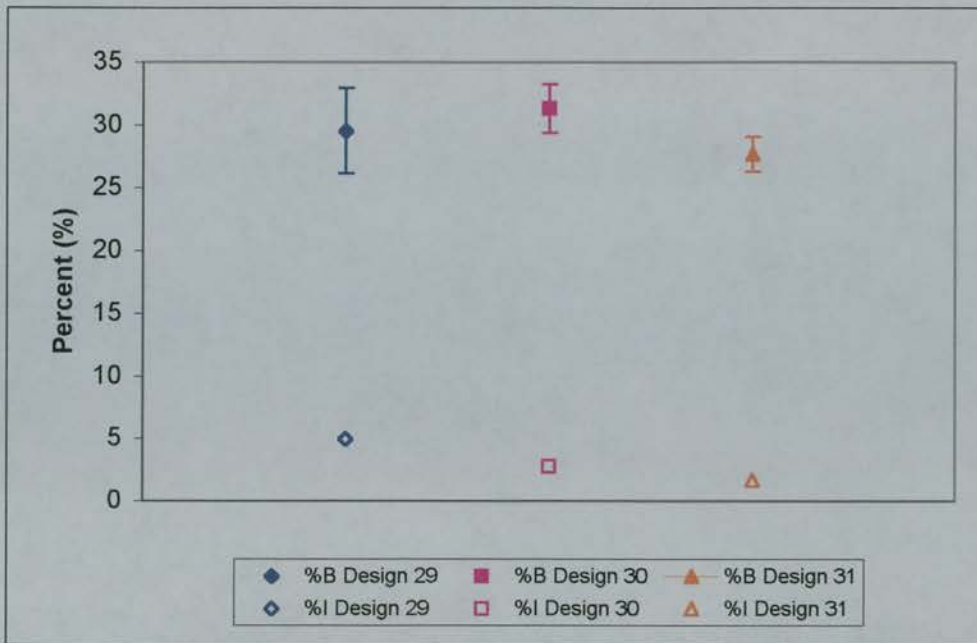


Figure 7.25 Mean percentage bias (%B) \pm 95% confidence interval and imprecision (%I) for the estimation of the volume of distribution of the central compartment (\bar{V}_1) of Antagonist G, using designs 29-31.

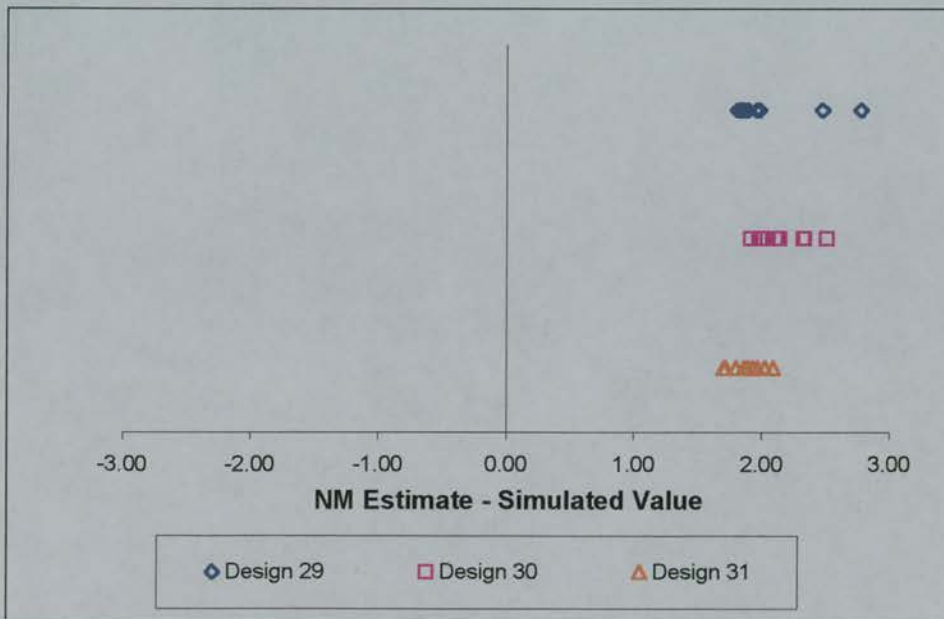


Figure 7.26 Comparison of mean simulated values with NONMEM population estimates of Antagonist G volume of the central compartment (\bar{V}_1).

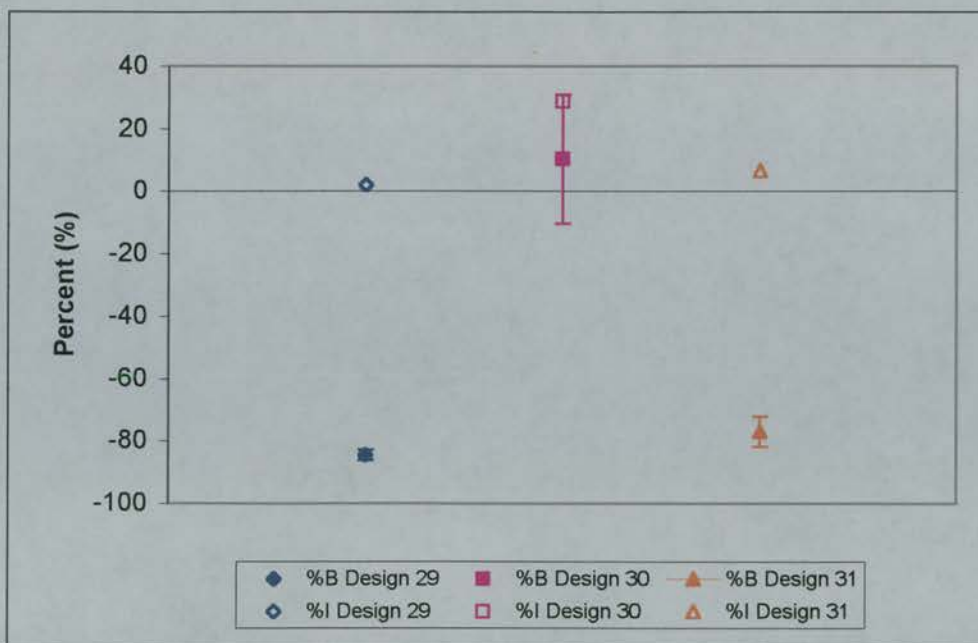


Figure 7.27 Mean percentage bias (%B) \pm 95% confidence interval and imprecision (%I) for the estimation of the volume of distribution of the peripheral compartment (\bar{V}_2) of Antagonist G, using designs 29-31.

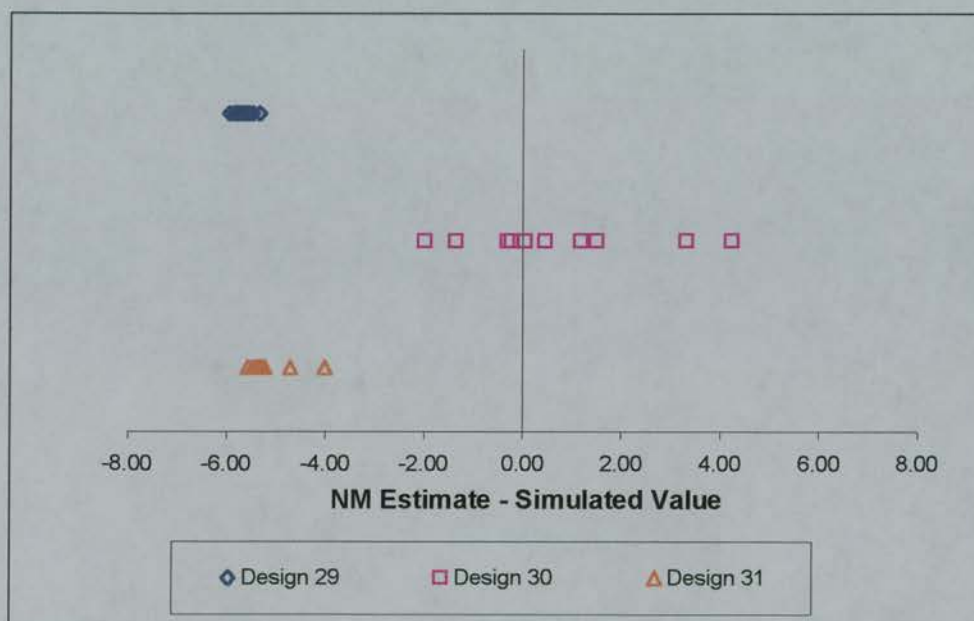


Figure 7.28 Comparison of mean simulated values with NONMEM population estimates of Antagonist G volume of the peripheral compartment (\bar{V}_2).



Figure 7.29 Mean percentage bias (%B) \pm 95% confidence interval and imprecision (%I) for the estimation of the inter-compartmental clearance (\bar{Q}) of Antagonist G, using designs 29-31.

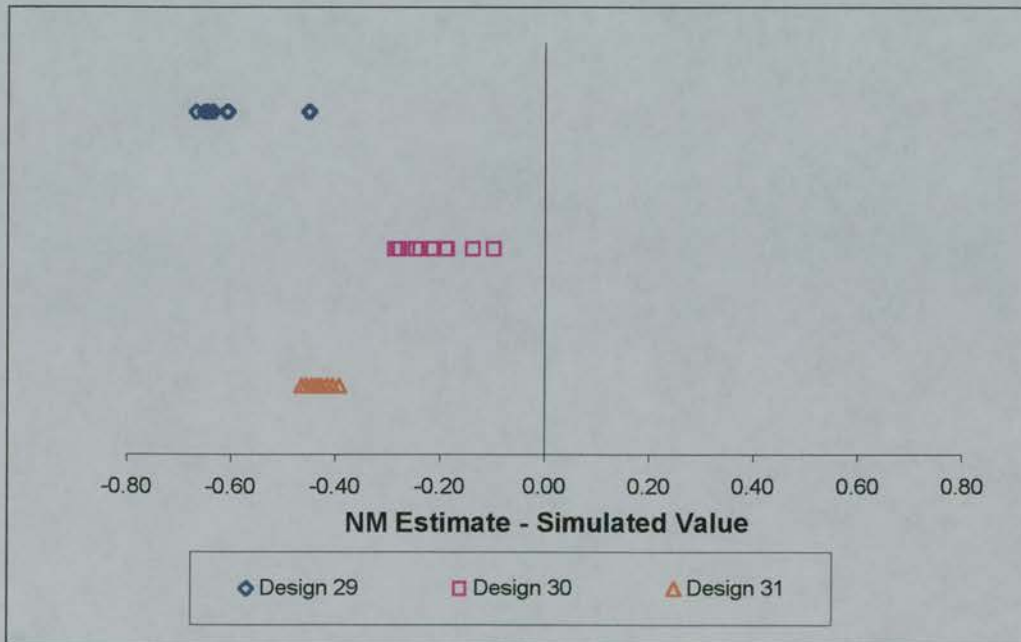


Figure 7.30 Comparison of mean simulated values with NONMEM population estimates of Antagonist G inter-compartmental clearance (\bar{Q}).

Estimation of Population Standard Deviation of Clearance (ω_{Cl})

The variability in clearance (ω_{Cl}) was estimated poorly with all three designs (mean bias of -100% (figure 7.31)). Similar to the patterns of estimation seen for the fixed effects, the imprecision was low at less than 2%. All designs performed equally and the spread of results is shown in figure 7.32.

Estimation of Population Standard Deviation of the Volume of Distribution of the Central Compartment (ω_{V_1})

The estimation of the variability of the volume of distribution of the central compartment (ω_{V_1}) was improved compared to ω_{Cl} , but remained poor with a mean bias of -44% for all designs. Similar to the estimation of ω_{Cl} the imprecision was low at less than 5% (figures 7.33 and 7.34).

Estimation of Population Standard Deviation of the Volume of Distribution of the Peripheral Compartment (ω_{V_2})

Design 31 had the lowest mean bias of -41% for the estimation of the variability in the peripheral compartment (ω_{V_2}) and the imprecision was 33% (figures 7.35 and 7.36). Design 29 with 14 samples and design 30 with six samples performed poorest with mean bias of 100% and imprecision of 47% and almost 0%, respectively.

However, no design offered a reasonable overall estimate of ω_{V_2} .

Estimation of Population Standard Deviation of the Inter-Compartmental Clearance (ω_Q)

The bias in the estimation of the bias variability in the inter-compartmental clearance (ω_Q) was the poorest of all the parameters, ranging from 245% to 1530%. The imprecision was equally poor ranging from 36% to 700%. As shown in figures 7.37 and 7.38, design 29 was poorest with mean bias of 1530% and imprecision of 700%.

Estimation of the Proportional Component of Random Intra-Subject Error (σ_1)

Of all of the fixed and random effects, the proportional intra-subject random error component was the only parameter estimated with any accuracy. All estimates of bias were within 7% and design 30, using the times selected from the sensitivity analysis was best with less than 2% bias. The imprecision for all designs was less than 3%. (Figures 7.39 and 7.40).

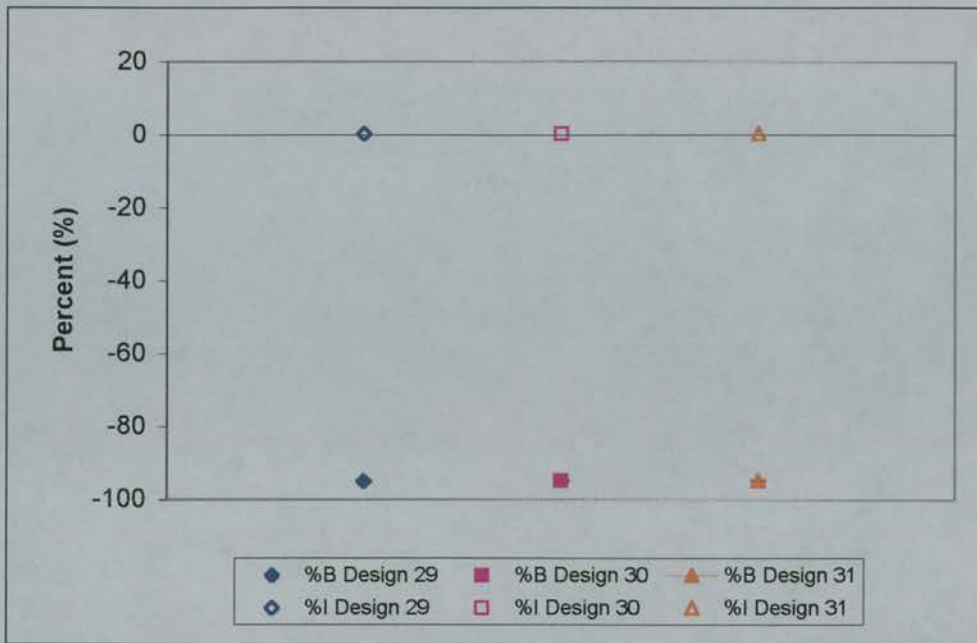


Figure 7.31 Mean percentage bias (%B) \pm 95% confidence interval and imprecision (%I) for the estimation of the standard deviation of clearance of Antagonist G (ω_{Cl}), using designs 29-31.

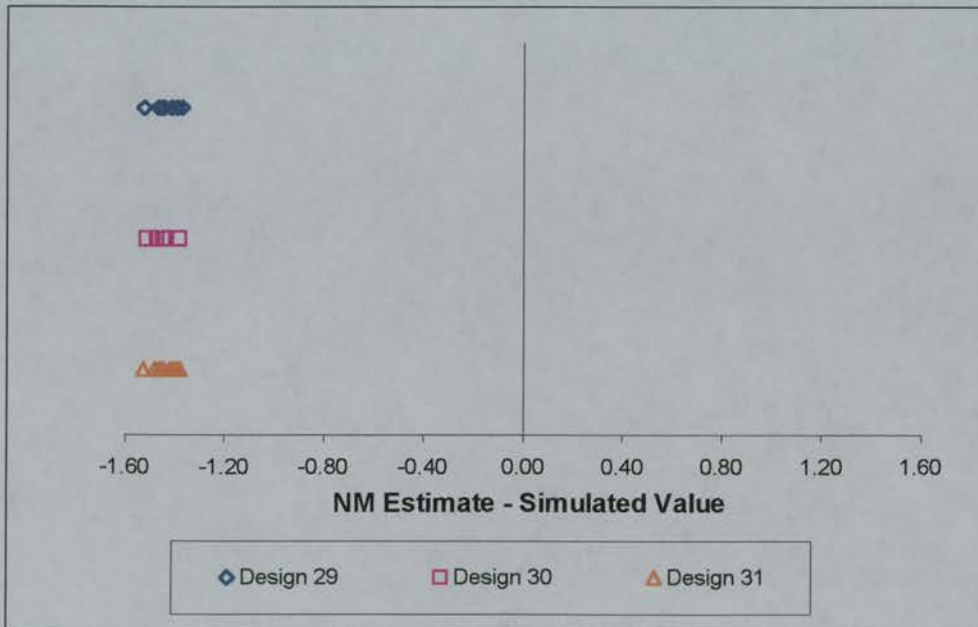


Figure 7.32 Comparison of mean simulated values with NONMEM population estimates of standard deviation of Antagonist G clearance (ω_{Cl} .)

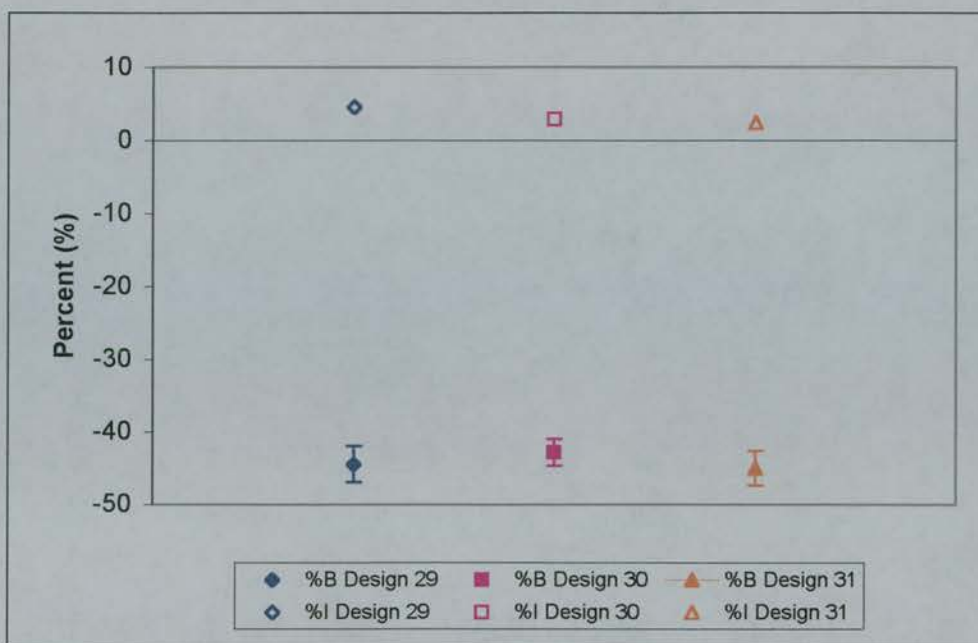


Figure 7.33 Mean percentage bias (%B) \pm 95% confidence interval and imprecision (%I) for the estimation of the standard deviation of the volume of distribution of the central compartment of Antagonist G (ω_{V_1}), using designs 29-31.

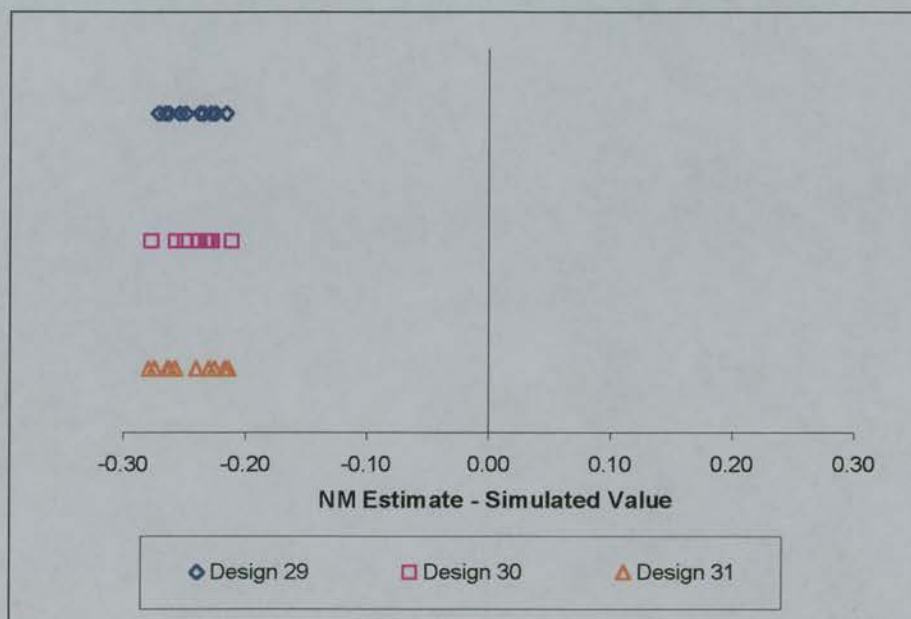


Figure 7.34 Comparison of mean simulated values with NONMEM population estimates of standard deviation of Antagonist G volume of the central compartment (ω_{V_1} .)

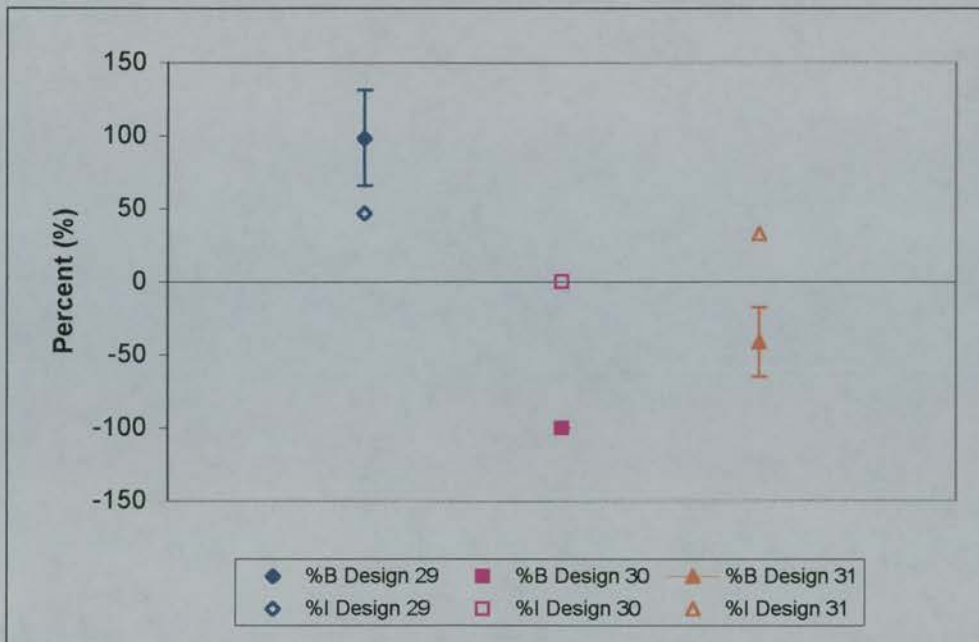


Figure 7.35 Mean percentage bias (%B) \pm 95% confidence interval and imprecision (%I) for the estimation of the standard deviation of the volume of distribution of the peripheral compartment of Antagonist G (ω_{V_2}), using designs 29-31.

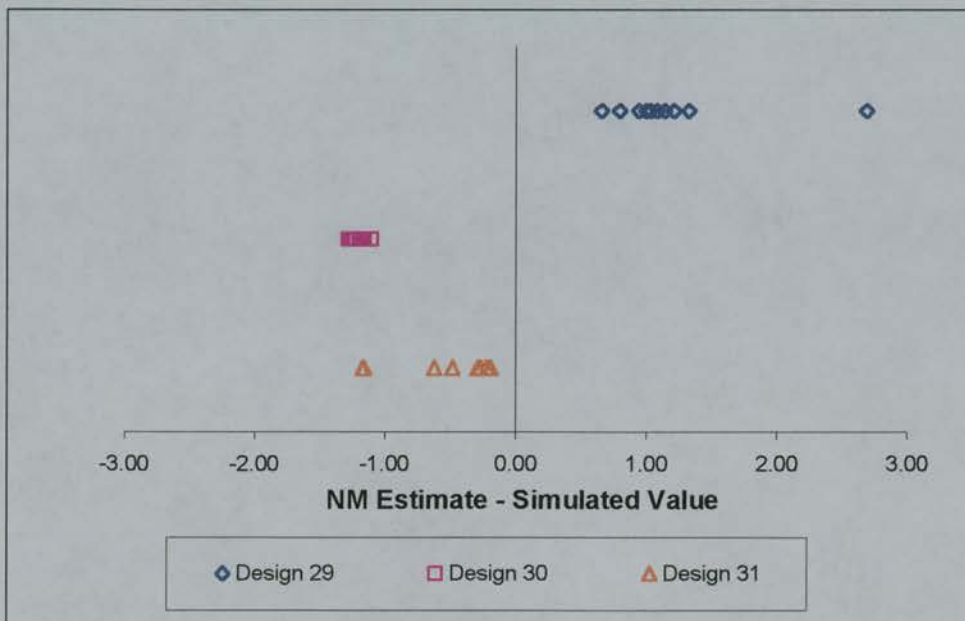


Figure 7.36 Comparison of mean simulated values with NONMEM population estimates of standard deviation of Antagonist G volume of the peripheral compartment (ω_{V_2}).

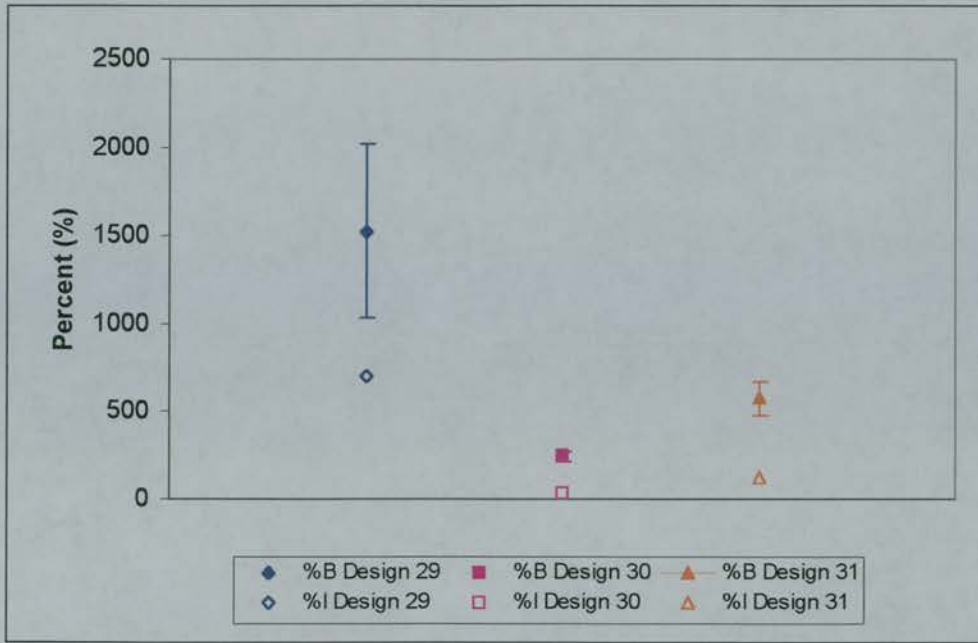


Figure 7.37 Mean percentage bias (%B) \pm 95% confidence interval and imprecision (%I) for the estimation of the standard deviation of the inter-compartmental clearance of Antagonist G (ω_G), using designs 29-31.

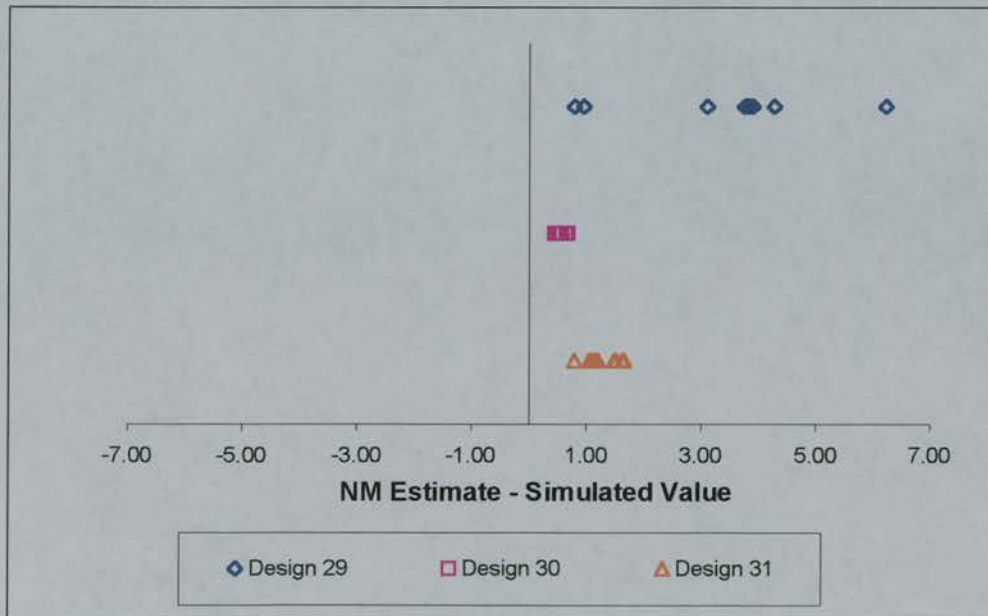


Figure 7.38 Comparison of mean simulated values with NONMEM population estimates of standard deviation of Antagonist G inter-compartmental clearance (ω_G).

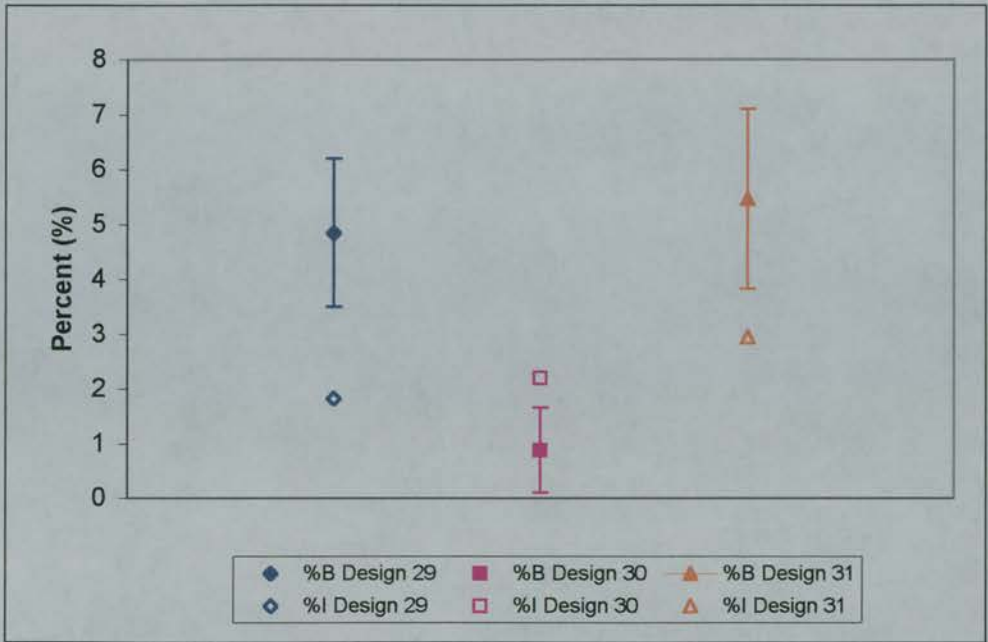


Figure 7.39 Mean percentage bias (%B) \pm 95% confidence interval and imprecision (%I) for the estimation of the proportional intra-subject error in Antagonist G concentration (σ_1), using designs 29-31.

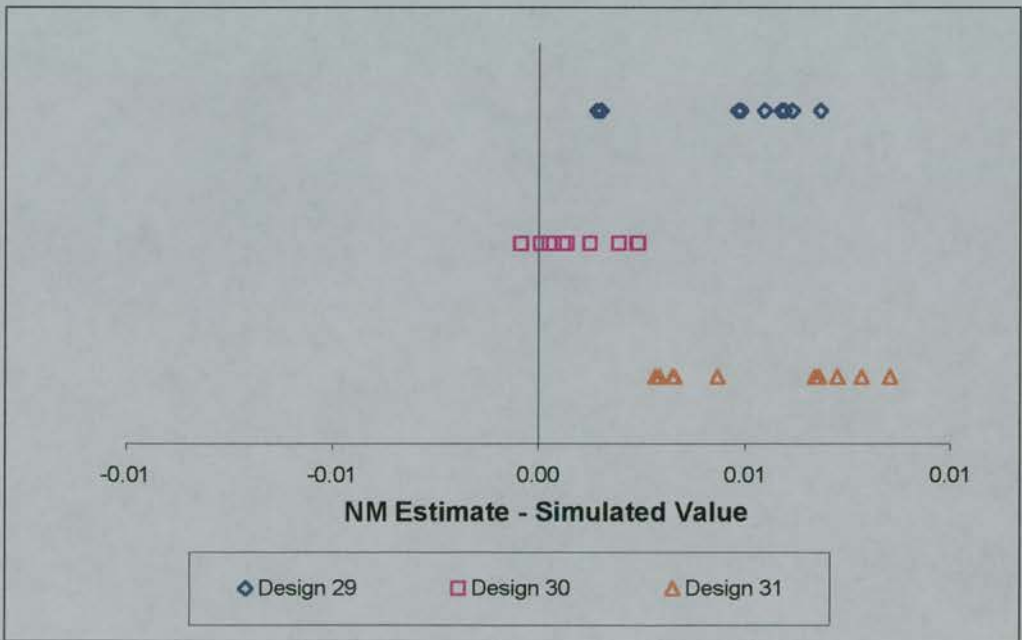


Figure 7.40 Comparison of mean simulated values with NONMEM population estimates of standard deviation of the proportional intra-subject error in Antagonist G concentration (σ_1 .)

7.5.3 Discussion

The results for the Antagonist G simulations were disappointing when compared to the simulations of a two-compartment model in chapter 6. All results except the estimation of the residual error model were biased, although precise, suggesting that there was a problem of model identifiability. The most probable cause was that the population average values \bar{V}_1 and \bar{V}_2 , and hence the rate constants k_{12} and k_{21} , were almost equal. Using the FO method in NONMEM, all individuals are ascribed the same parameter values i.e. the population averages, and this could lead to the model not being sustainable. The FOCE method should have alleviated this problem by allowing each individual to have his own set of parameter values, but NONMEM would not terminate using this method.

As the results were so poor no conclusions could be drawn regarding the use of the 'optimal' designs over the original full sampling design. However, it should be noted that the designs with five and six samples based on sensitivity analysis gave results that were similar to those obtained with the fourteen-sample design.

In the designs with five and six samples, the last sample collection was at 10.4 hours. This would mean one day spent at hospital for this study, e.g., from 0800 to 1900 hr, allowing for starting the infusion. The original sampling schedule required a 12 and 24 hr sample, which required a stay up to 2000 hr, or later depending on delays, for both patient and staff. In addition, the collection of the 24 hr sample required attendance by the patient the following morning. The reduced sampling designs removed eight samples from the period 6 to 24 hr of the original design, which in addition to the reduced time attending the hospital would be more convenient for the patient.

Examination of the NONMEM output showed high correlations between the estimated parameters, when none were present in the simulated data. An example of the parameter estimates obtained using design 29 is shown in figure 7.41. The plots for designs 30 and 31 were similar, showing that the posthoc estimates were not

accurate when compared to the simulated values. However, the high correlations between the parameters allowed the concentrations to be well fitted by the model (figure 7.42).

In order for the parameters of a model to be identifiable, they have to exert an influence on the outcome variable (Williams 1990; Gabrielsson et al. 1997). In this case the outcome variable is concentration and, as the sensitivity analysis showed, clearance was the parameter with greatest influence. Hence, perhaps it is not surprising that the parameter estimates were so poor. However, clearance, which did influence the outcome, was not estimated accurately either.

The population model for Antagonist G was only developed from patients 13-24 in the phase I study and perhaps further work, refining the model with the use of covariates would have allowed all data to be included. There is a suggestion in figure 7.18 of a dose dependent reduction in clearance which was not explored fully at this stage. A more accurate population model may have selected times that would be different to those used and hence, perhaps in the situation described in this thesis the 'optimal' design for a population PK study of Antagonist G has not been identified.

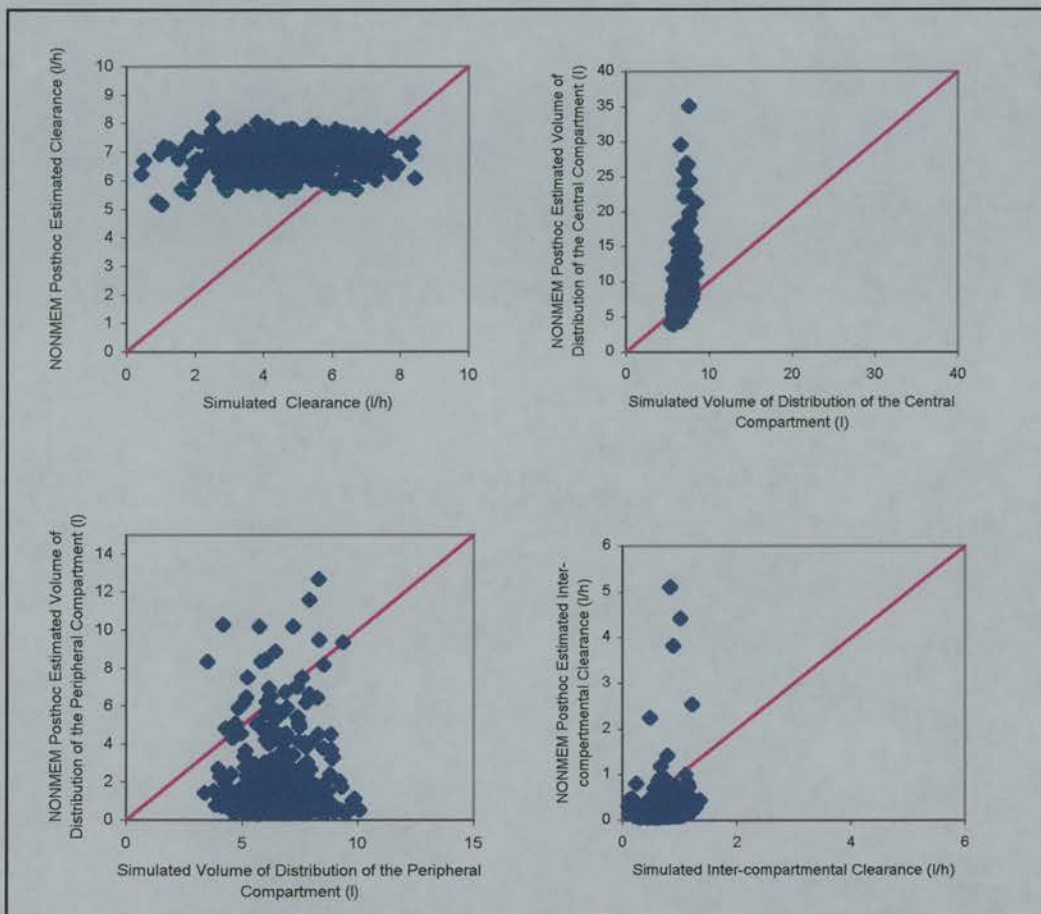


Figure 7.41 Comparison of a set of 500 simulated parameter estimates with NONMEM posthoc parameter estimates, using 14 fixed sampling times (Design 29). The line of identity is shown in pink.

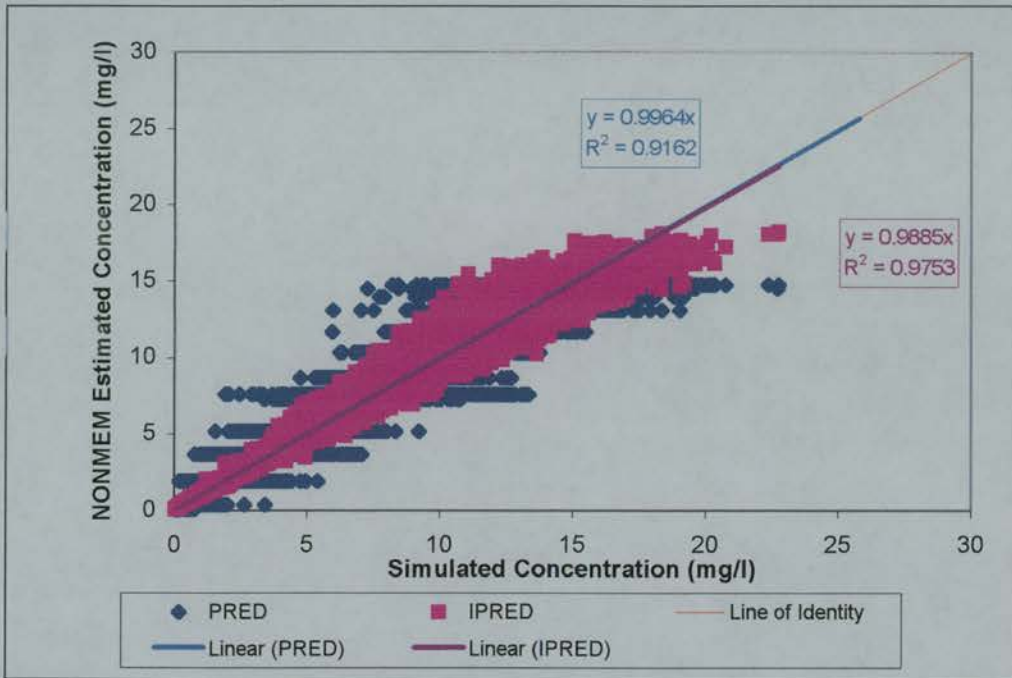


Figure 7.42 Comparison of the simulated concentrations for 500 subjects with the NONMEM population predicted concentrations (PRED) and the NONMEM posthoc predicted concentrations for each individual (IPRED), using 14 fixed sampling times (Design 29). The line of identity is shown in red and the linear regression lines (and corresponding equations) for the PRED and IPRED concentrations are shown in blue and purple, respectively.

7.6 Conclusion

The first part of this chapter has shown that for a one-compartment PK model the equations derived in chapter 3 were scaleable to 'real' values of PK parameters, when applied to a modified carboplatin model. The sampling schedules derived from the times of peak concentration variance performed as well as published sampling schedules, but allowed a reduction in the number of samples that were required for accurate parameter estimation. In addition, selecting sampling times close to the 'optimal' times based on sensitivity analysis also gave accurate parameter estimates. This was particularly true if these samples were taken at times where the amount of information about the parameter remained high in relation to the total height of the peak. This result indicates that designing population PK studies based on optimal design strategy allows a degree of flexibility in when the sample is taken, but only in the situation in which the time is recorded accurately, similar to those designs incorporating sampling windows.

The results from the second part of the chapter were disappointing when the optimal design strategy was applied to clinical data from the phase I trial of the broad-spectrum neuropeptide antagonist, Antagonist G. Model identifiability problems with NONMEM resulted in biased parameter estimates that were highly correlated. As such no conclusions could be drawn about the 'optimal' designs investigated, other than the fact that the reduced designs of five and six samples resulted in parameter estimates with similar bias to the fourteen-sample design.

As the population model for Antagonist G was not explored fully in terms of covariate effects, investigation of this in the future may result in an improved sampling design. The results from this section emphasise the reliance that optimal design strategies have on the *a priori* identification of the correct PK model (Silvey 1980; Jacquez 1998).

In conclusion, this chapter has shown that the use of an 'optimal' sampling strategy allows population PK studies to be designed around times that will allow accurate

parameter estimation, perhaps from a reduced number of samples. Specifically, if the design does not call for a minimum number of samples, then these sampling times should be utilised as the starting point for the addition of further samples and should be included.

Chapter 8

8 Conclusions and Further Investigations

The aim of the studies described in this thesis was to investigate the efficiency of different study designs in the estimation of population PK parameters. Designs were simulated with sparse data for each subject included in the populations as this is the nature of the population approach to pharmacokinetics. In general, this type of analysis is carried out in a clinical setting where the primary goal may not be to investigate pharmacokinetics, but to investigate therapeutic efficacy and tolerability. Hence, often only a small amount of PK data is collected per individual, which if considered alone would not give accurate estimates of their PK parameters.

The strength of the population approach to PK analysis is that mixed effect modelling techniques allow analysis of the population as a whole. In this situation each individual ‘borrows strength’ from the others in the population, and the distribution of the PK parameters can be obtained. The advantage of this technique over other techniques, e.g., the standard two-stage method, is that the inclusion of covariate data may allow the model to be refined and the residual random error partitioned into that due to inter and intra-individual error.

Selection of Sampling Times

An important aspect of the design of population PK studies is the number and timing of the samples. The timing of the samples was investigated in this thesis using sensitivity analysis (chapter 3), which allowed the definition of a minimum number of samples to be collected. The sampling times were selected by relating the variability in the outcome parameter of the PK model (concentration) to the variability in the input parameters (e.g., clearance and volume of distribution), and the ‘optimal’ sampling times corresponded to peaks in concentration variance. This method was similar to the most commonly used design criterion, D-optimality, and allowed investigation of the effect of increasing the variability in the parameters. D-optimality only considers the mean PK parameter values. One result was that the sampling time related to clearance was shown to move slightly to later times when the variability in the parameters was greater.

Selection of sampling times using sensitivity analysis resulted in the definition of an optimal sampling strategy consisting of two sampling times for the one-compartment PK model - as early as possible for the estimation of volume of distribution and $1.44*t_{1/2}$ for estimating clearance. Designs for a two-compartment model were defined graphically, as the equations were intractable, and resulted in a five or six-sample strategy dependent on the values of the parameters.

Comparison of 'Optimal' Sampling Schedules with Empirical Designs

Comparison of the sampling designs from sensitivity analysis with empirically selected designs and published sampling strategies showed that the use of optimal sampling techniques allowed a reduction in the number of samples while resulting in equally accurate parameter estimation (chapters 4 & 6). In addition it was shown that the use of a sampling window around the optimal time had no detrimental effect on the bias and precision of the estimates and, in fact, the estimation of random effects was improved (chapter 5 & 6). This was most apparent when the size of the window was relatively large in relation to the half-life of the drug. The addition of further samples to the minimum number defined by sensitivity analysis, improved the estimation of the random error terms, but the times of the extra samples was not as important as their inclusion (chapter 5).

Application of Sensitivity Analysis to Carboplatin and Antagonist G

The approach to sampling design described in this thesis was applied to two drugs - one in routine clinical use, carboplatin, and a novel anticancer agent in early clinical development, Antagonist G (chapter 7). When simulations were used to compare the designs described in this thesis to published sampling strategies for carboplatin, the two-sample designs based on sensitivity analysis performed as well as a published four-sample design. However, when the designs were applied to a two-compartment population model described for Antagonist G the results were disappointing. This was probably due to the poor design of the original study which gave rise to

identifiability problems with the PK model and resulted in the average values of the rate constants k_{12} and k_{21} being approximately equal.

Investigation of covariate information for the population model should improve the population PK model for Antagonist G and hence solve these problems. However, it was noted that the five and six-sample designs had similar parameter estimates to those obtained with the original fourteen-sample design used in the phase I clinical trial.

The results from the Antagonist G data serve to stress the key aspect in the use of optimal sampling techniques - that the PK model must be defined *a priori*, along with estimates of the parameter values.

Conclusions

Overall, this thesis has shown the development of a technique which may be used for population PK study design and which allows accurate parameter estimation from a reduced number of samples.

As stated previously, optimal sampling strategies rely on the definition of the PK model *a priori*, and hence will require that classical PK studies are carried out initially using a full sampling strategy. Specifically, the sampling times defined in this thesis could be incorporated into the classical design by utilising them as the starting point. Further samples could be added around them and sampling windows defined to allow identification of the appropriate PK model. Once the PK model has been defined and is stable, sampling may be reduced to the minimum number defined for the model. The use of sampling windows would allow flexibility in sampling in a clinical situation with the restriction that the times of the samples must be recorded accurately. In addition, the collection of a reduced number of samples could allow data to be collected during routine outpatient clinic visits, leading to an increased number of subjects in the population study. This in turn may result in

identification of covariate effects and an improved description of the PK model for the drug.

Further Investigations

Investigations which may follow from the studies described in this thesis are:

- full development of the PK model for Antagonist G, with investigation of covariate affects, to allow examination of an optimal sampling strategy for this compound.
- investigation of the optimal sampling times for other routes of administration, e.g., infusion regimes.
- investigation of the optimal sampling times for other PK models, e.g., nonlinear models.
- investigation of sampling designs when the times are recorded inaccurately.
- simulations examining when to switch from full to limited sampling, in terms of numbers of subjects required.

References

References

- Aarons, L. (1991). "Population kinetics: theory and practice." *British Journal of Clinical Pharmacology* **32**(6): 669-670.
- Aarons, L., L. P. Balant, F. Mentre, P. L. Morselli, M. Rowland, J. L. Steimer and S. Vozeh (1996). "Practical experience and issues in designing and performing population pharmacokinetic/pharmacodynamic studies." *European Journal of Clinical Pharmacology* **49**(4): 251-4.
- Al-Banna, M. K., A. W. Kelman and B. Whiting (1990). "Experimental design and efficient parameter estimation in population pharmacokinetics." *Journal of Pharmacokinetics & Biopharmaceutics* **18**(4): 347-360.
- Baille, P., R. Bruno, J. H. Schellens, L. K. Webster, M. Millward, J. Verweij and G. Montay (1997). "Optimal sampling strategies for bayesian estimation of docetaxel (Taxotere) clearance." *Clinical Cancer Research* **3**(9): 1535-8.
- Barford, N. C. (1967). *Experimental Measurements: Precision, Error and Truth*. Addison Wesley Company, London.
- Beal, S. L. and L. B. Sheiner (1998). *Conditional Estimation Methods*. NONMEM Users Guide Part VII. NONMEM Project Group, University of California, San Francisco.
- Bellissant, E., V. Seville and G. Paintaud (1998). "Methodological issues in pharmacokinetic-pharmacodynamic modelling." *Clinical Pharmacokinetics* **35**(2): 151-66.
- Bennett, J. E. and J. C. Wakefield (1996). "A comparison of a Bayesian population method with two methods as implemented in commercially available software." *Journal of Pharmacokinetics & Biopharmaceutics* **24**(4): 403-32.

Berg, M. J., R. K. Lantz, R. D. Schoenwald, M. I. Clarke and D. D. Schottelius (1983). "Optimization of pharmacokinetic monitoring: I. Linear pharmacokinetics." *Therapeutic Drug Monitoring* **5**(4): 379-87.

Boeckman, A. J., L. B. Sheiner and S. L. Beal (1992). *Introductory Guide*. NONMEM Users Guide Part V. NONMEM Project Group, University of California, San Francisco.

Box, G. and H. Lucas (1959). "Design of Experiments in Nonlinear Situations." *Biometrika* **46**: 77-90.

Calvert, A. H., D. R. Newell, L. A. Gumbrell, S. O'Reilly, M. Burnell, F. E. Boxall, Z. H. Siddik, I. R. Judson, M. E. Gore, et al. (1989). "Carboplatin dosage: prospective evaluation of a simple formula based on renal function." *Journal of Clinical Oncology* **7**(11): 1748-1756.

Canal, P., E. Chatelut and S. Guichard (1998). "Practical treatment guide for dose individualisation in cancer chemotherapy." *Drugs* **56**(6): 1019-38.

Chabot, G. G. (1995). "Limited sampling models for simultaneous estimation of the pharmacokinetics of irinotecan and its active metabolite SN-38." *Cancer Chemotherapy & Pharmacology* **36**(6): 463-472.

Chatelut, E., P. Canal, V. Brunner, C. Chevreau, A. Pujol, A. Boneu, H. Roche, G. Houin and R. Bugat (1995). "Prediction of carboplatin clearance from standard morphological and biological patient characteristics." *Journal of the National Cancer Institute* **87**(8): 573-580.

Chatelut, E., X. Pivot, J. Otto, C. Chevreau, A. Thyss, N. Renee, G. Milano and P. Canal (2000). "A limited sampling strategy for determining carboplatin AUC and monitoring drug dosage." *European Journal of Cancer* **36**(2): 264-9.

Clewell, H. J., 3rd, T. S. Lee and R. L. Carpenter (1994). "Sensitivity of physiologically based pharmacokinetic models to variation in model parameters: methylene chloride." *Risk Analysis* **14**(4): 521-31.

Cockroft, D. W. and H. Gault (1976). "Prediction of creatinine clearance from serum creatinine." *Nephron* **16**: 31-41.

CRC (1999). Cancer Stats: Survival., Cancer Research Campaign.

CRC (2000). Cancer Stats: Mortality., Cancer Research Campaign.

Danhof, M. (1996). "Applications of pharmacokinetic/pharmacodynamic research in rational drug development." *Methods & Findings in Experimental & Clinical Pharmacology* **18**(Suppl C): 53-54.

D'Argenio, D. Z. (1981). "Optimal sampling times for pharmacokinetic experiments." *Journal of Pharmacokinetics & Biopharmaceutics* **9**(6): 739-756.

D'Argenio, D. and K. Khakmahd (1983). "Adaptive control of theophylline therapy: importance of blood sampling times." *Journal of Pharmacokinetics & Biopharmaceutics* **11**(5): 547-59.

D'Argenio, D. Z. and A. Schumitsky (1997). *ADAPT II User's Guide: Pharmacokinetic /Pharmacodynamic Systems Analysis Software*. Biomedical Simulations Resource, University of Southern California, Los Angeles.

Desoize, B., P. Dumont, L. Manot, S. Urien, R. Dufour and G. Berthiot (1994a). "Comparison of two dose prediction models for cisplatin." *Anticancer Research* **14**(6a): 2285-2290.

Desoize, B. and J. Robert (1994b). "Individual dose adaptation of anticancer drugs." *European Journal of Cancer* **30A**(6): 844-851.

Dollery, C., Ed. (1999). *Therapeutic Drugs*. Second Edition. Churchill Livingstone, Edinburgh.

Donelli, M. G., M. Zucchetti, E. Munzone, M. D'Incalci and A. Crosignani (1998). "Pharmacokinetics of anticancer agents in patients with impaired liver function." *European Journal of Cancer* **34**(1): 33-46.

Døssing, M., A. Volund and H. E. Poulsen (1983). "Optimal sampling times for minimum variance of clearance determination." *British Journal of Clinical Pharmacology* **15**(2): 231-5.

Drusano, G. L., A. Forrest, M. J. Snyder, M. D. Reed and J. L. Blumer (1988). "An evaluation of optimal sampling strategy and adaptive study design." *Clinical Pharmacology & Therapeutics* **44**(2): 232-238.

Duffull, S. B. and B. A. Robinson (1997). "Clinical pharmacokinetics and dose optimisation of carboplatin." *Clinical Pharmacokinetics* **33**(3): 161-83.

Duffull, S. B., E. J. Begg and J. J. Deely (1999). "Development of a general method of limited sampling for the determination of AUC for a drug that displays two-compartment pharmacokinetics." *European Journal of Clinical Pharmacology* **55**(3): 213-9.

Egorin, M. J., D. A. Van Echo, E. A. Olman, M. Y. Whitacre, A. Forrest and J. Aisner (1985). "Prospective validation of a pharmacologically based dosing scheme for the cis-diamminechloroplatinum (II) analogue diamminecyclobutanedicarboxylatoplatinum." *Cancer Research* **45**: 6502-6506.

Egorin, M. J., A. Forrest, C. P. Belani, M. J. Ratain, J. S. Abrams and D. A. Van Echo (1989). "A limited sampling strategy for cyclophosphamide pharmacokinetics." *Cancer Research* **49**(11): 3129-3133.

Eisenberger, M. A., V. J. Sinibaldi, L. M. Reyno, R. Sridhara, D. I. Jodrell, E. G. Zuhowski, K. H. Tkaczuk, M. H. Lowitt, R. K. Hemady, et al. (1995). "Phase I and clinical evaluation of a pharmacologically guided regimen of suramin in patients with hormone-refractory prostate cancer." *Journal of Clinical Oncology* **13**(9): 2174-2186.

Endrenyi, L. (1981). Design of experiments for estimating enzyme and pharmacokinetic parameters. *Kinetic Data Analysis*. L. Endrenyi. New York, Plenum Press: 137-167.

Ette, E. I., H. Sun and T. M. Ludden (1998). "Balanced designs in longitudinal population pharmacokinetic studies." *Journal of Clinical Pharmacology* **38**(5): 417-23.

Evans, W. and M. Relling (1989). "Clinical pharmacokinetics-pharmacodynamics of anticancer drugs." *Clinical Pharmacokinetics* **16**(6): 327-336.

Gabrielsson, J. and D. Weiner (1997). *Pharmacokinetic and Pharmacodynamic Data Analysis: Concepts and Applications*. Swedish Pharmaceutical Press, Stockholm.

Gambus, P. (1996). "Structural Modeling - Simultaneous pharmacokinetic-pharmacodynamic modeling." *Methods & Findings in Experimental & Clinical Pharmacology* **18**(SC): 47-48.

Gentili, D., M. Zucchetti, V. Torri, C. Sessa, J. De Jong, F. Cavalli and M. D'Incalci (1993). "A limited sampling model for the pharmacokinetics of etoposide given orally." *Cancer Chemotherapy & Pharmacology* **32**(6): 482-486.

Ghazal-Aswad, S., A. H. Calvert and D. R. Newell (1996). "A single-sample assay for the estimation of the area under the free carboplatin plasma concentration versus time curve." *Cancer Chemotherapy and Pharmacology* **37**(5): 429-434.

Grasela, T. H., Jr., E. J. Antal, R. J. Townsend and R. B. Smith (1986). "An evaluation of population pharmacokinetics in therapeutic trials. Part I. Comparison of methodologies." *Clinical Pharmacology & Therapeutics* **39**(6): 605-12.

Griffiths, J. R. and J. D. Glickson (2000). "Monitoring pharmacokinetics of anticancer drugs: non-invasive investigation using magnetic resonance spectroscopy." *Advanced Drug Delivery Reviews* **41**(1): 75-89.

Hashimoto, Y. and L. B. Sheiner (1991). "Designs for population pharmacodynamics: value of pharmacokinetic data and population analysis." *Journal of Pharmacokinetics & Biopharmaceutics* **19**(3): 333-53.

Hassan, M., A. Fasth, B. Gerritsen, A. Haraldsson, Z. Syruckova, B. van den, M. Sandstrom, M. Karlsson, S. Kumlien, et al. (1996). "Busulphan kinetics and limited sampling model in children with leukemia and inherited disorders." *Bone Marrow Transplantation* **18**(5): 843-850.

Hetrick, D. M., A. M. Jarabek and C. C. Travis (1991). "Sensitivity analysis for physiologically based pharmacokinetic models." *Journal of Pharmacokinetics & Biopharmaceutics* **19**(1): 1-20.

Holz, J. B., H. Koppler, L. Schmidt, H. W. Fritsch, K. H. Pfluger and H. Jungclas (1995). "Limited sampling models for reliable estimation of etoposide area under the curve." *European Journal of Cancer* **31A**(11): 1794-1798.

Hon, Y. Y. and W. E. Evans (1998). "Making TDM work to optimize cancer chemotherapy: a multidisciplinary team approach." *Clinical Chemistry* **44**(2): 388-400.

Huizing, M. T., L. J. C. Van Warmerdam, H. Rosing, W. W. Ten Bokkel Huinink, M. B. Stewart, H. M. Pinedo and J. H. Beijnen (1995). "Limited sampling strategies for investigating paclitaxel pharmacokinetics in patients receiving 175 mg/m² as a 3-hour infusion." *Clinical Drug Investigation* 9(6): 344-353.

Jacquez, J. A. (1998). "Design of experiments." *Journal of the Franklin Institute-Engineering and Applied Mathematics* 335b(2): 259-279.

Jia, X. and J. R. Nedelman (1996). "Errors in time in pharmacokinetic studies." *Journal of Biopharmaceutical Statistics* 6(3): 303-318.

Jodrell, D. I., M. J. Egorin, R. M. Canetta, P. Langenberg, E. P. Goldbloom, J. N. Burroughs, J. L. Goodlow, S. Tan and E. Wiltshaw (1992). "Relationships between carboplatin exposure and tumor response and toxicity in patients with ovarian cancer." *Journal of Clinical Oncology* 10(4): 520-8.

Jodrell, D. I., L. M. Reyno, R. Sridhara, M. A. Eisenberger, K. H. Tkaczuk, E. G. Zuhowski, V. J. Sinibaldi, M. J. Novak and M. J. Egorin (1994). "Suramin: development of a population pharmacokinetic model and its use with intermittent short infusions to control plasma drug concentration in patients with prostate cancer." *Journal of Clinical Oncology* 12(1): 166-175.

Jodrell, D. I., L. S. Murray, J. Hawtof, M. A. Graham and M. J. Egorin (1996). "A comparison of methods for limited-sampling strategy design using data from a phase I trial of the anthrapyrazole DuP-941." *Cancer Chemotherapy & Pharmacology* 37(4): 356-362.

Jones, D. A., J. Cummings, S. P. Langdon and J. F. Smyth (1997). "Preclinical studies on the broad-spectrum neuropeptide growth factor Antagonist G." *General Pharmacology* 28(2): 183-9.

- Jonsson, E. N., J. R. Wade and M. O. Karlsson (1996). "Comparison of some practical sampling strategies for population pharmacokinetic studies." *Journal of Pharmacokinetics & Biopharmaceutics* **24**(2): 245-263.
- Kintzel, P. E. and R. T. Dorr (1995). "Anticancer drug renal toxicity and elimination: dosing guidelines for altered renal function." *Cancer Treatment Reviews* **21**(1): 33-64.
- Kobayashi, K., D. I. Jodrell and M. J. Ratain (1993). "Pharmacodynamic-pharmacokinetic relationships and therapeutic drug monitoring." *Cancer Surveys* **17**: 51-78.
- Koren, G., K. Beatty, A. Seto, T. R. Einarson and M. Lishner (1992). "The effects of impaired liver function on the elimination of antineoplastic agents." *Annals of Pharmacotherapy* **26**(3): 363-71.
- Levy, G. (1998). "What are narrow therapeutic index drugs?" *Clinical Pharmacology & Therapeutics* **63**(5): 501-5.
- Liliemark, J., F. Albertioni, G. Juliusson and S. Eksborg (1996). "A limited sampling strategy for estimation of the cladribine plasma area under the concentration versus time curve after intermittent i.v. infusion, s.c. injection, and oral administration." *Cancer Chemotherapy and Pharmacology* **38**(6): 536-540.
- Lindstrom, M. L. and D. M. Bates (1990). "Nonlinear mixed effects models for repeated measures data." *Biometrics* **46**(3): 673-87.
- Loadman, P. M. and M. C. Bibby (1994). "Pharmacokinetic drug interactions with anticancer drugs." *Clinical Pharmacokinetics* **26**(6): 486-500.

- Lum, B. L., K. J. Lane, T. W. Synold, A. Goram, S. B. Charnick and B. I. Sikic (1997). "Validation of a limited sampling model to determine etoposide area under the curve." *Pharmacotherapy* **17**(5): 887-890.
- Lustig, V., H. Rosing, L. J. C. Van Warmerdam, H. T. Huizing, W. W. Ten Bokkel Huinink, A. C. Dubbelman and J. H. Beijnen (1997). "Limited sampling models for the pharmacokinetics of docetaxel." *Clinical Drug Investigation* **13**(5): 247-254.
- Masson, E. and W. C. Zamboni (1997). "Pharmacokinetic optimisation of cancer chemotherapy. Effect on outcomes." *Clinical Pharmacokinetics* **32**(4): 324-343.
- Mathijssen, R. H. J., R. J. van Alphen, M. J. A. de Jonge, J. Verweij, P. de Bruijn, W. J. Loos, K. Nooter, L. Vernillet, G. Stoter, et al. (1999). "Sparse-data set analysis for irinotecan and SN-38 pharmacokinetics in cancer patients co-treated with cisplatin." *Anti-Cancer drugs* **10**(1): 9-16.
- McLeod, H. L., M. A. Graham, S. Aamdal, A. Setanoians, Y. Groot and B. Lund (1996). "Phase I pharmacokinetics and limited sampling strategies for the bioreductive alkylating drug EO9. EORTC Early Clinical Trials Group." *European Journal of Cancer* **32A**(9): 1518-1522.
- Mentré, F., P. Burtin, Y. Merlé, J. van Bree, A. Mallet and J.-L. Steimer (1995a). "Sparse-Sampling Optimal Designs in Pharmacokinetics and Toxicokinetics." *Drug Information Journal* **29**: 997-1019.
- Mentré, F. and R. Gomeni (1995b). "A two-step iterative algorithm for estimation in nonlinear mixed-effect models with an evaluation in population pharmacokinetics." *Journal of Biopharmaceutical Statistics* **5**(2): 141-58.
- Merlé, Y. and F. Mentré (1995). "Bayesian design criteria: computation, comparison, and application to a pharmacokinetic and a pharmacodynamic model." *Journal of Pharmacokinetics & Biopharmaceutics* **23**(1): 101-25.

Mick, R., E. Gupta, E. E. Vokes and M. J. Ratain (1996). "Limited-sampling models for irinotecan pharmacokinetics-pharmacodynamics: prediction of biliary index and intestinal toxicity." *Journal of Clinical Oncology* **14**(7): 2012-2019.

Minami, H., J. H. Beijnen, J. Verweij and M. J. Ratain (1996). "Limited sampling model for area under the concentration time curve of total topotecan." *Clinical Cancer Research* **2**(1): 43-46.

Moore, M. J. and C. Erlichman (1987). "Therapeutic drug monitoring in oncology. Problems and potential in antineoplastic therapy." *Clinical Pharmacokinetics* **13**(4): 205-27.

Moore, M. J., P. Bunting, S. Yuan and J. J. Thiessen (1993). "Development and validation of a limited sampling strategy for 5-fluorouracil given by bolus intravenous administration." *Therapeutic Drug Monitoring* **15**(5): 394-399.

Nakashima, H., R. Lieberman, A. Karato, H. Arioka, H. Ohmatsu, N. Nomura, J. Shiraishi, T. Tamura, K. Eguchi, et al. (1995). "Efficient sampling strategies for forecasting pharmacokinetic parameters of irinotecan (CPT-11): implication for area under the concentration-time curve monitoring." *Therapeutic Drug Monitoring* **17**(3): 221-229.

Nestorov, I. A., L. J. Aarons and M. Rowland (1997). "Physiologically based pharmacokinetic modeling of a homologous series of barbiturates in the rat: a sensitivity analysis." *Journal of Pharmacokinetics and Biopharmaceutics* **25**(4): 413-447.

Newell, D. R. (1989). "Pharmacokinetic determinants of the activity and toxicity of antitumour agents." *Cancer Surveys* **8**(3): 557-603.

- Newell, D. R. (1994). "Can pharmacokinetic and pharmacodynamic studies improve cancer chemotherapy?" *Annals of Oncology* **5**(Suppl 4): 9-14; discussion 15.
- Peck, C., W. Barr, L. Benet, J. Collins, R. Desjardins, D. Furst, J. Harter, G. Levy, T. Ludden, et al. (1992). "Opportunities for integration of pharmacokinetics, pharmacodynamics, and toxicokinetics in rational drug development." *Clinical Pharmacology & Therapeutics* **51**(4): 465-73.
- Peng, B., A. V. Boddy, M. Cole, A. D. Pearson, E. Chatelut, H. Rubie and D. R. Newell (1995). "Comparison of methods for the estimation of carboplatin pharmacokinetics in paediatric cancer patients." *European Journal of Cancer* **31A**(11): 1804-1810.
- Racine-Poon, A. and J. Wakefield (1998). "Statistical methods for population pharmacokinetic modelling." *Statistical Methods in Medical Research* **7**(1): 63-84.
- Ratain, M. J. and N. J. Vogelzang (1987). "Limited sampling model for vinblastine pharmacokinetics." *Cancer Treatment Reports* **71**(10): 935-939.
- Ratain, M. J., A. E. Staibus, R. L. Schilsky and L. Malspeis (1988). "Limited sampling models for amonafide (NSC 308847) pharmacokinetics." *Cancer Research* **48**(14): 4127-4130.
- Ratain, M. J., J. Robert and W. J. F. Van der Vijgh (1991). "Limited sampling models for doxorubicin pharmacokinetics." *Journal of Clinical Oncology* **9**(5): 871-876.
- Rescigno, A. (1999). "Compartmental analysis revisited." *Pharmacological Research* **39**(6): 471-8.

Roe, D. J. (1997). "Comparison of population pharmacokinetic modeling methods using simulated data: results from the Population Modeling Workgroup." *Statistics in Medicine* **16**(11): 1241-57.

Rosenthal, R. C. (1988). "The impact of pharmacokinetics on cancer chemotherapy." *Veterinary Clinics of North America: Small Animal Practice* **18**(6): 1133-9.

Sallas, W. M. (1995). "Development of limited sampling strategies for characteristics of a pharmacokinetic profile." *Journal of Pharmacokinetics & Biopharmaceutics* **23**(5): 515-529.

Samara, E. and R. Granneman (1997). "Role of population pharmacokinetics in drug development, a pharmaceutical industry perspective." *Clinical Pharmacokinetics* **32**(4): 294-312.

Scher, H. I., D. I. Jodrell, J. M. Iversen, T. Curley, W. Tong, M. J. Egorin and Forrest (1992). "Use of adaptive control with feedback to individualize suramin dosing." *Cancer Research* **52**(1): 64-70.

Sessa, C., M. Zucchetti, T. Cerny, O. Pagani, F. Cavalli, M. De Fusco, J. De, D. Gentili, C. McDaniel, et al. (1995). "Phase I clinical and pharmacokinetic study of oral etoposide phosphate." *Journal of Clinical Oncology* **13**(1): 200-209.

Sheiner, L. B. and S. L. Beal (1981). "Some suggestions for measuring predictive performance." *Journal of Pharmacokinetics & Biopharmaceutics* **9**(4): 503-12.

Sheiner, L. B. and S. L. Beal (1983). "Evaluation of methods for estimating population pharmacokinetic parameters. III. Monoexponential model: routine clinical pharmacokinetic data." *Journal of Pharmacokinetics & Biopharmaceutics* **11**(3): 303-19.

- Sheiner, L. B. (1984). "The population approach to pharmacokinetic data analysis: rationale and standard data analysis methods." *Drug Metabolism Reviews* **15**(1-2): 153-71.
- Silvey, S. D. (1980). *Optimal Design: An Introduction to the Theory for Parameter Estimation*. Monographs on Applied Probability and Statistics Chapman & Hall, London, New York.
- Spear, R. C. and F. Y. Bois (1994). "Parameter variability and the interpretation of physiologically based pharmacokinetic modeling results." *Environmental Health Perspectives* **102**(Suppl 11): 61-66.
- Sun, H., E. I. Ette and T. M. Ludden (1996). "On the recording of sample times and parameter estimation from repeated measures pharmacokinetic data." *Journal of Pharmacokinetics & Biopharmaceutics* **24**(6): 637-650.
- Sun, H., E. O. Fadiran, C. D. Jones, L. Lesko, S. M. Huang, K. Higgins, C. Hu, S. Machado, S. Maldonado, et al. (1999). "Population pharmacokinetics. A regulatory perspective." *Clinical Pharmacokinetics* **37**(1): 41-58.
- Thomson, A. H. and B. Whiting (1992). "Bayesian parameter estimation and population pharmacokinetics." *Clinical Pharmacokinetics* **22**(6): 447-467.
- Tod, M., F. Mentré, M. Y. and A. Mallet (1998). "Robust optimal design for the estimation of hyperparameters in population pharmacokinetics." *Journal of Pharmacokinetics & Biopharmaceutics* **26**(6): 689-716.
- Troconiz, I. F. (1996). "Population-based approach to the assessment of pharmacokinetic-pharmacodynamic data." *Methods & Findings in Experimental & Clinical Pharmacology* **18**(Suppl C): 51-52.

Vadiei, K., S. Troy, J. Korth-Bradley, S. T. Chiang and J. J. Zimmerman (1997). "Population pharmacokinetics of intravenous amiodarone and comparison with two-stage pharmacokinetic analysis." *Journal of Clinical Pharmacology* **37**(7): 610-7.

van der Vijgh, W. J. (1991). "Clinical pharmacokinetics of carboplatin." *Clinical Pharmacokinetics* **21**(4): 242-61.

van Warmerdam, L. J., S. Rodenhuis, O. van Tellingen, R. A. Maes and J. H. Beijnen (1994a). "Validation of a limited sampling model for carboplatin in a high-dose chemotherapy combination." *Cancer Chemotherapy & Pharmacology* **35**(2): 179-181.

van Warmerdam, L. J., H. ten Bokkel, R. A. Maes and J. H. Beijnen (1994b). "Limited-sampling models for anticancer agents." *Journal of Cancer Research & Clinical Oncology* **120**(7): 427-433.

van Warmerdam, L. J. C., B. J. F. van den Bemt, W. W. T. Huinink, R. A. A. Maes and J. H. Beijnen (1995). "Dose individualization in cancer-chemotherapy - pharmacokinetic and pharmacodynamic relationships." *Cancer Research Therapy & Control* **4**(4): 277-291.

van Warmerdam, L. J., G. J. Creemers, S. Rodenhuis, H. Rosing, M. de Boer-Dennert, J. H. Schellens, H. ten Bokkel, B. E. Davies, R. A. Maes, et al. (1996a). "Pharmacokinetics and pharmacodynamics of topotecan given on a daily-times-five schedule in phase II clinical trials using a limited-sampling procedure." *Cancer Chemotherapy & Pharmacology* **38**(3): 254-260.

van Warmerdam, L. J., S. Rodenhuis, E. van der Wall, R. A. Maes and J. H. Beijnen (1996b). "Pharmacokinetics and pharmacodynamics of carboplatin administered in a high-dose combination regimen with thiotepa, cyclophosphamide and peripheral stem cell support." *British Journal of Cancer* **73**(8): 979-984.

van Warmerdam, L. J. (1997). "Tailor-made chemotherapy for cancer patients." *Netherlands Journal of Medicine* **51**(1): 30-5.

Vozech, S., P. O. Maitre and D. R. Stanski (1990). "Evaluation of population (NONMEM) pharmacokinetic parameter estimates." *Journal of Pharmacokinetics & Biopharmaceutics* **18**(2): 161-73.

Vozech, S., J. L. Steimer, M. Rowland, P. Morselli, F. Mentre, L. P. Balant and Aarons (1996). "The use of population pharmacokinetics in drug development." *Clinical Pharmacokinetics* **30**(2): 81-93.

White, D. B., C. A. Walawander, Y. Tung and T. H. Grasela (1991). "An evaluation of point and interval estimates in population pharmacokinetics using NONMEM analysis." *Journal of Pharmacokinetics & Biopharmaceutics* **19**(1): 87-112.

Whiting, B., A. W. Kelman and J. Grevel (1986). "Population pharmacokinetics: theory and clinical application." *Clinical Pharmacokinetics* **11**(5): 387-407.

Williams, P. L. (1990). "Structural identifiability of pharmacokinetic models--compartments and experimental design." *Journal of Veterinary Pharmacology & Therapeutics* **13**(2): 121-31.

Yu, D. K., S. J. Hutcheson, G. Wei, V. O. Bhargava and S. J. Weir (1994). "A comparison of population and standard two-stage pharmacokinetic analyses of vigabatrin data." *Biopharmaceutics & Drug Disposition* **15**(6): 473-84.

Appendix 1

Mathematical Proofs

Introduction

Chapter 3 describes the use of sensitivity analysis to define sampling times for pharmacokinetic studies. This involved defining the times at which the model output (concentration) was most sensitive to changes in each model parameter (e.g., clearance and volume of distribution) by examining the partial derivatives of the output parameter with respect to each of the input parameters. The total variability in the output parameter was expressed in terms of factors relating to each of the input parameters. This appendix expands the equations used in chapter 3.

One Compartment IV Bolus

Assuming that any given dose distributed instantaneously into a one compartment PK system following an IV bolus (see figure A.1), the concentration was calculated from the following equation:

$$C_t = \frac{D}{V} \cdot e^{-\frac{Cl \cdot t}{V}} \quad \text{Equation A.1}$$

where C_t = Concentration, D = Dose, V = Volume of Distribution, Cl = Clearance and t = time after injection.

If it was assumed that there was no covariance between Cl and V , then the following equation was derived:

$$\omega_C^2 = \left(\frac{\partial C}{\partial Cl}\right)^2 \cdot \omega_{Cl}^2 + \left(\frac{\partial C}{\partial V}\right)^2 \cdot \omega_V^2 \quad \text{Equation A.2}$$

where ω_{Cl}^2 and ω_V^2 were variance in Cl and V , respectively and ω_C^2 was the variance in C .

Equation A.2 showed that the total variance in concentration was dependent on a factor from the variance in each of the parameters, clearance and volume of

distribution. Analysis of the partial derivatives of concentration with respect to Cl and V gave the following equation:

$$\frac{\partial C}{\partial Cl} = -\frac{t}{V} \cdot C \quad \text{Equation A.3}$$

and

$$\frac{\partial C}{\partial V} = \frac{1}{V^2} (Cl \cdot t - V) \cdot C \quad \text{Equation A.4}$$

and hence rewriting equation A.2 gave:

$$\omega_C^2 = \frac{t^2 C^2}{V^2} \cdot \omega_{Cl}^2 + \frac{(Cl \cdot t - V)^2}{V^4} \cdot C^2 \cdot \omega_V^2 \quad \text{Equation A.5}$$

Component of concentration variance due to clearance.

As described in chapter 3, setting ω_V^2 to zero allowed the component of variation in C due to Cl to be studied:

$$\omega_C^2 = \frac{t^2 C^2}{V^2} \cdot \omega_{Cl}^2 \quad \text{Equation A.6}$$

Therefore,

$$\omega_C^2 \propto t^2 C^2 \quad \text{Equation A.7}$$

as V and ω_{Cl}^2 were constant.

Times of maximum concentration variance arose when $\frac{\partial}{\partial t} \omega_C^2 = 0$ and therefore when:

$$t = \frac{V}{Cl} = \frac{1}{k_e} = 1.44 \cdot t_{1/2} \quad \text{Equation A.8}$$

where k_e was the elimination rate constant and $t_{1/2}$ was the half-life of the drug.

Component of concentration variance due to volume of distribution.

Similarly, when ω_{Cl}^2 was zero, the concentration variance due entirely to the volume component was examined.

$$\omega_C^2 = \frac{(Cl \cdot t - V)^2}{V^4} \cdot C^2 \cdot \omega_V^2 \quad \text{Equation A.9}$$

Therefore,

$$\omega_C^2 \propto (Cl \cdot t - V)^2 \cdot C^2 \propto (Cl \cdot t - V)^2 \cdot e^{-2\frac{Cl \cdot t}{V}} \quad \text{Equation A.10}$$

as V and ω_V^2 were constant.

Turning points again arise when $\frac{\partial}{\partial t} \omega_C^2 = 0$ i.e., when

$$t = \frac{1}{k_e} \quad \text{Equation A.11}$$

$$\text{and } t = \frac{2V}{Cl} = \frac{2}{k_e} \quad \text{Equation A.12}$$

In this case $t = \frac{1}{k_e}$ corresponds to a minimum, i.e., giving least information about V ,

whereas $t = \frac{2}{k_e}$ is a maximum associated with a peak in the concentration variance.

Also, $t = 0$ corresponds to a peak in ω_C^2 , although it is not a turning point and at this

$$\text{time, } \omega_C^2 = C^2 \cdot \frac{\omega_V^2}{V^2}.$$

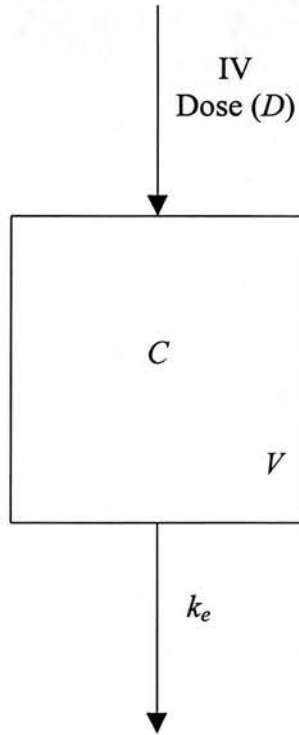


Figure A. 1 One-compartment pharmacokinetic model with IV bolus dose (D), volume of distribution (V) and first-order elimination (k_e).

Effects of random error in concentration on total concentration variance.

If the observed concentration, C , was associated with random error (intra-subject error), ε , then for the simplest case of an additive random error,

$$C = C^* + \varepsilon \quad \text{Equation A.13}$$

In the case of a proportional random error:

$$C = C^* + \varepsilon(C^*) \quad \text{Equation A.14}$$

The combination random error model gave:

$$C = C^* + \varepsilon_1(C^*) + \varepsilon_2 \quad \text{Equation A.15}$$

where C^* in all cases was the expected concentration before the addition of random error.

Therefore the variance in concentration was dependent on both the expected concentration variance and the variance of the error component(s), ω_ε^2 .

For the simple additive error model,

$$\omega_\varepsilon^2 = b^2 \quad \text{Equation A.16}$$

and

$$\omega_C^2 = (\omega_{C^*}^2) + b^2 \quad \text{Equation A.17}$$

If the error was proportional then

$$\omega_\varepsilon^2 = a^2 C^{*2} \quad \text{Equation A.18}$$

and

$$\omega_C^2 = (\omega_{C^*}^2) + a^2 C^{*2} \quad \text{Equation A.19}$$

Hence, if the error was a combination of both a proportional and an additive component then

$$\omega_g^2 = a^2 C^{*2} + b^2 \quad \text{Equation A.20}$$

and

$$\omega_C^2 = (\omega_{C^*}^2) + a^2 C^{*2} + b^2 \quad \text{Equation A.21}$$

Therefore, for a combination error model the total concentration variance was equal to:

$$\omega_C^2 = \frac{t^2 C^{*2}}{V^2} \cdot \omega_{Cl}^2 + \frac{(Cl \cdot t - V)^2}{V^4} \cdot C^{*2} \cdot \omega_V^2 + a^2 C^{*2} + b^2 \quad \text{Equation A.22}$$

Again, times of maximum concentration variance, when a combination error model was used, arose when $\frac{\partial}{\partial t} \omega_C^2 = 0$

i.e., at

$$t = \frac{(Cl_r + 3V_r) \pm \sqrt{(Cl_r - V_r)^2 - 4a^2(Cl_r + V_r)}}{2k_e(Cl_r + V_r)} \quad \text{Equation A.23}$$

where $Cl_r = \frac{\omega_{Cl}^2}{Cl^2}$ and $V_r = \frac{\omega_V^2}{V^2}$, i.e., (the coefficient of variation)² of each of Cl and V , respectively. This showed that when a combination random error model was used, the definition of sampling times using sensitivity analysis was more complex than the case of no error. This also represented the case for the proportional error model as $b = 0$ in equation A.22 giving the same derivation as A.23.

In the simplest case of the additive error model, $a = 0$ and for $k_e < 1$:

$$t_+ = \frac{1}{k_e} \quad \text{Equation A.24}$$

$$\text{and } t_- = \frac{2V_r}{k_e(Cl_r + V_r)} \quad \text{Equation A.25}$$

where t_+ and t_- represent the maximum and minimum concentration variance.

When $k_e > 1$, $t_+ = \frac{2V_r}{k_e(Cl_r + V_r)}$ and $t_- = \frac{1}{k_e}$, and when $Cl_r = V_r$, then $t_+ = t_- = \frac{1}{k_e}$.

In summary, these mathematical proofs showed that when there was no random error on concentration maximum concentration variance for a one-compartment PK model arose at the times $\frac{1}{k_e}$ and $\frac{2}{k_e}$, due to the clearance and volume components, respectively. If random error was added to concentration the times of maximum variance in concentration were more complex to define and included factors which were dependent on how much variance was present in the clearance and volume parameters.

Two Compartment IV Bolus

Similar to a one-compartment PK model, assuming that any given dose distributed instantaneously into a two-compartment system following an IV bolus, the concentration was calculated from the following equation:

$$C_t = Ae^{-\alpha t} + Be^{-\beta t} \quad \text{Equation A.26}$$

where C_t = Concentration, A and B = constants, α and β = the model macro rate constants, and t = time after injection.

The two-compartment model parameters for estimation in this thesis were Cl , V_1 , V_2 and Q . These were related to the constants A and B , and the macro and micro rate constants (k_{10} , k_{12} & k_{21}) as described below (see figure A.2):

$$k_{10} = \frac{Cl}{V_1} \quad \text{Equation A.27}$$

$$k_{12} = \frac{Q}{V_1} \quad \text{Equation A.28}$$

$$k_{21} = \frac{Q}{V_2} \quad \text{Equation A.29}$$

$$A = \frac{D(\alpha - k_{21})}{V_1(\alpha - \beta)} \quad \text{Equation A.30}$$

$$B = \frac{D(k_{21} - \beta)}{V_1(\alpha - \beta)} \quad \text{Equation A.31}$$

$$k_{21} = \frac{B \cdot \alpha + A \cdot \beta}{(A + B)} \quad \text{Equation A.32}$$

$$k_{10} = \frac{\alpha\beta}{k_{21}} \quad \text{Equation A.33}$$

$$k_{12} = \alpha + \beta - k_{21} - k_{10} \quad \text{Equation A.34}$$

$$\alpha = \frac{1}{2} \left[(k_{10} + k_{12} + k_{21}) + \sqrt{(k_{10} + k_{12} + k_{21})^2 - 4 \cdot k_{21} \cdot k_{10}} \right] \quad \text{Equation A.35}$$

$$\beta = \frac{1}{2} \left[(k_{10} + k_{12} + k_{21}) - \sqrt{(k_{10} + k_{12} + k_{21})^2 - 4 \cdot k_{21} \cdot k_{10}} \right] \quad \text{Equation A.36}$$

The sum of the micro rate constants, s_k , was

$$s_k = (k_{10} + k_{12} + k_{21}) = \frac{Cl}{V_1} + \frac{Q}{V_1} + \frac{Q}{V_2} \quad \text{Equation A.37}$$

The following expression, X , was a simplification for purposes of the mathematical proofs:

$$X = s_k^2 - 4 \cdot k_{21} \cdot k_{10} \quad \text{Equation A.38}$$

The relationships s_k and X lead to the following definitions of α , β and $\alpha - \beta$:

$$\begin{aligned} \alpha &= \frac{1}{2} \left[(k_{12} + k_{21} + k_{10}) + \sqrt{(k_{12} + k_{21} + k_{10})^2 - 4 \cdot k_{21} \cdot k_{10}} \right] \\ &= \frac{1}{2} \left[s_k + \sqrt{s_k^2 - 4 \cdot k_{21} \cdot k_{10}} \right] \\ &= \frac{1}{2} \left(s_k + X^{1/2} \right) \end{aligned} \quad \text{Equation A.39}$$

$$\begin{aligned} \beta &= \frac{1}{2} \left[(k_{12} + k_{21} + k_{10}) - \sqrt{(k_{12} + k_{21} + k_{10})^2 - 4 \cdot k_{21} \cdot k_{10}} \right] \\ &= \frac{1}{2} \left[s_k - \sqrt{s_k^2 - 4 \cdot k_{21} \cdot k_{10}} \right] \\ &= \frac{1}{2} \left(s_k - X^{1/2} \right) \end{aligned} \quad \text{Equation A.40}$$

$$\begin{aligned} \alpha - \beta &= \frac{1}{2} s_k + \frac{1}{2} \sqrt{s_k^2 - 4 \cdot k_{21} \cdot k_{10}} - \frac{1}{2} s_k + \frac{1}{2} \sqrt{s_k^2 - 4 \cdot k_{21} \cdot k_{10}} \\ &= \sqrt{s_k^2 - 4 \cdot k_{21} \cdot k_{10}} \\ &= X^{1/2} \end{aligned} \quad \text{Equation A.41}$$

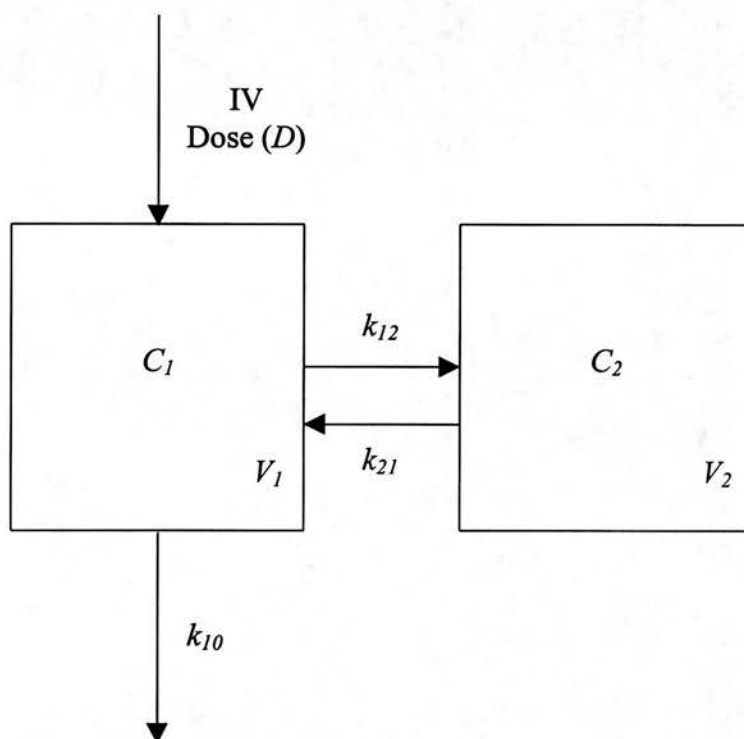


Figure A. 2 Two-compartment pharmacokinetic model with IV bolus dose (D), inter-compartmental transfer (k_{12} & k_{21}), volume of distribution of the central (V_1) and peripheral (V_2) compartments and first-order elimination (k_{10}).

Assuming no covariance between any of the parameters, then the variance in concentration was defined as:

$$\omega_C^2 = \left(\frac{\partial C}{\partial Cl}\right)^2 \cdot \omega_{Cl}^2 + \left(\frac{\partial C}{\partial V_1}\right)^2 \cdot \omega_{V_1}^2 + \left(\frac{\partial C}{\partial V_2}\right)^2 \cdot \omega_{V_2}^2 + \left(\frac{\partial C}{\partial Q}\right)^2 \cdot \omega_Q^2$$

Equation A.42

where ω_{Cl}^2 , $\omega_{V_1}^2$, $\omega_{V_2}^2$ and ω_Q^2 were variance in Cl , V_1 , V_2 and Q , respectively and ω_C^2 was the variance in C . Equation A.42 showed that the variance in concentration was dependent on a factor from the variance in each of the parameters. In order to define times of maximum concentration variance that arose with respect to each parameter it was necessary to differentiate equation A.26 with respect to each parameter, Cl , V_1 , V_2 and Q . (Equations A.43-A.46).

$$\begin{aligned} \frac{\partial C}{\partial Cl} &= \frac{\partial A}{\partial Cl} \cdot e^{-\alpha t} + \frac{\partial(e^{-\alpha t})}{\partial Cl} \cdot A + \frac{\partial B}{\partial Cl} \cdot e^{-\beta t} + \frac{\partial(e^{-\beta t})}{\partial Cl} \cdot B \\ &= \frac{\partial A}{\partial Cl} \cdot e^{-\alpha t} - A \cdot t \cdot e^{-\alpha t} \frac{\partial \alpha}{\partial Cl} + \frac{\partial B}{\partial Cl} \cdot e^{-\beta t} - B \cdot t \cdot e^{-\beta t} \frac{\partial \beta}{\partial Cl} \end{aligned} \quad \text{Equation A.43}$$

$$\begin{aligned} \frac{\partial C}{\partial V_1} &= \frac{\partial A}{\partial V_1} \cdot e^{-\alpha t} + \frac{\partial(e^{-\alpha t})}{\partial V_1} \cdot A + \frac{\partial B}{\partial V_1} \cdot e^{-\beta t} + \frac{\partial(e^{-\beta t})}{\partial V_1} \cdot B \\ &= \frac{\partial A}{\partial V_1} \cdot e^{-\alpha t} - A \cdot t \cdot e^{-\alpha t} \frac{\partial \alpha}{\partial V_1} + \frac{\partial B}{\partial V_1} \cdot e^{-\beta t} - B \cdot t \cdot e^{-\beta t} \frac{\partial \beta}{\partial V_1} \end{aligned} \quad \text{Equation A.44}$$

$$\begin{aligned} \frac{\partial C}{\partial V_2} &= \frac{\partial A}{\partial V_2} \cdot e^{-\alpha t} + \frac{\partial(e^{-\alpha t})}{\partial V_2} \cdot A + \frac{\partial B}{\partial V_2} \cdot e^{-\beta t} + \frac{\partial(e^{-\beta t})}{\partial V_2} \cdot B \\ &= \frac{\partial A}{\partial V_2} \cdot e^{-\alpha t} - A \cdot t \cdot e^{-\alpha t} \frac{\partial \alpha}{\partial V_2} + \frac{\partial B}{\partial V_2} \cdot e^{-\beta t} - B \cdot t \cdot e^{-\beta t} \frac{\partial \beta}{\partial V_2} \end{aligned} \quad \text{Equation A.45}$$

$$\frac{\partial C}{\partial Q} = \frac{\partial A}{\partial Q} \cdot e^{-\alpha t} + \frac{\partial(e^{-\alpha t})}{\partial Q} \cdot A + \frac{\partial B}{\partial Q} \cdot e^{-\beta t} + \frac{\partial(e^{-\beta t})}{\partial Q} \cdot B$$

$$= \frac{\partial A}{\partial Q} \cdot e^{-\alpha t} - A \cdot t \cdot e^{-\alpha t} \frac{\partial \alpha}{\partial Q} + \frac{\partial B}{\partial Q} \cdot e^{-\beta t} - B \cdot t \cdot e^{-\beta t} \frac{\partial \beta}{\partial Q} \quad \text{Equation A.46}$$

Equations A.43 – A.46 could not be solved without the derivative of each of A , α , B and β with respect to each of the parameters Cl , V_1 , V_2 and Q . Since α and β were defined with the use of s_k and X above, these also had to be differentiated with respect to each of the parameters Cl , V_1 , V_2 and Q .

The derivatives of s_k with respect to each parameter were as follows:

$$\frac{\partial s_k}{\partial Cl} = \frac{\partial \left[\frac{Cl}{V_1} + \frac{Q}{V_1} + \frac{Q}{V_2} \right]}{\partial Cl} = \frac{1}{V_1} \quad \text{Equation A.47}$$

$$\frac{\partial s_k}{\partial V_1} = \frac{\partial \left[\frac{Cl}{V_1} + \frac{Q}{V_1} + \frac{Q}{V_2} \right]}{\partial V_1} = -\frac{Cl}{V_1^2} - \frac{Q}{V_1^2} \quad \text{Equation A.48}$$

$$\frac{\partial s_k}{\partial V_2} = \frac{\partial \left[\frac{Cl}{V_1} + \frac{Q}{V_1} + \frac{Q}{V_2} \right]}{\partial V_2} = -\frac{Q}{V_2^2} \quad \text{Equation A.49}$$

$$\frac{\partial s_k}{\partial Q} = \frac{\partial \left[\frac{Cl}{V_1} + \frac{Q}{V_1} + \frac{Q}{V_2} \right]}{\partial Q} = \frac{1}{V_1} + \frac{1}{V_2} \quad \text{Equation A.50}$$

The derivatives of X with respect to each parameter are as follows:

$$\frac{\partial X}{\partial Cl} = \frac{\partial \left[s_k^2 - 4 \cdot \frac{Cl}{V_1} \cdot \frac{Q}{V_2} \right]}{\partial Cl} = 2 \cdot s_k \cdot \frac{1}{V_1} - \frac{4Q}{V_1 \cdot V_2} \quad \text{Equation A.51}$$

$$\frac{\partial X}{\partial V_1} = \frac{\partial \left[s_k^2 - 4 \cdot \frac{Cl}{V_1} \cdot \frac{Q}{V_2} \right]}{\partial V_1} = 2 \cdot s_k \cdot \left(-\frac{Cl}{V_1^2} - \frac{Q}{V_1^2} \right) + 4 \cdot \frac{Q}{V_2} \cdot \frac{Cl}{V_1^2} \quad \text{Equation A.52}$$

$$\frac{\partial X}{\partial V_2} = \frac{\partial \left[s_k^2 - 4 \cdot \frac{Cl}{V_1} \cdot \frac{Q}{V_2} \right]}{\partial V_2} = -2 \cdot s_k \cdot \frac{Q}{V_2^2} + 4 \cdot \frac{Cl}{V_1} \cdot \frac{Q}{V_2^2}$$

Equation A.53

$$\frac{\partial X}{\partial Q} = \frac{\partial \left[s_k^2 - 4 \cdot \frac{Cl}{V_1} \cdot \frac{Q}{V_2} \right]}{\partial Q} = 2 \cdot s_k \cdot \left(\frac{1}{V_1} + \frac{1}{V_2} \right) - 4 \cdot \frac{Cl}{V_1 \cdot V_2}$$

Equation A.54

Redefining A in terms of s_k and X gave:

$$A = \frac{D}{V_1} \cdot \left(\frac{\alpha - k_{2l}}{\alpha - \beta} \right) = \frac{D}{2 \cdot V_1} \cdot \left(s_k - \frac{2Q}{V_2} + X^{1/2} \right) \cdot X^{-1/2}$$

Equation A.55

Therefore, the derivatives of A with respect to each parameter are as follows:

$$\frac{\partial A}{\partial Cl} = \frac{D}{2 \cdot V_1} \cdot X^{-1/2} \cdot \left(\frac{\partial s_k}{\partial Cl} + \frac{1}{2} \cdot X^{-1/2} \cdot \frac{\partial X}{\partial Cl} \right) - \frac{A}{2} \cdot X^{-1} \cdot \frac{\partial X}{\partial Cl}$$

Equation A.56

$$\frac{\partial A}{\partial V_1} = \frac{D}{2 \cdot V_1} \cdot X^{-1/2} \cdot \left(\frac{\partial s_k}{\partial V_1} + \frac{1}{2} \cdot X^{-1/2} \cdot \frac{\partial X}{\partial V_1} \right) - \frac{A}{2} \cdot X^{-1} \cdot \frac{\partial X}{\partial V_1} - \frac{A}{V_1}$$

Equation A.57

$$\frac{\partial A}{\partial V_2} = \frac{D}{2 \cdot V_1} \cdot X^{-1/2} \cdot \left(\frac{\partial s_k}{\partial V_2} + \frac{2Q}{V_2^2} + \frac{1}{2} \cdot X^{-1/2} \cdot \frac{\partial X}{\partial V_2} \right) - \frac{A}{2} \cdot X^{-1} \cdot \frac{\partial X}{\partial V_2}$$

Equation A.58

$$\frac{\partial A}{\partial Q} = \frac{D}{2 \cdot V_1} \cdot X^{-1/2} \cdot \left(\frac{\partial s_k}{\partial Q} - \frac{2}{V_2} + \frac{1}{2} \cdot X^{-1/2} \cdot \frac{\partial X}{\partial Q} \right) - \frac{A}{2} \cdot X^{-1} \cdot \frac{\partial X}{\partial Q}$$

Equation A.59

The derivatives of α with respect to each parameter were as follows:

$$\frac{\partial \alpha}{\partial Cl} = \frac{1}{2} \left(\frac{\partial s_k}{\partial Cl} + \frac{1}{2} X^{-1/2} \cdot \frac{\partial X}{\partial Cl} \right)$$

Equation A.60

$$\frac{\partial \alpha}{\partial V_1} = \frac{1}{2} \left(\frac{\partial s_k}{\partial V_1} + \frac{1}{2} X^{-1/2} \cdot \frac{\partial X}{\partial V_1} \right)$$

Equation A.61

$$\frac{\partial \alpha}{\partial V_2} = 1/2 \left(\frac{\partial s_k}{\partial V_2} + 1/2 X^{-1/2} \frac{\partial X}{\partial V_2} \right) \quad \text{Equation A.62}$$

$$\frac{\partial \alpha}{\partial Q} = 1/2 \left(\frac{\partial s_k}{\partial Q} + 1/2 X^{-1/2} \frac{\partial X}{\partial Q} \right) \quad \text{Equation A.63}$$

The differentiations of β with respect to each parameter were as follows:

$$\frac{\partial \beta}{\partial Cl} = 1/2 \left(\frac{\partial s_k}{\partial Cl} - 1/2 X^{-1/2} \frac{\partial X}{\partial Cl} \right) \quad \text{Equation A.64}$$

$$\frac{\partial \beta}{\partial V_1} = 1/2 \left(\frac{\partial s_k}{\partial V_1} - 1/2 X^{-1/2} \frac{\partial X}{\partial V_1} \right) \quad \text{Equation A.65}$$

$$\frac{\partial \beta}{\partial V_2} = 1/2 \left(\frac{\partial s_k}{\partial V_2} - 1/2 X^{-1/2} \frac{\partial X}{\partial V_2} \right) \quad \text{Equation A.66}$$

$$\frac{\partial \beta}{\partial Q} = 1/2 \left(\frac{\partial s_k}{\partial Q} - 1/2 X^{-1/2} \frac{\partial X}{\partial Q} \right) \quad \text{Equation A.67}$$

Redefining B in terms of s_k and X gave:

$$B = \frac{D}{V_1} \cdot \left(\frac{k_{2l} - \beta}{\alpha - \beta} \right) = \frac{D}{V_1 \cdot 2} \cdot X^{-1/2} \cdot \left(\frac{2Q}{V_2} - s_k + X^{1/2} \right) \quad \text{Equation A.68}$$

Therefore, the derivatives of B with respect to each parameter were as follows:

$$\frac{\partial B}{\partial Cl} = \frac{D}{2 \cdot V_1} \cdot X^{-1/2} \cdot \left(-\frac{\partial s_k}{\partial Cl} + 1/2 \cdot X^{-1/2} \frac{\partial X}{\partial Cl} \right) - \frac{B}{2} \cdot X^{-1} \cdot \frac{\partial X}{\partial Cl} \quad \text{Equation A.69}$$

$$\frac{\partial B}{\partial V_1} = \frac{D}{2 \cdot V_1} \cdot X^{-1/2} \cdot \left(-\frac{\partial s_k}{\partial V_1} + 1/2 \cdot X^{-1/2} \frac{\partial X}{\partial V_1} \right) - \frac{B}{2} \cdot X^{-1} \cdot \frac{\partial X}{\partial V_1} - \frac{B}{V_1} \quad \text{Equation A.70}$$

$$\frac{\partial B}{\partial V_2} = \frac{D}{2 \cdot V_1} \cdot X^{-1/2} \cdot \left(-\frac{2Q}{V_2^2} - \frac{\partial s_k}{\partial V_2} + 1/2 \cdot X^{-1/2} \frac{\partial X}{\partial V_2} \right) - \frac{B}{2} \cdot X^{-1} \cdot \frac{\partial X}{\partial V_2} \quad \text{Equation A.71}$$

$$\frac{\partial B}{\partial Q} = \frac{D}{2 \cdot V_1} \cdot X^{-1/2} \cdot \left(\frac{2}{V_2} - \frac{\partial s_k}{\partial Q} + \frac{1}{2} \cdot X^{-1/2} \frac{\partial X}{\partial Q} \right) - \frac{B}{2} \cdot X^{-1} \cdot \frac{\partial X}{\partial Q} \quad \text{Equation A.72}$$

In summary the mathematical proofs for a two-compartment IV bolus model showed that it was not possible to define times of maximum concentration variance by equation alone as there were too many contributing factors from each parameter.

The equations were put into a computer program so that each parameter value could be input and plotted over time, in order to define sampling times for a two-compartment IV bolus model (see chapter 3). This allowed the variance for all parameters except one to be set to zero and peaks or troughs in concentration variance attributed to a single parameter. The program also allowed the plotting of the total concentration variance profile where it became clear the magnitude of each parameter's peak in relation to the others and therefore, which peaks were more relevant in relation to sampling times.

Appendix 2

Simulation Programs

Input File for One-Compartment IV Bolus Simulations

The example shown is the input file for the simulation of design 1.

```
dose clpop sdcl vpop sdv
100 10.0 1.0 10.0 1.0
sdconcadd sdconcprop
0.0 0.1
nsubjects points niterations
500 2 100
nran xlimit
250 3.0
output file (no extension)
Design1
t sdt
0.1 0
1.0 0
```

Simulation Program for a One-Compartment IV Bolus PK Model

Program CGEN was used for designs 1-8 and designs 20-28.

```
REM      CGEN.BAS
REM
REM      1 comp model
REM      Generates Concentration data for
REM      NSUBS, NPOINTS and creates NSET of NONMEM input files.

OPTION BASE 1
DEFINT I-N

DIM t(100), sdt(100)
izero = 0
ione = 1
zero = 0!

INPUT "Input file name..... "; filein$
INPUT "Random no. seed (-32676- 32676) "; xr
RANDOMIZE (xr)

GOSUB design:
fout$ = RTRIM$(fout$)

FOR iset = 1 TO nsets
app$ = STR$(iset)
app$ = RTRIM$(app$)
app$ = LTRIM$(app$)
fileout$ = fout$ + app$ + ".var"
parout$ = fout$ + app$ + ".par"
parout2$ = fout$ + app$ + "B" + ".par"

OPEN fileout$ FOR OUTPUT AS #1
CLOSE #1

OPEN parout$ FOR OUTPUT AS #2
CLOSE #2

OPEN parout2$ FOR OUTPUT AS #3
CLOSE #3

OPEN fileout$ FOR APPEND AS #1
OPEN parout2$ FOR APPEND AS #3
PRINT #3, "  i      time      Cexp      Err_Add Err_prp Prop_Er  Conc"

      FOR i = 1 TO nsubjects
          GOSUB parameters:
          PRINT #1, USING "##### # # ###.### ###.### ###.###
#####.### ###.###"; i; ione; ione; dose; zero; zero; zero; zero
          c0 = dose / vol
          GOSUB conc
      NEXT i

CLOSE #1
CLOSE #3

NEXT iset
```

```

END

parameters:
Cl:
  GOSUB rannum:
  Cl = clpop + rn * sdcl
  IF Cl <= .2 THEN GOTO Cl
vol:
  GOSUB rannum
  vol = volpop + rn * sdvol
  IF vol <= .2 THEN GOTO vol
  xke = Cl / vol
  IF xke > 20 THEN GOTO Cl
  OPEN parout$ FOR APPEND AS #2
    PRINT #2, USING "#####   ###.###   ###.###"; i; Cl; vol
  CLOSE #2
RETURN

conc:
  FOR j = 1 TO npoints
newtime:
  tt = t(j)
  GOSUB rannum:
  tt = tt + rn * sdt(j)
  IF tt <= 0 THEN GOTO newtime
  ttest = t(1)
  IF (j > 1 and tt <= ttest) THEN GOTO newtime

conc2:
  concl = c0 * EXP(-xke * tt)
  GOSUB rannum:
  erradd = rn * sdconcadd
  GOSUB rannum:
  errprop = sdconcpro * rn * concl
  conc = concl + erradd + errprop
  IF conc <= 0! THEN GOTO conc2
  PRINT #1, USING "##### # # ###.### ###.### ###.###
###.### ###.###"; i; izero; izero; zero; tt; conc; Cl; vol
  PRINT #3, USING "##### ###.### ###.### ###.### ###.###
###.### ###.###"; i; tt; concl; erradd; errprop; errprop / concl;
conc
  PRINT "set="; iset; " sub="; i; " cl="; Cl; " V="; vol; " t="; tt; "
c("; j; ")="; conc
  NEXT
RETURN

rannum:
nextrand:
  sum = 0
  FOR kk = 1 TO nran
    sum = sum + RND
  NEXT kk
  rn = (sum - xnran1) / SQR(nran / 12)
  IF ABS(rn) > xlimit THEN GOTO nextrand
RETURN

design:
  OPEN filein$ FOR INPUT AS #1
    LINE INPUT #1, xin$
    INPUT #1, dose, clpop, sdcl, volpop, sdvol

```

```
LINE INPUT #1, xin$
INPUT #1, sdconcadd, sdconcpro
LINE INPUT #1, xin$
INPUT #1, nsubjects, npoints, nsets
LINE INPUT #1, xin$
INPUT #1, nran, xlimit
LINE INPUT #1, xin$
INPUT #1, fout$
LINE INPUT #1, xin$
FOR i = 1 TO npoints
    INPUT #1, t(i), sdt(i)
NEXT i
CLOSE #1
xnrans1 = nran / 2
RETURN
```

Simulation Program for a One-Compartment IV Bolus PK Model with Fixed Sampling Times (Selects Optimal Sampling Times for each Individual)

Program CGEN2 was used for design 9.

```
REM      CGEN2.BAS
REM
REM      1 comp model
REM      Generates Concentration data for
REM      NSUBS, NPOINTS and creates NSET of NONMEM input files.
REM      uses one early time point and the "best" second time for
REM      EACH individual
```

```
OPTION BASE 1
DEFINT I-N
```

```
DIM t(100), sdt(100)
izero = 0
ione = 1
zero = 0!
```

```
INPUT "Input file name..... "; filein$
INPUT "Random no. seed (-32676- 32676) "; xr
RANDOMIZE (xr)
```

```
GOSUB design:
fout$ = RTRIM$(fout$)
```

```
FOR iset = 1 TO nsets
app$ = STR$(iset)
app$ = RTRIM$(app$)
app$ = LTRIM$(app$)
fileout$ = fout$ + app$ + ".var"
parout$ = fout$ + app$ + ".par"
parout2$ = fout$ + app$ + "B" + ".par"
```

```
OPEN fileout$ FOR OUTPUT AS #1
CLOSE #1
```

```
OPEN parout$ FOR OUTPUT AS #2
CLOSE #2
```

```
OPEN parout2$ FOR OUTPUT AS #3
CLOSE #3
```

```
OPEN fileout$ FOR APPEND AS #1
OPEN parout2$ FOR APPEND AS #3
PRINT #3, " i      time      Cexp      Err_Add Err_prp Prop_Er  Conc"
```

```
      FOR i = 1 TO nsubjects
          GOSUB parameters:
          PRINT #1, USING "##### # # ###.### ###.### ###.###
###.### ###.###"; i; ione; ione; dose; zero; zero; zero; zero
          c0 = dose / vol
          xke = cl / vol
          GOSUB conc
```

```

        NEXT i

CLOSE #1
CLOSE #3

NEXT iset
END

parameters:
cl:
    GOSUB rannum:
    cl = clpop + rn * sdcl
    IF cl <= 0! THEN GOTO cl
vol:
    GOSUB rannum
    vol = volpop + rn * sdvol
    IF vol <= 0! THEN GOTO vol
    OPEN parout$ FOR APPEND AS #2
        PRINT #2, USING "##### ###.### ###.###"; i; cl; vol
    CLOSE #2
RETURN

conc:
    FOR j = 1 TO npoints
newtime:
    IF j = 1 THEN
        tt = t(j)
        GOSUB rannum:
        tt = tt + rn * sdt(j)
        IF tt <= 0 THEN GOTO newtime
    END IF
    IF j = 2 THEN
        IF xke <= 1 THEN
            tt = 1 / xke
        ELSE
            tt = 2 * xke / (1 + xke * xke)
        END IF
    END IF

conc2:
    conc1 = c0 * EXP(-xke * tt)
    GOSUB rannum:
    erradd = rn * sdconcadd
    GOSUB rannum:
    errprop = sdconcpro * rn * conc1
    conc = conc1 + erradd + errprop
    IF conc <= 0! THEN GOTO conc2
    PRINT #1, USING "##### # # ###.### ###.### ###.###
###.### ###.###"; i; izero; izero; zero; tt; conc; cl; vol
    PRINT #3, USING "##### ###.### ###.### ###.### ###.###
###.### ###.###"; i; tt; conc1; erradd; errprop; errprop / conc1;
conc
        NEXT
RETURN

rannum:
nextrand:
    sum = 0
    FOR kk = 1 TO nran
        sum = sum + RND

```



```

NEXT kk
rn = (sum - xnrn1) / SQR(nran / 12)
IF ABS(rn) > xlimit THEN GOTO nextrand
RETURN

design:
OPEN filein$ FOR INPUT AS #1
  LINE INPUT #1, xin$
  INPUT #1, dose, clpop, sdcl, volpop, sdvol
  LINE INPUT #1, xin$
  INPUT #1, sdconcadd, sdconcpro
  LINE INPUT #1, xin$
  INPUT #1, nsubjects, npoints, nsets
  LINE INPUT #1, xin$
  INPUT #1, nran, xlimit
  LINE INPUT #1, xin$
  INPUT #1, fout$
  LINE INPUT #1, xin$
  FOR i = 1 TO npoints
    INPUT #1, t(i), sdt(i)
  NEXT i
CLOSE #1
xnrn1 = nran / 2
RETURN

```

Simulation Programs for a One-Compartment IV Bolus PK Model with Three Sampling Times

Program CGEN3A was used for designs 10a and 10b, where the third sample was added between the two optimal sampling times.

```
REM      CGEN3A.BAS
REM
REM      1 comp model
REM      Generates Concentration data for
REM      NSUBS, NPOINTS and creates NSET of NONMEM input files.

OPTION BASE 1
DEFINT I-N

DIM tmean(100), t(100), sdt(100)
izero = 0
ione = 1
zero = 0!

INPUT "Input file name..... "; filein$
INPUT "Random no. seed (-32676- 32676) "; xr
RANDOMIZE (xr)

GOSUB design:
fout$ = RTRIM$(fout$)

FOR iset = 1 TO nsets
app$ = STR$(iset)
app$ = RTRIM$(app$)
app$ = LTRIM$(app$)
fileout$ = fout$ + app$ + ".var"
parout$ = fout$ + app$ + ".par"
parout2$ = fout$ + app$ + "B" + ".par"

OPEN fileout$ FOR OUTPUT AS #1
CLOSE #1

OPEN parout$ FOR OUTPUT AS #2
CLOSE #2

OPEN parout2$ FOR OUTPUT AS #3
CLOSE #3

OPEN fileout$ FOR APPEND AS #1
OPEN parout2$ FOR APPEND AS #3

PRINT #3, "  i      time      Cexp      Err_Add Err_prp Prop_Er  Conc"

      FOR i = 1 TO nsubjects
          GOSUB parameters:
          PRINT #1, USING "##### # # ###.### ###.### ###.###
#####.### ###.###"; i; ione; ione; dose; zero; zero; zero; zero
          c0 = dose / vol
          GOSUB times
          GOSUB conc
      NEXT i
```

```

CLOSE #1
CLOSE #3

NEXT iset
END

parameters:
Cl:
    GOSUB rannum:
    Cl = clpop + rn * sdcl
    IF Cl <= .2 THEN GOTO Cl
vol:
    GOSUB rannum
    vol = volpop + rn * sdvol
    IF vol <= .2 THEN GOTO vol
    xke = Cl / vol
    IF xke > 20 THEN GOTO Cl
    OPEN parout$ FOR APPEND AS #2
        PRINT #2, USING "#####   ###.###   ###.###"; i; Cl; vol
    CLOSE #2
RETURN

times:
newtime1:
    tt = tmean(1)
    GOSUB rannum:
    tt = tt + rn * sdt(1)
    IF tt <= 0 THEN GOTO newtime1
    t(1) = tt
newtime3:
    tt = tmean(3)
    GOSUB rannum:
    tt = tt + rn * sdt(3)
    IF tt <= t(1) + 1 / 6 THEN GOTO newtime3
    t(3) = tt
newtime2:
    tt = tmean(2)
    GOSUB rannum:
    tt = tt + rn * sdt(2)
    IF tt <= t(1) + 1 / 12 THEN GOTO newtime2
    IF tt >= t(3) - 1 / 12 THEN GOTO newtime2
    t(2) = tt

RETURN

conc:
    FOR j = 1 TO npoints
        tt = t(j)
conc2:
    conc1 = c0 * EXP(-xke * tt)
    GOSUB rannum:
    erradd = rn * sdconcadd
    GOSUB rannum:
    errprop = sdconcpro * rn * conc1
    conc = conc1 + erradd + errprop
    IF conc <= 0! THEN GOTO conc2
    PRINT #1, USING "##### # # ###.###   ###.###   ###.###
#####   ###.###"; i; izero; izero; zero; tt; conc; Cl; vol

```

```

        PRINT #3, USING "##### ###.### ###.### ###.### ###.###
###.### ###.###"; i; tt; concl; erradd; errprop; errprop / concl;
conc
PRINT "set="; iset; " sub="; i; " cl="; Cl; " V="; vol; " t="; tt; "
c("; j; ")="; conc
        NEXT
RETURN

rannum:
nextrand:
    sum = 0
    FOR kk = 1 TO nran
        sum = sum + RND
    NEXT kk
    rn = (sum - xnran1) / SQR(nran / 12)
    IF ABS(rn) > xlimit THEN GOTO nextrand
RETURN

design:
    OPEN filein$ FOR INPUT AS #1
        LINE INPUT #1, xin$
        INPUT #1, dose, clpop, sdcl, volpop, sdvol
        LINE INPUT #1, xin$
        INPUT #1, sdconcadd, sdconcpro
        LINE INPUT #1, xin$
        INPUT #1, nsubjects, npoints, nsets
        LINE INPUT #1, xin$
        INPUT #1, nran, xlimit
        LINE INPUT #1, xin$
        INPUT #1, fout$
        LINE INPUT #1, xin$
        FOR i = 1 TO npoints
            INPUT #1, tmean(i), sdt(i)
        NEXT i
    CLOSE #1
    xnran1 = nran / 2
RETURN

```

Program CGEN3B was used for designs 11 and 12, where the third sample was added after the two optimal sampling times.

```

REM      CGEN3B.BAS
REM
REM      1 comp model
REM      Generates Concentration data for
REM      NSUBS, NPOINTS and creates NSET of NONMEM input files.

OPTION BASE 1
DEFINT I-N

DIM tmean(100), t(100), sdt(100)
izero = 0
ione = 1
zero = 0!

INPUT "Input file name..... "; filein$
INPUT "Random no. seed (-32676- 32676) "; xr

```

```

RANDOMIZE (xr)

GOSUB design:
fout$ = RTRIM$(fout$)

FOR iset = 1 TO nsets
app$ = STR$(iset)
app$ = RTRIM$(app$)
app$ = LTRIM$(app$)
fileout$ = fout$ + app$ + ".var"
parout$ = fout$ + app$ + ".par"
parout2$ = fout$ + app$ + "B" + ".par"

OPEN fileout$ FOR OUTPUT AS #1
CLOSE #1

OPEN parout$ FOR OUTPUT AS #2
CLOSE #2

OPEN parout2$ FOR OUTPUT AS #3
CLOSE #3

OPEN fileout$ FOR APPEND AS #1
OPEN parout2$ FOR APPEND AS #3
PRINT #3, " i time Cexp Err_Add Err_prp Prop_Er Conc"
FOR i = 1 TO nsubjects
GOSUB parameters:
PRINT #1, USING "##### # # ###.### ###.### ###.###
###.### ###.###"; i; ione; ione; dose; zero; zero; zero; zero
c0 = dose / vol
GOSUB times
GOSUB conc
NEXT i
CLOSE #1
CLOSE #3
NEXT iset
END

parameters:
Cl:
GOSUB rannum:
Cl = clpop + rn * sdcl
IF Cl <= .2 THEN GOTO Cl

vol:
GOSUB rannum
vol = volpop + rn * sdvol
IF vol <= .2 THEN GOTO vol
xke = Cl / vol
IF xke > 20 THEN GOTO Cl
OPEN parout$ FOR APPEND AS #2
PRINT #2, USING "##### ###.### ###.###"; i; Cl; vol
CLOSE #2

RETURN

times:
newtime1:
tt = tmean(1)
GOSUB rannum:
tt = tt + rn * sdt(1)

```

```

        IF tt <= 0 THEN GOTO newtime1
        t(1) = tt
newtime2:
        tt = tmean(2)
        GOSUB rannum:
        tt = tt + rn * sdt(2)
        IF tt <= t(1) + 1 / 6 THEN GOTO newtime2
        t(2) = tt
newtime3:
        tt = tmean(3)
        GOSUB rannum:
        tt = tt + rn * sdt(3)
        IF tt <= t(2) + 1 / 12 THEN GOTO newtime3
        t(3) = tt
RETURN

conc:
        FOR j = 1 TO npoints
                tt = t(j)
conc2:
                conc1 = c0 * EXP(-xke * tt)
                GOSUB rannum:
                erradd = rn * sdconcadd
                GOSUB rannum:
                errprop = sdconcpro * rn * conc1
                conc = conc1 + erradd + errprop
                IF conc <= 0! THEN GOTO conc2
                PRINT #1, USING "##### # # ###.### ###.### ###.###
###.### ###.###"; i; izeo; izeo; zero; tt; conc; Cl; vol
                PRINT #3, USING "##### ###.### ###.### ###.### ###.###
###.### ###.###"; i; tt; conc1; erradd; errprop; errprop / conc1;
conc
                PRINT "set="; iset; " sub="; i; " cl="; Cl; " V="; vol; " t="; tt; "
c("; j; ")="; conc
        NEXT
RETURN

rannum:
nextrand:
        sum = 0
        FOR kk = 1 TO nran
                sum = sum + RND
        NEXT kk
        rn = (sum - xnran1) / SQR(nran / 12)
        IF ABS(rn) > xlimit THEN GOTO nextrand
RETURN

design:
        OPEN filein$ FOR INPUT AS #1
                LINE INPUT #1, xin$
                INPUT #1, dose, clpop, sdcl, volpop, sdvol
                LINE INPUT #1, xin$
                INPUT #1, sdconcadd, sdconcpro
                LINE INPUT #1, xin$
                INPUT #1, nsubjects, npoints, nsets
                LINE INPUT #1, xin$
                INPUT #1, nran, xlimit
                LINE INPUT #1, xin$
                INPUT #1, fout$

```

```
LINE INPUT #1, xin$
FOR i = 1 TO npoints
    INPUT #1, tmean(i), sdt(i)
NEXT i
CLOSE #1
xnrans1 = nran / 2
RETURN
```

Input File for Two-Compartment IV Bolus Simulations

The example shown is the input file for the simulation of design 15.

```
dose clpop sdcl v1pop sdv1 v2pop sdv2 qpop sdq
100 10 1.0 10 1.0 20 2.0 15 1.5
sdconcadd sdconcprop
0.35 0.05
nsubjects points niterations
500 4 10
nran xlimit
250 3.0
output file (no extension)
Design15
t sdt
0.1 0
0.4 0.28
1.0 0.84
2.5 1.4
```


Simulation Program for a Two-Compartment IV Bolus PK Model

Program CGENWIN1 was used for designs 13-19.

```
REM      CGENWIN1.BAS
REM
REM      2 comp model
REM      Generates Concentration data for
REM      NSUBS, NPOINTS and creates NSET of NONMEM input files.
REM      puts sampling window on times

OPTION BASE 1
DEFINT I-J, L-N

DIM tmean(100), t(100), sdt(100)
izero = 0
ione = 1
zero = 0!

INPUT "Input file name..... "; filein$
INPUT "Random no. seed (-32676- 32676) "; xr
RANDOMIZE (xr)

GOSUB design:
fout$ = RTRIM$(fout$)

FOR iset = 1 TO nsets
  app$ = STR$(iset)
  app$ = RTRIM$(app$)
  app$ = LTRIM$(app$)
  fileout$ = fout$ + app$ + ".var"
  parout$ = fout$ + app$ + ".par"
  parout2$ = fout$ + app$ + "B" + ".par"

  OPEN fileout$ FOR OUTPUT AS #1
  CLOSE #1

  OPEN parout$ FOR OUTPUT AS #2
  PRINT #2, " a      al      b      be      cl      v1      v2
q      k10      k12      k21"
  CLOSE #2

  OPEN parout2$ FOR OUTPUT AS #3
  PRINT #3, " i      time      Cexp      Err_Add Err_prp Prop_Er
Conc"
  CLOSE #3

  OPEN fileout$ FOR APPEND AS #1
  OPEN parout2$ FOR APPEND AS #3

  FOR i = 1 TO nsubjects
    GOSUB parameters:
    PRINT #1, USING "##### # # ###.### ###.### ###.###
###.### ###.### ###.### ###.###"; i; ione; ione; dose; zero; zero;
zero; zero; zero; zero
    GOSUB times
    GOSUB conc
```

```

        NEXT i
        CLOSE #1
        CLOSE #3
NEXT iset
END

parameters:
cl:
    GOSUB rannum:
    cl = clpop + rn * sdcl
    IF cl <= .2 THEN GOTO cl
voll1:
    GOSUB rannum
    v1 = v1pop + rn * sdvoll1
    IF v1 <= .2 THEN GOTO voll1

voll2:
    GOSUB rannum
    v2 = v2pop + rn * sdvoll2
    IF v2 <= .2 THEN GOTO voll2

q:
    GOSUB rannum
    q = qpop + rn * sdq
    IF q <= .02 THEN GOTO q

    k10 = cl / v1
    k12 = q / v1
    k21 = q / v2
    ksum = k10 + k12 + k21
    ksumsq = ksum * ksum - 4 * k21 * k10
    IF ksumsq < 0 THEN GOTO parameters

    sq = SQR(ksumsq)
    al = (ksum + sq) / 2
    be = (ksum - sq) / 2
    a = dose * (al - k21) / (v1 * (al - be))
    b = dose * (k21 - be) / (v1 * (al - be))

    OPEN parout$ FOR APPEND AS #2
    PRINT #2, USING "##.### ##.### ##.### ##.### ##.### ##.###
###.### ##.### ##.### ##.### ##.###"; a; al; b; be; cl; v1; v2; q;
k10; k12; k21
    CLOSE #2
RETURN

times:
newtime1:
    tt = tmean(1)
    GOSUB rannum:
    tt = tt + rn * sdt(1)
    IF tt <= 0 THEN GOTO newtime1
    t(1) = tt

    FOR jj = 2 TO npoints
newtime2:
    tt = tmean(jj)
    GOSUB rannum:
    tt = tt + rn * sdt(jj)

```

```

                IF tt <= t(jj - 1) + 1 / 6 THEN GOTO newtime2
                t(jj) = tt
        NEXT
RETURN

conc:
    FOR j = 1 TO npoints
        tt = t(j)
conc2:
        conc1 = a * EXP(-al * tt) + b * EXP(-be * tt)
        GOSUB rannum:
        erradd = rn * sdconcadd
        GOSUB rannum:
        errprop = sdconcpro * rn * conc1
        conc = conc1 + erradd + errprop
        IF conc <= 0! THEN GOTO conc2
        PRINT #1, USING "##### # # ###.### ###.### ###.###
###.### ###.### ###.### ###.###"; i; izero; izero; zero; tt; conc;
cl; v1, v2, q
        PRINT #3, USING "##### ###.### ###.### ###.### ###.###
###.### ###.###"; i; tt; conc1; erradd; errprop; errprop / conc1;
conc
    NEXT
RETURN

rannum:
nextrand:
    sum = 0
    FOR kk = 1 TO nran
        sum = sum + RND
    NEXT kk
    rn = (sum - xnran1) / SQR(nran / 12)
    IF ABS(rn) > xlimit THEN GOTO nextrand
RETURN

design:
    OPEN filein$ FOR INPUT AS #1
        LINE INPUT #1, xin$
        INPUT #1, dose, clpop, sdcl, v1pop, sdvol1, v2pop,
sdvol2, qpop, sdq
        LINE INPUT #1, xin$
        INPUT #1, sdconcadd, sdconcpro
        LINE INPUT #1, xin$
        INPUT #1, nsubjects, npoints, nsets
        LINE INPUT #1, xin$
        INPUT #1, nran, xlimit
        LINE INPUT #1, xin$
        INPUT #1, fout$
        LINE INPUT #1, xin$
        FOR i = 1 TO npoints
            INPUT #1, tmean(i), sdt(i)
        NEXT i
    CLOSE #1
    xnran1 = nran / 2
RETURN
RETURN

```

Input File for Two-Compartment IV Infusion Simulations

The example shown is the input file for the Antagonist G simulation of design 29.

```
dose tinf clpop sdcl v1pop sdv1 v2pop sdv2 qpop sdq
622 6.0 4.92 1.54 6.86 0.56 6.7 1.21 0.72 0.23
sdconcadd sdconcprop
0.0 0.1
nsubjects points niterations
500 14 10
nran xlimit
250 3.0
output file (no extension)
Design29
t sdt
1.0 0
5.0 0
6.0 0
6.08 0
6.17 0
6.33 0
6.5 0
6.75 0
7.0 0
7.5 0
8.0 0
9.0 0
12.0 0
24.0 0
```

Simulation Program for a Two-Compartment IV Infusion PK Model

Program COMP2INF was used for designs 29-31.

```
REM      COMP2INF
REM
REM      2 comp model - INFUSION
REM      Generates Concentration data for
REM      NSUBS, NPOINTS and creates NSET of NONMEM input files.

OPTION BASE 1
DEFINT I-J, L-N

DIM tmean(100), t(100), sdt(100)
izero = 0
ione = 1
zero = 0!

INPUT "Input file name..... "; filein$
INPUT "Random no. seed (-32676- 32676) "; xr
RANDOMIZE (xr)

GOSUB design:
fout$ = RTRIM$(fout$)

FOR iset = 1 TO nsets
app$ = STR$(iset)
app$ = RTRIM$(app$)
app$ = LTRIM$(app$)
fileout$ = fout$ + app$ + ".var"
parout$ = fout$ + app$ + ".par"
parout2$ = fout$ + app$ + "B" + ".par"
errout$ = fout$ + app$ + ".err"

OPEN fileout$ FOR OUTPUT AS #1
CLOSE #1

OPEN parout$ FOR OUTPUT AS #2
PRINT #2, " A      alpha  B      beta      Cl      V1      V2      Q
k10      k12      k21"
CLOSE #2

OPEN parout2$ FOR OUTPUT AS #3
CLOSE #3

OPEN errout$ FOR OUTPUT AS #4
PRINT #4, " A      alpha  B      beta      Cl      V1      V2      Q
k10      k12      k21"
CLOSE #4

OPEN fileout$ FOR APPEND AS #1
OPEN parout2$ FOR APPEND AS #3
PRINT #3, " i      time      Cexp      Err_Add Err_prp Prop_Er  Conc"
FOR i = 1 TO nsubjects
GOSUB parameters:
PRINT #1, USING "##### # # ###.### ###.### ###.###
###.### ###.### ###.###"; i; ione; ione; dose; rate; zero; zero;
zero; zero
```

```

                GOSUB times
                GOSUB conc
        NEXT i
CLOSE #1
CLOSE #3
NEXT iset
END

parameters:
cl:
    GOSUB rannum:
    cl = clpop + rn * sdcl
    IF cl <= .2 THEN GOTO cl
v1:
    GOSUB rannum
    v1 = v1pop + rn * sdvol1
    IF v1 <= .2 THEN GOTO v1
V2:
    GOSUB rannum
    V2 = v2pop + rn * sdvol2
    IF V2 <= .2 THEN GOTO V2

Q:
    GOSUB rannum
    Q = qpop + rn * sdq
    IF Q <= 0.1 THEN GOTO Q

    k10 = cl / v1
    k12 = Q / v1
    k21 = Q / V2
    ksum = k10 + k12 + k21
    ksumsq = ksum * ksum - 4 * k21 * k10
    IF ksumsq < 0 THEN
        OPEN errout$ FOR APPEND AS #4
        PRINT #4, USING "###.### ###.### ###.### ###.### ###.###
###.### ###.### ###.### ###.### ###.### ###.###"; a; al; b; be; cl; v1;
V2; Q; k10; k12; k21
        CLOSE #4
        GOTO cl
    END IF

    sq = SQR(ksumsq)
    al = (ksum + sq) / 2
    be = (ksum - sq) / 2
    a = rate * (al - k21) / (v1 * (al - be))
    b = rate * (k21 - be) / (v1 * (al - be))

    OPEN parout$ FOR APPEND AS #2
    PRINT #2, USING "###.### ###.### ###.### ###.### ###.### ###.###
###.### ###.### ###.### ###.### ###.###"; a; al; b; be; cl; v1; V2; Q;
k10; k12; k21
    CLOSE #2
RETURN

times:
    ttest = 0
    FOR j = 1 TO npoints
newtime:
    tt = tmean(j)

```

```

        GOSUB rannum:
        tt = tt + rn * sdt(j)
        IF tt <= ttest THEN GOTO newtime
        t(j) = tt
        ttest = tt
    NEXT
RETURN

conc:
    FOR j = 1 TO npoints
        tt = t(j)
        t1 = tt
        IF t1 > tinf THEN t1 = tinf
conc2:
        conc1 = a * (EXP(al * t1) - 1) * EXP(-al * tt)
        conc1 = conc1 + b * (EXP(be * t1) - 1) * EXP(-be * tt)
        GOSUB rannum:
        erradd = rn * sdconcadd
        GOSUB rannum:
        errprop = sdconcpro * rn * conc1
        conc = conc1 + erradd + errprop
        IF conc <= 0! THEN GOTO conc2
        PRINT #1, USING "##### # # ###.### ###.### ###.###
###.### ###.### ###.###"; i; izero; izero; zero; zero; tt; conc; cl;
v1
        PRINT #3, USING "##### ###.### ###.### ###.### ###.###
###.### ###.###"; i; tt; conc1; erradd; errprop; errprop / conc1;
conc
    NEXT
RETURN

rannum:
nextrand:
    sum = 0
    FOR ii = 1 TO nran
        sum = sum + RND
    NEXT ii
    rn = (sum - xnran1) / SQR(nran / 12)
    IF ABS(rn) > xlimit THEN GOTO nextrand
RETURN

design:
    OPEN filein$ FOR INPUT AS #1
        LINE INPUT #1, xin$
        INPUT #1, dose, tinf, clpop, sdcl, v1pop, sdvol1, v2pop,
sdvol2, qpop, sdq
        LINE INPUT #1, xin$
        INPUT #1, sdconcadd, sdconcpro
        LINE INPUT #1, xin$
        INPUT #1, nsubjects, npoints, nsets
        LINE INPUT #1, xin$
        INPUT #1, nran, xlimit
        LINE INPUT #1, xin$
        INPUT #1, fout$
        LINE INPUT #1, xin$
        FOR i = 1 TO npoints
            INPUT #1, tmean(i), sdt(i)
        NEXT i
    CLOSE #1

```

```
rate = dose / tinf  
xnran1 = nran / 2  
RETURN
```


Appendix 3

Presentations

S.J. Carmichael, A.W. Kelman, L.S. Murray, D.I. Jodrell (1997) Predicted Population Concentration Distributions.
Pharmacokinetics (U.K), Newcastle. Poster Presentation.

S.J. Carmichael, A.W. Kelman, L.S. Murray, D.I. Jodrell (1998) Comparison of NONMEM FO Estimation vs FOCE for Sparse Concentration Data.
Pharmacokinetics (U.K), Manchester. Poster Presentation.

S.J. Carmichael, A.W. Kelman, L.S. Murray, D.I. Jodrell (1999) Comparison of NONMEM FO Estimation vs FOCE for Sparse Concentration Data.
Scottish NHS Research Day, Royal College of Physicians, Edinburgh. Poster Presentation

S.J. Carmichael, A.W. Kelman, L.S. Murray, D.I. Jodrell (2000) Limited Sampling Designs for a Two-Compartment PK Model.
Scottish NHS Research Day, The University of Stirling. Poster Presentation